DESIGN AND EVALUATION OF TWO-LAYER ROLLER COMPACTED CONCRETE

By

Haneen Adil Mohammed

Thesis submitted to the University of Nottingham

for the degree of Doctor Philosophy

Department of Civil Engineering

May 2018

DEDICATION

WHEN YOU TRUST GOD TO FULFILL THE PROMISES HE'S GIVEN YOU, ALL THE FORCES OF DARKNESS CANNOT STOP GOD FROM BRINGING YOUR DREAMS TO PASS.

TO MY BELOVED FAMILY

ABSTRACT

Roller Compacted Concrete (RCC) is a mixture of well graded aggregates, cement and water. It is placed with a high compaction asphalt type paver and compacted to high density by vibratory rollers to provide a high strength and durable pavement structure. RCC requires no formwork, surface finishing, dowelled joints or reinforcement. These characteristics make RCC simple, fast and economical. However, it also presents difficulties with high-speed applications related to surface texture and surface evenness. These difficulties have so far restricted the use of RCC to the lower layers of normal roads.

A two-layer RCC pavement system is a type of composite pavement consisting of two concrete layers. The two layers are paved in either a "wet-on-wet" technique or "wet-on-dry" technique. The bottom layer serves as the main bending-resistant component of the composite slab, while the top lift is generally constructed with higher-quality constituent materials for improved surface characteristics such as noise and skid resistance.

The aim of this research is to evaluate and design two-layer RCC systems with different aggregate sizes and types and different placement conditions in order to expand the application of RCC in pavements. Mechanical properties, bond strength properties, durability characteristics, surface properties, fatigue damage, joint deterioration and pavement design are the main objectives in this research. A range of testing equipment, methodologies and tools have been used in this investigation.

The findings of this study showed that a two-layer RCC system can achieved good strength and stiffness for each of the mixtures in the two layers. Also,

the inter-layer bond was found to be strong when the two layers were placed within one hour, but weaker when the upper layer was placed three hours after the lower layer. Moreover, the durability of the two-layer RCC system was found to be acceptable, especially when the upper layer was placed within an hour of the lower layer. The surface characteristics for the upper layer of RCC showed that the minimum requirement for skid resistance and texture depth have been achieved. However, it is suggested that further investigation is needed, particularly into the evenness of RCC.

The investigation into the effect of dynamic load on the two-layer RCC system demonstrated a good fatigue strength for each RCC mixture and for the two layers together, compared to conventional concrete pavements. Also, the results of load transfer stiffness and joint deterioration showed acceptable performance with regard to crack or joint width, shear stress and placement conditions. The effect of other parameters such as moisture and differential temperature requires a separate investigation and is recommended for future work.

The results of the design and analysis of two-layer RCC using KENSLAB, a finite element program, indicted that RCC could perform successfully in pavements with a long service life.

In conclusion, the results obtained show that the two-layer RCC are a valid alternative for pavements. On one hand, the use of a harder and more resistance aggregate at the top layer guarantees higher skid resistance and durability, while limiting for the use of high quality aggregate. On the other hand, the results show that adequate construction techniques can alleviate the problems arising from the lack bond between layers.

ACKNOWLEDGEMENTS

First of all, I want to thank Allah almighty who gave me the power, the patience and the love to be able to complete my study in the best way.
I gratefully acknowledge the support and guidance from my supervisors Dr. Nick Thom and Mr. Andrew Dawson. They helped me a lot and gave me from their immense knowledge and experience, without their guidance this thesis would not have been possible. I am very grateful for the great assistance, motivation and encouragement given by my supervisors. I would like to express my sincere gratitude to Dr. Nick who gave me a lot of his scientific, practical experience and his time. My supervisors, I will never forget your help.
I am grateful to my internal assessor Dr. Luis Neves for his kind advices during my research.
Special thanks to Higher Committee for Education Development in Iraq (HCED) who sponsored this research and funded me for the study period.
I am grateful to all technical staff of NTEC (Nottingham Transportation Engineering Centre) who were very helpful and friendly in my laboratory work: Jon Watson, Richard, Matt and Laura. Special thanks to Mr. Martyn Barret for his help in the difficult and long-time test. Also, to the staff of Structural & Concrete Laboratory for their help with concrete tests, especially Mr. Nigel Rook.
Big thanks to my colleagues at the Nottingham Transportation Engineering Centre for their support, encourage and useful discussion. Big thanks to my colleague Samuel Leworthy for his valuable help in my research. Deep thanks to my special friends and colleagues Doha, Hadel, Siham and

Sarah for the beautiful time that I spent during my study. I am also very grateful to Dr. Hasan Al-mosawe and Dr. Ameer Hilal for their help when I first came to the UK and in the beginning of my research.

Finally, I want to express my deep and warm thanks to my father, mother and my beloved sister (Zainab) for their endless love, support, encourage, believe and prayers, I ask God to bless them all. I hope I could make you proud of my work. Also, I am grateful to my lovely aunt Nadia and her daughter Faroha for their love and positive energy. My thanks cannot be end without saying big thanks to my real friends in Baghdad and Nottingham (Fatima, Rana and Aza) for the big love, beautiful times and motivation to finish my study successfully.

DECLARATION

This is to declare that the contents of this thesis are my own work and were performed at the University of Nottingham from 2014 to 2018. This thesis has not been submitted to any other institution for another degree.

Haneen Adil Mohammed

Nottingham, March 2018

Email: haneen.mohammed@nottingham.ac.uk, haneen.civil.2009@gmail.com

Contents

List of Figures

Tables

Chapter 1

Introduction

1.1 General

Roller-compacted concrete (RCC) derives its name from the heavy vibratory steel drum and rubber-tired rollers that are used to compact it to its final form. RCC has similar strength properties and consists of the same materials as conventional concrete, which are well-graded aggregates, cementitious materials, and water, but it has different mixture proportions (Harrington et al., 2010). ACI-116 (2000) defines roller compacted concrete as a 'concrete compacted by roller compaction; that in its unhardened state will support a roller while being compacted.' Moreover, Donegan (2011) described roller compacted concrete (RCC) as an engineered mixture of dense-graded aggregates, cement and water. It is a zero-slump concrete, which is placed with a high compaction asphalt type paver and compacted to high density by vibratory rollers to provide a high strength and durable pavement structure. RCC requires no formwork, surface finishing, dowelled joints or reinforcement. These characteristics make RCC simple, fast and economical (ACI-325.10R, 2001).

Roller compacted concrete is used in two general areas of engineered construction, which are dams and pavements. In addition, ACI-309 (2000) explains that roller compacted concrete (RCC) has become an accepted material for constructing dams and pavements, rehabilitating and modifying existing concrete dams, and providing overflow protection to embankment dams and spillways. Its production provides a rapid method of concrete construction similar in principle to soil-cement and other earthwork construction. From these definitions, the similarity of RCC with other types of concrete can be noticed and also its potential benefits for use in the various applications.

The main drawback of RCC pavement is the surface texture and evenness that made the pavement can only carry traffic at relatively low speeds. Therefore, to improve the surface, asphalt overlays have been applied with success. However, these pavements have lack in the strength and durability of a rigid pavement system and some problems with reflective cracks have been identified (Kreuer, 2006). Thus, a two-layer RCC system can provide an economical pavement that is both strong and durable.

Figures 1.1 and 1.2 show two different applications of RCC in pavements.

Figure 1.1: *RCC pavement used for a local street (Harrington et al., 2010)*

Figure 1.2: *RCC used to reconstruct shoulders on I-285 near Atlanta, GA, USA (Harrington et al., 2010)*

1.1.1 Benefits of RCC in pavements

RCC has proven to have similar strength and performance of conventional concrete. It is commonly used in parking areas, equipment yards, container ports, rail freight terminals, and increasingly, in highways. RCC's economic advantages relate to high-volume, high-speed construction methods and it is preferable to asphalt in many aspects such as material costs, placement time, labour cost and time and traffic opening time (Donegan, 2011).
In addition, RCC has a higher reflectivity than asphalt, when it is used

as a surfacing material. This benefit mitigates some of the problems of the urban heat island effect which is commonly linked to dark surfaces absorbing heat (Harrington et al., 2010). RCC can be open to traffic within two days in warm weather and three to four days in cooler weather and in certain applications immediately. The opening time of RCC depends on some factors such as mechanical properties, pavement loading, RCC mixture and ambient day and night temperature. Therefore, RCC should be allowed to gain adequate flexural and compressive strength prior to opening to traffic (Donegan, 2011; Harrington et al., 2010).

The most important advantages for RCC in pavements are summarised in Table 1.1 according to Donegan (2011) and Harrington et al. (2010).

Table 1.1: *Features and advantages of roller compacted concrete (RCC)*

Features	Advantages
Low paste content	Less concrete shrinkage
Low permeability	Enhances durability and resistance to chemical attack
High flexural strength	Supports heavy, repetitive loads without failure, which reduces maintenance costs and down time
High compressive strength	Withstands high concentrated loads and heavy industrial and military applications
High shear strength	Reduces rutting and subsequent repairs
Aggregate interlock	Provides high shear resistance at joints to prevent vertical displacement or faulting
No steel reinforcement or dowels No forms or finishing	Speeds and simplifies construction, reduces cost and minimises labour
No formed or sawn joints	Speeds construction and reduces cost
Light coloured surface	Lighting requirements are reduced for parking and storage areas

1.2 Significance of research

RCC has been used successfully for different applications because of the ease of construction, low cost and the availability of materials and equipments. Although there are clear advantages of RCC when used, there are certain limitations that have affected its use in high speed applications and other types of pavement. RCC presents difficulties related to surface texture and surface evenness, the latter possibly partially due to high lift thickness of RCC. These difficulties have so far restricted the use of RCC to certain pavement applications such as parking areas and low speed roads. Two-layer systems, which have been used before for different types of concrete pavement, can provide good surface properties such as low noise and high friction when using high quality aggregate and long lives. The use of two-layer system in pavements has been restricted by the lack of understanding of the bond between different layers and long term performance of joints. These phenomena are studied herein using both experimental and analytical tools.

Thus, a two-layer RCC system with different aggregate sizes and types under different placement conditions will be evaluated in this research, and the possibility of expanding RCC pavement applications will be investigated.

1.3 Research aim and Objectives

The aim of this research is to design and evaluate a two-layer RCC system in pavements with different aggregate sizes and types under different

placement conditions in order to investigate the possibility of expanding the application of RCC in pavements.

To achieve this aim, the following steps have been taken:

- Design and produce two mixtures with different aggregate sizes and types in order to use them in a two-layer RCC system.
- Examine the mechanical properties of each mixture in terms of compressive strength, flexural strength, indirect tensile strength and modulus of elasticity. Also, the density and compacity of the two mixtures is assessed in this study.
- Study the bond strength between the two RCC layers using a shear bond strength test and the indirect tensile strength test.
- Assess the durability of the two-layer RCC in terms of a cyclic freezing and thawing test.
- Evaluate the surface characteristics of the upper RCC layer through the pendulum test for skid resistance and the sand patch test for texture depth.
- Investigate the performance of the two-layer RCC system under repeated load by assessing the evolution of damage due to fatigue determined by a four-point bending test.
- Examine the joint deterioration in terms of load transfer stiffness through a cyclic shear test.
- Analyse and design two-layer RCC systems using KENSLAB, a finite element program, to predict the design life of the RCC and the deterioration of joints in a two-layer system for pavements.

1.4 Layout of thesis

This thesis consists of eight chapters:

- Chapter 2 presents an overview of the previous work on roller compacted concrete in construction. The chapter also presents the use of RCC in constructions such as dams and pavements, the differences between RCC and other types of pavements, the applications of RCC in pavements and the limitations of RCC in pavements.

- Chapter 3 explains the production of RCC and its mix design with regard to selection of materials, gradation of aggregate and methods of producing RCC samples. Mechanical properties of each mixture are also discussed in terms of compressive strength, flexural strength, indirect tensile strength and modulus of elasticity. Density and compacity are also studied.

- Chapter 4 investigates the two-layer RCC pavement system by measuring the bond strength between the two layers and the durability of the two-layer RCC. The bond strength is presented in terms of shear bond strength and indirect tensile strength and the durability is assessed by a freezing and thawing test.

- Chapter 5 briefly explains the surface characteristics of the surface layer of RCC with regard to microtexture, macrotexture, megatexture and roughness. Skid resistance properties are evaluated through the pendulum test and the sand patch test.

- Chapter 6 assesses the performance of the two-layer RCC system under repeated load. This chapter investigates the fatigue damage of the

RCC mixtures and the two-layer system by means of the four-point bending test to draw a relationship between stress ratio and number of cycles to failure. In addition, the load transfer stiffness across the joint was studied using a cyclic shear test and an equation derived to predict joint deterioration.

- Chapter 7 focuses on structural design and analysis of the two-layer RCC system using a mechanistic-empirical approach through KENSLAB, a finite element program, to find maximum stresses and deflections. In this chapter, the effect of load transfer stiffness is examined and the effect of different slab thicknesses and lengths also are observed. The design life and the joint deterioration are also investigated.

- Chapter 8 states the conclusions achieved from this research and suggests recommendations for future work.

Figure 1.3: *Flow chart for the research methdology*

Chapter 2

Previous work of Roller Compacted Concrete (RCC)

2.1 Introduction

Concrete pavements have been used in various applications such as highways, airports, streets, local roads, parking lots, industrial facilities, and other types of infrastructure. Concrete pavements can provide high durability for long service life with little or no maintenance. The first concrete pavement was built in Bellefontaine, Ohio, in 1891, by George Bartholomew. Different types of concrete pavement have been built and are commonly used. They have two important requirements, namely to resist traffic loads and also the effect of drying shrinkage of the concrete and subsequent thermal effects (Delatte, 2014).

Types of concrete pavement are:

1. Conventional concrete pavements which are generally either jointed plain (JPCP), jointed reinforced (JRCP), or continuously reinforced (CRCP). Figure 2.1 shows different types of concrete pavement.

2. Prestressed and precast concrete pavements (PCP) that are used for similar applications to conventional concrete pavements.

3. Other types of concrete pavement include roller compacted concrete (RCC) and pervious or porous concrete, commonly used for industrial or parking lot applications.

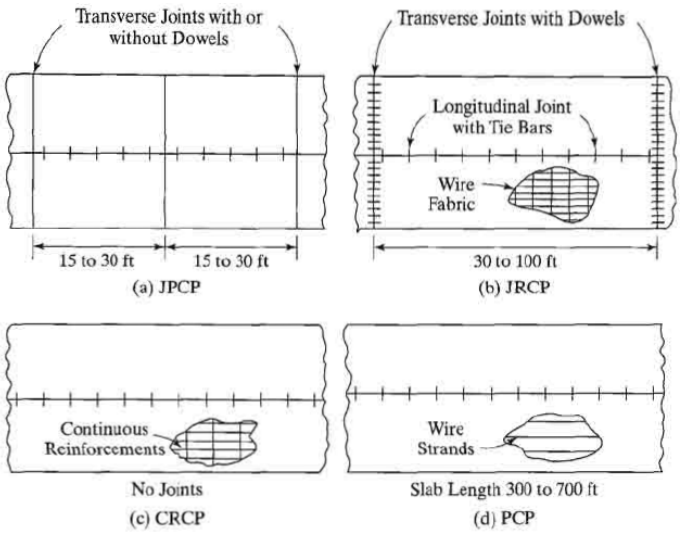

Figure 2.1: *Types of concrete pavement (Huang, 2004)*

2.2 Background

For many years cement–treated base (CTB) has been used in pavements with a protective asphalt surface, where the cementitious base was designed to carry logging equipment loads, and where the asphalt surface tended to become damaged from heavily loaded tyres in hot summer temperatures. The suggestion was made to try increasing the cement content of the soil cement from 6% to 12% by weight, making it stronger and probably more resistant to freeze/thaw damage. The exposed cementitious pavement was successful in that the asphalt layer was never applied and thus roller com-

pacted concrete was formed (Piggott 1999).

RCC has been used for a long time in a variety of applications. The needs for a new pavement material with high strength and low initial cost on certain industrial projects has led to the use of RCC with wider applications. The two important characteristics of RCC, durability and low maintenance requirements, have been proved to provide these needs effectively. In the 1930s, RCC pavements were built in Sweden and in 1942, the U.S. Army Corps of Engineers (USACE) built an RCC runway in Yakima, Washington that provided a durable and strong concrete pavement (Delatte, 2004). The 1970s saw the first widespread use of RCC by the Canadian logging industry when the new land-based log sorting methods needed a strong, fast and economic paving system that could take heavy loads and handling equipment (ERMCO-Guide, 2013). During the early 1980s, engineers at the United States Army Corps of Engineers started studying the use of RCC for pavement construction at military facilities. In 1984, the durability of RCC in terms of freezing and thawing was seen to require more investigation. Hence, the Corps of Engineers constructed a full scale test pavement at the Cold Regions Research Engineering Laboratory in Hanover, NH, USA.

During 2000 – 2010, RCC pavements gained popularity for constructing low to moderate traffic streets and secondary highways with over 70 projects and 7.4 million m^2 placed. From 2011 until 2013, RCC utilization expanded into many other applications such as hike and bike trails, local streets and roads, commercial parking lots, while continuing to be used in traditional industrial type applications (ACI-325.10R, 2001; Harrington et al., 2010; Zollinger, 2015).

Figure 2.2 illustrates the growth of RCC in terms of cumulative and individual square yards of RCC per year, (where 1 square yard = 0.83 m^2).

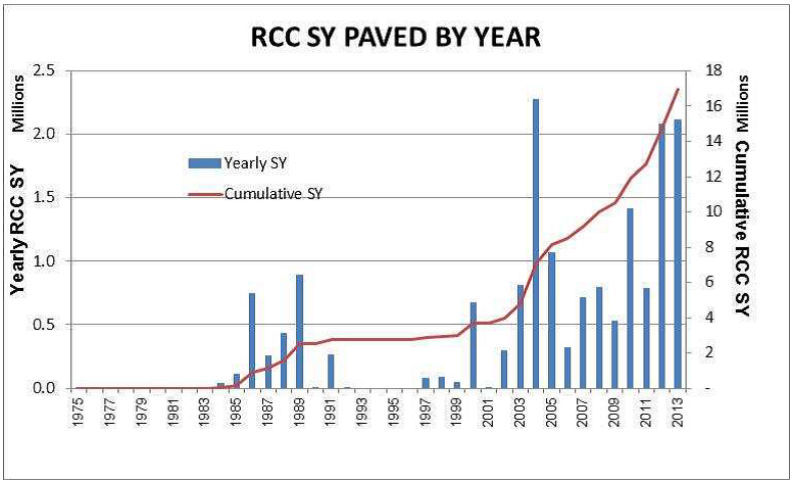

Figure 2.2: *Summary of RCC yd^2 Placed in the United States (Zollinger, 2015)*

Over the years, several developments were introduced to RCC; most were directed towards improving quality, including smoothness and durability. An improvement in ride-ability came when asphalt pavers were used to place RCC. Therefore, RCC combines the performance of concrete and the low cost of asphalt (Delatte, 2004; Piggott, 1999).

RCC pavement has been widely used for heavy load traffic in maintenance, container storage, parking, or low speed roadway applications. The development of more advanced paving machines designed specifically for RCC and improved construction techniques and procedures has resulted in higher quality pavements. These improvements have led to the possibility of utilizing RCC for high speed applications (Shoenberger, 1994).

In recent years, there are some improvements towards the ductile behaviour of RCC and reduces the environmental effect to become more sustainable material. Xu (2014) stated that the utilisation of bonded concrete overlays (BCOs) can be more sustainable, environmentally friendly and cost

effective than the complete removal and replacement of the old concrete pavement. Therefore, she designed a unique mix of steel fibres, RCC and polymer modified bonded concrete overlays to achieve good mechanical performance and rapid construction process.

Khayat and Libre (2014) investigated the optimization of RCC mixture depending on a proper selection of aggregate combination to achieve a high packing density and optimum particles size distribution. They found that compressive strength of the optimized RCC mixtures was almost equal to that of conventional concrete (wet-formed concrete). While, flexural strength increased by 20 % to 25 % than the conventional concrete.

In addition, Mohammed and Adamu (2018) study the effect of using crumb rubber and nano silica on RCC mixture. They found that using 10 % of crumb rubber by volume of fine aggregate with 1.13 % of nano silica by weight of cement can give a high strength, durable and ductile RCC for pavement applications.

2.3 Using RCC in construction work

2.3.1 RCC for dams

Roller compacted concrete is used worldwide for constructing new gravity dams and arch dams. RCC has also been used to provide stability berms for static and seismic requirements. It has been developed as a result of efforts to design and build concrete dams that can be constructed rapidly and economically.

One of the successful RCC dams is the 52-m-high Willow Creek Dam, which

confirmed that economy and rapid construction is possible with RCC. This dam contained 330000 m^3 of RCC and was placed in less than five months, with in-place RCC cost averaging about \$26 per m^3. Moreover, the U.S. Bureau of Reclamation's (USBR) used RCC for the 90-m high Upper Stillwater Dam, which was completed in 1987, containing 1.12 million of RCC. More than 280 RCC dams, are located in 39 countries, mainly in Japan and China. The United States has 37 RCC dams with the highest being Olivenhain Dam in San Diego, CA which was completed in 2003 as shown in Figure (2.2) (Adaska, 2006; Saucier, 1994).

Figure 2.3: *Olivenhain Dam in San Diego (Adaska, 2006)*

2.3.2 RCC for pavements

RCC pavements combine the properties of conventional concrete pavement materials with the construction practices of asphalt pavements. RCC pavements are compacted with an asphalt-type pavers and have similar aggregate gradations to asphalt pavements, while the materials and structural performance properties of RCC are similar to those of conventional concrete. RCC pavements can achieve high strength properties equal to or exceeding conventional concrete, if using well-graded aggregates, suitable

cement and water content and sufficient compaction (Harrington et al., 2010).

RCC pavements have proven to be economical to construct as compared to jointed plain concrete pavements (JPCP). RCC pavements do not require forms, dowels or tie bars, or labour for texturing and finishing, therefore, construction costs are lower. Maintenance costs are also found to be lower than for other pavement types. In the past ten years RCC has continued to be a cost-effective for many conventional pavement applications such as warehouse facilities, industrial access roads, large commercial parking areas, roadway inlays, and residential streets (Harrington et al., 2010). It may be considered for aprons, massive open foundations, base slabs, massive backfill, riprap for bank protection, as a repair material, and for pavement construction (Saucier, 1994).

Traditionally, RCC pavements have rough surfaces because of the construction process which means that RCC unsuitable for high speed traffic. Therefore, Kreuer (2006) suggested an investigation into using bonded concrete overlays on RCC, and a trial pavement has been built at an industrial facility in Michigan, USA. The results of this trial showed that compressive strength between 19 MPa and 28 MPa without signs of debonding between the RCC base and the overlay.

Furthermore, Zollinger (2015) proposed grading the RCC surface after hardening to remove the roller marks and create a smooth surface. He also indicated the effort that have been made to eliminate the need for rolling and to use only the densification provided by the paver screed to meet the compaction specifications.

This approach results in a much smoother surface at a lower cost while

still meeting the required strength and specified density.

2.4 How RCC pavement differs from soil–cement treated base (CTB) and conventional concrete pavement (PCC)

The RCC pavement mixes have different cement and paste contents with smaller coarse aggregate than typically used in dams. Typical cementitious material contents range from 10-17%, and the maximum size of coarse aggregate is usually 20 mm. These factors along with a different approach to mix design produce a much more workable mix than that used for dams, although it is still a no-slump mix, stiff enough to support vibratory rollers (Keifer, 1986).

On the other hand, the use of RCC for pavements developed from the use of soil cement and cement treated base (CTB) courses. RCC for pavements requires better controls on proportioning; also, a paving machine is normally used for placing and finishing the RCC pavement while less advanced placing and spreading equipment is often used for CTB or soil cement. The RCC pavement mix has considerably more cementitious material than CTB, and differs from soil cement which may contain coarser aggregates.

Furthermore, according to Shoenberger (1994) and Donegan (2011), CTB can be differentiated from RCC by the compressive strengths achieved. CTB and other similar materials such as econocrete and dry rolled lean concrete normally obtain compressive strengths of 7 MPa or less at 28 days, while RCC normally obtains compressive strengths of 28 to 69 MPa,

similar to conventional PCC.

Yet, RCC pavements are unlike conventional concrete pavements in many ways, especially during production with different mixture proportions and placement. They are engineered and constructed differently from conventional concrete and require different placement and design considerations even though they are made of the same constituent materials which are aggregate, portland cement, supplementary cementitious materials, chemical admixtures and water (Burwell et al., 2014).

Figure (2-4) shows the different types of concrete pavement which contain different amounts of cement and water content.

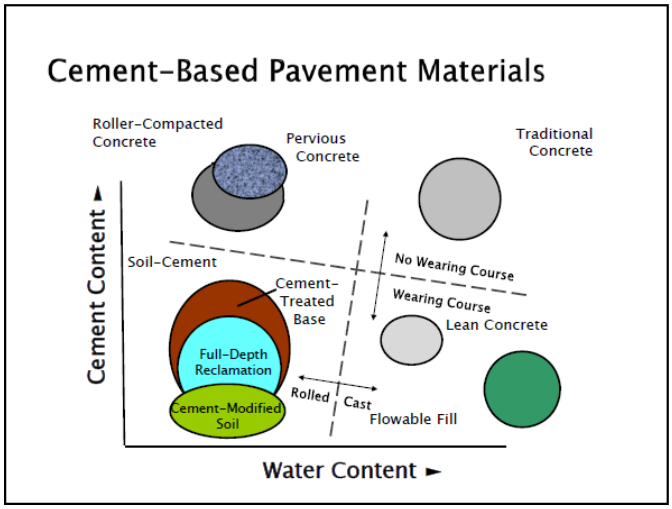

Figure 2.4: *Different types of concrete pavements (Prusinski, 2013)*

2.5 Applications of RCC in different types of pavement

RCC is economical, fast-construction and beneficial for many pavement applications. In the past, RCC pavements have been used mainly for

maintenance and parking areas or as low speed access roads because of its relatively coarse surface. These areas have been used for low speed, heavy load and tracked vehicles. From the beginning of using RCC in pavement, it was used in harsh and mild climates under all types of wheel loadings.

The intended use of the pavement surface and the cost-effectiveness of RCC are normally the deciding factors in the selection of RCC over either asphalt concrete (AC) or conventional concrete (PCC) (Shoenberger, 1994). In recent years, RCC has started to be used in commercial areas and for local streets and highways as improved design and construction techniques have been developed (Harrington et al., 2010).

Thus, Donegan (2011) indicated the common applications of RCC which are:

- Intermodal terminals.
- Stock yards (coal, compost, wood chips).
- Military facilities.
- Truck terminals-distribution centres.
- Low to medium speed roads (exposed or with surfacing).
- Hard shoulders and inlays to highways (with surfacing).
- Container handling yards.
- Warehouse floors.
- Parking areas.

Application of RCC is often considered when it is economically competitive with other construction methods. Figures (2.4), (2.5) and (2.6) show different applications of using RCC around the world.

Figure 2.5: *Residential Street, Columbus, OH (Harrington et al., 2010)*

Figure 2.6: *Tattershall Quarry Haul road, UK (ERMCO-Guide, 2013)*

Figure 2.7: *Construction for commercial and heavy industrial applications (Garber et al., 2011)*

2.6 Limitations of RCC for pavements

There are limitations to the use of RCC pavemet. Pittman (1994) pointed out that the smoothness of RCC has not met the requirements for high-speed applications, such as interstate highways or airfield runways. The surface roughness is primarily a result of the rolling process, which may affect the evenness of the paving lane along a longitudinal profile.

He also observed that the surface texture is not appropriate for RCC pavements in high-speed applications as it could result in raveling of surface fines under traffic. This occurs when the surface of the RCC is inadequately cured, and when excessive fine material joint is not removed from the surface.

Harrington et al. (2010) summarized the possible limitations and challenges of RCC pavements:

- RCC smoothness is not adequate for high-speed pavement applications.
- Multiple lifts must be placed within an hour to ensure good bonding

and monolithic pavements.

- RCC pavement edges require 96% dry density on cold joints instead of the 98% required on interior pavement sections because of the difficulty of compaction according to Harrington et al. (2010).

- RCC pavements in hot weather require more attention to reduce evaporation and water loss.

2.7 Summary

This chapter has presented background and overview of literature of RCC usage in different application such as dams and pavements. RCC has been used for a long time and this has proven the sustainability of using it in many successful applications.

There are also several developments that have occurred for RCC, particularly in pavements, related to mix design and selection materials, compaction and thickness design that made RCC a viable choice for pavement construction. However, there are also some limitations that restrict the use of RCC to certain applications such as heavy duty surfaces, storage area and parks area. These limitations are surface texture and evenness that need more consideration in order to expand the application of RCC.

Thus, this research aims to use a two-layer of RCC pavement system with different aggregate types and sizes and different placement conditions in order to achieve improvement in the performance of RCC so that it will be more suitable for normal roads and highways.

Chapter 3

Producing RCC for pavement

3.1 Introduction

This chapter presents the production of two-layer RCC for pavements with regard to mix design, material selection, sample production and some initial properties. The purpose of designing two layer RCC in this research with different aggregate sizes and types is to investigate the possibility of expanding the application of RCC in pavements for wider applications and to improve the skid resistance and evenness of RCC surfaces.

There are several methods to produce and design RCC for pavements to achieve good quality, high strength and durability. A number of successful methods have been used for RCC mixture proportioning to produce mixtures for mass concrete applications, pavements and other concrete construction applications. Proportioning selection is necessary to ensure that the RCC mix has sufficient percentage of paste compared to aggregate particles in order to sufficiently fill the voids of the compacted mix so that it behaves integrally.

The most common method of proportioning aggregate, cementitious ma-

terials and water to design a RCC mix is based on evaluating compacted laboratory specimens. The equipment and procedures are very similar to those used for determining maximum dry density and optimum moisture content for aggregates and soils (ACI-116, 2000; Halsted, 2009).
Therefore, ACI-207.5R (1999) and Donegan (2011) classified the various procedures into three categories:

- Proportioning method of RCC that depends on workability and suitable consistency.
- Method for selecting mixture proportions to achieve the most economical aggregate-cement combination.
- Proportioning method of RCC according to soil compaction concepts.
- Proportioning of RCC depending on the solid suspension model.
- The optimal paste volume method.

Obviously, the methods depend on different criteria that make them suitable for different applications and, from experience, the most appropriate one can be decided. These methods differ significantly for a number of reasons. Mainly, the reasons relate to the aggregate, whether it is used for conventional concrete or for stabilized materials. Also, the size of aggregate affects the design method, whether it is for dams or pavements, and it influences the workability of the concrete.
On the other hand, Tangtermsirikul et al. (2004) illustrated that there are two main approaches for proportioning RCC mixtures, the soil and concrete approaches. In the soil approach, RCC is considered as a cement-enriched processed soil, where the mix design is based on moisture – density

relationships and the compaction method. In the concrete approach RCC is considered as a normal concrete where the mix design depends on the water–cement relationship, which affects the strength and other properties of RCC.

Furthermore, Amer et al. (2008) evaluated two methods of mixing and producing RCC mixtures. First, the U.S Army Corps of Engineering (USACE) procedure depends on determining the performance requirements for the RCC pavement, such as strength and durability. Second, the procedure of the American Society for Testing and Materials ASTM D 1557 is used to determine the maximum dry density and optimum moisture content for a RCC mixture.

Thus, Harrington et al. (2010) reported that whichever approach is used, the aim is to produce a RCC mixture that has:

- Sufficient cement to aggregates ratio to fill the voids between them in order to gain a sufficiently well compacted mixture.
- The required mechanical strength and elastic properties.
- Good workability characteristics to achieve the required density.
- Enough durability to withstand any given environment.

In brief, there are several methods used for the design RCC mixtures ; however, they differ depending on the application of the RCC construction.

3.2 Mix design of RCC for pavement

In this research, the design of RCC mixtures follows the soil compaction concept. This proportioning method is based on forming a relationship

between the dry density and moisture content of the RCC by compacting specimens at a given compactive effort over a range of moisture content. It is similar to the method used in soils and soil-aggregate mixtures (ACI-116, 2000).

This is the most commonly used method of mix design in the UK, as it establishes the optimum moisture content to achieve maximum dry density which is essential in order to establish field controls for compaction (Donegan, 2011). It involves determining the maximum dry density of materials using modified Proctor compaction procedures and it can be considered an extension of soil-cement technology. Optimum water contents are established using the same procedures as for establishing the optimum water content of embankment material and soil cement as described in BS EN 13286-4:2003. Compaction is dependent upon the energy imparted to the specimen. Hence, Choi and Groom (2001) pointed out that the general methodology to proportion RCC mixes with the soils approach consists of:

- Select a suitable aggregate for the RCC.
- Choose various cement contents for a range of trial mixtures.
- Determine a desirable moisture content to prepare RCC specimens for each trial mix.
- Prepare RCC specimens for compressive strength testing.
- Select mix proportions based on laboratory test results.

Arnold (2004) reported that there are two common types of soil compaction test that are used for monitoring and controlling fill placement material.

They are the standard Proctor test (ASTM D 698) and the modified Proctor test (ASTM D 1557). These two tests depend on determining the optimum moisture content that gives the maximum dry density of the material, but they are different in compaction effort. From previous experience, the modified Proctor in ASTM D 1557 has been shown to be more suitable for roller compacted concrete (RCC). This is due to the coarse nature of RCC and because the modified Proctor has proved to have the ability to achieve high compactive effort similar to that applied in the field. Table 3.1 summarises the general requirement for RCC mix design according to previous references and specifications.

Table 3.1: *Summary of the requirement for RCC mix design depending on different specifications and references*

Property	ACI 207.5R	Tangterm-isrikul et al. (2004)	USACE	ASTM D 1557	Harrington et al. (2010)	BS EN 13286-4
Density	√	√		√		√
Workability	√				√	
Strength		√	√	√	√	√
Durability		√	√		√	

On this basis the most suitable method for designing RCC is the geotechnical approach of ASTM D 1557 which simulates the condition in the field and gives an indication of the best composition of the mixture.

3.2.1 Fabrication of test specimens in the laboratory stage

There are several pieces of equipment for the preparation of specimens at the laboratory stage that have been used as representative of actual field placement conditions.

The preparation equipment includes: 10-ton vibratory roller, Hilti or Kango vibrating hammer, Vebe table, roller compactor and Proctor test. The effectiveness of the different methods of specimen preparation varies based on the workability of the RCC mixture as stated by Arnold (2004).

Choi and Groom (2001) reported on RCC fabricated in accordance with a geotechnical approach. There are two common methods to prepare RCC cylinder samples:

- Using modified proctor hammer (ASTM D 1557).
- Using a vibrating hammer (ASTM C 1435).

On the other hand, ACI-325.10R (2001), adopting a concrete design approach, states that the procedures most frequently used for preparing RCC mixtures involve vibrating the fresh RCC sample on a vibrating table then compacting the sample with some type of compaction hammer following the procedures of ASTM D 1557. It stated that complete compaction of RCC specimens may be difficult when using only a vibrating table as samples taken from RCC pavements sometimes have unit weights greater than vibrating table specimens of similar age and moisture content. In contrast, specimens compacted by vibrating hammer may have unit weights approximately equal to samples taken from RCC pavements.

Khayat and Libre (2014) argued that one technique for making RCC spec-

imens that has proven itself in recent years, both in the field and the laboratory, is the vibrating hammer. This technique provides cylinders for compressive strength, prisms for flexural strength and several other specimen geometries, such as rectangular prisms for scaling resistance testing. It involves compacting fresh RCC with an impact hammer with an appropriate compaction head in to a steel mould.

According to Khayat and Libre (2014), the procedure for producing RCC specimens for compressive testing using a vibrating hammer and vibrating table are described in ASTM C 1435 and ASTM C 1176, respectively, and the equipment is shown in Figure 3.1.

Figure 3.1: *Hammer, rectangular head and circular heads used for compacting RCC samples (Khayat and Libre, 2014)*

Marques Filho et al. (2008) designed a new device for RCC sample manufacture to simulate actual site conditions. The apparatus was composed of a rail system on which a roller-compacting structure moved. In an area at the center of the rails there was a pit into which a mould was fixed. The mould remains entirely below floor level. The apparatus basically comprises three systems: one for horizontal movement, another for vertical movement, and a third for load application. The device is shown in Figure

3.2.

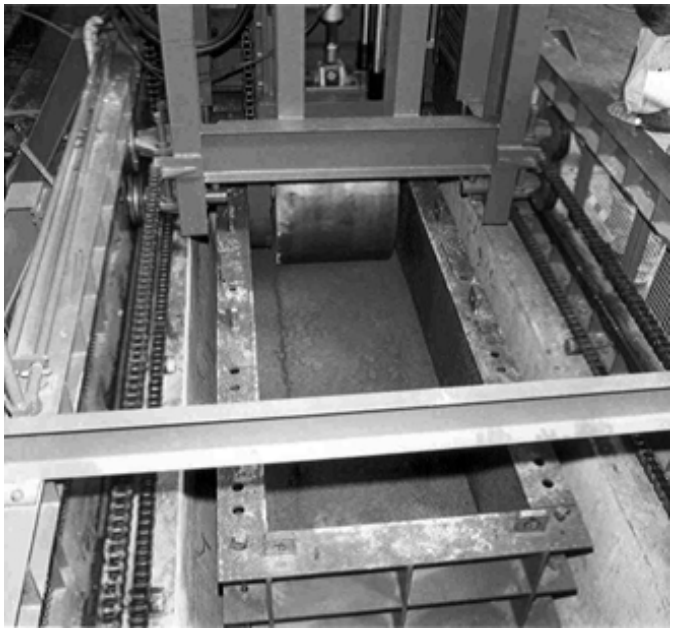

Figure 3.2: *General view of apparatus at setup stage (Marques Filho et al., 2008)*

Furthermore, Sarsam et al. (2012) created an apparatus that was designed to simulate a steel roller of the type that is usually used on site for compaction. It compacted slab moulds with dimensions 380 x 380 x 100 mm. It consists of a steel skeleton with a solid cylinder 150 mm diameter, 360 mm in length and 15 kg in weight fixed between two ball bearings to allow movement of the roller during compaction as shown in Figure 3.3. The total weight of this apparatus was 24 kg. It had a container to load the standard steel roller with a weight up to 183 kg.

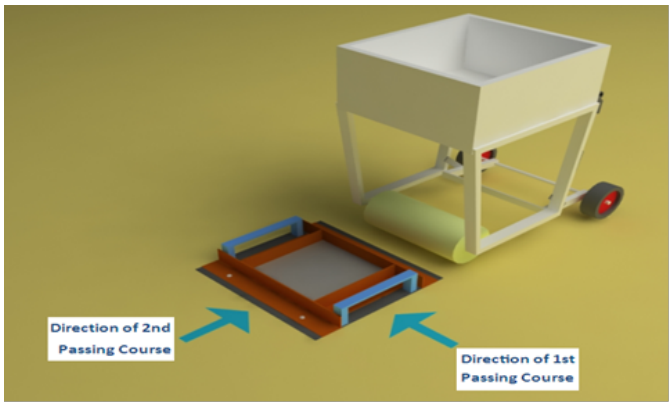

Figure 3.3: *General view of apparatus (Sarsam et al., 2012)*

In this research, the standard Cooper Research Technology roller compactor (asphalt slab compactor) has been used to compact loose material in order to allow the aggregate particles to bond with cement paste and achieve a target density in a manner similar to the compaction process in the field. Unlike the previous methods, the roller is actively processed against the sample until the desired density is achieved. The slabs that are produced measure 305 x 305 mm. Figure 3.4 illustrates the roller compaction machine.

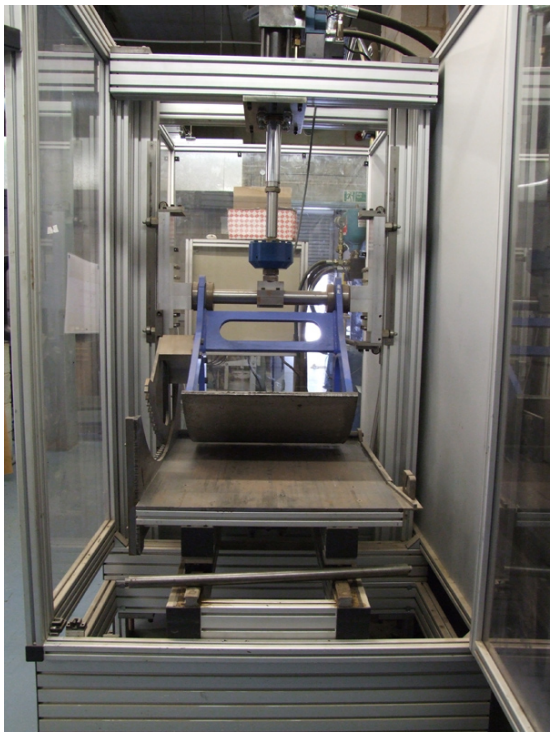

Figure 3.4: *The machine of roller compactor –steel roller*

3.3 Experimental work

This section summarizes the experimental work carried out on two-layer roller compacted concrete (RCC) and describes the materials selection, characterisation and mix design methodology for the RCC pavements.

3.3.1 Material selection

Figures 3.5 and 3.6 show the aggregates used in this research.

Figure 3.5: *Granite aggregate*

Figure 3.6: *Limestone aggregate*

3.3.1.1 Aggregates

The aggregates used for this project were crushed limestone and granite since they are readily available in the UK, for fine and coarse aggregates. These aggregates are available in different sizes, namely 20 mm, 14 mm, 10 mm, 6 mm, dust and filler, chosen according to MCHW-800 (2009) and conforming to BS EN 14227-1:2013. The choice of granite aggregate for the upper layer depended on its high skid resistance and abrasion resistance, while the limestone is chosen as a cheap material with high strength for the lower layer. The gradation of each aggregate type and size are shown

in Figures 3.7, 3.8, 3.9 and 3.10 and they are compared with maximum and minimum values from the European specification. Tables 3.2 and 3.3 show the particle densities for each type and size of aggregate.

Table 3.2: *Particles densities of limestone aggregate*

aggregate size	Particle density of aggregate
20 mm	2.633
14 mm	2.067
10 mm	2.68
6 mm	2.427
Dust(0/4)	2.668

Table 3.3: *Particle densities of granite aggregate*

aggregate size	Particle density of aggregate
10 mm	2.83
6 mm	2.84
Dust (0/4)	2.8
Filler	2.7

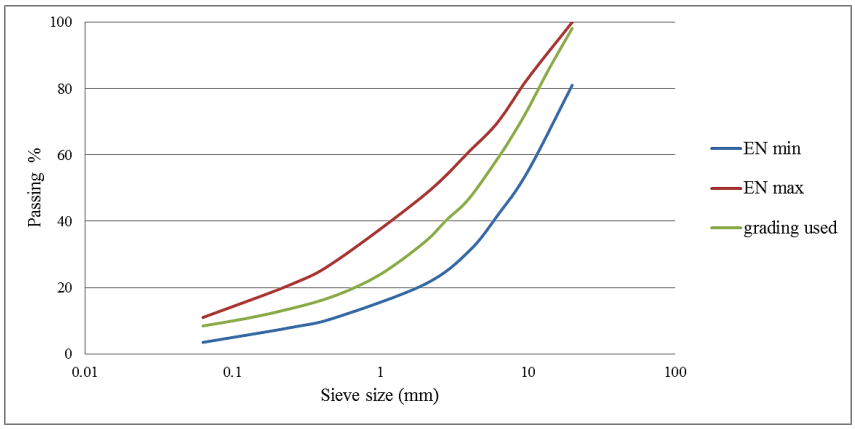

Figure 3.7: *Gradation of 0/20 mm combined limestone aggregate*

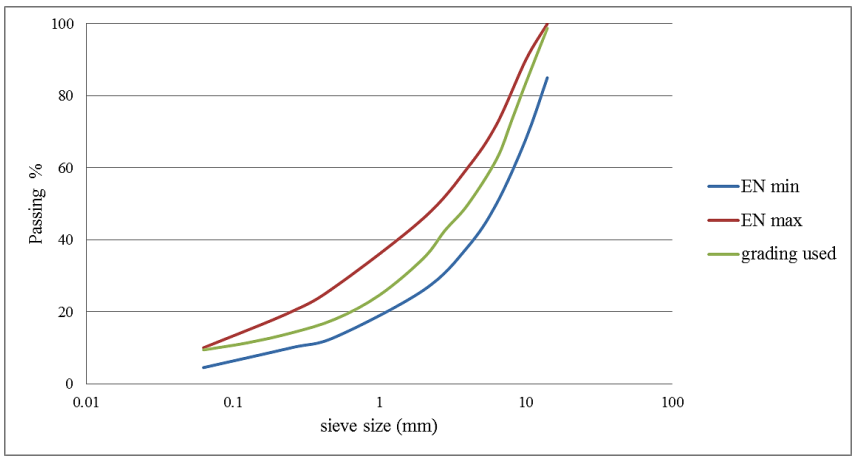

Figure 3.8: *Gradation of 0/14 mm combined limestone aggregate*

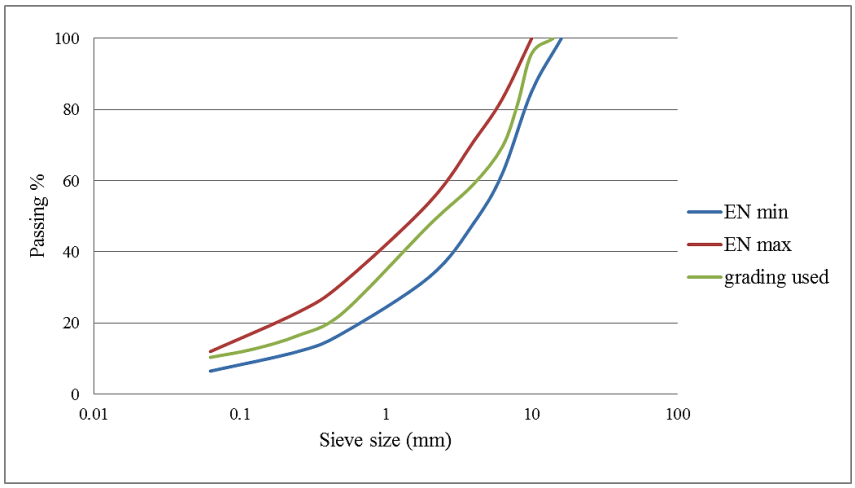

Figure 3.9: *Gradation of 0/10 mm combined limstone aggregate*

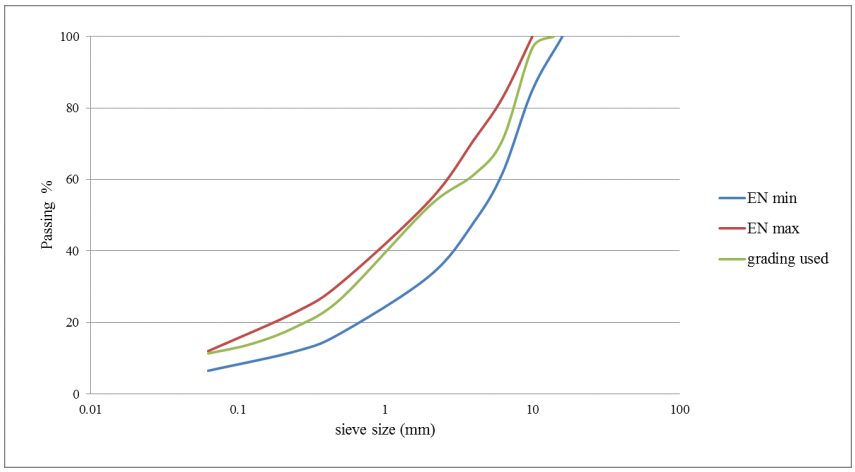

Figure 3.10: *Gradation of 0/10 mm combined granite aggregate*

3.3.1.2 Cement

The cement type used in this project was Portland cement CEM I- 42.5/52.5N conforming to BS EN 197-1 (2011) as the principal binder for RCC pavement. Table 3.4 shows its physical and chemical properties.

Table 3.4: *Physical and chemical properties of cement*

Physical properties	**Determined as**
Specific gravity	3.15
Fineness	420
Chemical properties	**Determined as %**
SiO_2	19.6
Al_2O_3	4.9
Fe_2O_3	3.1
CaO	63.1
MgO	1.2
SO_3	3.4
LOI	2.7
Chloride as C1	0.05
Alkalis as (Na_2O)	0.74

3.3.1.3 Water

Clean tap water was used throughout this work for both casting and curing of specimens.

3.3.2 Mix design methodology

The mixture of RCC in this research was designed according to the geotechnical approach by developing a relationship between the moisture content and maximum dry density. This will give an indication of the optimum water content in order to achieve maximum dry density. Also, it gives an estimated achievable density for the mixture. In accordance with ASTM D 1557, the test was completed with five moisture contents; 5%, 6%, 7%, 8% and 9% by mass, were chosen based on previous studies (Harrington et al., 2010; Marchand et al., 1997). Three percentages of cement were trialled within allowable limits for RCC, which were 10%, 12% and 14% by mass for each gradation.

The samples were prepared in steel cylinder moulds of 150 mm diameter by 116 mm height and 100 mm diameter by 116 mm height depending on whether the maximum aggregate size was more or less than 20 mm. After calculating the proportions of the materials, the empty moulds were cleaned and weighed. The materials were mixed for 1 minute, after which water was added and mixing continued until a homogeneous mix was obtained.

The next step was to compact the mixture with a modified Proctor hammer (4.5 kg) in five layers with either 56 blows or 25 blows depending on the size of the mould. The same procedures were done for each moisture

content and each percentage of cement. Table 3.5 shows the results of moisture content and dry density, and hence the optimum water content and maximum density were obtained, as shown in Figures 3.11, 3.12, 3.13 and 3.14.

Table 3.5: *Results of maximum dry density and water content for different cement content and aggregate size*

Cement content % (by dry mass)	Maximum dry density (gm/cm^3)			Moisture content % (by dry mass)		
	20 mm	14 mm	10 mm	20 mm	14 mm	10 mm
10	2.32	2.25	2.21	7	7.5	6.5
12	2.37	2.20	2.243	7	8	7
14	2.34	2.16	2.22	7	8	7.5

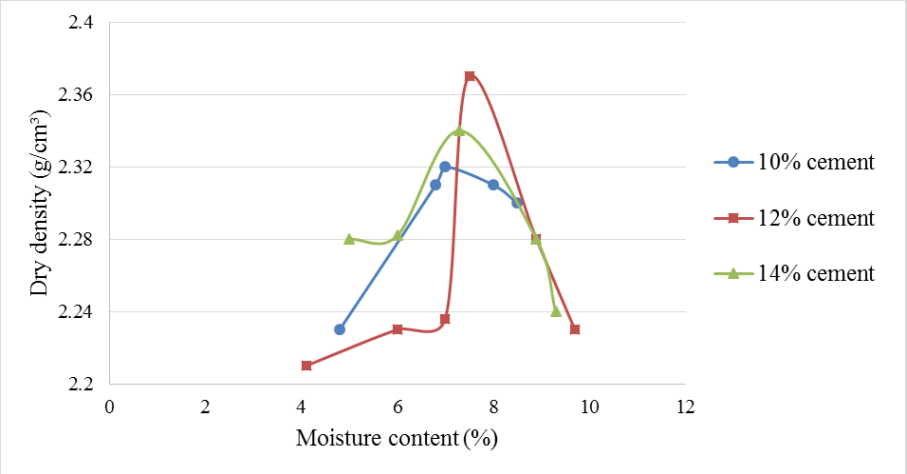

Figure 3.11: *The relationship between moisture content (%) and dry density (gm/cm^3) for 0/20 mm limestone aggregate*

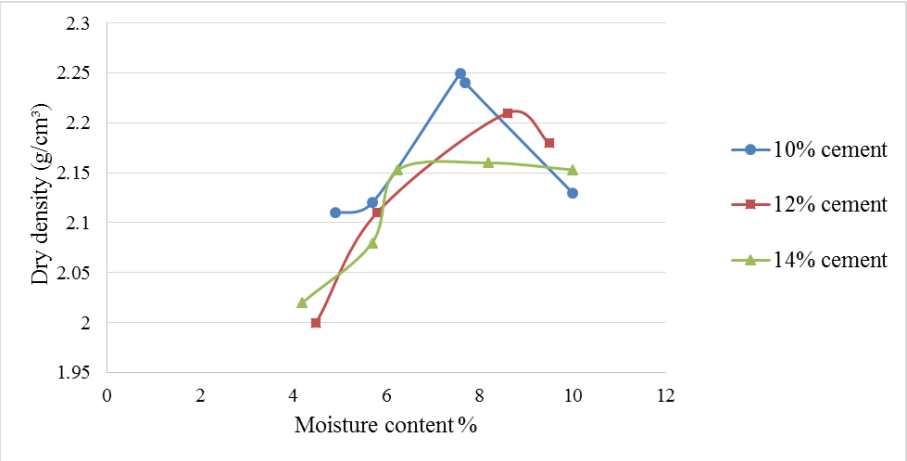

Figure 3.12: *The relationship between moisture content (%) and dry density (gm/cm^3) for 0/14 mm limestone aggregate*

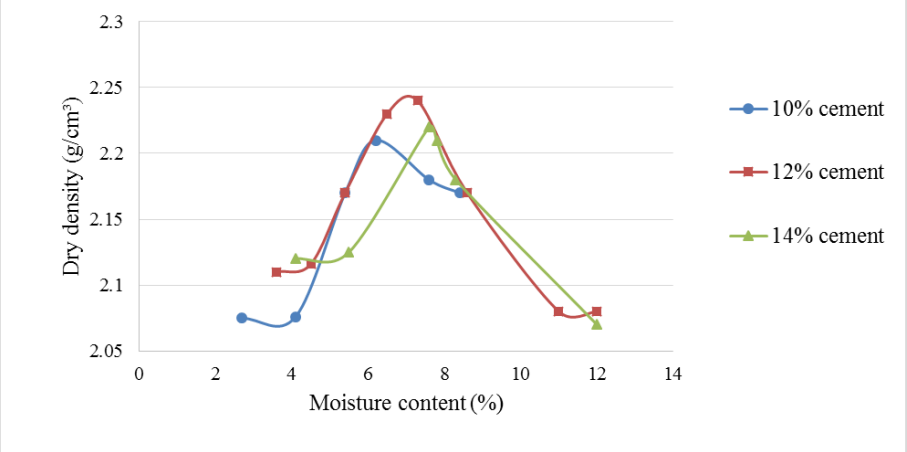

Figure 3.13: *The relationship between moisture content (%) and dry density (gm/cm^3) for 0/10 mm limestone aggregate*

The second stage, in the design of the RCC materials was to find the required cement content depending on the compressive strength. The materials were batched with three different percentages of cement 10%, 12% and 14%. Then, the dry mixture was mixed in the mixer as shown in Figure 3.15 and gradually the water was added in order to gain a consistent mixture. The next step was to fill the mould with the mixture. Slab specimens were then prepared as shown in Figure 3.16 with dimensions 305 x 305 x 100 mm^3 according to EN 12697-33:2013. The roller compactor compacted

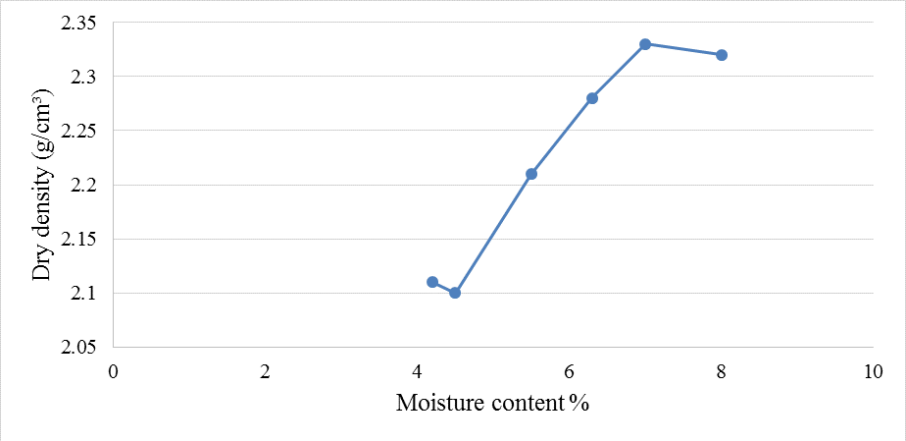

Figure 3.14: *The relationship between moisture content (%) and dry density (gm/cm^3) for 0/10 mm granite aggregate*

the mixture in two orientations to an approximate height of 100 mm, then the specimens were left in moulds for 24 hours before putting them in curing water. The slabs were then cured in water for 7 days before cutting them into cubes in order to test the specimens. Based on the results of the compressive strength test, suitable cement contents were chosen.

Figure 3.17 shows the results of compressive strength of RCC for different cement contents for both limestone and granite aggregates. It can be observed that increasing the cement content increased the compressive strength for different aggregate sizes and types, however, 10 mm limestone aggregate showed higher strength than 14 mm, this might be related to the proper compaction for the sample. The 10 mm granite present relatively similar strength to 14 mm limestone, this increased strength for the same aggregate size is a consequence of the higher strength of granite aggregate when compared to the limestone used.

Figure 3.15: *Mixing of materials in mixer machine*

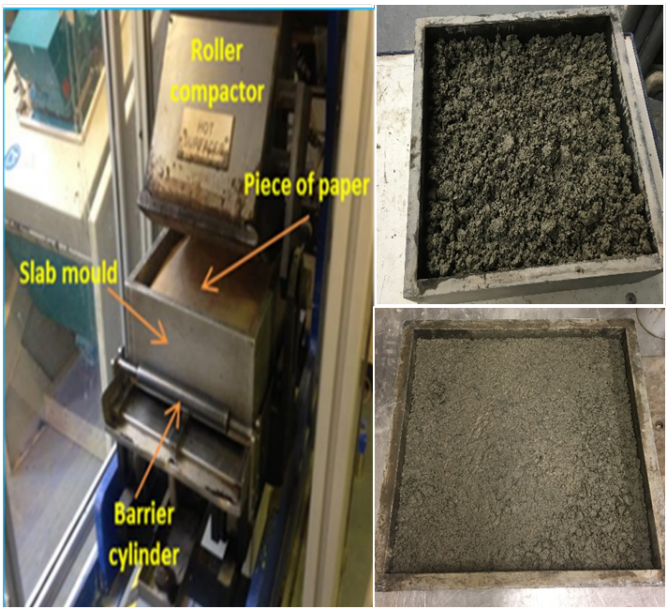

Figure 3.16: *Preparation of RCC samples by roller compactor*

In the Third stage, in order to prepare RCC samples for the different tests, the percentages of cement and water were specified as 12% and 7% respectively for all mix types as it gives acceptable strength, then the slab samples were prepared by roller compactor. However, for comparison purposes between different production methods, a set of samples was prepared

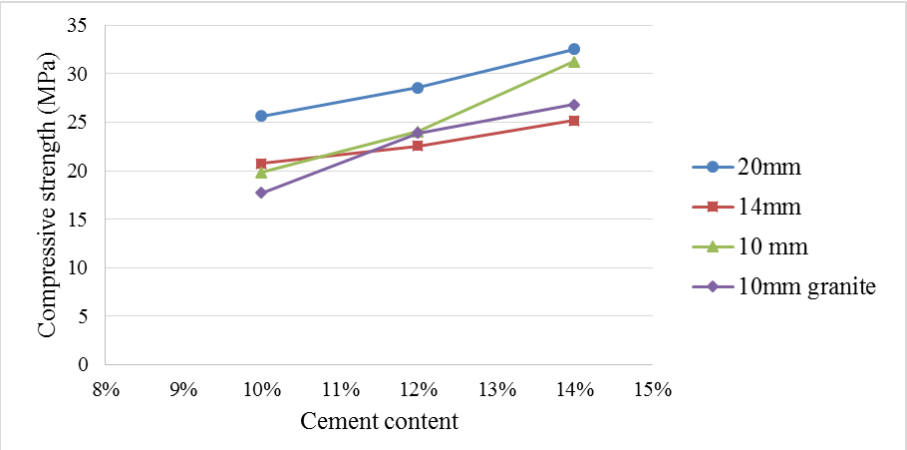

Figure 3.17: *Results of compressive strength for different cement contents and aggregates sizes*

by vibrating hammer as shown in Figure 3.18 in order to show the effectiveness of using the laboratory roller compactor.

Figure 3.18: *Producing samples by vibrating hammer*

In this research, two layers of RCC were produced together as well as separately, to evaluate the bond between these layers as a function of any delay that may happen during construction.

3.4 Properties of RCC for pavements

3.4.1 Density and Compacity

The density of the compacted mixture represents an important parameter that significantly affects its final performance. Density of RCC depends primarily on aggregate density and the degree of compaction (Fuhrman, 2000). It is very important to perform the compaction adequately. In the field, the density achieved also depends on the layer thickness and degree of support given by the underlying layer, and the compaction is normally specified to be not less than 95% of maximum density (Donegan, 2011; Thompson, 2001).

Density plays a significant role in the performance of RCC in both the laboratory and field. Williams (1988) reported that a 5% reduction in mixture density causes a 40-50% reduction in compressive strength of the mixture. There are different methods to check the density of RCC, whether on site or in the laboratory. In-place density of compacted RCC is determined by nuclear gage according to ASTM C 1040 and it should be checked at random locations, while in the laboratory, the maximum dry density can be measured according to ASTM D 1557 (ACI-309, 2000).

The density in this research was measured after curing of cubical samples cut from roller compacted slabs using the water displacement method. The method involves taking the sample weight in air and in water and then calculating the density using equation 3.1:

$$\rho_b = \frac{w_a}{w_a - w_w}.1000 \tag{3.1}$$

where ρ_b is the bulk density in kg/m^3, w_a is the weight of specimen in air and w_w is the weight of specimen in water.

The efficiency of compaction can be checked in different ways. In hydraulically bound materials (aggregate with cement binder), its effectiveness is commonly quantified by the term 'compacity', which means the ratio of achieved to maximum theoretical density. As soil mechanics principles are used here in RCC design, the effectiveness of compaction is also assessed by comparing the achieved dry density to the maximum dry density that can be achieved in the laboratory.

The compacity was calculated according to BS EN 14227-1:2013 using equation 3.2:

$$C = (\frac{\gamma_m}{100}) \times (\frac{a}{\gamma_A} + \frac{b}{\gamma_B} + \frac{c}{\gamma_C}...) \tag{3.2}$$

where C is the compacity, γ_m is the actual achieved density of the mixture and γ_A, γ_B, γ_C are particle densities of coarse aggregate, fine aggregate and cement, with percentages a, b, and c respectively.

3.4.2 Mechanical properties of RCC pavement

The following sections describe the testing procedure used to evaluate the mechanical properties of RCC for pavements. The mechanical properties of RCC depend on the amount of cementitious materials, water-cement ratio, quality of aggregates, and degree of compaction of the concrete. Gener-

ally, RCC pavements have compressive and flexural strengths comparable to those of conventional concrete pavements (Harrington et al., 2010).

The compressive and flexural strengths of RCC mixes are usually higher than those of conventional concrete with the same cement content especially at early ages. A flexural strength of 7 MPa at 90 days is readily achievable with good aggregate selection and grading (Donegan, 2011).

The compressive strength of RCC typically ranges from 28 to 41 MPa. Some projects (Harrington et al., 2010; Khayat and Libre, 2014) have reported that compressive strength could be higher than 48 MPa; however, practical construction and cost considerations would suggest increasing the thickness rather than the strength. The densely graded aggregates used in RCC mixtures have a significant influence on achieving high levels of compressive strength. Also, the low water-cement ratio of RCC mixtures reduces the porosity of the cement matrix which leads to a high compressive strength of the concrete. However, very low water-cement ratio will result in a dry mix that cannot be compacted thoroughly (Harrington et al., 2010; Khayat and Libre, 2014).

Adaska (2006) observed that the degree of compaction will affect compressive strength, where lower compaction increased voids in the matrix of the concrete resulting in decreased strength. This is because of its dry consistency, so the compaction of RCC requires more effort than conventional concrete while delays in compaction result in a decrease in compressive strength.

Tensile strength of concrete is an important property as it affects its brittleness (low tensile strength is associated with greater brittleness). Applying direct, uni-axial, tension is difficult because the brittleness of concrete will

often produce local failure at an end. Therefore, to evaluate and determine the tensile strength of the concrete, there are two different commonly used tests which are :

1. Flexural strength or modulus of rupture which is a significant parameter in designing both conventional concrete pavements and RCC. Fuhrman (2000) stated that the flexural strength of RCC depends on loading rate, moisture content, curing temperture and the age of RCC. Meanwhile, Khayat and Libre (2014) claimed that flexural strength depended on unit weight and compressive strength of the concrete mixture. They also found that the flexural strength of RCC ranged from 3.5 to 7 MPa.

Fatigue behaviour is influenced by the flexural strength of concrete because the most common critical stresses in RCC pavements are flexural. Therefore, using a dense mix can reduce the development of fatigue cracking and increase the flexural strength (Harrington et al., 2010; Khayat and Libre, 2014).

Moreover, Harrington et al. (2010) stated that the in situ flexural strength of RCC is difficult to obtain because of the shape of the specimens, where it is difficult to cut prisms samples from the field. Khayat and Libre (2014) noted that the ratio between flexural strength and compressive strength of RCC is about 0.15.

2. Indirect tensile strength or splitting tensile strength: This property is dependent on same factors that affected flexural strength, additionally, cementitious material, aggregate strength, the bond characteristics of the cement paste with the aggregate and the degree of compaction (Fuhrman, 2000).

Regarding the loading type on a concrete pavement, the tensile stresses

that are developed at the bottom of the pavement are induced by bending. Therefore, the flexural test is generally used for determining the tensile strength of RCC pavement instead of the splitting tensile test as it generates tensile failure in a similar manner to that found in the pavement. ACI-325.10R (2001) suggests that the splitting tensile strength of pavement RCC ranged from about 2.8 to over 4.1 MPa at 28 days depending on the cementitious content of the mix.

The modulus of elasticity expresses the ratio between the applied stress and strain in the linear region. It represents the propensity of a material to undergo reversible elastic deformation in response to a stress. The modulus of elasticity of concrete is influenced by the modulus of elasticity of aggregate in the concrete (Neville, 2011). Many studies indicate that RCC modulus of elasticity values are similar to or slightly higher than those of conventional concrete when the mixes have similar cement contents (ACI-325.10R, 2001; Fuhrman, 2000; Harrington et al., 2010).

Neville (2011) reported that ACI 318-02 recommended an equation to estimate modulus of elasticity of concrete as a proportion of the compressive strength using this formula:

$$E_c = 4.73\sqrt{f_c} \tag{3.3}$$

where E_c is the modulus of elasticity (GPa), and f_c is compressive strength of the concrete (MPa).

3.5 Results and discussions of properties of RCC

In this section, the test results are summarized in order to evaluate the test procedures and the properties of RCC for different aggregate size and types.

3.5.1 Density and Compacity

The results of density and compacity for two-layer RCC are shown in Figures 3.19 and 3.20 when using different compaction methods. It can be seen that the density of each layer is within the limits of the density requirement for RCC. The higher density for the mixture with limestone aggregate is related to well packed aggregate that leads to fewer voids to be filled by the cement paste. Where the air voids content in the mixture of limestone aggregate was about 1.61%, while for granite mixture was 2.69% ; these values are less than the optimum air content of concrete mixture as reported by Neville (2011). Also, the laboratory roller compactor delivered a dense mixture for the RCC. However, the vibrating hammer gave slightly higher density for both mixtures because of the combined effect of compaction and vibrating.

In addition, the compacity for both compaction methods is within the recommended limits and the difference between the vibrating hammer and laboratory roller compactor is between 1.9%-2.7% for both mixture with granite aggregate and mixture with limestone aggregate that confirmed to Parsons et al. (1992) investigation on different types of compaction machine. It can be concluded that using a laboratory roller compactor as a production method could give a dense mixture and acceptable compaction,

similar to field density and compaction.

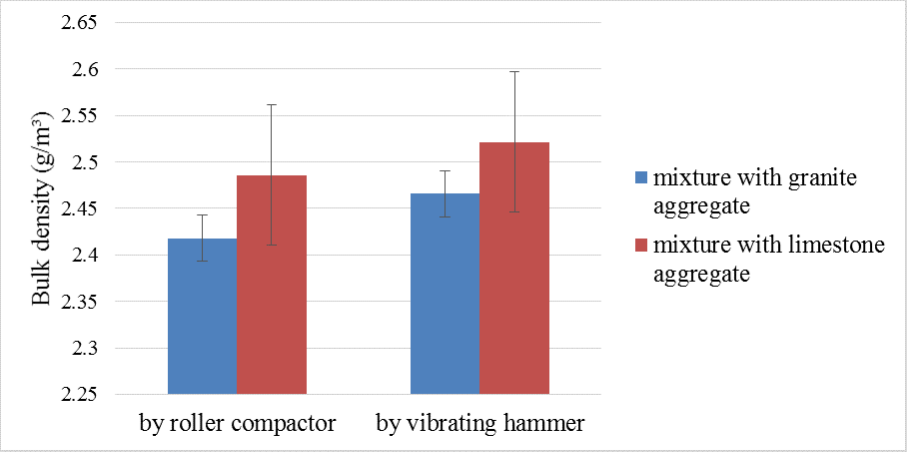

Figure 3.19: *Results of bulk density for the two RCC layers compacted by roller compactor and vibrating hammer*

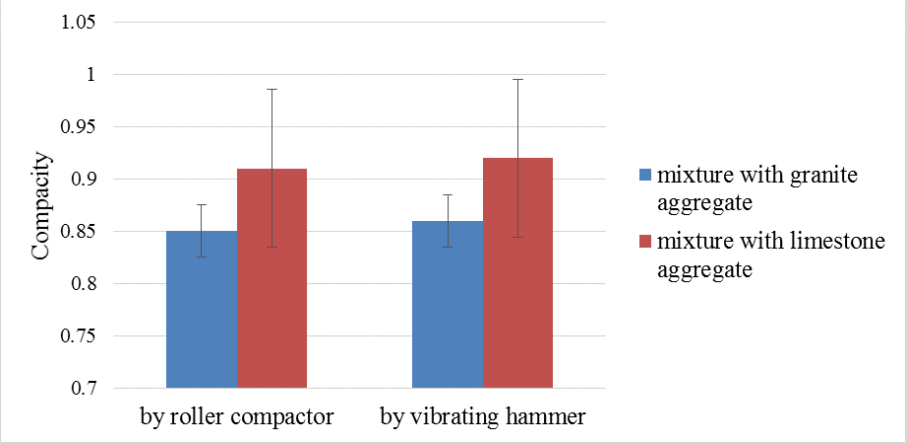

Figure 3.20: *Results of compacity for two layers RCC pavement compacted by roller compactor and vibrating hameer*

3.5.2 Compressive strength

Compressive strength is an important property of RCC that gives an indication about the mixtures load-carrying capacity and the durability of the mixture. It is influenced by the water-cement ratio, age of specimen, proper curing and the compaction effort.

The compressive strength of each layer was measured on 100 mm cubes in a Contest Instruments Limited machine with a capacity of 2500 kN, conforming to BS EN 12390-3:2002 as shown in Figure 3.21. The results of compressive strength tests are shown in Figure 3.22. In each mixture the mean of three measurements is plotted and error bars indicate the total range of the results.

It can be seen from these figures that the compressive strength of the limestone mixture is higher than that of the mixture with granite aggregate indicating that the limestone aggregate interacts better with the cement paste then increasing the compressive strength. Moreover, the vibrating hammer compaction method delivered a higher strength than the laboratory roller compactor as the vibrating effort reduced the voids and increased the density of the mixture. However, the laboratory roller compactor was shown to be competent and it delivered acceptable compressive strengths that were comparable to those of Harrington et al. (2010).

Figure 3.21: *Compressive strength machine test*

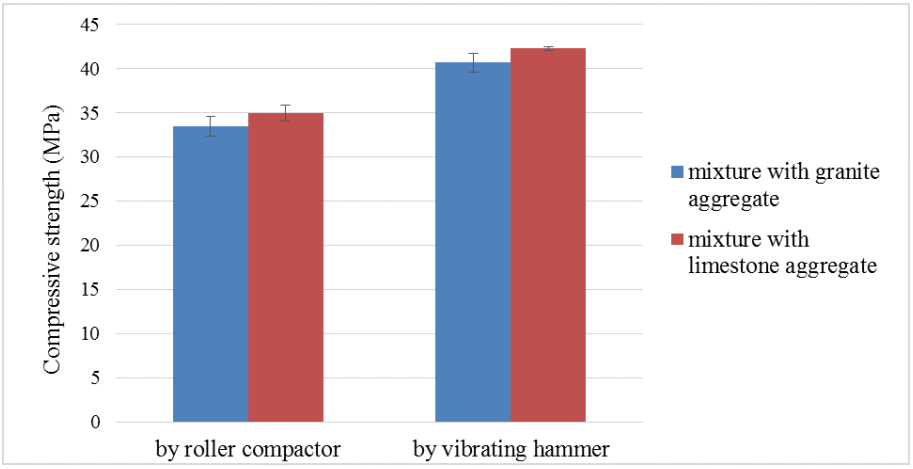

Figure 3.22: *results of compressive strength for the two layers RCC compacted by roller compactor and vibrating hammer*

3.5.3 Flexural strength

The flexural strength test was performed to determine the modulus of rupture and it was carried out in a Denison machine with capacity of 3000 kN as shown in Figure 3.23 in center point bending mode on prism specimens

with 100 x 100 x 300 mm dimensions where the prisms were cured for 28 days according to BS EN 12390-5:2009. Two rigid supports were located at each side of the specimen. The load was applied gradually at a rate 0.22 N/mm^2.s, and the failure load (P) was recorded. Flexural modulus of rupture, MR (MPa) was calculated using this equation:

$$MR = \frac{3PL}{2bd^2} \tag{3.4}$$

where P is the maximum load (N), L is the distance between the supporting rollers (mm), b is the width of the prism (mm) and d is the thickness of the prism (mm).

After testing three samples of each material and compaction method, the results are shown in Figure 3.24. The mixture with limestone aggregate and maximum size 20 mm had a higher flexural strength than the mixture with granite aggregate and a maximum size 10 mm. This can be explained in terms of the size of aggregate where the coarse particles act as crack arresters (Neville, 2011).

The laboratory roller compactor delivered a good and acceptable flexural strength for both two layers (although it is less than the value obtained by vibrating hammer). Thus, it is suggested, to simulate the reality of the field, to use the laboratory roller compactor to produce RCC samples.

Figure 3.23: *Flexural strength machine test*

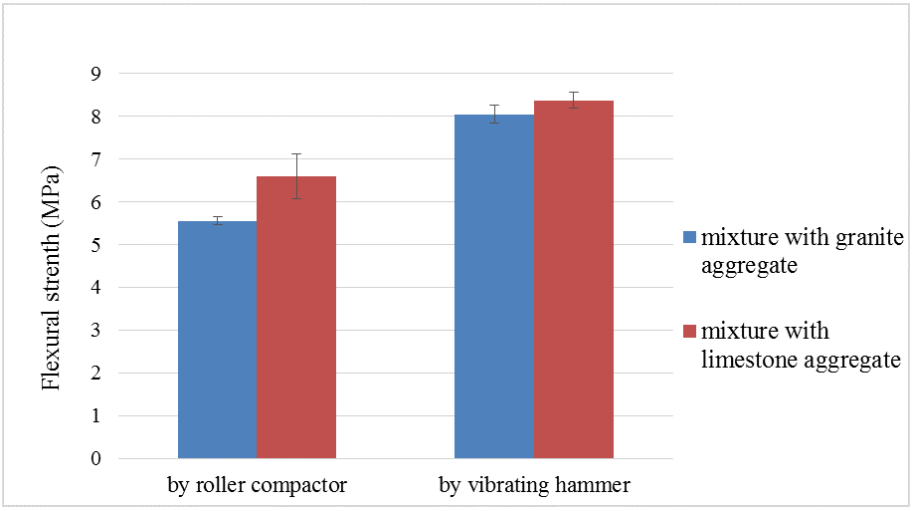

Figure 3.24: *Results of flexural strength for the two RCC layers compacted by roller compactor and vibrating hammer*

3.5.4 Indirect tensile strength

The structural properties of concrete such as shear resistance, bond strength and resistance to cracking depend on the tensile strength; the higher the tensile strength the better these structural properties (Babu, 2009).

Indirect tensile strength was performed at 28 days in accordance with BS EN 13286-42:2003. A 200 kN capacity Instron universal testing machine was used on cylinder samples with dimensions 85 mm diameter and 50 mm

Figure 3.25: *Indirect tensile strength test setup*

thickness as shown in Figure 3.25. The indirect tensile strength (ITS, in MPa) was calculated using the following equation:

$$ITS = \frac{2P}{\pi hd} \tag{3.5}$$

where P is the failure load (N), h is the thickness of specimen (mm) and d is the diameter of the specimen (mm).

The results of indirect tensile strength are presented in Figure 3.26. It can be observed that the lower layer of RCC with limestone aggregate has a higher indirect tensile strength, whether using the vibrating hammer or the laboratory roller compactor, than the lower layer with granite aggregate and the same compaction method. The higher indirect tensile strength is also linked to the higher compressive strength. Using larger maximum size of aggregate was found to improve the strength and the stiffness of the mixture.

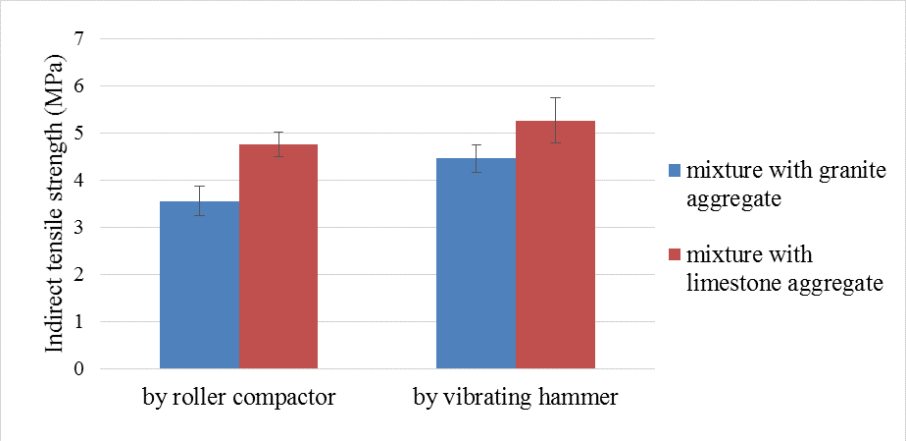

Figure 3.26: *Results of indirect tensile strength for the two RCC layers compacted by roller compactor and vibrating hammer*

3.5.5 Modulus of Elasticity

Modulus is normally considered jointly with the ITS value to classify a cement-bound mixture as specified in BS EN 14227-1:2013. This evaluation was performed in parallel with the ITS test in according with BS EN 13286-42:2003 by measuring the lateral deformation of the samples for each applied load as shown in Figure 3.27.

The static modulus of elasticity should be computed based on a load that is 30% of the ultimate indirect tensile load and its corresponding lateral deformation. However, estimating modulus of elasticity utilizing the formula provided in the latter specification (BS EN 14227-1:2013) would give inaccurate results since this formula is derived and used for a specific LVDT arrangement in which both LVDTs are mounted diametrically opposite to each other. Accordingly the following formula was used as provided by Solanki and Zaman (2013).

$$E = \frac{2P}{\pi.d.t.\Delta H_T(D^2 + D_g^2)}[(3+\upsilon)D^2.D_g + (1-\upsilon)D_g^3 - 2D(D^2 + D_g^2)tan^{-1}(\frac{D_g}{D})] \qquad (3.6)$$

where: E = modulus of elasticity (GPa); P = load (N); D = diameter of sample (mm); t = sample thickness (mm); ΔH_T = lateral deformation; D_g

= LVDT gauge distance (mm); and υ = Poisson's ratio.

The results of the modulus of elasticity are summarized in Figures 3.28

Figure 3.27: *Modulus of elasticity testing configuration*

and 3.29. It can be concluded that the two layers with different aggregate sizes and types have a similar stiffness despite the different methods of compaction and they conformed with ACI-318 results. Thus, stiffness appears to be less sensitive than strength to void content and aggregate size.

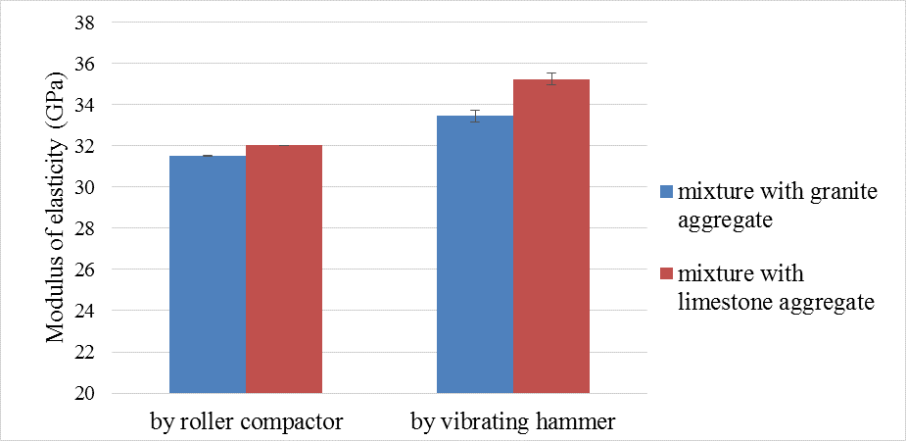

Figure 3.28: *Results of modulus of elasticity for the two RCC layers compacted by roller compactor and vibrating hammer*

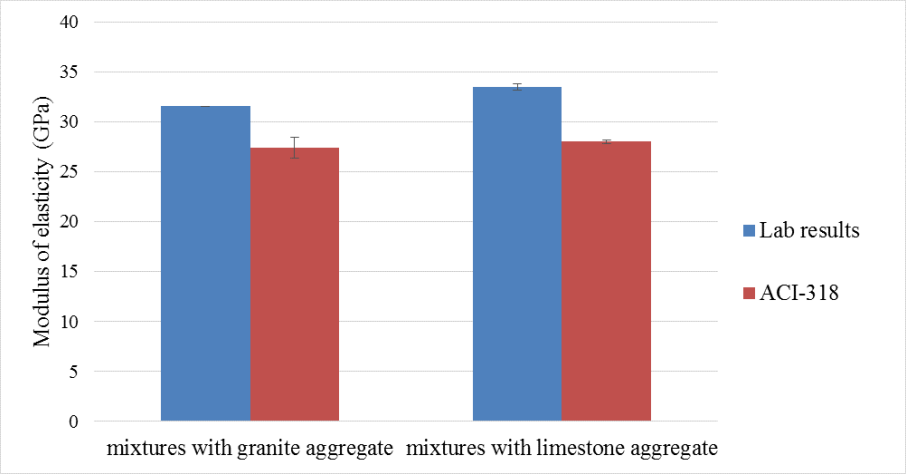

Figure 3.29: *Results of modulus of elasticity for the two RCC layers compacted by roller compactor compared to ACI-318 equation*

3.6 Summary

This chapter has presented the production of RCC for pavements with regard to mix design methodology; then the materials that have been used have been evaluated with two types of compaction. The initial properties have been investigated with regard to density and compacity and mechanical properties.

There are various methods to design RCC mixture for pavements. The

geotechnical method appears to be the best approach as it develops the relationship between maximum dry density and optimum water content which reflects the likely content parameters in situ. Therefore, it is recommended by different specifications for highways and roads.

Selecting appropriate materials for the RCC mixture plays a significant role in the performance of RCC in the pavement and, also, the production method has an effect on the properties of RCC. The different types and sizes of aggregates that were chosen in this research are designed to produce a two-layer system of RCC that has a capability to be used in wider application by improving the skid resistance and evenness of RCC surface. Moreover, it can be concluded from the results presented that the two mixtures have sufficient density and strength to be used in any pavement with acceptable performance and that the laboratory roller compactor provides an appropriate and adequate mass of forming specimens.

Chapter 4

Two layer RCC for pavement system

4.1 Introduction

Multi-layer pavement systems are normally used for high speed road applications. Two lifts in construction means placing two layers with different properties for the purpose of reducing noise, increasing skid resistance and lowering costs by using low cost materials for the lower layer and high quality material for the surface layer. Rao et al. (2013) states that there are two types of multi-layer pavement, hot mix asphalt (HMA) with a concrete base (PCC) (HMA/PCC) and a thin layer of concrete (PCC) on top of a thicker concrete layer (PCC) (PCC/PCC).

The use of two-layer systems for concrete pavements has been common practice for a long time as this method gives good performance, low cost and can provide better skid resistance. The next paragraphs will present the historical development of using two lifts in pavements in different regions.

Two-layer concrete pavement construction is an old technique. Historically, the first US concrete pavement was constructed in 1891 in Bellefontaine,

Ohio. It consisted of a two-layer system (Rao et al., 2013). After that, in 1915, two streets in Wisconsin in the US were constructed by the same process, where the bottom layer was constructed from locally available dolomite limestone rock, while the top layer used quartzite rock for the first street and granite for the second street (Cable et al., 2004).

From 1950 to the mid-1970s, two-layer PCC became common in the United States, where the typical construction practice placed the full PCC slab as two homogeneous half-slabs with wire mesh reinforcement between them (Tompkins et al., 2009).

From 1970 to 2000, the concrete paving industry moved from a mesh reinforcement design to a plain pavement design, with or without dowels, based on traffic volumes. Eliminating the mesh and shortening panels from as much as 30 m to 4.6 m or 6 m pattern eliminated the need to pave with a two-lift process (Cable et al., 2004).

The High Performance Concrete Pavement (HPCP) project was aimed at developing experimental two-layer PCC sections in the 1990s in Michigan and Kansas. These sections were made in order to better understand two-layer PCC and its performance, economy, manner of construction and ability to accommodate innovative designs and materials (Tompkins et al., 2009). Grove and Taylor (2010) reported a number of test sections in the west of Abilene, Kansas in 2008. They observed that the two-lift paving process was found to be a very practical approach that worked well with the paving methods and equipment employed by United States contractors. Figure 4.1 shows this paving operation in progress.

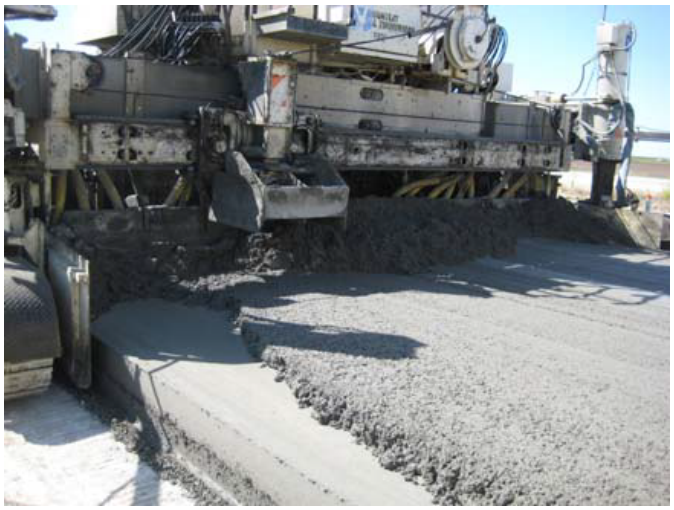

Figure 4.1: *Two-lift Concrete Pavement Construction, Salina County, Kansas, 2008 (Grove and Taylor, 2010)*

Two-lift concrete pavement construction has also been used in a number of European countries since the 1930's. In the European Union, two-layer PCC paving construction has been utilized for structural, economic, environmental, or safety reasons much more commonly than in the United States (Tompkins et al., 2009). Austria in particular uses this method as their standard method of concrete pavement construction. A significant research effort has been devoted to improve construction techniques and to use recycled materials, for example, aggregates (Grove and Taylor, 2010). In France, continuous reinforced concrete pavement was placed on two traffic lanes of a highway using a two-layer system. The bottom layer, which was greater than 5 cm thick, used local limestone aggregates. The top layer of this pavement, about 5 cm thick, was made up of harder aggregates. These aggregates provided low noise and high friction for the pavement surface. Therefore, using the two-lift method reduced costs less because it required less expensive concrete over most of the pavement thickness while still obtaining the desired concrete surface (Cable et al., 2004).

In addition, in Germany, Munich airport was paved using the two-lift method. The bottom layer thickness was approximately 24 cm and used local gravel as an aggregate. The top layer thickness was 14 cm and used crushed granite as an aggregate. The same two aggregates were used for the two layers of an Autobahn project in Berlin (Cable et al., 2004). In this way the overall cost was kept low by limiting use of the high quality, and more expensive aggregate to the surface layer.

Two-layer paving is mainly a wet on wet process where the surface layer is placed over the lower layer while the concrete is still wet. The placement of the surface lift is scheduled when the bottom layer is stiff enough to resist the mixing of the materials but sufficiently wet to get a good bond to form a monolithic concrete structure. The time of placing of the upper layer is generally within one hour (ACI-325.10R, 2001).

Tompkins et al. (2009) state that the upper layer of a two-layer PCC pavement must contain high quality, highly durable aggregate in order to improve the surface texture and act as a safe (frictional) and quiet roadway. Also, he suggested in the United States that the maximum size of aggregate for the upper layer should be between 8 mm and 11 mm to keep noise to a minimum while providing excellent skid resistance.

With regard to the benefits of a two-layer system, the most important benefit is that the design of the top lift can improve skid resistance. A part from reducing the need for hard and costly aggregate to be used throughout the pavement. Another important advantage of a two-layer concrete pavement is that the second paver only has to place a limited amount of concrete, so that a higher degree of evenness can be obtained (Hu et al., 2014).

In summary, two-layer systems have been used around the world as an effective method to get better serviceability of pavements, reduce noise, increase skid resistance and lower costs. Therefore, the necessity of understanding this technique becomes obvious for alternative concrete pavement types such as roller compacted concrete (RCC) in order to expand the application of RCC for pavements.

4.2 Multi-lift considerations for RCC

Multiple lifts are routinely used for RCC pavements when the thickness is more than 250 mm to ensure adequate compaction of each lift and develop sufficient bond at the interface of the multiple lifts so as to be considered monolithic. This assumption is used in most RCC pavement design procedures. However, proper procedures need to be followed in two-layer systems to ensure that a good bond between lifts is achieved (ACI-325.10R, 2001).

The lower lift is typically compacted and kept moist until the upper lift is placed, which is generally recommended to be completed within 1 hour. When these recommendations can not be met due to unexpected delay, an interlayer bonding agent can be used to develop good bond between lifts such as a cement slurry or a sand-cement grout. When a slurry or grout is used, sufficient time should be allowed for the lower lift to gain sufficient strength prior to placing and compacting the upper lift (ACI-325.10R, 2001).

Adequate adhesion between the two layers is important because this bond will have to withstand heavy loads and also the stresses resulting from

freeze-thaw cycles, shrinkage, curling and temperature effects (Kreuer, 2006).

In addition, one of the main drawbacks of RCC pavement is the surface unevenness. Therefore, RCC is commonly used as a base layer for hot asphalt mixture or conventional concrete pavement because it reduces the surface thickness necessary and provides a good construction base. Thus, using RCC as a base layer in multi-layer systems can be cost effective for long term performance in highway, airport and heavy industrial applications (Harrington et al., 2010).

From the above, it can be concluded that RCC has proven to have a good performance as a base layer and it could also be a good choice for a two-layer system with wider applications in pavements, depending on factors such as mix design and material selection, evenness, good bond strength and good durability .

4.3 Bond strength properties of two-layer RCC for pavements

Bond strength at the interface of RCC lifts is a critical engineering property. The purpose of measuring the bond strength is to determine whether the multi-lift construction will behave as a monolithic layer or as partially bonded or unbonded lifts. Bonded lifts will carry heavier load than partially bonded or unbonded, and the interface layer should be at least 50% of the strength of RCC (ACI-325.10R, 2001).

Furthermore, the desired minimum bond strength can be determined depending on fatigue tests and freeze-thaw durability tests where these tests

will indicate the strength of the bond between layers required to withstand the stresses during its service life (Kreuer, 2006).

The two tests that express the bond strength of a two-layer system in this research, which are the shear bond strength and the tensile bond strength. In this research, three different cases with different RCC placement conditions have been investigated in order to evaluate the bond strength between layers and the effect of any delay that may happen during construction. In the first case, the two layers were placed within one hour. In the second case, the upper layer was placed three hours after the lower layer. In the third case, the upper layer was placed 24 hours after the lower layer.

4.3.1 Shear bond strength test

The shear bond strength test is used to evaluate the mechanical properties of an interface when tested on standard cubic shaped specimens. A simple shear test was conducted using an Instron hydraulic machine with Rubicon software to determine the shear strength of a two-layer RCC specimen. This test was carried out according to BS EN 12697-48:2013. The interlayer bond strength was measured by using a shear mould specifically designed for the shear strength test in this study as shown in Figure 4.2 and 4.3. The shear was applied at a rate of 20 mm/min and the resulting load was recorded to the nearest 0.1 kN. The test was stopped when the interface failed by rupture. Shear bond strength was calculated by dividing the maximum shear load by the cross sectional area of the interface as shown in Equation 4.1.

$$\tau = \frac{F_{max}}{A} \tag{4.1}$$

where τ is the shear bond strength , F is the maximum shear force and A is the cross sectional area of a specimen.

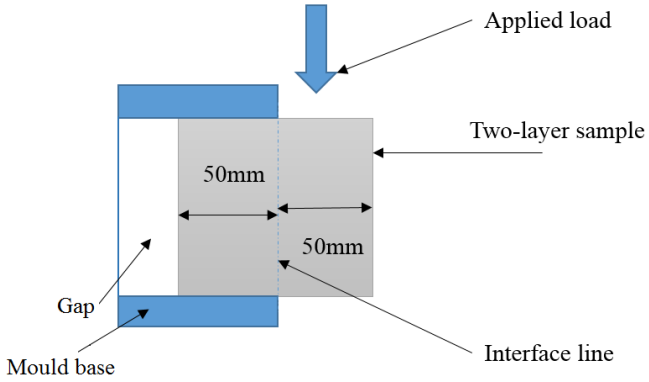

Figure 4.2: *Shear bond strength test configaration*

Figure 4.3: *Shear bond strength test*

4.3.2 Indirect tensile strength (ITS)

The ITS test involves applying diametric compression to 85 mm diameter and 50 mm thickness specimen at a constant deformation rate of 50 $\pm$ 2 mm/min to samples between two loading strips, which creates tensile

stresses along the vertical diametral plane causing a splitting failure. The test was conducted using INSTRON test equipment in accordance with BS EN 12697-23. Figure 4.4 shows the indirect tensile strength configuration where the load was applied vertically at the interface of the two RCC layers. The indirect tensile strength (ITS) was calculated as in Equation 4.2:

$$ITS = \frac{2P}{\pi DH} \tag{4.2}$$

where:

ITS = Indirect tensile strength

P = The peak load

D = The diameter of the specimen

H = The height of the specimen

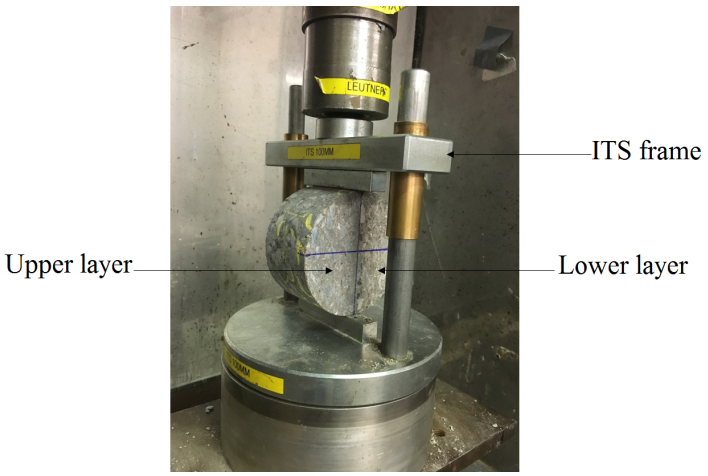

Figure 4.4: *Indirect tensile strength test*

4.4 Results of bond strength tests

Figures 4.5 and 4.6 show the results of shear bond strength and indirect tensile strength as an average of three samples for each test, where :
Case 1 the two layers were placed within one hour of each other.
Case 2 the upper layer was placed three hours after the lower layer.
Case 3 the upper layer was placed 24 hours after the lower layer.
Where these cases are chosen depending on specifications recommendations, field experience and some expectations for the worse case scenario.
The results of shear bond strength and indirect tensile bond strength show that the first and second cases which are wet-on-wet placements, have a reasonably good bond between the two layers. This means that the placement technique in a wet condition gives strong adhesion between layers.
Meanwhile the third case, which is a wet on dry placement condition (after 24 hours), had a low shear bond strength, showing that the dry surface of the bottom layer caused the adhesion with the top layer to be weak.
With regard to the indirect tensile strength of the two layers, the results clearly indicate a relatively similar indirect tensile strength for the first and second cases to the strengths of each layer separately. whereas the third case shows a considerably lower indirect tensile strength.

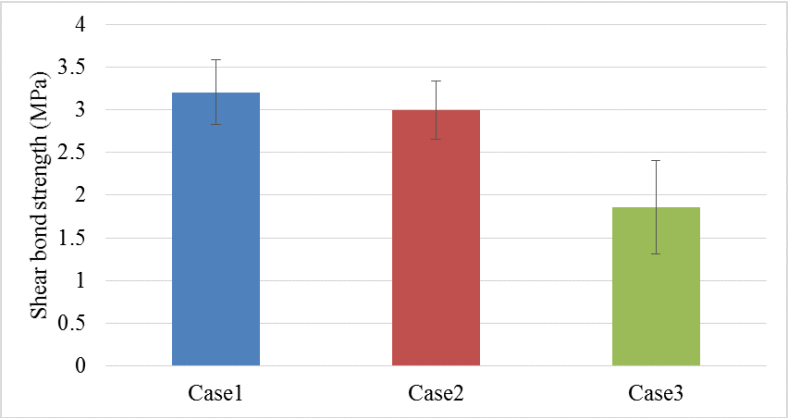

Figure 4.5: *shear bond strength test*

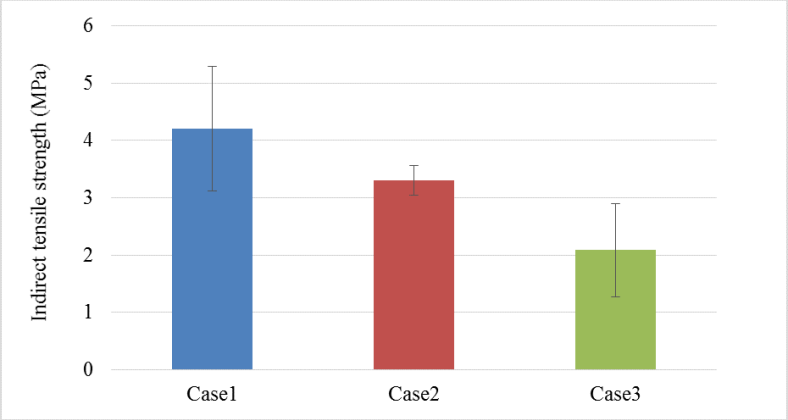

Figure 4.6: *Indirect tensile strength test*

4.4.1 Enhancing the bond strength

Given the weak bond observed where there was a 24 hours delay between layer placements, two methods were tried in an attempt to improve the bond strength of two-layer RCC when using wet-on-wet (Case 2) and wet-on-dry (Case 3) placement techniques.

1. **Using an inter-layer bonding agent such as cement mortar**

   This method is recommended by ACI-325.10R (2001) in any case of delay in placing the upper layer of more than 1 hour, to develop a good bond between two lifts. The mortar used in this research was

a conventional mixture with a 1:3 cement to sand ratio by weight as recommended by ASTM C 270.

Figures 4.7 and 4.8 show the results of shear bond strength and indirect tensile strength when using this cement mortar as a bond enhancer with the wet-on-dry placement technique (Case 3*) with an average of three samples for each test. It can be seen that there is some improvement; however, the improvement is not sufficient to achieve the same results as Case 1 or Case 2. The dry surface in Case 3 clearly limited the adhesion between the cement mortar and the upper layer resulting in less strength.

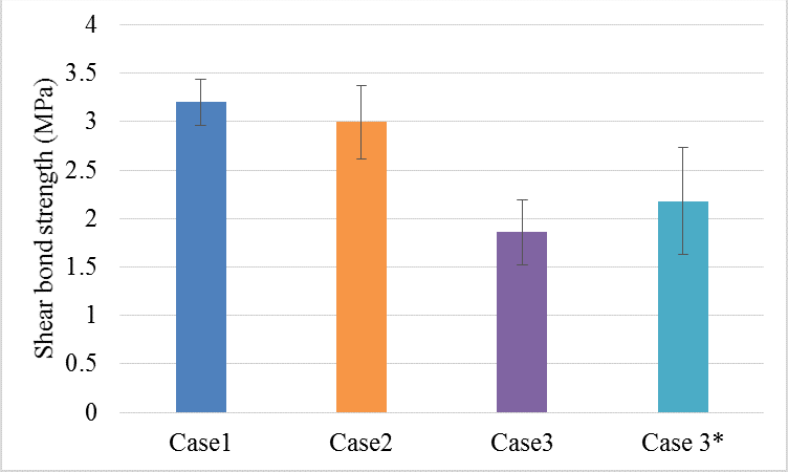

Figure 4.7: *Results of shear bond strength with inter-layer bond*

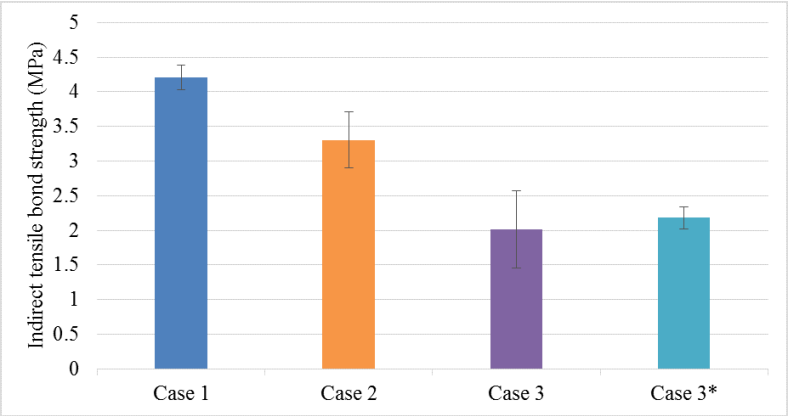

Figure 4.8: *Results of indirect tensile strength with inter-layer bond*

2. **Roughening the surface**

   Roughening of the surface is usually used with two-layer concrete to rehabilitate an old surface prior to overlaying with new concrete. Momayez et al. (2004) pointed out that the bond strength was improved with greater surface roughness.

   In addition, Knutson (1990) found that bond strength between old and new concrete is affected by the surface texture and moisture conditions of the existing concrete. In this study, the surface roughening was obtained by making longitudinal and transverse grooves across the surface while it was still unhardened (after approximately 1 hour) with a groove thickness of about 5 mm then scratching the surface as shown in Figure 4.9 for Case 2 (upper layer placed 3 hours after lower layer) and Case 3 (the upper layer placed 24 hours after lower layer).

   Shear bond strength and indirect tensile bond strength with a roughened surface showed strange results without any improvement for Cases 2 and 3 as shown in Figures 4.10 and 4.11. It can be seen that the shear bond strength for the roughened Case 2 is virtually the

Figure 4.9: *Stages of roughening the surface of the bottom layer*

same as the roughened Case 2 but for Case 3 the reduction reached about 60%. However, for the indirect tensile strength in Case 2, the roughening influenced the bond strength and decreased it by about 19% while for Case 3 is stayed the same without any improvement. It seems that roughening still requires more experience and knowledge in order to make the two layers connecting well and be more monolithic where any excessive roughening may increase the voids between layers as a result of poor connection thereby affecting the adhesion between the layers.

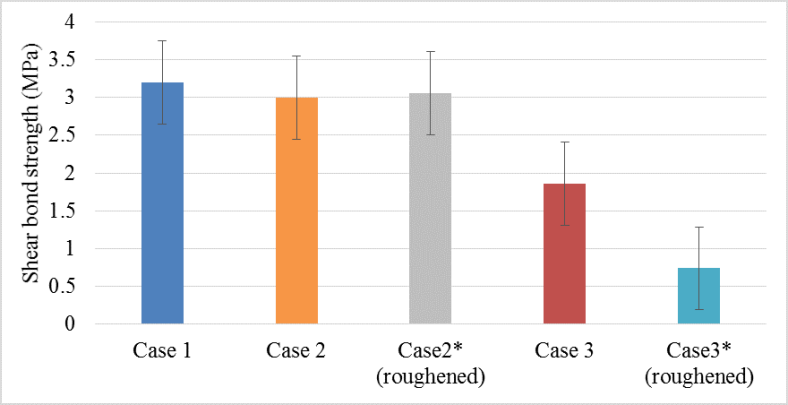

Figure 4.10: *Results of shear bond strength with roughening*

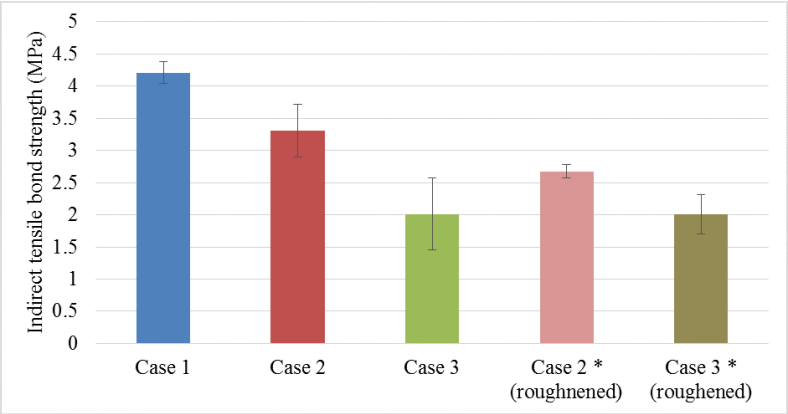

Figure 4.11: *Results of indirect tensile bond strength with roughening*

4.5 Durability characteristics of two layer RCC pavements

Durability is the ability of concrete to withstand a harsh environment. Durability of RCC is usually considered in terms of abrasion, erosion, or damage from freezing and thawing, but not often in terms of all three together.

The durability of concrete depends on its water permeability which is defined as "the property that governs the rate of flow of a fluid into a porous material under pressure". The permeability of concrete can be measured by determining the rate of water flow under pressure through the concrete. The porosity of concrete can significantly affect the permeability. In concrete, porosity mainly appears at the interface between the aggregate and the cement past where increasing porosity will affect on the bond between cement and aggregate and being a weak region for the durability of concrete (Mardani-Aghabaglou et al., 2013).

With regard to durability of RCC pavements against erosion and abrasion phenomena at heavy duty facilities such as log-storage yards and coal stor-

age areas, it can be observed that RCC has a good durability properties and no obvious wear deterioration under severe conditions. Erosion tests in test flumes have indicated the excellent erosion resistance of RCC. However, there have been conflicting results with respect to resistance of RCC to freezing and thawing (Saucier, 1994).

Furthermore, Halsted (2009) pointed out that RCC pavement has an excellent durability, both in terms of environmental effects, and the physical wearing caused by equipment operations. In some cases, if the pavement surface is not sufficiently bonded during construction, a small amount of wear will occur. However, this wear will stop and will not increase even after years of traffic and abrasion as indicated by various different experiences.

Nanni (1989) stated that concrete used as a paving material must possess an abrasion resistance adequate for the vehicle types and traffic of each specific application. Abrasion resistance is a surface property that depends primarily on surface layer characteristics. He also reported that cement content, water-cement ratio, type of finish, and curing affect the characteristics of the concrete surface layer. Furthermore, in order to achieve a high abrasion resistance, a high compressive strength is often specified.

On the other hand, ACI-116 (2000) observed that RCC needs some protection against deterioration due to cycles of freezing and thawing, such as air-entrainment to improve the durability of RCC in some pavements. However, if the RCC does not contain sufficient water content, proper air entrainment will be difficult to achieve.

Therefore, the ERMCO-Guide (2013) argues that RCC is similar to concrete block paving achieving its resistance to freezing and thawing cycles

by entrained air voids. However, the experiences on RCC showed that air entrainment is not normally needed, even in conditions where there is the potential for freeze-thaw damage. There are some reasons for this; firstly, the good freeze-thaw resistance of aggregates, secondly, sufficient amounts of fine material that gives a closed structure and thirdly, compaction of RCC as required by the specification.

Furthermore, Chun et al. (2008) found that a good resistance to freezing and thawing can be obtained through many factors such as using pug-mill mixing and using a dense, well compacted and high strength RCC. Also, they observed that the resistance to freezing and thawing cycles can be improved by using silica fume or by a combination of silica fume, super-plasticizer, and air-entraining admixture in RCC.

In addition, RCC pavements in cold weather are generally exposed to two types of damage caused by freeze-thaw cycles. These are internal cracking and surface scaling. These two types of damage may occur simultaneously. The internal cracking damage may happen when the RCC contains a large amount of moisture, which can affect the dynamic modulus of elasticity and lead to expansion or freezing. Also, when there is significant moisture in RCC surface scaling damage can occur during freezing and thawing cycles. Therefore, RCC mixes have to be designed to resist both types of attack caused by freezing and thawing cycles (Harrington et al., 2010; Khayat and Libre, 2014).

Harrington et al. (2010) reported that there are some important factors that should be considered for freezing and thawing resistance in RCC pavements:

1. Proper materials selection: where the type and quality of aggregate

might affect the freeze-thaw durability, it should meet the requirement in ASTM C33. The selection of well-graded aggregate will provide optimum compaction and maximum density in the field.

2. The quality and quantity of cement binder is important to provide sufficient strength and reduce the permeability.

3. The compaction of RCC to the maximum density and highest strength is needed to achieve durable RCC for pavements.

4. Curing of the pavement surface plays a significant role in the resistance of RCC to freezing thawing cycles by reducing the moisture loss from the surface and preventing drying.

4.5.1 Freezing and thawing cyclic test

Freeze-thaw damage is commonly observed on concrete paving blocks and road structures. The most common damage is cracking and spalling of concrete caused by progressive expansion of the cement paste matrix from repeated freezing and thawing cycles.

Testing of freezing and thawing cycles was conducted according to ASTM 666-procedure B. Each cycle consisted of freezing at $-20°C$ in air for 7 hours and thawing in water at $+20°C$ for 17 hours. Figure 4.12 illustrates one cycle of freezing and thawing.

Figure 4.12: *Freezing and thawing cycles*

4.5.1.1 Results of freezing and thawing cyclic test

The results of durability of two-layer RCC measured in the freezing and thawing (F & T) test, determined in terms of the shear strength after 5 cycles of F & T for each case, give an indication of good durability with a reduction in strength for the first and second cases of between 5 and 15%. In contrast, the third case showed poorer durability and the reduction reached 55% after exposure to 5 cycles of F & T. The reduction in durability for the third case suggests a weak and voided interface between the two layers. Figure 4.13 presents the results of shear bond strength before and after F & T cycling with an average of three samples for each case.

With regard to enhancing Case 3 with cement mortar, the results for shear bond strength after F & T cycling showed less deterioration of inter-layer bond, with the reduction reaching 34% as shown in Figure 4.14. However, roughening the surface for Case 3 showed more deterioration after 5 cycles of F & T and the reduction reached 46% as shown in Figure 4.15.

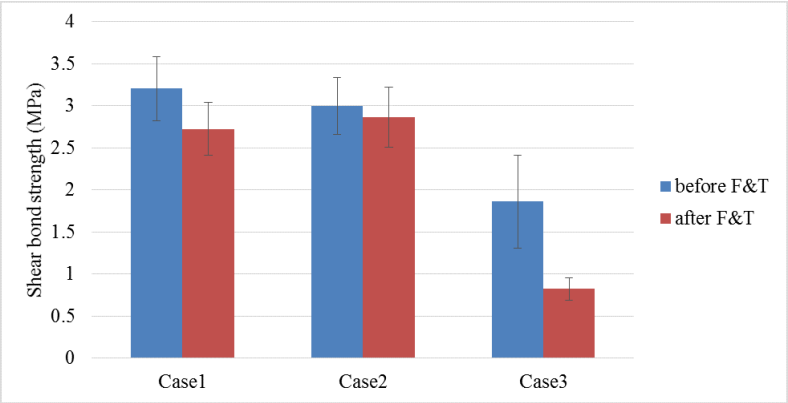

Figure 4.13: *Results of shear bond strength before and after 5 F & T cycles*

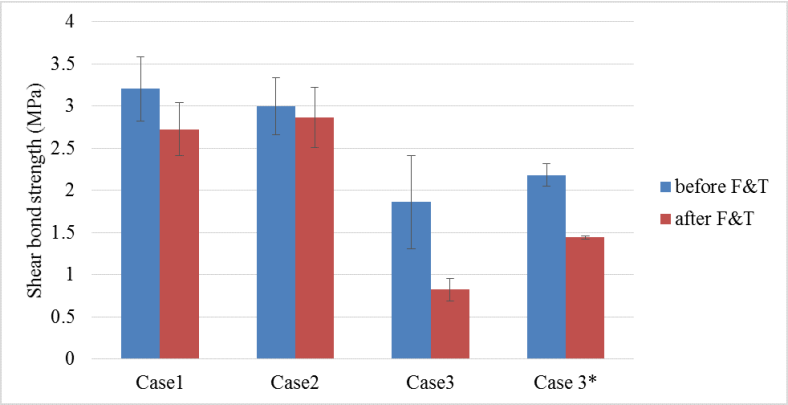

Figure 4.14: *Results of shear bond strength with bond layer before and after 5 F & T cycles using inter-layer bond*

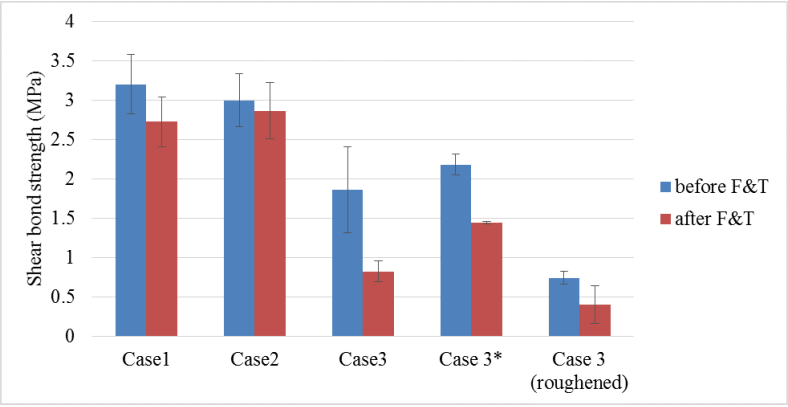

Figure 4.15: *Results of shear bond strength with roughening before and after 5 F & T cycles with roughening*

4.6 Summary

This chapter has introduced the concept of a two-layer system for concrete pavements and the feasibility of applying this technique to expand the ap-

plication of RCC in pavements. The benefits of using a two-layer system in pavements in terms of optimizing the skid resistance and minimizing use of relatively costly aggregates has made this technique preferable for conventional concrete paving in many countries.

Test results of two-layer systems for RCC showed good performance in terms of inter-layer bond strength, in particular for Case 1 (second layer placed within 1 hour) and Case 2 (second layer placed after 3 hours) with regard to both shear and indirect tensile strength.

For Case 3 (second layer placed after 24 hours) the results of shear bond strength and indirect tensile strength were poorer due to the dry surface of the bottom layer affecting the adhesion with the upper layer.

In addition, two methods of enhancing the bond were investigated, using a bonding layer and roughening the surface between the two layers in Cases 2 and 3. There was some improvement with a cement mortar bonding layer but a continuing poor bond with a roughened surface. Thus the cement mortar could be of some use if any delay occurs during construction.

The durability of two-layer RCC in terms of resistance to freezing and thawing cycles was good for Cases 1 and 2 . However, Case 3 showed less resistance to freezing and thawing cycles because of the voided interface that leads to weak adhesion between the two layers.

In conclusion, using a two-layer system of RCC for a pavement can give a good performance in terms of inter-layer bond increasing the possibility of using RCC in wider applications, but long delays between layer placement can bring problems.

Chapter 5

Surface characteristics of RCC pavement

5.1 Introduction

This chapter identifies the importance of surface characteristics for pavements. It describes surface properties for conventional concrete and roller compacted concrete (RCC) pavements in order to study the effect of using a two-layer system to reduce noise, improve evenness and increase skid resistance. It discusses ways of achieving high levels of these important characteristics in pavements.

5.2 Surface characteristics of rigid pavements

Surface characteristics are considered as a critical issue in pavements. For conventional concrete pavements, it has long been recognized that the texture of the surface directly influences friction and safety characteristics. Many methods have been developed to form and measure the texture of

pavement surfaces, and efforts have been made to correlate the textural properties with skid resistance parameters. Many of the accidents on wet highways are caused as a result of slippery conditions or lack of sufficient shear forces between tyres and pavement (Gallaway et al., 1971).

In general, the characteristics of the surface texture are defined according to the extent of microtexture, macrotexture, megatexture and roughness (unevenness), which have effects on the road functions such as the friction, tyre-pavement noises, splash and spray, tyre abrasion, rolling resistance and the ride quality according to the characteristics of the pavement texture in wet conditions as shown in Figure 5.1 according to World Road Association (PIARC).

Traditionally, the principal limitation to the wider use of RCC has been its texture, specifically the roughness of the surface. RCC is characterized by an uneven surface texture. The appearance of the surface texture is significantly affected by the aggregate size and type, where a smaller maximum size coarse aggregate will produce a finer pavement texture.

The use of a two-layer system could improve surface characteristics of RCC by using different aggregate sizes and types in the upper-most layer that can interact with vehicle tyres more effectively. This research has therefore evaluated the effect of surface properties, namely skid resistance and texture depth. In order to understand the importance of surface properties, a brief description of each property will be given for conventional concrete pavement and RCC. Figure 5.1 shows the relationship of pavement surface texture with different surface characteristics according to Cackler et al. (2006). Figure 5.2 identifies different scales of texture, explaining the details of texture length and depth according to HD36/06 (2006).

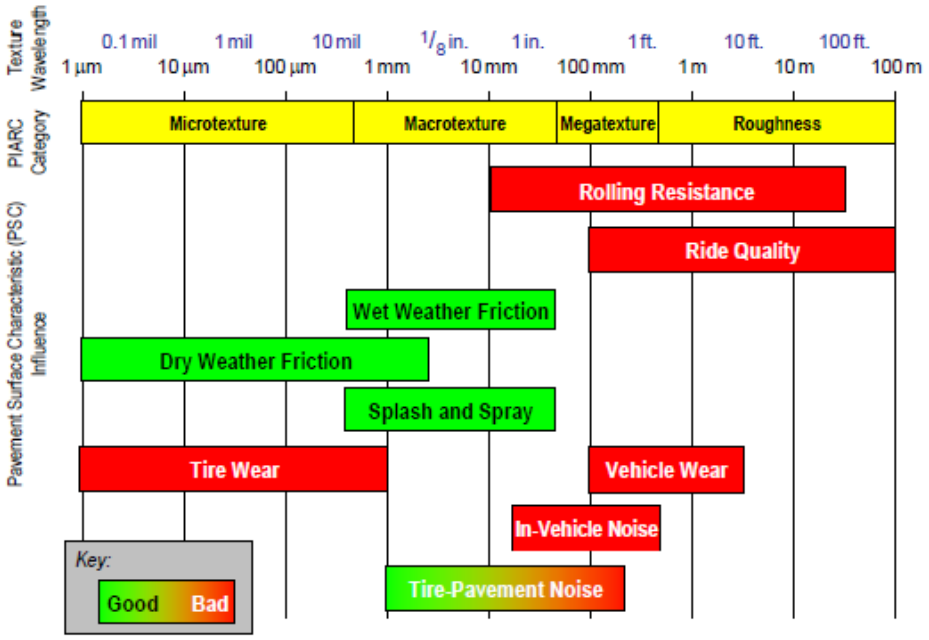

Figure 5.1: *The relationship of pavement surface texture with different surface characteristics (Cackler et al., 2006)*

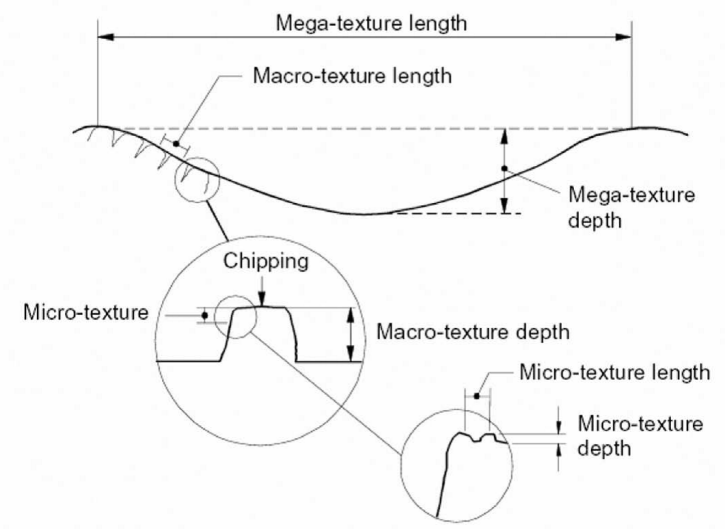

Figure 5.2: *Details of texture length and depths (HD36/06, 2006)*

5.2.1 Microtexture

Microtexture is the amplitude of pavement surface deviations from the plane with wavelengths less than or equal to 0.5 mm. It consists of irregularities that are often not readily visible. This includes texture from fine sands and the surface roughness on the aggregate particles themselves. Microtexture does not significantly contribute to tire-pavement noise at highway speeds, but it influences other surface characteristics, such as pavement friction (Cackler et al., 2006).

HD36/06 (2006) states that microtexture describes the roughness of the surface aggregate, which is associated with the crystalline structure of the coarse aggregate and the sand particles in the surface of a brushed concrete surface.

The fine scale microtexture of the surface aggregate is the main contributor to skidding resistance and is the dominant factor in determining skidding resistance at lower speeds (HD36/06, 2006). Microtexture is desirable because it provides adhesion, which is necessary for friction resistance. However, excessive adhesion may also increase noise (Cackler et al., 2006).

5.2.2 Macrotexture

The macrotexture of a pavement is an important category of texture because it is a primary contributor to pavement noise and other pavement surface characteristics including friction and splash and spray. The wavelength values of macrotexture are between 0.5 and 50 mm on pavement surfaces. Macrotexture can be produced by grooving, indenting or forming

small surface channels in the pavement surface (Cackler et al., 2006).

HD36/06 (2006) reportes that macrotexture provides rapid drainage routes between the tyre and the road surface and contributes to the wet skidding resistance at higher speeds. It also allows air trapped beneath the tyre to escape. Ergun et al. (2005) observed that macrotexture has a direct effect on skid resistance; the better the macrotexture, the smaller the slope of the friction coefficient speed function.

The texture depth is a measure of the macrotexture and is an important factor influencing skidding in wet conditions on high speed (> 65 km/h) roads. However, on lower speed roads, microtexture is the major factor in maintaining skid resistance, although texture depth is still important.

Figure 5.3 shows the differences between conventional concrete (PCC), hot mix asphalt (HMA) and RCC with regard to the surface macrotexture and it can be concluded that the RCC is less smooth than other types depending on the nature of the mixture used.

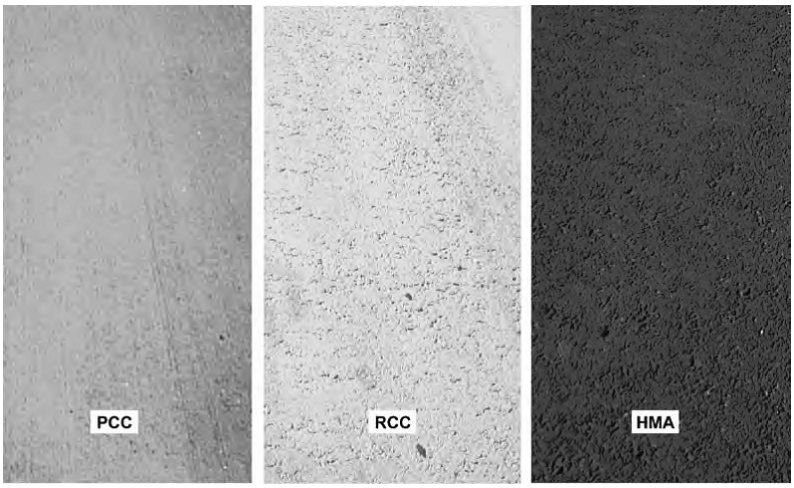

Figure 5.3: *Surface texture of RCC compared to conventional concrete (PCC) and asphalt (HMA) (Harrington et al., 2010)*

5.2.3 Megatexture

This represents the degree of smoothness of the surface, considered as an important surface characteristic for the travelling public. It is a primary measure of how comfortable a pavement surface feels to ride on. Megatexture is defined by wavelength values ranging from 50 to 500 mm. The variations in this level of the texture result from poor construction practices, surface deterioration or local settlements (Cackler et al., 2006).

HD36/06 (2006) observes that concrete surfaces laid with a slip-form or fixed form paver may have megatexture undulations caused by the paver. These arise from the natural irregularities of the paver method of working. Megatexture is undesirable, as it can be a major cause of tyre-pavement noise and noise inside the vehicle.

In conventional concrete pavements, this type of texture can be minimized through use of a transverse finishing screed in advance of a longitudinal oscillating float. The aim is to maintain the aggregate surface as close to a plane level as possible. The result will be improved smoothness and reduced noise (Cackler et al., 2006). On conventional concrete pavements, ride smoothness is also influenced by joints, warp or curl phenomena, faulting, load transfer devices or pavement surface distress.

Halsted (2009) observed that RCC pavements are not as smooth as conventional PCC pavements. In ports, this may be acceptable as, typically, RCC pavement operating speeds do not exceed 55-65 kph. In addition, Halsted (2009) determined the following steps that can be taken to improve the surface smoothness:

- Reduce the maximum size of aggregate.
- Use a two layer system when the pavement layers exceed 200 mm in

thickness in order to control the evenness.

• Use a high-density paver with string-line grade control and achieve compaction without excessive rolling.

Furthermore, Guyer (2013) stated that checking of the smoothness should be carried out immediately behind the finishing roller to avoid any excessive variations in the surface that would then need to be corrected with the finishing roller. He also observed that the megatexture across fresh and cold joints is a critical area for surface variations and a skilled vibratory roller operator can reduce smoothness problems.

5.2.4 Roughness

The structural performance of a road and ride quality are both related to the accuracy to which the various layers of material are laid. To achieve optimum performance within a given design, the aim should be to have an even surface profile and layers that are as uniform in thickness as possible (McLellan, 1982). Roughness (i.e. unevenness) is technically classified as texture with wavelengths of 500 mm.

Spielhofer (2007) reported that longitudinal evenness is an important influencing factor on road safety in terms of ruts and aquaplaning, ride comfort and on the durability of roads as well. Concerning the longitudinal eveneness of roads, three phenomena are generally distinguished:

• General unevenness

• Periodical unevenness

• Singular obstacles

Among the surface characteristics of a road pavement, evenness is probably the factor to which road users are most sensitive when it comes to assigning a level of quality to that pavement. Generally, roughness affects rolling resistance, vehicle wear, ride quality and pavement noise. Therefore, avoiding roughness helps enhance ride quality (Cackler et al., 2006). RCC pavements typically have a rougher surface (i.e. higher international roughness index, IRI), more like an asphalt pavement, than other concrete pavements . For this reason, it is typically used for lower volume and lower speed applications such as shoulders, parking lots, and local roads. It can also be used as a base for a composite pavement (ACI-325.10R, 2001).

The aim of measuring roughness and setting acceptable limits is to connect the requirements of the user with the technological capabilities in order to achieve good levels of evenness on the various types of road. The results of roughness measurements are mainly used to assess the quality of road works against specified criteria. Moreover, roughness criteria throughout the world can be expressed in terms of IRI (International Roughness Index) units. This reference scale was established to allow comparison of evenness measurements carried out with different instruments, and also for specified acceptability thresholds (Fuchs, 1991).

Fuchs (1991) concluded that to achieve good evenness in conventional concrete pavements the following principal factors should be taken into consideration:

1- A homogeneous mixture with suitable workability for the laying machines;

2- The guidance of the laying machines, including the setting up of forms or guide wires and the evenness of rolling paths;

3- Steady supply of concrete and proper distribution before the paver;
4- Regular progress of the paver without stoppage, at a speed adapted to the consistency of the concrete and conditions on the site;
5- The use of specific equipment to smooth out small irregularities behind the paver such as correcting beams and longitudinal mechanical floats.
Table 5.1 demonstrates the tolerance in surface levels of pavement courses and derived thickness tolerance for pavements in the UK according to Highways England (2016).

Table 5.1: *Tolerances in surface levels of pavement courses (Highways England 2016)*

Road surfaces -general -adjacent to a surface water channel	 ± 6 mm + 10 - 0 mm
Binder course	± 6 mm
Base	± 15 mm
Subbase under concrete pavement surface slabs laid full thickness in one operation by machines with surface compaction	± 10 mm
subbases other than above	+ 10 - 30 mm

5.3 Evaluating surface properties of concrete pavements

5.3.1 British pendulum test

The British pendulum tester is one of the simplest and cheapest instruments used in the measurement of friction characteristics of pavement sur-

faces. The British pendulum tester is operated by releasing a pendulum arm from a height that is adjusted so that a rubber slider on the pendulum head contacts the pavement surface over a fixed length. The pavement surface is usually wet to ensure that the surface voids are saturated. The difference between the initial and recovered pendulum heights is a representation of the loss in energy due to friction between the slider and the pavement surface. The pendulum test value is calculated as the mean of five swings (Alshareef, 2011; ASTM-E303, 2013).

The pendulum test was carried out in this research for the upper layer of RCC which incorporated granite aggregate with 10mm maximum size. The pendulum value from the test was 54.2 as an average of 5 swings. The temperature was fixed ($25°C \pm 3°C$) during the work to avoid any effect of temperature. This result gives an indication of acceptable skid resistance comparing to Kokkalis and Panagouli (1998) and Hosking (1992), which could allow RCC to be used in broader applications in pavements. Figure 5.4 shows the pendulum test in use on the upper RCC layer. Table 5-2 shows the minimum values of skid resistance as suggested by Hosking (1992).

Figure 5.4: *British pendulum test*

Table 5.2: *suggested minimum values of skid resistance numbers (Hosking, 1992)*

Category	Type of site	Minimum skid resistance value (wet surface)
A	Difficult sites such as: (i) Roundabouts, (ii) Bends with radius less than 150m on unrestricted, (iii) Gradients, 1 in 20 or steeper, of lengths greater than 100m, (iv) Approaches to traffic lights on unrestricted roads	65
B	Motorways, trunk and class 1 roads and heavily trafficked roads in urban areas (carrying more than 2000vehicles per day)	55
C	All other sites	45

5.3.2 Surface texture

The surface texture of a pavement influences various characteristics related to the tyre, including dry-weather friction, rolling resistance, and tire wear.

However, there are many features of the surface that will affect the texture of a pavement which are the combinations of texture depth (amplitude) and feature length, the contributions of aggregate texture and gradation, pavement finishing techniques, and pavement wear. Therefore, it is important to be able to classify pavement texture in order to explain the effect of pavement surface texture on pavement performance characteristics (Pidwerbesky et al., 2006).

In addition, for RCC pavement, Donegan (2011) suggested an approach to improve surface texture by increasing the cement content, reducing the maximum size of aggregate, using a high compaction paver and avoiding the over-use of steel drum rollers. Also, he recommended that surface grinding (groove forming) can be carried out to improve the macrotexture of an RCC surface if required.

Several volumetric methods are used to measure the surface texture such as ASTM-E965 which measures the mean texture depth of pavement macrotexture (MTD) by spreading a known volume of glass spheres and measuring the covered area. ASTM-E1845 (2001) states that there is a difference between the values of mean profile depth (MPD) and MTD due to the size of the glass spheres used in the volumetric technique and also the MPD is derived from a two dimensional profile rather than a three-dimensional surface. Figure 5.5 illustrates the mean profile depth computation according to ASTM-E1845 (2001).

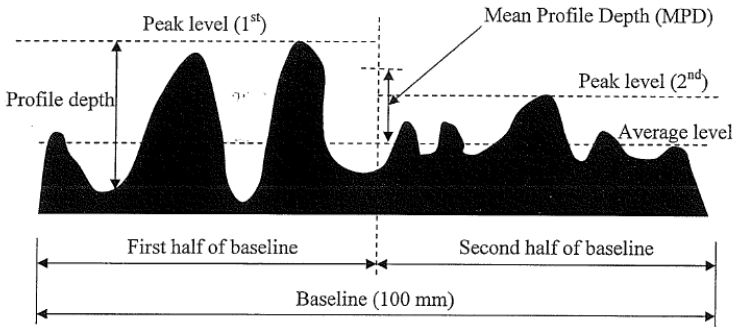

Figure 5.5: *Illustration of mean profile depth computation (ASTM-E1845, 2001)*

5.3.2.1 Texture depth test

The texture depth of the surface layer can also been evaluated by the sand patch test. The sand patch method determines the mean texture depth of pavement surfaces by applying and smoothing a known volume of sand grains to make a circle on the pavement surface in a similar manner to that of ASTM E-1845 described above. In this research, the sand patch test was carried out according to BS 598-105:1990 and Nicholls (1997) which defines the test as a measurement of the average depth of the road surface macro-texture below the general level of the peaks.

It is calculated for concrete pavements depending on this equation:

$$\text{Texture depth}(mm) = \frac{31,830}{D^2} \tag{5.1}$$

where D is the mean diameter of the sand patch in millimeters.

Table 5.2 presents grading and macrotexture depth requirements according to notes for guidance on the specification for highway works in UK MCHW-1000 (2016). The result of the mean texture depth for the upper layer of RCC in this research was 0.793 mm, obtained from the sand patch test as shown in Figure 5.6. From this result, it can be concluded that the upper layer of RCC with granite aggregate and maximum size 10 mm meets the

minimum limits for surface texture confirming to MCHW-900 (2012) as shown in table 5.3. It similarly meets the requirement of the Highways Department in China RD/GN/032 (2007).

Figure 5.6: *Sand patch test*

Table 5.3: *Retained Surface Macrotexture Requirements according to MCHW-900 (2012)*

Surfacing type	Average texture depth per 1000 m section, mm
Hot applied thin surface course systems with an upper (D) aggregate size of 14 mm	0.9
Hot applied thin surface course systems with an upper (D) aggregate size of 10 mm	0.8
Hot applied thin surface course systems with an upper (D) aggregate size of 6 mm	0.7
Cold applied ultra thin surface course systems produced using surface dressing techniques	1.0

5.4 Summary

This chapter has briefly described the surface characteristics of concrete pavement and RCC in terms of microtexture, macrotexture, megatexture and roughness. These are important pavement characteristics which need to be delivered at an appropriate level when using a two-layer system.

Surface properties are considered as a critical issue in pavements as they influence the serviceability of the pavement and affect the performance and safety of any pavement. RCC typically has a high international roughness index (IRI) that inhibits using it on highways and normal roads; however, using a two-layer system with smaller maximum size for the upper layer could improve the microtexture and macrotexture of the surface to a level suitable for many road pavement applications.

Furthermore, it can be seen from the result of the upper layer RCC that the skid resistance, which was evaluated using the British pendulum test,

showed a skid number for the upper layer that met the minimum requirements. Also, the results of surface texture were assessed in terms of texture depth, and these showed acceptable properties related to surface specifications when using 10 mm maximum size aggregate for the upper layer. These results suggested similar texture to asphalt pavement that could have similar level of noise to be considered in the design of surface layer according to HD36/06 (2006) design guide.

Chapter 6

Performance of two layer RCC under repeated load

6.1 Introduction

Sustainability of concrete pavements depends, in part, on the rate of pavement deterioration. Cracks, as the main reason behind deterioration of concrete pavements, are initiated at the top or the bottom of the concrete slab and they then propagate through the concrete due to fatigue action (Darestani, 2007). Normally, highway mixtures are characterized under repeated load, while conventional concrete mixtures in constructions is may be assessed under static load.

Concrete cracks when the tensile stress is equal to the tensile strength of the concrete. In fact, the tensile strength is defined as the magnitude of tensile stress which causes the concrete to crack. Concrete can also crack when subjected to repetitions of tensile stress of magnitude less than the tensile strength, which is called fatigue cracking. Both of these mechanisms of cracking are important in the consideration of concrete pavement

thickness design and joint spacing (Pittman, 1994).

Therefore, this chapter investigates the performance of two-layer RCC in a pavement under cyclic load to understand the behaviour of two-layer RCC with different aggregate sizes and types in the two layers and different placement conditions. This chapter includes determination of fatigue lines and equations and the performance of two-layer RCC under cyclic shear load in order to obtain a load transfer stiffness.

6.2 Fatigue of concrete pavements

Generally, the usual stresses caused by a single load are less than the strength of the material; however, repetition of these loads will slowly damage the material over time and eventually result in fatigue failure (Harrington et al. 2010).

Li et al. (2007) stated that fatigue failure occurs in concrete pavements when exposed to a large number of cycles with a stress less than the design load. They defined fatigue as a 'process of progressive and permanent internal damage in a material subjected to repeated loading'. The exposure to repeated flexural loading reduces the stiffness of the pavement which leads to the propagation of internal microcracks resulting in fatigue failure.

There are various parameters that influence the fatigue performance of a concrete pavement such as loading conditions, load frequency, stress level (stress ratio), number of cycles, type of mixture, environmental conditions and mechanical properties. In addition, the flexural fatigue of plain concrete is affected by the water–cement ratio, where the fatigue strength is

decreased for a low water–cement ratio in the concrete (Li et al., 2007). Ameen and Szymanski (2006) argued that fatigue failure is caused by the deterioration of the bond between the coarse aggregate and the paste matrix. Antrim (1965) reported that fatigue failure in plain concrete is based on small cracks that are formed in the cement paste and this results in weakening of the mixture bond until it cannot sustain the applied load. Therefore, it can be concluded that fatigue in concrete is based around microcracks. Some of these may be formed due to local strains that develop under loading due to incompatible stiffness between the different parts of the mix. These may occur due to early-life shrinkage. The microcracks probably grow between the cement matrix and the aggregate as well as in the cement-matrix itself.

Farhan (2016) found that there is no certainty about the location of fatigue failure in cement bound materials whether from the top or bottom of the layer because the behaviour is complex and depends on different factors, for example, thickness and stiffness of different sub-layers, the cement content and the condition of underlying courses. He suggested performing a structural analysis to assess the critical criteria.

Ahsan (1982) investigated a plain concrete subjected to repeated compressive loads, indicating that fatigue strength is 50 to 55 % of the static ultimate strength at 7000 cycles of load. Concrete subjected to repeated flexural loads has a similar resistance, although it has been found to vary from 33 to 64 % depending on moisture, aggregate and curing. Ahsan also found a relationship between the fatigue strength of concrete in tension and the modulus of rupture between 50 - 55 %. Mechanical properties of the hardened concrete and its components, environmental effects and loading

conditions can affect concrete fatigue life (Darestani, 2007).

Furthermore, fatigue strength is affected by age and curing of concrete. Concrete that is carefully cured and aged displays greater resistance to fatigue than concrete inadequately cured and aged. In addition, there are indications that concrete of a rich mix and a low water/cement ratio has a slightly higher fatigue strength (Ahsan, 1982).

Two types of fatigue loading can result in different failure characteristics, namely, low-cycle fatigue and high-cycle fatigue. Low-cycle fatigue means that the load is applied at high stress levels for a relatively low number of cycles, while the high-cycle fatigue corresponds to a large number cycles at lower stresses. A low cycle fatigue is important for structures subjected to earthquake loads (Naik et al., 1993).

In addition, the stress range (difference between maximum and minimum stresses in a cycle) does not significantly influence concrete fatigue life in low-cycle fatigue, as in airports pavements, where the applied peak stress primarily controls the number of repetitions to failure. In high cycle fatigue, which is applicable for highway applications, peak stress and stress range are both influential and affect the number of cycles to failure (Roesler et al. 2005).

Thus, there are may parameters that have an influence on the fatigue damage and controlling these parameters will improve the fatigue strength in concrete pavements.

6.2.1 Evolution of damage of RCC due to fatigue

The most common failure modes that occur in concrete pavements are fatigue cracking in the concrete slab and erosion of materials in sub-layers.

Both are related to excessive stresses and deflections (Parjoko, 2012). Because the critical stresses in RCC pavements are flexural, fatigue due to flexural stress is used for thickness design. Stress ratio, as used in fatigue relationships, is the ratio of flexural stress to flexural strength (Harrington et al., 2010).

The concept of fatigue is important to the design of concrete pavement. It helps designers know what the design stress should be for a given strength of concrete and desired number of load repetitions (Pittman, 1994). ACI-325.10R (2001) found from results of fatigue tests on beams obtained from a full-scale test section incorporating four different RCC mixtures that the fatigue behaviour of RCC is similar to that of conventional concrete.

The Portland Cement Association (PCA) suggested that RCC has similar fatigue characteristics to conventional concrete, but tends to deteriorate more rapidly at lower stress ratios than conventional concrete. In contrast, the Waterways Experiment Station (WES) observed that RCC has similar or better fatigue characteristics as compared to conventional concrete. The PCA used their flexural fatigue data to develop a design curve used in their design procedure for RCC pavements. This design curve was conservatively set about 15 percent below a line parallel to the PCA regression line at which 95 percent of the PCA data was greater, as shown in Figure 6.1. The design curve suggests that RCC can withstand an unlimited number of load applications at a stress ratio of 0.40 (Pittman, 1994).

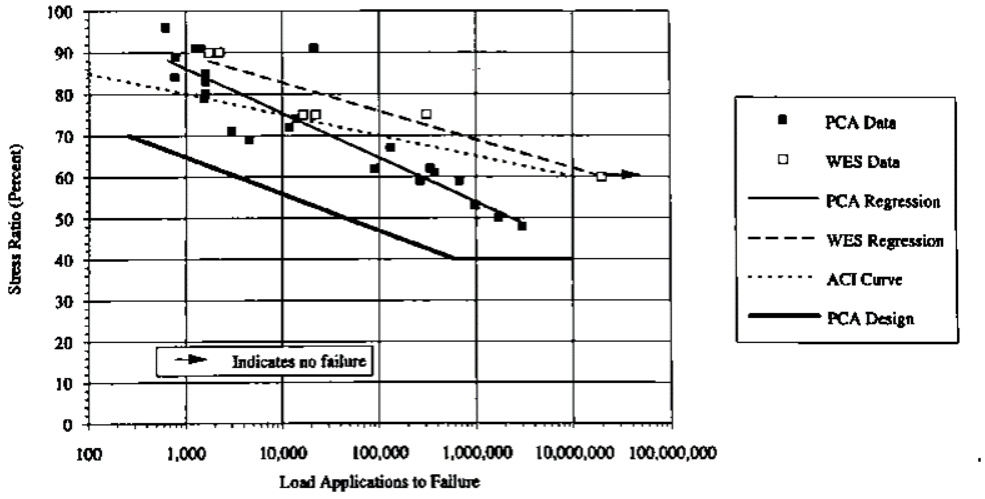

Figure 6.1: *RCC fatigue test results (Pittman, 1994)*

6.3 Experimental producers of fatigue test

Different testing methods have been developed to assess the fatigue behaviour of construction materials. These methods have been utilized based on simplicity, ability to simulate field conditions and applicability of the test results to design a pavement against fatigue cracking (de Oliveira, 2006). These include two-point bending, three-point bending, four-point bending, indirect tensile, compressive, tension-compression and wheel tracking as presented in Figure 6.2.

Regarding the configuration of test, fatigue tests are conducted either in stress control or strain control modes. In the stress control mode, the stress amplitude is maintained while the strain amplitude increases as the materials overall stiffness reduces due to the damage caused by the cyclic application of stress. In the strain control mode, the amplitude of strain is kept constant while the resulting stress decreases due to the stiffness reduction caused by crack propagation. The choice of either stress or strain controlled mode depends on the field situation that is to be simulated,

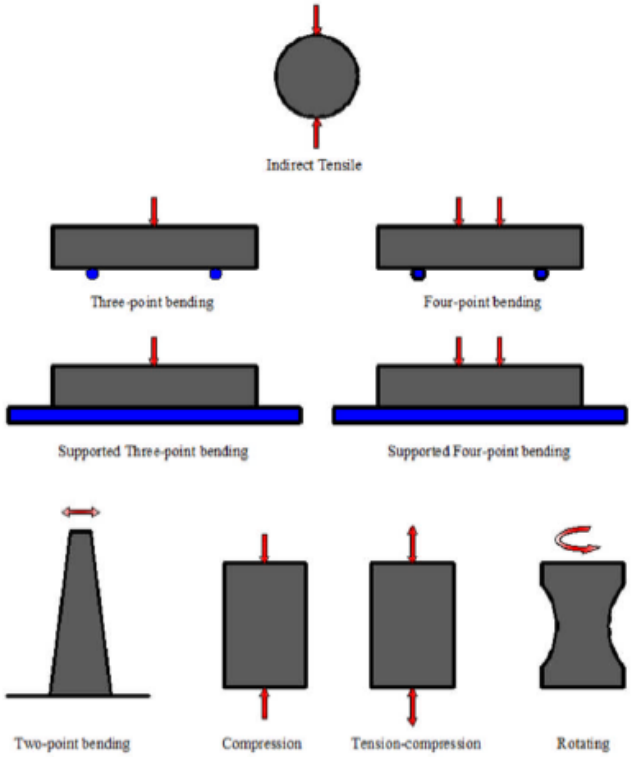

Figure 6.2: *Different fatigue test arrangements*

where the stress control mode is normally used for thicker pavement layers (Farhan, 2016).

In a stress controlled fatigue test, the failure is assumed to occur either at the full fracture of the sample or when the mixture stiffness reaches 10% of its original value. The reason for adopting 10% stiffness in stress controlled mode is because the cracks propagate very quickly towards the end of cycling which makes the number of cycles at 50% stiffness reduction approximately equal to that at which the collapse occurs. For the controlled stress mode the specimen has a relatively short crack propagation period, so the failure point is close to the moment when the specimen has completely fractured, as shown in Figure 6.3 (Farhan, 2016; Li et al., 2007).

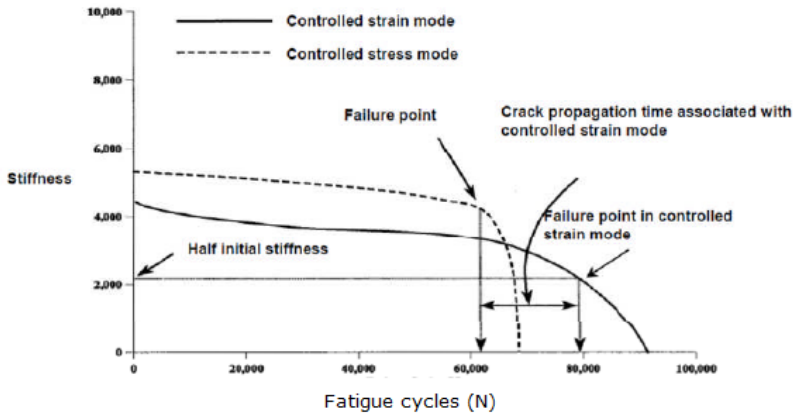

Figure 6.3: *Representation of the failure points for the two modes of loading (Li et al., 2007)*

The fatigue property of materials is usually defined by S-N curves, where S is the stress ratio and N is the number of loading cycles. S is the ratio of the current stress and ultimate strength of the material. The general beam fatigue equation for concrete as recommended by PCA (Packard, 1984) is expressed as shown below :

$$log(N_f) = f_1 - f_2[\frac{\sigma}{MOR}] \tag{6.1}$$

where N_f = number of load applications until failure, σ = applied maximum stress level, and MOR = modulus of rupture of the concrete. However, the Portland Cement Association recommended these particular fatigue equations for different stress ratios:

For $\frac{\sigma}{MOR} \geq 0.55$:

$$log(N_f) = 11.73 - 12.077[\frac{\sigma}{MOR}] \tag{6.2}$$

For $0.45 < \frac{\sigma}{MOR} < 0.55$:

$$N_f = (\frac{4.2577}{\sigma/MOR - 0.4325})^{3.268} \tag{6.3}$$

For $\frac{\sigma}{MOR} \leq 0.45$:

$$N_f = unlimited \tag{6.4}$$

Thus, a fatigue test for a two-layer RCC will depend on the stress ratio as a percentage of the flexural strength of the two layers to obtain fatigue lines and equations, in order to use it in thickness design and service life prediction.

6.3.1 Development of fatigue test facility

The test used in this research was the four-point apparatus designed by de Oliveira (2006) and manufactured at the University of Nottingham since it has been found not to be prone to anomalous results that can result from poorly determined support conditions. The test frame was built such that the clamps and specimen supports have free rotation. This avoids internal stresses and strains being imposed on the specimen leading to consistent support of specimens.

A MAND servo-hydraulic testing machine was used to apply load to the 4-point bending frame. The machine was controlled by a Rubicon digital servo control system. The 4-point bending frame was attached to the testing machine and the alignment adjusted. The beam with dimensions 60 x 60 x 305 mm was placed centrally into the test frame and clamped as shown in Figure 6.4.

The load was applied at 2 Hz since for concrete materials, the rate of loading does not have a significant effect on the fatigue life for frequencies between 1 and 15 Hz (Sobhan and Mashnad, 2000) and the test was conducted under load control. The load was expressed in terms of the stress ratio, being the ratio of the applied flexural stress to the static flexural strength of the material. The flexural strength had previously been determined for each material as described in Chapter 3 and the results for

two-layer system will present in next section. The selected stress ratios for this study were 0.75, 0.8, 0.85 and 0.9 according to previous studies and as they are suitable for strong concrete materials. Two beams were tested at the selected stress ratio until the specimen failed as the stiffness is not measured, where failure was defined as the complete fracture of the specimen.

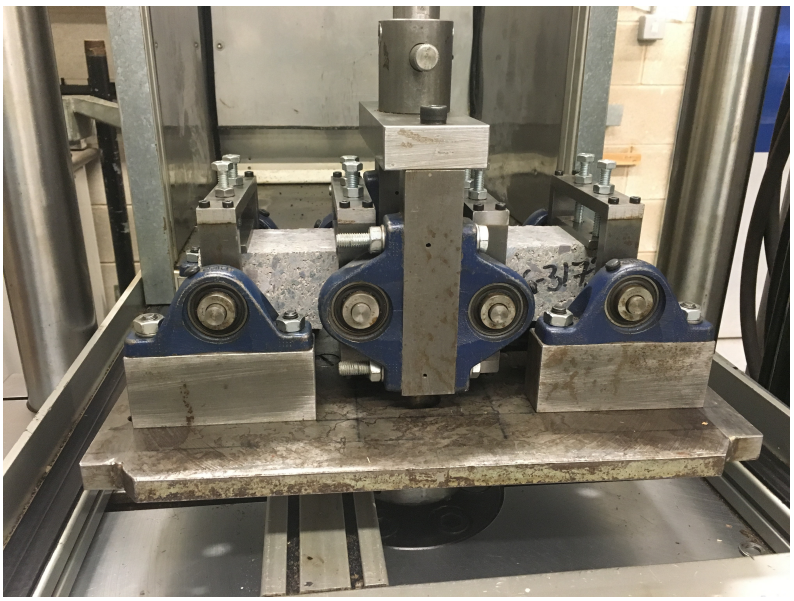

Figure 6.4: *Four-point bending frame*

6.3.2 Results and discussions of fatigue test

The flexural fatigue testing method was preferred here since it is simulative of in-service stress conditions and due to its simplicity. The relationships between the fatigue life (N) and stress ratio (S) for each individual material and for two-layer specimens with different placement conditions are shown in Figure 6.6, where in Case 1, the two layers were placed within one hour, Case 2 means the upper layer was placed three hours after the lower layer and Case 3 means the upper layer was placed 24 hours after the lower layer. Figure 6.5 presents the flexural strength measured for each case. Table 6.1 presents the S–N equations and their respective coefficients of correlation for potential use in designing RCC pavements.

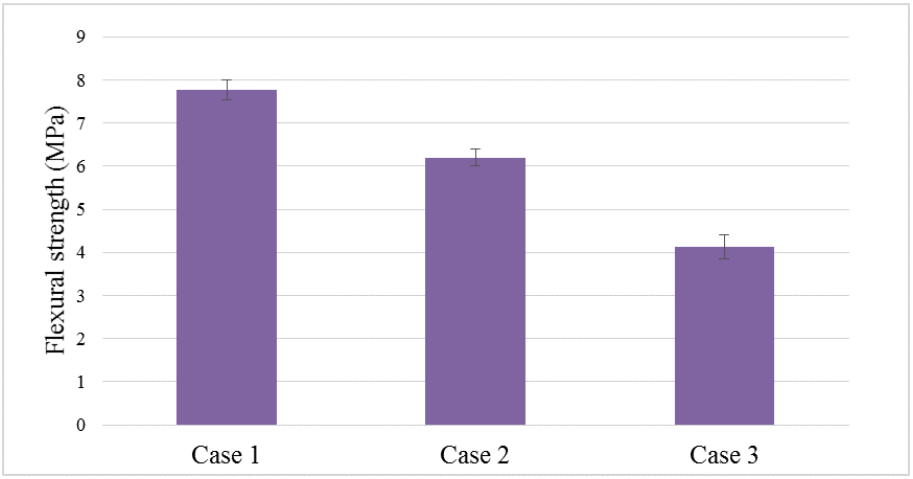

Figure 6.5: *Results of flexural strength for two-layer RCC*

It can be seen from Figure 6.6 that the fatigue resistance (relative to each materials/ arrangements slab strength) of individual layers is similar to that of two layer specimens with different placement conditions. Moreover, the techniques of two layer placement gave very similar fatigue characteristics relative to that of each layer tested separately. However, Figure 6.7,

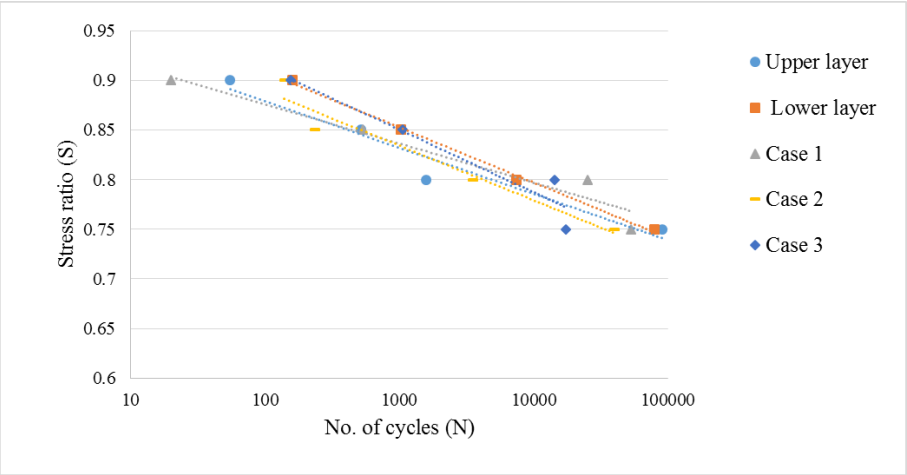

Figure 6.6: *S-N curves for RCC mixtures*

Table 6.1: *Fatigue S-N equations for different RCC specimens each relative to S=1 for the same mixture arrangement*

Mix no.	Fatigue equation	R^2
Upper layer	Log (N_f) = 21.33-21.95 SR	0.94
Lower layer	Log (N_f) = 18.45-18.09 SR	0.997
Case 1	Log (N_f) = 24.38-25.55 SR	0.943
Case 2	Log (N_f) = 18.083-18.096 SR	0.941
Case 3	Log (N_f) = 16.73-16.085 SR	0.92

where stress ratio for Case 2 and 3 has been calculated using the flexural strength for Case 1, the relative effect of placement conditions on the fatigue performance can be noted. Clearly, where Case 3 shows a significant reduction relative to Case 1.

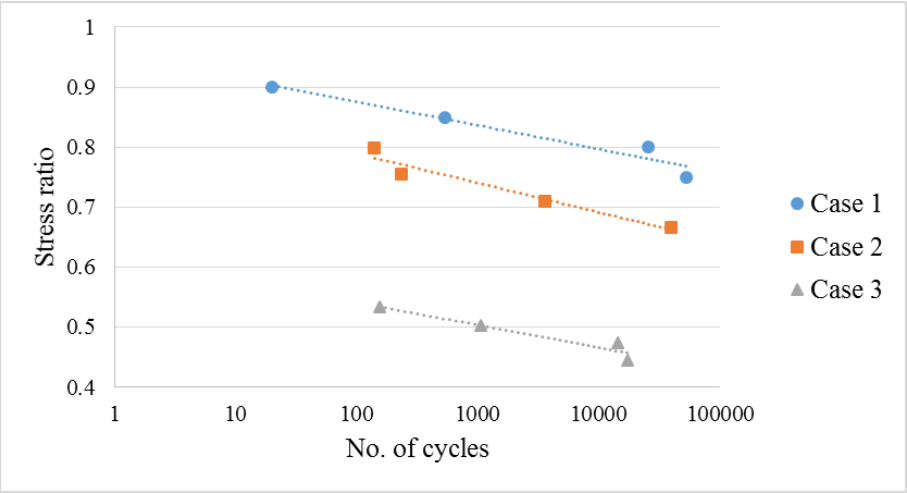

Figure 6.7: *Reduction of S-N curve for two layer RCC, relative to S=1 for Case 1*

In conclusion, the fatigue resistance for each layer separately shows similar behaviour to that of conventional concrete pavement. For a two-layer system with different placement conditions, the fatigue resistance varied as a function of the stress applied relative to the flexural strength. The design life for a two-layer RCC in which the second layer had been placed almost immediately exhibited significantly more load repetitions. When placement of the second layer was delayed only for few hours very significant life reduction was noted, and for a 1 day delay the composite bending action was effectively lost all together.

6.4 Joints in concrete pavements

Concrete pavements comprise different types; these can be either jointed plain, or jointed reinforced with steel bars, mesh or fibres. The purpose of incorporation of joints for all types is to enable movement, relieve the stresses and prevent random cracking (Deen et al., 1979). Normally, the joints are placed approximately every 5 m in plain concrete pavements, and

the spacing can reach to 35 m if heavily reinforced. The stresses eliminated by the joints are caused by temperature and moisture movements in the slabs (Arnold, 2004).

Load transfer is important to the performance of concrete pavements because it reduces the amount of stress in a concrete slab at the joint due to an applied load. Also, load transfer could be an essential part of the thickness design procedure (Griffiths and Thom, 2007).

Jointed plain concrete pavement (JPCP) consists of unreinforced concrete slabs with lengths between 3.6 – 6.0 m and transverse contraction joints between the slabs. The joints should spaced relatively closely together so that uncontrolled cracks will not form in the slabs during the service life of the pavement. For JPCP, two mechanisms contribute to providing load transfer, namely aggregate interlock and dowels (Delatte, 2014).

The performance of concrete pavements depends to a large extent on the performance of the joints. Most failures in jointed concrete pavement result from failures at the joint. Distress types that may result from joint failure include faulting, pumping, spalling, corner breaks, blowups, and mid-panel cracking. Adequate load transfer and proper concrete consolidation can provide satisfactory joint performance as identified through research and field experience (FHWA, 1990).

Delatte (2014) stated that FHWA (1990) classified the common types of joint as:

1. A transverse contraction joint which is defined as "a sawed, formed, or tooled groove in a concrete slab that creates a weakened vertical plane". It is used to define the locations of cracks caused by dimensional changes in the slab. For light loading, jointed pavement contraction joints depend on

aggregate interlock across joints, while for heavy load, pavements generally use dowels to give a load transfer mechanism across the joints.

The primary purpose of transverse contraction joints is to control the cracking that results from the tensile and bending stresses in concrete slabs caused by the cement hydration process, traffic loading and the environment. The performance of transverse contraction joints is related to three major factors: joint spacing, load transfer across the joint, and joint shape and sealant properties.

2. Longitudinal joints are joints between two lines of slabs which allow slab warping without cracking of the slabs. Longitudinal joints are used to relieve warping stresses and are generally needed when slab widths exceed 4.6 m. Load transfer at longitudinal joints is achieved through aggregate interlock and supported by tie bars.

3. Construction joints are defined as "joints between slabs that result when concrete is placed at different times". This type of joint can be further broken down into transverse and longitudinal joints.

4. Expansion joints are defined as "joints placed at specific locations to allow the pavement to expand without damaging adjacent structures or the pavement itself". They are generally transverse joints to relief compressive stresses (Huang, 2004).

6.4.1 Joint behaviour for RCC pavement

Roller compacted concrete (RCC) is a form of jointed plain concrete pavement (JPCP). An important role of aggregate in concrete pavements is to provide load transfer across joints and cracks by using aggregate interlock,

which in theory can eliminate the need for load transfer devices.

Joints in RCC pavement are the most critical areas for obtaining adequate smoothness and density. RCC is similar to conventional concrete in that it can have different types of joints such as construction joints, sawed (contraction) joints, and expansion joints. Longitudinal and transverse construction joints are necessary for the construction of RCC pavements. Longitudinal and transverse sawed joints are normally used to control random cracking and to provide a mechanism to control the spacing of cracks (Harrington et al., 2010; White, 1986).

Joints can be sawn every 8-12 meters to reduce most of the random shrinkage cracking and to improve the appearance of the final RCC pavement. Early-entry saw cutting can be performed on RCC usually within a few hours of compaction (Vahidi and Malekabadi, 2012).

Generally, regarding the economy of construction, RCC pavements have been allowed to crack naturally and this has proven to be very successful. When RCC is allowed to crack naturally, aggregate interlock usually provides adequate load transfer across the cracks. The first cracks will appear within 24 hours of placement because of shrinkage and will typically be spaced from 10 to 25 m apart. Therefore, contraction joints are typically sawn in slabs at regular intervals along the length of the slab, usually within the first 24 hours, to control the location of the cracks by creating a weakened plane in the slab, and thus reduction on shrinkage which will lead to reduced curling and warping stresses (Pittman and Ragan, 1998). On other hand, Harrington et al. (2010) reported that cracks typically occur at 6.1 to 18.3 m intervals, depending on the properties of RCC and pavement thickness. Contraction joints can be constructed using early-

entry sawing to a depth of 1/4 to 1/3 of the total layer thickness usually within two to three hours in order to maintain the highest load transfer across a joint. PCA recommends that the joints should be spaced no more than 6 m apart and for slab thickness less than 200 mm, joint spacing should be between 4.6-6 m (ACI-325.10R, 2001; Harrington et al., 2010). Figure 6.8 illustrates the mechanism of load transfer depending on aggregate interlock.

An important characteristic of concrete pavement joints in design procedures is load transfer and joint efficiency. Load transfer refers to the ability of a crack to transfer load from one slab to an adjacent slab, thereby reducing the amount of load and therefore stress which must be considered in the design of the slab thickness.

Joint efficiency indicates to the portion of deflection due to a load on one slab that is transferred to an adjacent slab through the joint. The importance of this phenomenon is to keep the slabs vertically aligned at the joint during loading and helping to prevent faulting, or permanent vertical misalignment of the edges of the slabs at the joints. It has been found that load transfer and joint efficiency are improved by limiting the spacing between joints (Pittman, 1994).

6.4.2 Mechanism of load transfer

Natural load transfer occurs across cracks that form naturally after placing the concrete slab, or that were designed, when inserting a device to form the crack. Load transfer is a complex mechanism that can vary with concrete pavement thickness, joint spacing, temperature, moisture content,

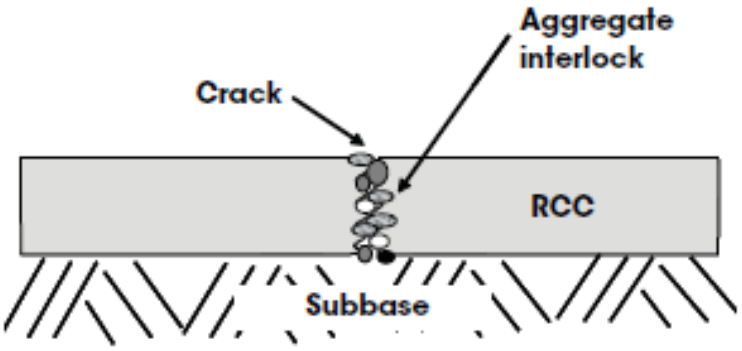

Figure 6.8: *Typical RCC design relies on aggregate interlock at cracks (Garber et al., 2011)*

aggregate type and size, age, construction quality, magnitude and repetition of load, and type of joint (Pittman, 1994). Ioannides and Korovesis (1990) suggested that a pure shear load transfer mechanism is preferable to transmitting bending because of the warping effect inducing further stress when movement is prevented.

The concept of load transfer in a jointed concrete pavement is very important based on the Corps of Engineers and Federal Aviation Administration (FAA) design procedures for rigid pavement. The procedures assume that 25 % of the load applied at the edge of a concrete pavement slab, which is considered the most critical loading position, is transferred through the joint to the adjacent unloaded slab. Therefore, this reduces the edge stress in the loaded slab by 25 % from a maximum free edge condition thereby allowing for a reduced slab thickness. The 25 % load transfer assumption in the Corps of Engineering and FAA design procedures is a simplifying assumption. If the load transfer assumption is not met, the life of the pavement may be significantly reduced from the expected design life (Pittman, 1994).

6.4.2.1 Aggregate interlock

Aggregate interlock is one of the most fundamental mechanisms of load transfer in concrete pavements. When reinforcement is not used and the cracking pattern is unknown, aggregate interlock becomes the only mechanism for transferring load. Even in situations where additional load transfer devices are provided, aggregate interlock still makes a significant contribution (Abdel-Maksoud et al., 1997). Load transfer in RCC pavements is achieved solely through aggregate interlock, which relies on the shear force developed from the friction at the rough vertical interface of a concrete pavement joint (Pittman, 1994).

Arnold (2004) stated that the aggregate effect is approximately 75-90% of the total load transfer for cracks between 0.25 and 0.76 mm wide containing dowel bars. In addition, the type and quality of aggregate, and its bond with the cement matrix, are very important factors in the aggregate interlock load transfer mechanism. If the aggregate is weak and allows cracking to propagate through it, then a smooth face will occur and interlock will be limited. When stronger aggregates are used the bond between the aggregate and the cement mortar is found to be the weakest point, resulting in aggregate protrusion and higher amounts of load transfer (Arnold, 2004). The joint efficiency endurance of slabs which contain crushed limestone and gravel was found to be better than that for slabs containing slag or recycled gravel concrete aggregate, and slightly better for slabs containing 38.1 mm versus 25.4 mm maximum size aggregate (Pittman, 1994).

Two aggregate interlock models have been widely discussed, the local and global roughness models, where local roughness refers to micro-texture causing interlocking of the fine aggregate particles, which is principally a

bearing or crushing action. Global roughness that refer to macro-texture causing interlocking of coarser aggregate particles, principally a sliding and overriding mechanism (Thompson, 2001).

Raja and Snyder (1991) found that local roughness is responsible for most aggregate interlock effects when the crack width is less than 0.25 mm, also, that it provides the interlock mechanism in the early load cycles while global roughness provides the interlock later. Figure 6.9 shows the local and global roughness model.

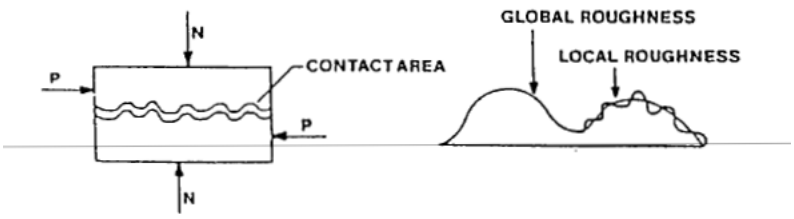

Figure 6.9: *Local and global roughness model (Raja and Snyder, 1991)*

6.4.2.2 Joint effectiveness

A number of methods have been used to calculate the effectiveness of load transfer. Many of these are based on deflections either side of a known joint or crack from an applied load, with a percentage mark given to illustrate the deflection being transferred from one slab to another. Other methods utilise the variation in stress under the slab edge or use finite element modelling to predict the load transfer (Arnold, 2004).

Load transfer is commonly known in terms of load transfer efficiency (LTE). This is often derived from deflection measurements on laboratory test slabs or in situ using a falling weight deflectometer (FWD). LTE is determined

from deflection measurements on account of the relative ease of measuring deflection rather than stress. LTE represents the ratio between the deflections on the unloaded side of the crack and the loaded side of the crack, as shown in equation below (Thompson, 2001).

$$LTE = \frac{\delta_{UL}}{\delta_L}.100 \tag{6.5}$$

where LTE is load transfer efficiency, δ_{UL} is the deflection on the unloaded side of the crack and δ_L is on the loaded side. Figure 6.10 illustrates load transfer and joint efficiency depending on aggregate interlock.

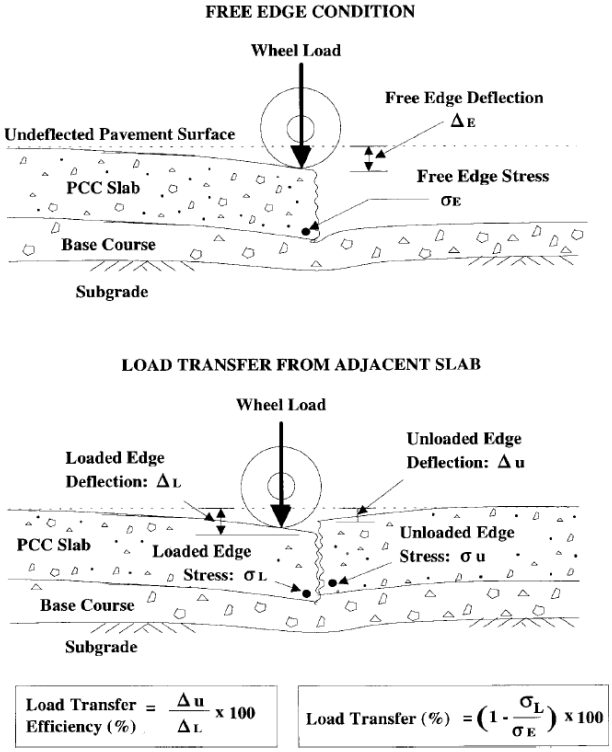

Figure 6.10: *Mechanism of load transfer and efficiency due to aggregate interlock (ACI-325.10R, 2001)*

The minimum level of joint efficiency is different in each design method. The UK minimum level of acceptance for highway pavements is 75 % (Grif-

fiths and Thom, 2007). The PCA stated that for roller compacted concrete crack efficiencies of 60 % are achieved with saw-cut joints and 60-90 % for naturally cracked joints are expected (Griffiths and Thom, 2007). Moreover, Harrington et al. (2010) reported that the joint efficiency of RCC ranges between 22 % to 89 % depending on the type of joint or crack test. The actual efficiency varies from joint to joint and it is affected by the slab temperature. The UK highways agency advise that joint efficiency should not be measured at a temperature more than 15°C in order to avoid deceptively high results (Griffiths and Thom, 2007).

LTE is of practical measure of the behaviour of a pavement under an applied load. Thompson (2001) claimed that LTE could be used to indirectly compare stresses in cement bound materials and strains in the asphalt. He also observed that when LTE is high, the loaded and unloaded sides of a crack deflect by a similar amount. When the LTE is low, little load is transferred across the crack, causing an increase in the deflection of the loaded side of the crack. Harrington et al. (2010) pointed out the factors that may reduce the joint efficiency of RCC, which are repetition of heavy loads, smaller coarse aggregates, cold pavement temperature and large crack or joint openings.

6.4.2.3 Joint stiffness

The stiffness of a joint as described by Huang (2004) is represented by two terms, a shear spring constant C_ω which is defined as shear force per unit length of joint divided by the difference in deflections between two slabs, and a moment spring constant C_θ described as the moment per unit length

of joint divided by the difference in rotations between the two slabs. It is generally accepted that load is transferred across a joint by shear, where Huang (2004) stated that moment transfer across joints with large openings is negligible.

Figure (6.11) shows the shear transfer through a joint by aggregate interlock, as indicated by a spring constant C_ω.

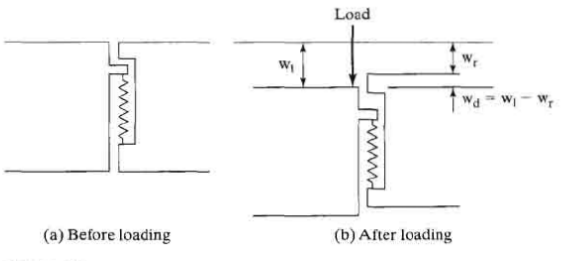

Figure 6.11: *Shear transfer through joint by aggregate interlock (Huang, 2004)*

Hammons (1998) reported that in 1949 Mikhail S. Skarlatos defined a dimensionless joint stiffness (f) in terms of the radius of relative stiffness (l), modulus of subgrade reaction (k), and a parameter (q) which represents the force transferred across a unit length of joint per unit differential deflection across the joint (spring constant C_ω) as follows:

$$f = \frac{q}{kl} \tag{6.6}$$

He carried out analytical development work into closed-form relationships related to deflection load transfer efficiency, LTE_δ, stress load transfer efficiency, LTE_σ, f, and a dimensionless measure of the loaded area size, ε/l. Non-linear regression was used to develop an expression for LTE_δ as a function f and ε/l as follows:

$$LTE_{\delta} = \frac{1}{1 + log^{-1}[\frac{0.214 - 0.183(\varepsilon/l) - logf}{1.180}]} \tag{6.7}$$

Furthermore, Ioannides and Korovesis (1990) defined a non-dimensional joint stiffness, by dividing the aggregate interlock factor (AIF) which represents the stiffness of a joint (spring constant C_{ω}) by the subgrade modulus and radius of relative stiffness. They demonstrated a relationship between LTE and the spring constant used in the ILLISLAB95 program to transfer load in shear as shown in Figure 6.12.

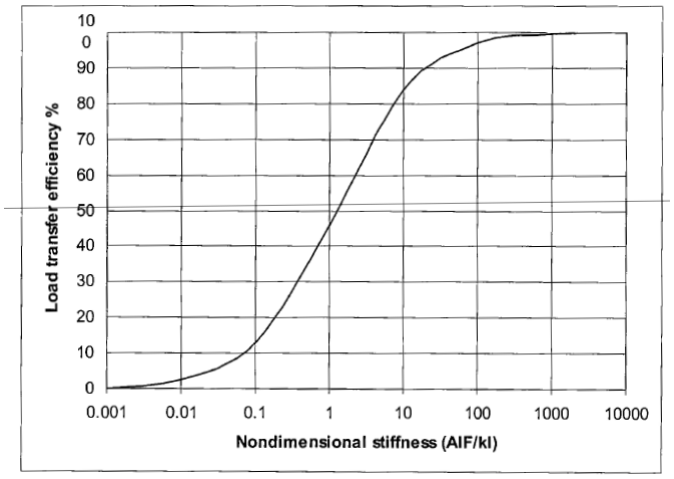

Figure 6.12: *Load transfer efficiency as a function of dimensionless joint stiffness (Ioannides and Korovesis, 1990)*

Thompson (2001) observed in situ that AIF was in the range of 217± 89 MPa for a natural crack in cement-bound materials. Also, he noted that the crack stiffness values correlated with the observed crack widths, where cracks with a low AIF were generally found to be wide, whereas cracks with a high AIF were generally found to be narrow.

Moreover, Thompson (2001) analysed two slabs of cement bound material with one joint to design a base layer of a composite pavement, using a

relationship between joint spring stiffness per unit area obtained from the cyclic shear test in terms of load transfer stiffness (LTS) and joint spring stiffness per unit length in terms of aggregate interlock factor (AIF) in order to find the critical stresses along the joint using Equation 6.8. He found that an increase in the aggregate interlock factor reduces the critical stress significantly where the reduction reached 30% for AIF between 70 MPa and 7000 MPa.

$$AIF = LTS \times D \tag{6.8}$$

where D is the depth of the slab.

6.5 Cyclic shear test

This test was carried out on two-layer RCC prism samples to investigate the crack interface properties where any improvement in the shear properties of a transverse crack would improve the load transfer characteristics of a two-layer RCC pavement. This will benefit the structure in two ways, first by reducing the stresses imposed in bending on the road base and second by reducing the damaging strains that cause reflection cracking through the surface layer (Thompson, 2001).

The dynamic shear characteristic of two-layer RCC pavements was investigated at three approximate crack widths, 0.2 mm, 0.5 mm and 1 mm depending on approximate joint spacing and opening which will discussed in Chapter 7. Two cracks were induced in each prism, vertically, after making 8 notches around each prism as shown in Figure 6.13 to a depth

of approximately 5 mm using a steel saw and a small hammer. The presence of the crack was confirmed by visual inspection of the beam and by measuring the crack width using DEMEC pips mounted on the face of the specimen as shown in Figure 6.14.

Historically, this test arrangement had followed previous investigation into methods to measure shear. Initially a specimen with a single crack was used, with one end of the specimen clamped and the other loaded. Horizontal measurement during these tests showed that significant movement was taking place in this mode due to normal stresses that were introduced under relative vertical movement. The two crack set up developed for this study had the benefit of balancing out these horizontal forces, without casing movement of the end section. Therefore, this arrangement was considered a more realistic approach than the single crack test arrangement (Thompson, 2001).

The test was carried out on prism specimens with dimensions 60 x 60 x 300 mm and load ranges of ± 1.4 kN, ± 1.8 kN, ± 2 kN depending on the shear stress expected across transverse joints in the RCC and the sample dimensions. A positive load represents load in an upward direction and a negative load was downwards. Before starting the test, the average cross sectional area at each notch was calculated by measuring the width and thickness of the beam with a vernier gauge. The number of cycles of each test was 1000 cycles for each load, where for each specimen three different loads were applied, with the same number of cycles. Crack widths were measured using a DEMEC gauge once the cracked beam had been mounted in the test rig and clamps fully tightened. Machine control and data acquisition were automated using MOOG software and a servo hydraulic load

frame machine with 100 kN capacity as shown in Figure 6.15.

Figure 6.13: *Method used to induce cracks in beam specimens*

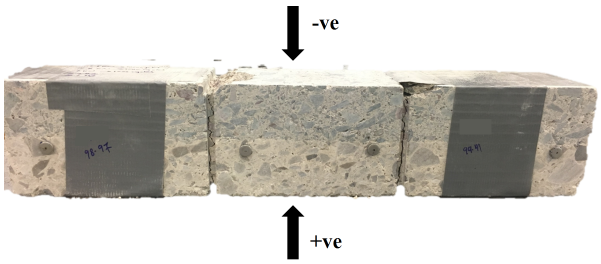

Figure 6.14: *Test specimen before testing*

6.5.1 Results and discussions of cyclic shear tests

In this section, the results for two-layer RCC with different aggregate sizes and types are discussed in terms of the effect of different crack widths, different shear stresses and different placement conditions. Tests were carried out in series, each series comprising a 'start' shear test and an 'end'

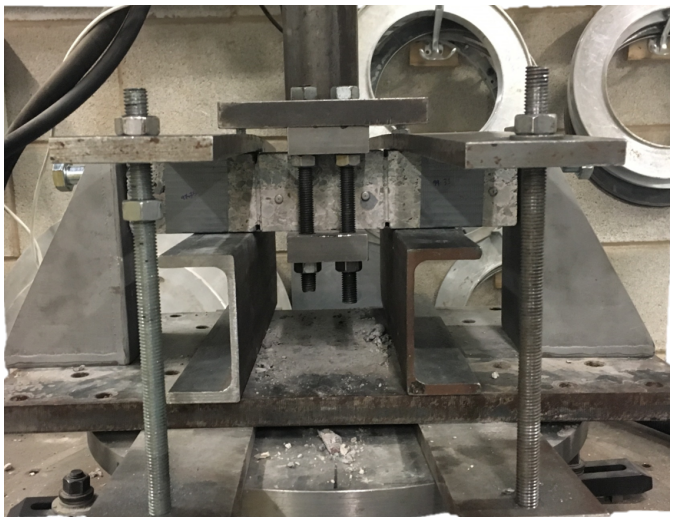

Figure 6.15: *Cyclic shear test arrangement*

shear test. The start and end tests evaluated the average of load-shear slip response over ten cycles.

Figure 6.16 and 6.17 show the effect of different crack width (0.2 mm, 0.5 mm and 1 mm) at 1.4 kN for the first case of placement (the upper layer was placed within one hour of the lower layer) in the beginning and the end of the test. The relation between applied load and shear slip (where shear slip was defined as the vertical distance moved under the applied load) indicated that the shear slip increases with increasing crack width, signifying an increasing deterioration of the joint with larger cracks. At low crack widths, the load-shear slip response was often approximately linear, while at higher crack widths, the relationship between load and shear slip was non-linear.

It appears that when the crack width is low, the whole crack face contributes to shear resistance. This results in a linear load-shear slip relationship, and maintains small shear slips and deterioration rates. However, the non-linear relation might be explained where the finer aggregate is no longer contributing to aggregate interlock, with the load being carried by

the larger aggregate only. The results for Case 2 (the upper layer placed three hours after the lower layer) are slightly less stiff while, for Case 3 (the upper layer placed 24 hours after the lower layer) there is significantly increased shear slip, as shown in Appendix A, resulting from the weak bond between the two layers especially for Case 3.

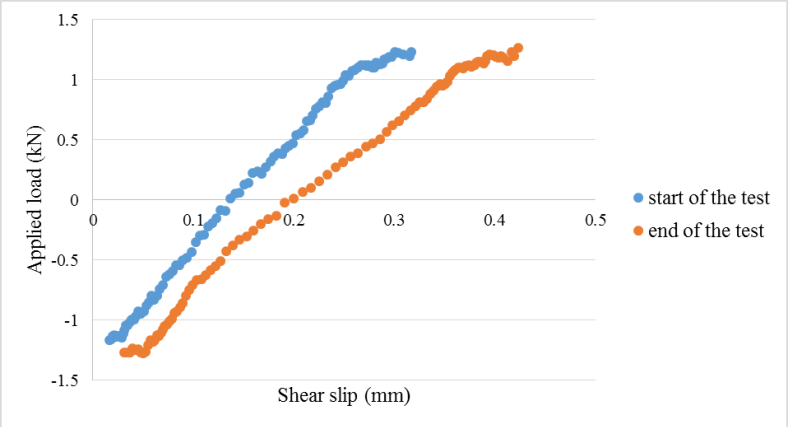

Figure 6.16: *Typical relationship between applied load and shear slip for 0.2 mm crack width*

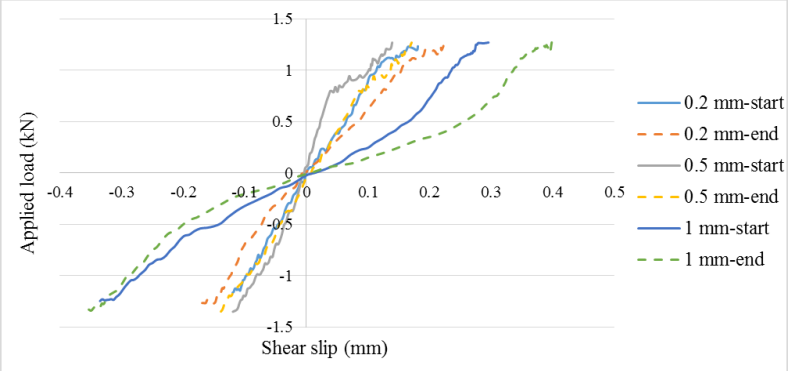

Figure 6.17: *Relationship between applied load and shear slip for Case 1 at 1.4 kN for different crack widths*

In addition, Figures 6.18 presents the relationship between the applied shear stress and shear slip for Case 2 placement of two-layer RCC at 0.2 mm crack width. This figure explains the effect of shear stress on the deterioration of the cracks, particularly the narrow cracks. It can be observed that increasing shear stress from 195 kPa to 278 kPa has a small effect on shear slip. The reason for that is related to the relatively good bond strength of two layers and increasing of frictions at small cracks. However, the results for Case 3 showed a large reduction in shear slip, where for large crack widths, the specimen did not withstand the applied load. All the results for different crack widths and applied loads are presented in appendix A.

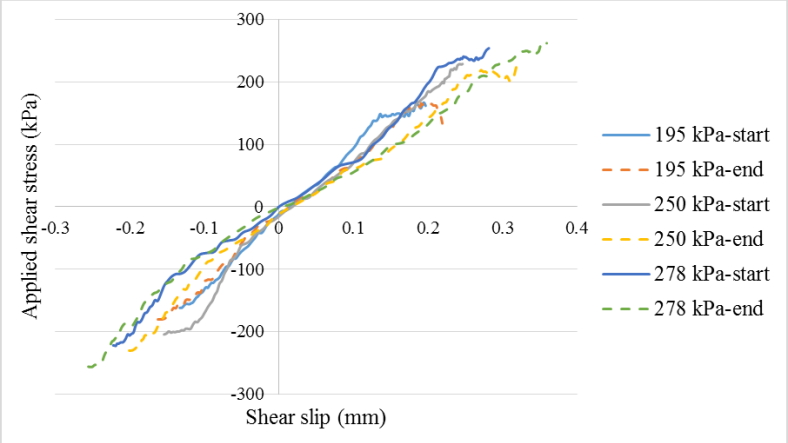

Figure 6.18: *Relationship between applied shear stress and shear slip for Case 2 at 0.2 mm crack at different shear stresses*

Furthermore, Figures 6.19 shows the relationship between applied shear stress and shear slip for different placement conditions at 0.5 mm crack width. It can be concluded that poorer bond quality between the layers leads to weak joint efficiency and rapid deterioration, resulting from the reduction in the load transferring across the joint or crack. The results for

different crack widths and applied shear stresses are shown in appendix A.

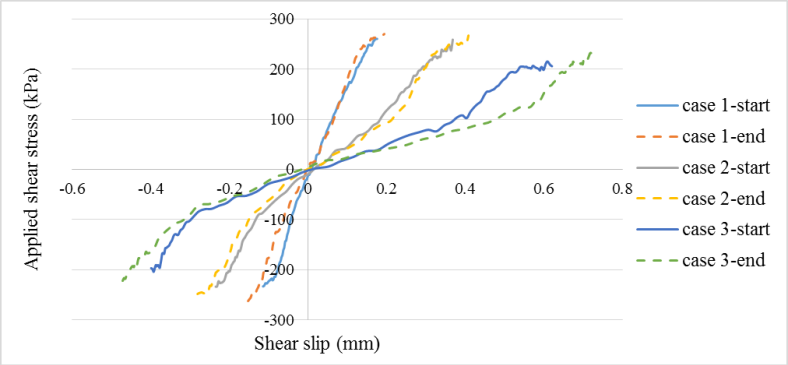

Figure 6.19: *Relationship between applied shear stress and shear slip at 0.5 mm crack width and 278 kPa shear stress*

6.5.1.1 Results of load transfer stiffness

From the load-shear slip data, load transfer stiffness (LTS) was calculated based on the applied shear stress (τ) per unit shear slip (y). For each test, the applied load (F) and the cross sectional area of both crack faces (A) remained constant. Therefore, any increase in the shear slip (y) during the tests resulted in a reduction in the load transfer stiffness. The shear slip is a measure of the total movement between the maximum and minimum loads; therefore, calculating the load transfer stiffness is by using Equation 6.9.

$$LTS = \frac{\tau}{y} = \frac{F}{A(y)} \tag{6.9}$$

The results of load transfer stiffness (as an average of the results for the beginning and the end of the test) for different crack widths, shear stresses and placement conditions are summarized in Tables 6.2, 6.3 and 6.4.

Table 6.2: *Results of load transfer stiffness in MN/m^3 for Case 1*

	Crack width		
Shear stress	0.2 mm	0.5 mm	1 mm
195 kPa	5058	3120	871
250 kPa	3812	1721	680
278 kPa	3867	740	638

Table 6.3: *Results of load transfer stiffness in MN/m^3 for Case 2*

	Crack width		
Shear stress	0.2 mm	0.5 mm	1 mm
195 kPa	3674	836	765
250 kPa	3442	826	464
278 kPa	2972	811	418

Table 6.4: *Results of load transfer stiffness in MN/m^3 for Case 3*

	Crack width		
Shear stress	0.2 mm	0.5 mm	1 mm
195 kPa	917	770	587
250 kPa	891	778	427
278 kPa	841	649	0

It can be observed from Figures 6.20, 6.21 and 6.22 that the load transfer stiffness for Case 1 is higher than for Case 2 and for Case 3 because the poor bond between the two layers decreased the shear resistance of the two-layer RCC. In addition, the load transfer stiffness for small crack widths showed better performance than for wider cracks. However, increasing shear stress slightly reduced the load transfer stiffness.

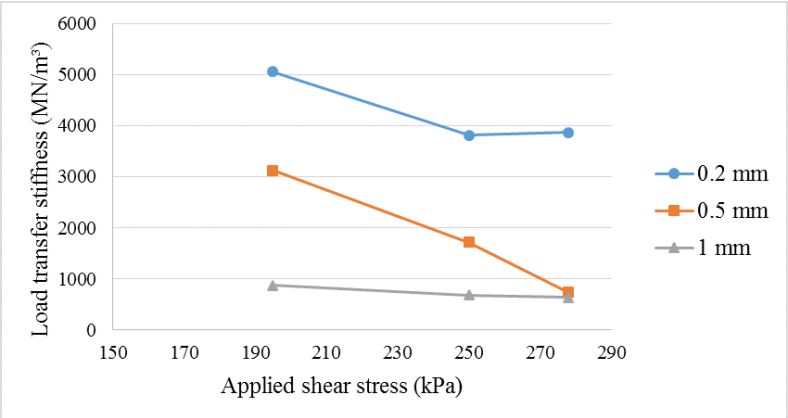

Figure 6.20: *Relationship between load transfer stiffness and applied shear stress for case 1 at different crack width*

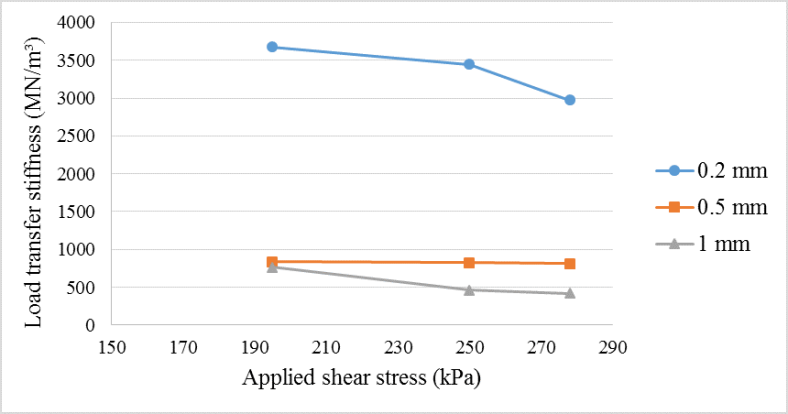

Figure 6.21: *Relationship between load transfer stiffness and applied shear stress for case 2 at different crack width*

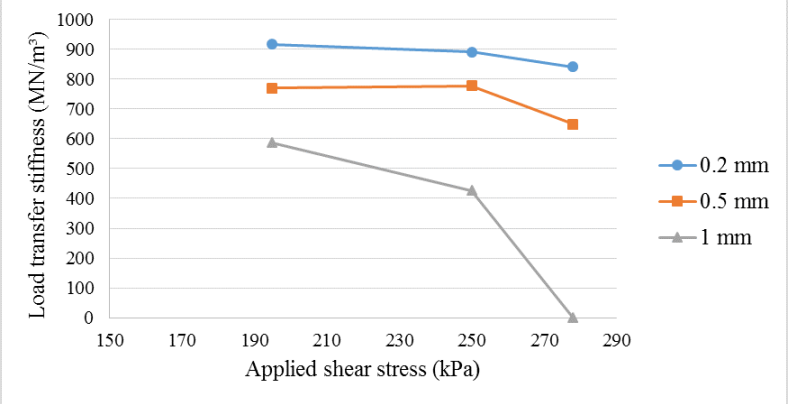

Figure 6.22: *Relationship between load transfer stiffness and applied shear stress for case 3 at different crack width*

Furthermore, an attempt to improve the load transfer stiffness of two-layer RCC, roughening of the upper surface of the lower layer was used for Case 2 and Case 3 (designated Case 2^* and Case 3^*). Roughening the surface is a technique used to increase the friction between two layers and may develop a connection to transfer the load through the cracks. Tables 6.5 and 6.6 illustrate the results of load transfer stiffness with the roughening technique for Case 2^* and Case 3^*.

Figures 6.23 and 6.24 present the relationship between the load transfer stiffness in (MN/m^3) and applied shear stress (kPa) for Case 2^* and Case 3^*, where the roughening improved the load transfer stiffness at a given crack width.

Roughening has a big positive effect. Comparing these results with the results of roughening in Chapter 5 (where roughening did not achieve much) seems to show that roughening is valuable for fatigue/repeated shear situations but not for static shear situations. This might be related to quick rupture under static load while in fatigue have more time to deteriorate.

Table 6.5: *Results of load transfer stiffness in MN/m^3 for Case* 2^*

	Crack width		
Shear stress	0.2 mm	0.5 mm	1 mm
195 kPa	3329	2666	2007
250 kPa	2794	2417	1828
278 kPa	2630	2324	1532

Table 6.6: *Results of load transfer stiffness in MN/m^3 for Case 3**

Shear stress	Crack width		
	0.2 mm	0.5 mm	1 mm
195 kPa	3119	2443	1148
250 kPa	3019	2438	1173
278 kPa	2599	2081	1095

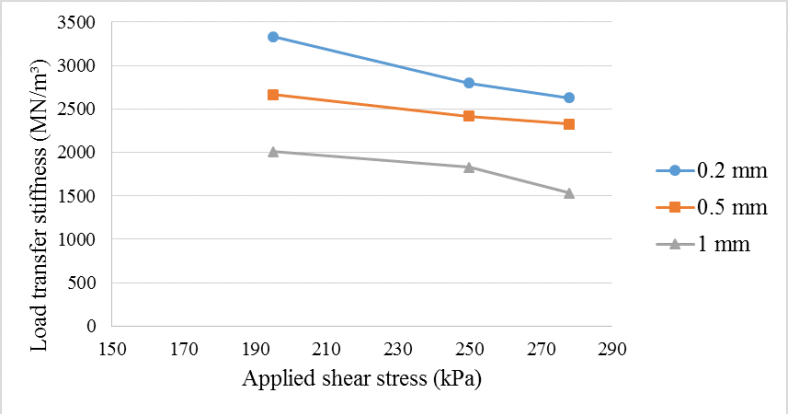

Figure 6.23: *Relationship between load transfer stiffness and applied shear stress for Case 2* at different crack width*

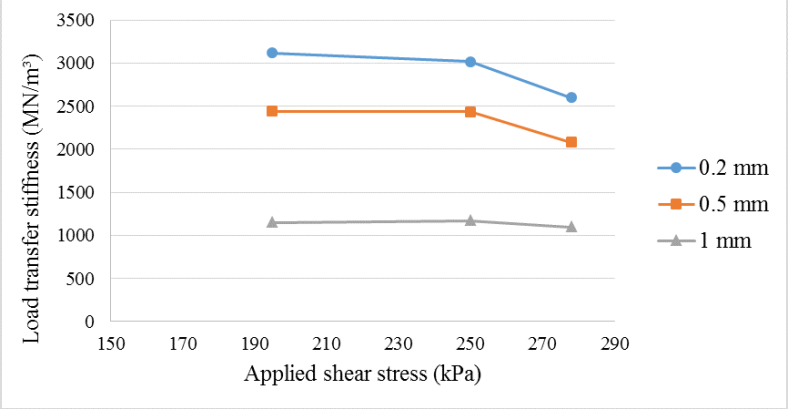

Figure 6.24: *Relationship between load transfer stiffness and applied shear stress for Case 3* at different crack width*

In addition, the deterioration of joints has been observed for the two-layer RCC. The results of load transfer stiffness are presented in Figures 6.25, 6.26 and 6.27 for each placement case with an average for the beginning and the end of the test. It can be concluded that the deterioration of the

cracks in two-layer RCC system increased with increasing number of cycles and shear stress with regard to increase crack width. Also, the placement conditions increased the rate of deterioration as the poor bond reduced transferring load across the crack.

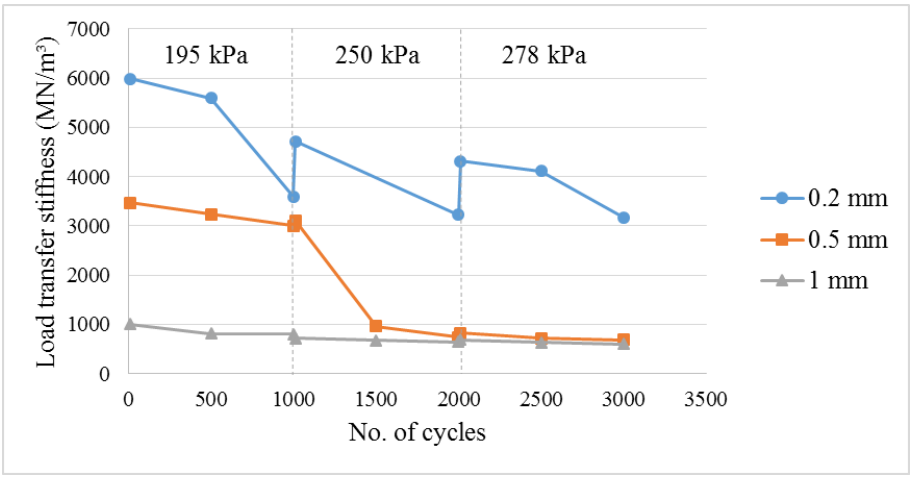

Figure 6.25: *Relationship between load transfer stiffness and number of cycles at different crack width for Case 1*

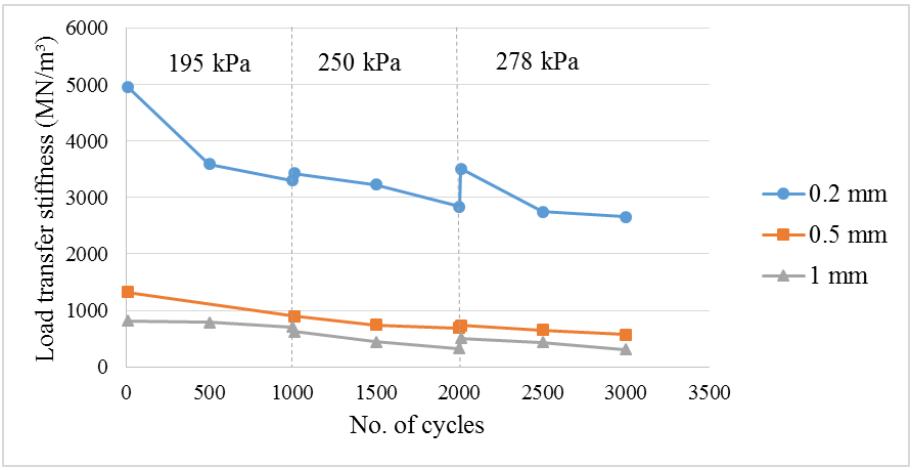

Figure 6.26: *Relationship between load transfer stiffness and number of cycles at different crack width for Case 2*

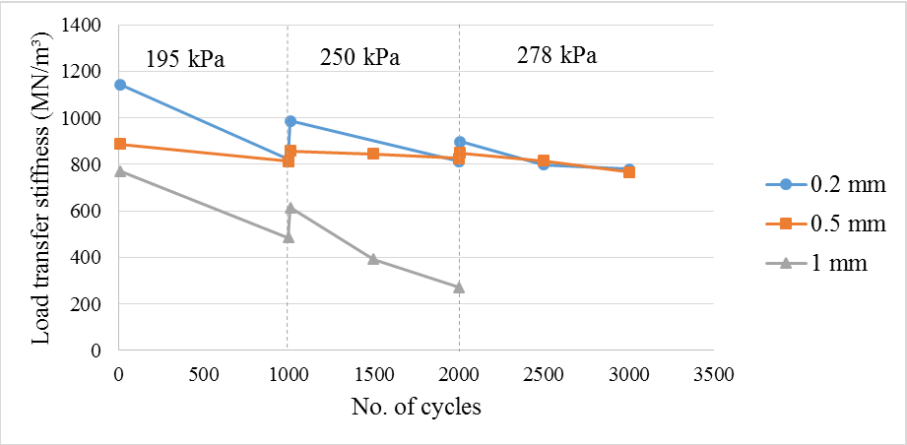

Figure 6.27: *Relationship between load transfer stiffness and number of cycles at different crack width for Case 3*

6.5.1.2 Joint stiffness equation

The cyclic shear test results combined three effects on load transfer stiffness; namely, crack width, number of cycles and applied stress. A non-linear analysis was used to drive an approximate mathematical equation that could predict joint deterioration for a two-layer RCC pavement which could be used then in pavement design.

The equation was estimated depending on non-linear relationships between test variables, with 26 data points from the start and end points of cyclic shear tests. A simple Matlab code was created to find the constants of the equation by trial and error, then the equation was validated against laboratory results and confirmed with the findings of Thompson (2001) on cement-bound material as shown in Figure 6.28. The equation is presented as shown below:

$$LTS = \frac{22\left(\frac{\tau}{MOR}\right)^{-2.2}}{W(29 + N^{0.4})} \tag{6.10}$$

where LTS is load transfer stiffness (MN/m^3), τ is the shear stress (kPa), MOR is modulus of rupture (kPa), W is the crack width (mm) and N is the number of cycles.

The correlation between the computed load transfer stiffness (LTS) and measured LTS from cyclic shear test indicated the usefulness of this equation to predict joint deterioration under repeated load, as shown in Figure 6.29.

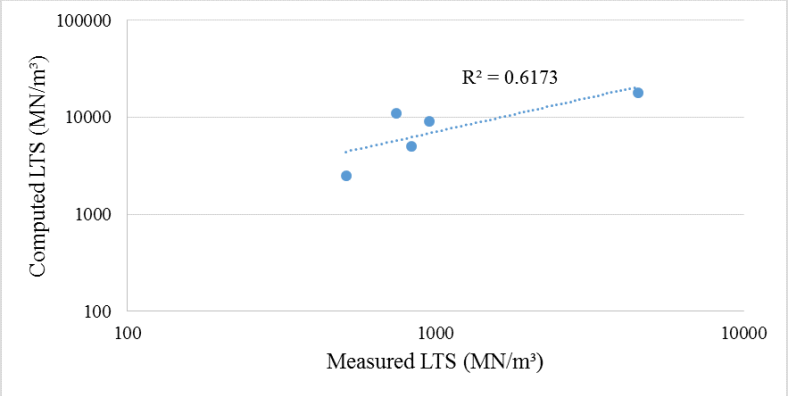

Figure 6.28: *Relationship between computed load transfer stiffness and measured load transfer stiffness based on Thompson (2001)*

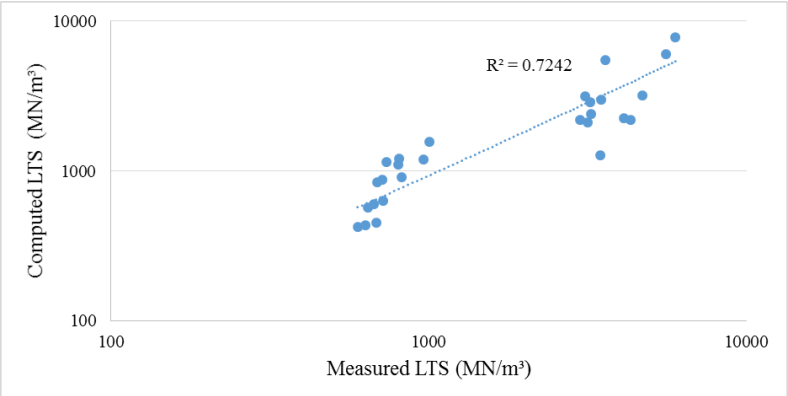

Figure 6.29: *Relationship between computed load transfer stiffness and measured load transfer stiffness according to laboratory findings*

The computed joint deterioration for different crack widths can be seen in Figures 6.30, 6.31 and 6.32 as estimated from Equation 6.10. It can be observed that increasing crack width affects significantly the stiffness of the joint after a large number of repeated loads. However, increasing the shear stress has a minor effect.

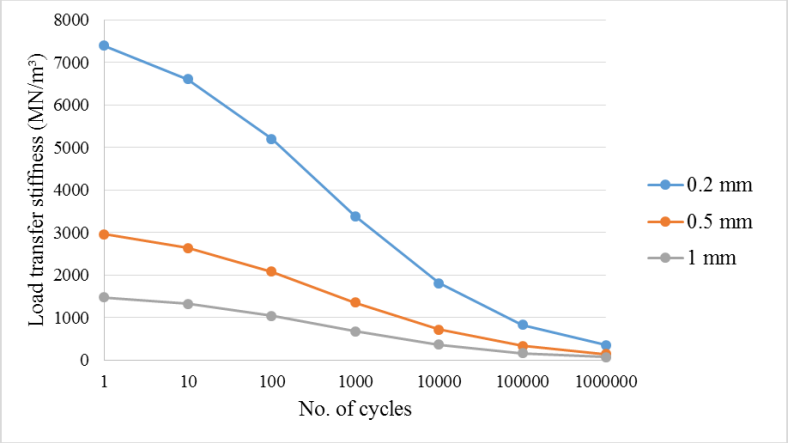

Figure 6.30: *Relationship between computed load transfer stiffness and no. of cycles for different crack widths at 200 kPa shear stress*

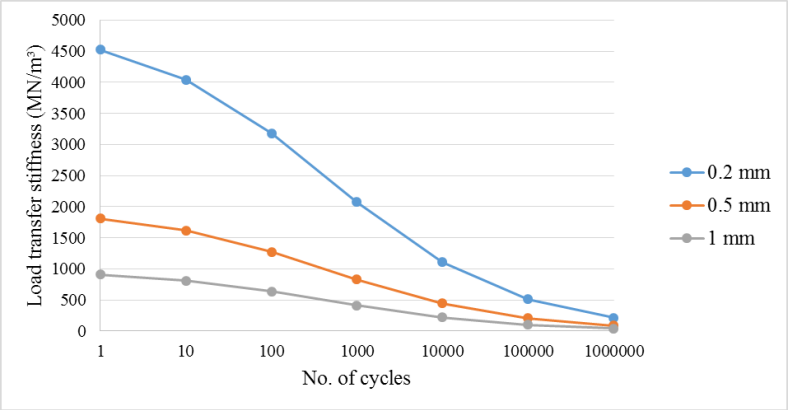

Figure 6.31: *Relationship between computed load transfer stiffness and no. of cycles for different crack widths at 250 kPa shear stress*

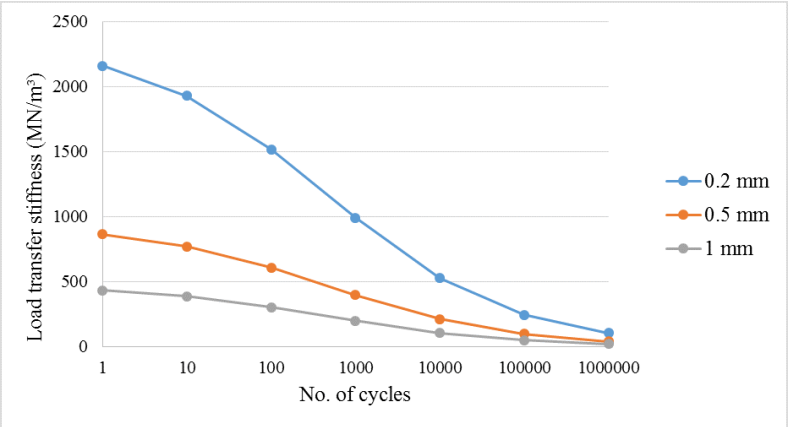

Figure 6.32: *Relationship between computed load transfer stiffness and no. of cycles for different crack widths at 350 kPa shear stress*

6.6 Summary

This chapter has summarized the effect of dynamic load on two-layer RCC pavement materials with different aggregate sizes and types and different placement conditions. The upper layer is formed of RCC with smaller aggregate size than the lower layer. The effect of flexural fatigue and joint stiffness of two-layer RCC was assessed in terms of 4-point bending and cyclic shear tests respectively.

In the flexural fatigue test, results were obtained for each layer of RCC separately as well as for the two layers combined with different placement conditions. It was found that the two-layer RCC has high fatigue life compared to conventional concrete and it is decreased for the two layers as the bond between them was less competent. These results can indicate the performance and design life of two-layer RCC pavement.

The importance of joints in two-layer RCC lies in its efficiency in transferring the load and this is given by the stiffness of joint. The cyclic shear tests were conducted to find the joint stiffness of two-layer RCC. The results showed that joint stiffness depends significantly on crack width and

then on the number of cycles and the applied shear stress.

It can be concluded from the test results that the crack deteriorates relatively quickly when the width is more than 0.2 mm and when the placement conditions weaken the bond between layers, that affects the joint deterioration. An equation of joint load transfer stiffness was designed to predict the deterioration of a joint under a large number of cycles as a function of RCC material properties. The aim was to provide a tool to assist in the design of two-layer RCC pavement. In brief, the design of two-layer RCC will depend on both fatigue resistance and joint stiffness.

Chapter 7

Rigid pavement analysis and design

7.1 Introduction

The purpose of this chapter is to give a simple guide for the design two-layer RCC pavement for different pavement applications such as local roads and industrial roads in order to expand the use of this type of concrete pavement into wider applications.

It demonstrates the influence of different parameters on the performance of two-layer RCC pavement. Also, the effect of joint deterioration of two-layer RCC on the design life is investigated with regard to traffic load and differential temperatures. The sensitivity of stresses in two-layer RCC with different slab lengths and thicknesses is evaluated using KENPAVE, a finite element program.

7.2 Design and analysis of concrete pavement

Rigid pavements are constructed of Portland cement concrete and are commonly analysed by means of plate theory. Plate theory is a simplified

version of layered theory that assumes the concrete slab to be a medium thick plate with a plane before bending which remains a plane after bending. Plate theory is useful when the wheel load is applied near to an edge or a joint (Huang, 2004). Concrete pavements are primarily designed in terms of thickness, but there are other important elements such as spacing of joints, subgrade and subbase properties, which contribute to providing good performance (Delatte, 2014). Figure 7.1 shows the cross section of rigid pavements as assumed by Huang (2004).

A rigid pavement system consists of a number of relatively thin Portland cement concrete slabs, finite in length and width, over one or more foundation layers. When a slab is subjected to a wheel load, it develops bending stresses and distributes the load over the foundation. However, the response of these finite slabs is controlled by joint or edge discontinuities. Joints are structurally weakening components of the system. Thus, the response and effectiveness of joints are of primary importance in rigid pavement analysis and design (Hammons and Ioannides, 1997).

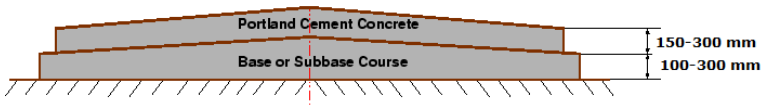

Figure 7.1: *Cross section of rigid pavements (Huang, 2004)*

Concrete pavements respond to loading in a variety of ways that affect the performance both initially and in the long term. The three principal responses are:

1. Curling stress: differences in temperature between top and bottom surfaces of a concrete slab will cause the slab to curl. Since slab weight and connection with the base restrict its movement, stresses are formed.

2. Load stress: Loads on concrete pavement will create both compressive and tensile stresses within the slab.

3. Shrinkage and expansion: Environmental temperature changes will cause a concrete slab to expand when it is hot and contract when it is cold and will cause joint movement.

Three typical locations are analysed by plate theory, termed the critical positions, namely the interior, edge and corner as shown in Figure 7.2.

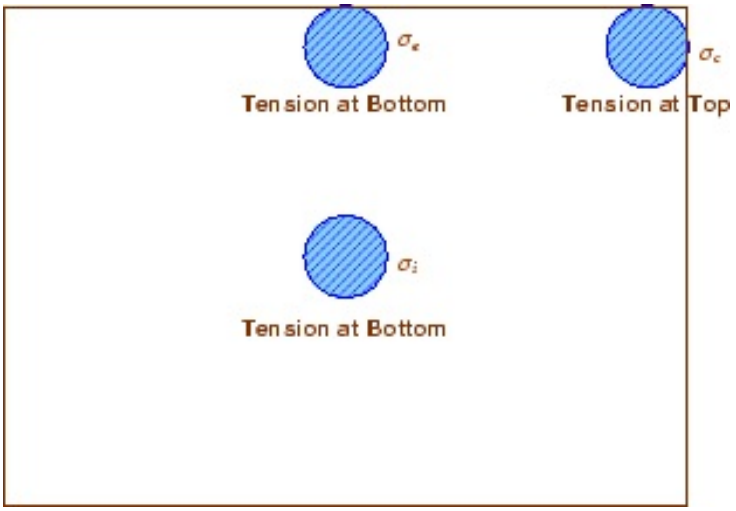

Figure 7.2: *Critical stress locations (Mathew and Rao, 2007)*

7.2.1 Stiffness and strength of support layers

In concrete pavements, the quality of the support layers to the pavement slab, their moisture susceptibility and frost susceptibility are important parameters for high performance (Delatte, 2014). The quality of the support layers is characterised by a k value which is known as the modulus

of subgrade reaction representing a set of elastic springs. It is defined as the load per unit area causing unit deflection. Values of k range between 0.01 N/mm^3 and 0.1 N/mm^3 depending on soil types and are usually determined from plate-loading tests. The standard plate load test is conceptually based on the volumetric method of calculating k. In this method the total applied load is divided by the volume of the deflection basin (Jafarifar, 2012).

This model is also called a dense liquid foundation where the modulus of subgrade reaction is equal to the unit weight of a virtual liquid support. A more realistic approach to define the support under a concrete pavement is to determine the k-values for the subgrade and the granular subbase combined, and then consider the base course as a structural layer (Jafarifar, 2012). Figure 7.3 shows this model of the foundation layers. Therefore, for simple analysis of two-layer RCC, the liquid foundation has been used in this research to calculate the stresses and deflections.

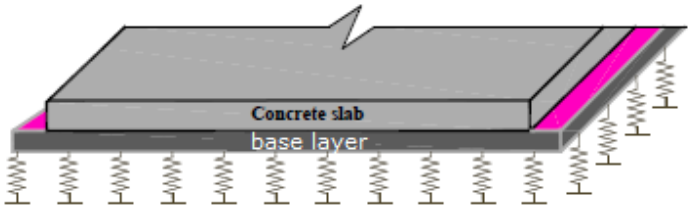

Figure 7.3: *Modelling of the foundation layers (Jafarifar, 2012)*

7.2.2 Failure criteria

In the design of any civil engineering structure, it is critical to have a good understanding of its failure modes in service. Brown (2013) stated that

most pavement structures will not fail suddenly but they will deteriorate gradually with time under repeated traffic load and environmental factors. Traffic loading is a major factor in the deterioration of a pavement, affected by the number and magnitude of the wheel loads. The stresses which develop in a concrete pavement slab due to applied loads present a more complex analytical problem than the simply supported beam in a flexural strength test. Perhaps the best-known closed-form solution developed for calculating the maximum tensile stresses in a concrete slab due to applied loads in three different places (internal, edge and corner) was presented by Westergaard in 1926. In his analysis, Westergaard assumed the slab to act "as a homogeneous isotropic elastic solid in equilibrium, and the reactions of the subgrade to be vertical only and proportional to the deflections of the slab" as shown in Figure 7.4 (Huang, 2004; Pittman, 1994). Figure 7.5 presents the distribution of bending stresses in beams and slabs of concrete.

In a concrete pavement, the most critical failure mode is fatigue cracking resulting from the tensile stress at the bottom of the layer and joint deterioration. Three methods can be used to determine the stresses and deflections in concrete pavements: closed-form formulae, influence charts, and finite-element computer programs (Huang, 2004).

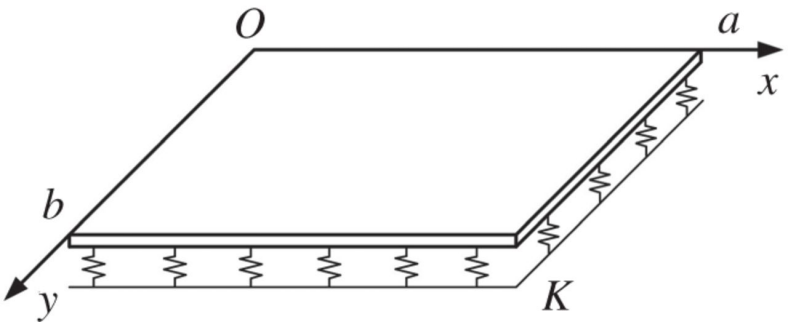

Figure 7.4: *Liquid foundation depending on theory of Westergaard (Huang, 2004)*

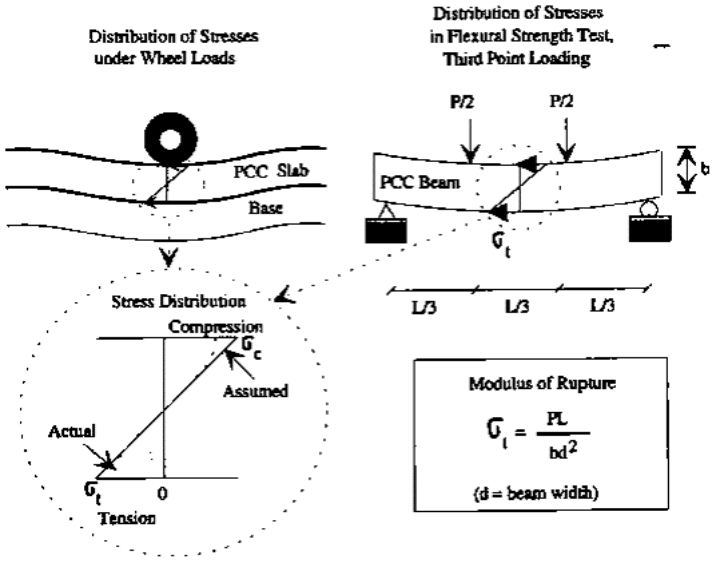

Figure 7.5: *Distribution of bending stresses in concrete beams and slabs (Pittman, 1994)*

7.3 Basis for RCC design

RCC is designed as a rigid pavement similar to conventional concrete pavements in the mode of failure. However, RCC has less shrinkage and it is cracking naturally. Generally, the inputs to the design process are the bearing capacity of the subgrade, the type and thickness of subbase, the flexural tensile strength of the RCC and the type and frequency of loading (ERMCO-Guide, 2013; Guyer, 2013).

The thickness design of both conventional concrete and RCC pavements is

based on keeping the flexural stresses and fatigue damage in the pavement caused by wheel loads within allowable limits. Stresses and fatigue damage are greatly influenced by wheel load placement. There is a greater effect from loads placed along edges and joints and less at interior locations in the pavement because joints are weak points (ACI-325.10R, 2001).

In structural design of concrete pavements, pavement thickness is a function of expected loads, concrete strength (modulus of rupture), and soil characteristics. The minimum thickness of a RCC pavement is typically 10 cm with a single-lift and the maximum thickness is 25.4 cm for multi-lift (Guyer, 2013; Harrington et al., 2010).

Shin and Carboneau (2010) demonstrated that many methods are used for the design of conventional concrete pavement and are suitable for RCC pavement such as the AASHTO 1993 design procedure, ACI Committee 325 design guides, and American Concrete Pavement Association (ACPA) design guide. They depend on different computer programs such as PCA/RCC-Pave and Street-Pave which are popular design tools for RCC pavement because of their efficiency and simplicity. PCA/RCC-Pave is suitable for the design of heavy duty industrial pavements, which have simple traffic patterns, while Street-Pave is suitable for the design of pavements carrying mixed vehicle traffic (Harrington et al., 2010).

In addition, Huang (2004) at the University of Kentucky developed a finite element program for calculating stresses and deflections in jointed rigid pavements called KENPAVE. The program can analyse a certain number of slabs with aggregate interlock or dowels as load transfer devices.

The design approach for RCC pavements is based upon limiting the stress in the pavement to a level such that the pavement structure can withstand

repeated loadings of this stress magnitude without failing in fatigue.

7.3.1 Thickness design procedures

Thickness design procedures for RCC pavements for certain applications such as ports and multimodal terminals have been developed by the Portland Cement Association (PCA) and U.S. Army Corps of Engineers (USACE). The design approach involves the assumption that the pavement structure can withstand loads of certain magnitudes at certain repetition levels without failing. According to previous studies (ACI-325.10R, 2001; Guyer, 2013; Harrington et al., 2010), the critical stresses in RCC are flexural, fatigue due to flexural stress is used for thickness design. The stress ratio, as used in fatigue relationships, is the ratio of flexural stress to flexural strength (ACI-325.10R, 2001).

In RCC thickness design, the pavement thickness is increased or the strength of the concrete is increased until the stress ratio is reduced sufficiently to provide adequate fatigue performance (Harrington et al., 2010).

Halsted (2009) clarified that to determine the appropriate pavement design, it should withstand the expected traffic, expressed in terms of wheel loads, load configuration, and number of load applications expected over the design period, which is typically of 20 to 30 years. In the design process, the economic and structural aspects of the following three parameters should be considered with regard to the applied wheel loads and number of expected load applications:

1. Foundation support (modulus of subgrade reaction).
2. Concrete properties (flexural strength and elastic modulus of the con-

crete mix).

3. Pavement thickness.

The PCA procedure is primarily used for industrial pavements but can be applicable for similar paving applications, where it is based on the interior load condition and uses a unique design fatigue relationship for RCC paving material (ACI-325.10R, 2001; Harrington et al., 2010). Moreover, to use the PCA procedure, the following information is needed. 1. Supporting strength of subgrade or subbase/subgrade combination.

2. Vehicle characteristics:

a) Wheel loads.

b) Wheel spacing.

c) Tire characteristics.

d) Number of load repetitions during the design life.

e) Flexural strength of RCC.

f) Modulus of elasticity of RCC.

Figure 7.6 shows the design charts for a single wheel.

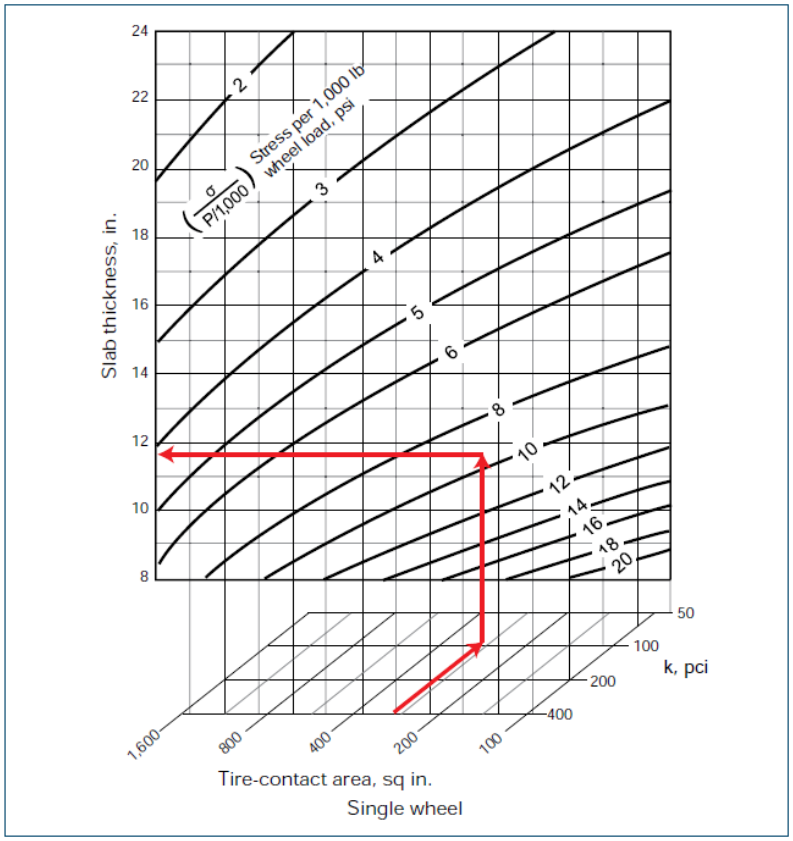

Figure 7.6: *Design chart for single-wheel loads according to PCA 1987 (Harrington et al., 2010)*

On the other hand, the U.S. Army Corps of Engineers (USACE) argued that there is a difference between designing the thickness of RCC pavement and PCC related to the assumptions of load transfer at joints, which directly affects the design stress and the thickness of the pavement. Thus, they concluded that the assumption of 25 % load transfer at joints in open storage areas and airfields constructed of plain concrete may not be valid for RCC pavement thickness design. Therefore, their approach was to base the thickness design of RCC pavement on no load transfer at the joints by assuming all joints/cracks give a free edge condition (ACI-325.10R, 2001; Harrington et al., 2010; Shoenberger, 1994).

The USACE procedure can be performed manually, using tables and nomographs, or electronically, using the USACE software and Figure 7.7 is used

for design of both PCC and RCC pavements.

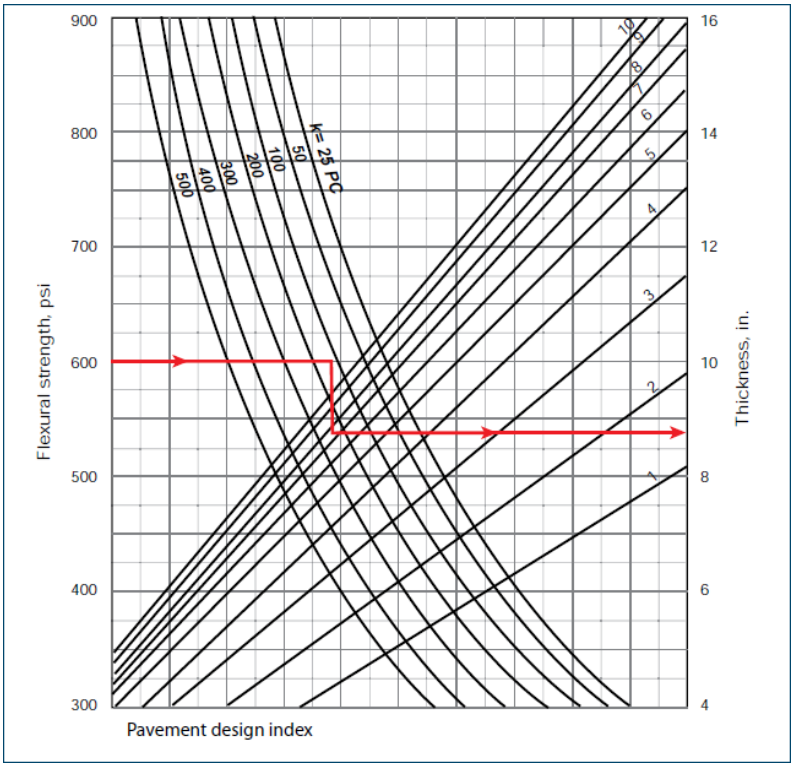

Figure 7.7: *Design chart for conventional concrete and RCC for roads and streets pavement according to USACE (Harrington et al., 2010)*

Furthermore, ACI design procedures are depended on manual design methods (tables) to determine RCC pavement thickness for streets, local roads and parking lots that carry mixed vehicle traffic. ACI-325.12R (2002) suggested different values for thickness of low-volume concrete roads as a function of subgrade support and concrete flexural strength with or without integral or tied curb and gutter.

7.4 Theoretical analysis of two-layer RCC pavement

The finite-element computer program KENPAVE has been used to investigate the influence of a number of common variables in a concrete pavement. The program was developed at the University of Kentucky in the United States by Huang (2004) for calculating stresses and deflections in jointed rigid pavements. Huang (2004) stated that the purpose of mechanistic procedures are mostly to improve reliability of design, prediction of distress types and the possibility of drawing conclusions from limited laboratory and field data. The KENPAVE program consists of two parts, one to deal with asphalt pavements called KENLAYER and the second part called KENSLAB deals with concrete.

The KENSLAB program is based on the finite-element method, in which the slab is divided into rectangular finite elements with a large number of nodes. Both wheel loads and subgrade reactions are applied to the slab as vertical concentrated forces at the nodes (Hammons and Ioannides, 1997; Huang, 2004). The program allows two slab layers, either bonded or unbonded. The two layers can be Hot Asphalt Mixture (HMA) on top of a conventional concrete pavement (PCC) or PCC over a cement-treated base. The program allows a maximum of 6 slabs, 7 joints and 420 nodes, and each slab can have a maximum of 15 nodes in the x direction and 15 nodes in the y direction (Chen, 2005; Huang, 2004).

The critical stress in a two-layer RCC pavement has been investigated assuming various aggregate interlock factors, slab lengths and depths and differential temperatures. Longitudinal surface profiles were plotted so that the vertical deflections on either side of a loaded and unloaded crack/joint

could be compared. From this, and based on laboratory test data, a design method will be presented and recommendations made as to how two-layer RCC pavement performance may be designed in practice.

7.5 Design Parameters

The two-dimensional mesh used in the finite element analysis is shown in Figure 7.8 and analysed as a linear elastic model. Four slabs were analysed with different dimensions and four joints with different stiffnesses (LTS).

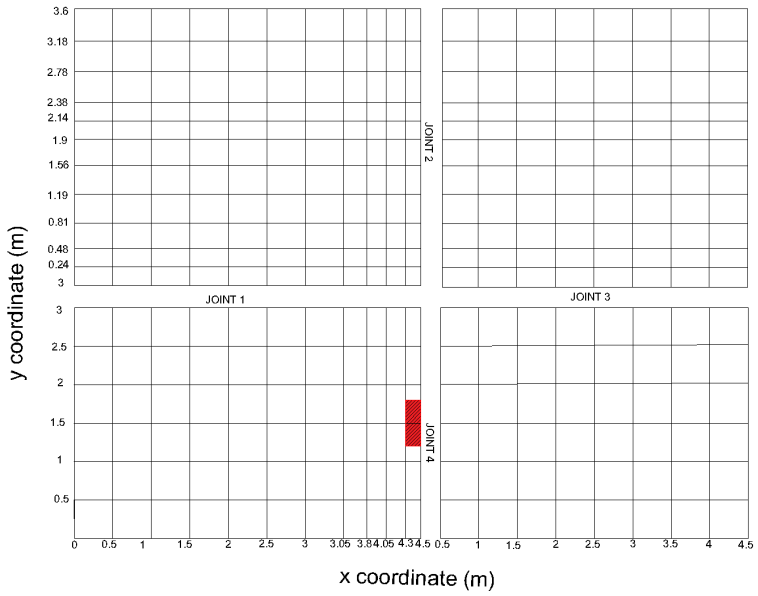

Figure 7.8: *Finite element grid for two-layer RCC pavement analysis*

In this analysis, a single axle load as a uniform load was placed directly on a rectangular area on the edge of the surface layer of the RCC pavement near a transverse joint at 1.5 m from the joint end. The constant parameters were: wheel load (F = 83 kN) and tyre pressure (P = 690 kPa) are assumed according to Huang (2004), slab stiffness as measured in the laboratory test (E for surface layer = 31530 MPa, E for base layer = 33470 MPa), modulus of subgrade reaction (k = 50 kN/m^3) was chosen from the ACI design charts and differential temperatures (-8° C, 11° C) were chosen depending on previous studies (Hiller, 2001; Huang, 2004; Pittman, 1994).

The input variables were: slab depth in mm (D = 150, 175, 200 and 250), slab length in m (L = 3.6, 4 and 4.5) and load transfer stiffness in MN/m^3 (LTS = 100, 1000, 10000). The output data were the maximum deflection, maximum tensile stress, maximum shear stress and number of cycles to failure which was calculated based on maximum stresses.

7.6 Pavement analysis results

7.6.1 Results of stresses in two-layer RCC pavement

The effect of traffic load is the major cause of stresses and deflections in the slab of concrete pavements. Therefore, computing the critical stresses is important in the design of concrete pavements. From analysis of two-layer RCC pavement by KENSLAB with transverse joints, the most critical stresses are found to be along the edge of the slab near the joint in the bottom layer under the load as shown in Figures 7.9, 7.10 and 7.11 for

the tensile stresses, in which it may be observed that the joint stiffness has a major effect on these stresses. Figures 7.13, 7.14 and 7.15 present the relationship between tensile stress and slab thickness for different slab lengths.

It can be seen from these results that while the joint stiffness and slab thickness have a significant effect on the tensile stresses in the lower layer of RCC pavement, the slab length has a relatively minor effect. The reduction in stress is about 25% when the joint stiffness increases from 100 MN/m^3 to 10000 MN/m^3 for a slab thickness 200 mm and this agrees well with Thompson (2001) work on cement bound material. While the reduction in stresses reached to 58% when increased the slab thickness from 150 mm to 250 mm at 1000 MN/m^3 along the joint. In contrast, the reduction was only 2.66% when increasing the slab length from 3.6 m to 4.5 m at 1000 MN/m^3 joint stiffness and 200 mm slab thickness.

Note that increasing slab thickness to 250 mm with a load transfer stiffness 10000 MN/m^3 at slab lengths of 4 m and 3.6 m led to a program error and therefore no results.

Thus, to keep stresses low and, hence, pavement life long, the design should be on the maximum stresses with reasonable slab thickness and sufficient load transfer stiffness.

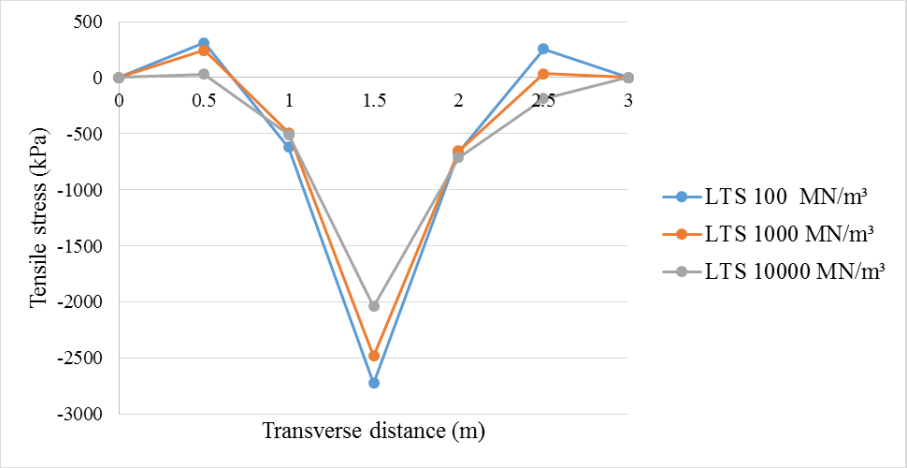

Figure 7.9: *Relationship between tensile stress and transverse distance along the joint at slab thickness 250 mm and slab length 4.5 m (load at transverse distance of 1.5 m)*

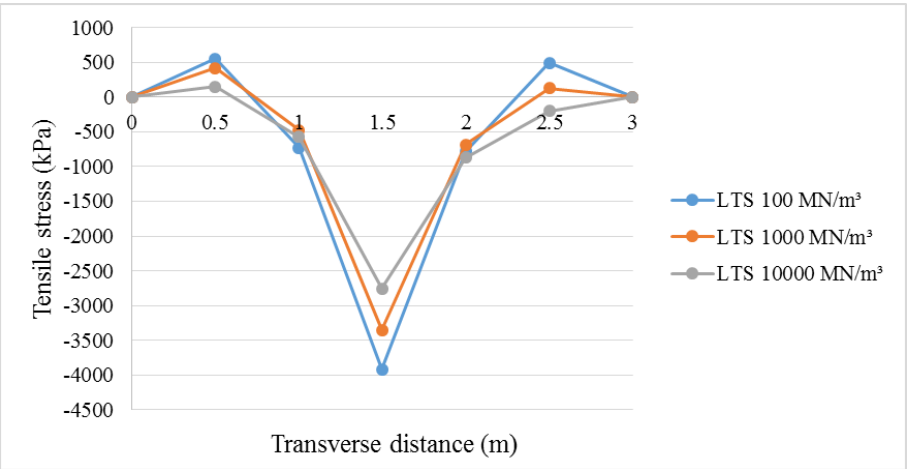

Figure 7.10: *Relationship between tensile stress and transverse distance along the joint at slab thickness 200 mm and slab length 4.5 m (load at transverse distance of 1.5 m)*

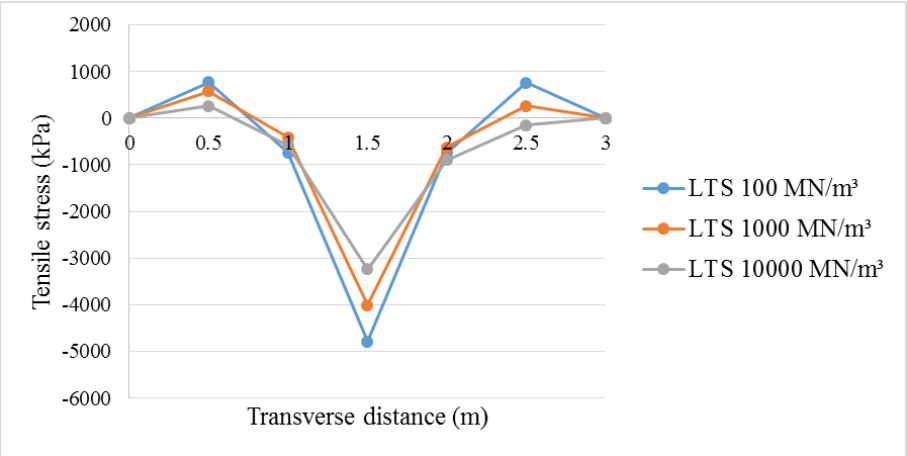

Figure 7.11: *Relationship between tensile stress and transverse distance along the joint at slab thickness 175 mm and slab length 4.5 m (load at transverse distance of 1.5 m)*

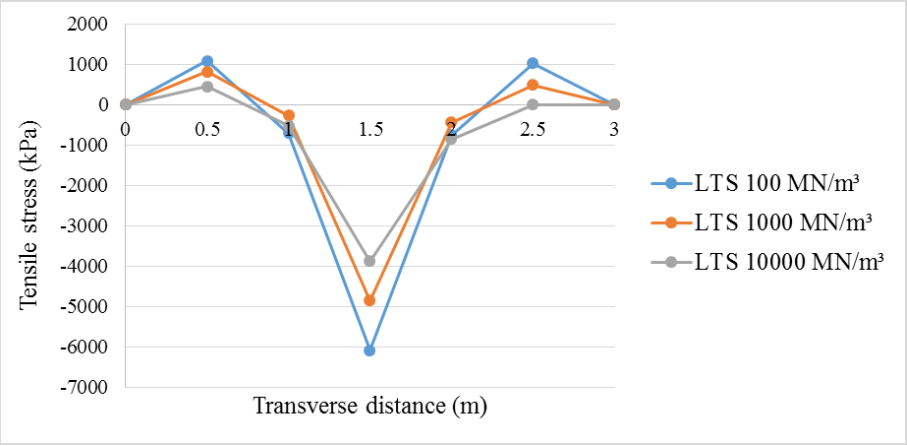

Figure 7.12: *Relationship between tensile stress and transverse distance along the joint at slab thickness 150 mm and slab length 4.5 m (load at transverse distance of 1.5 m)*

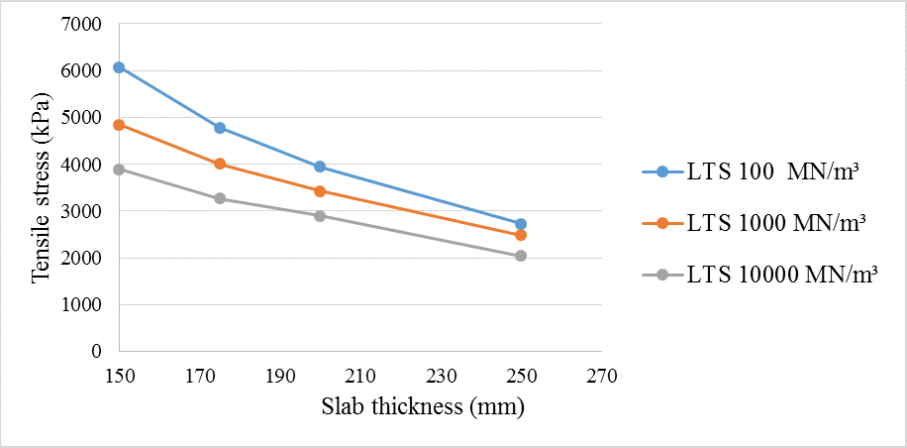

Figure 7.13: *Results for tensile stress at different slab thicknesses with different joint stiffnesses and slab length 4.5 m*

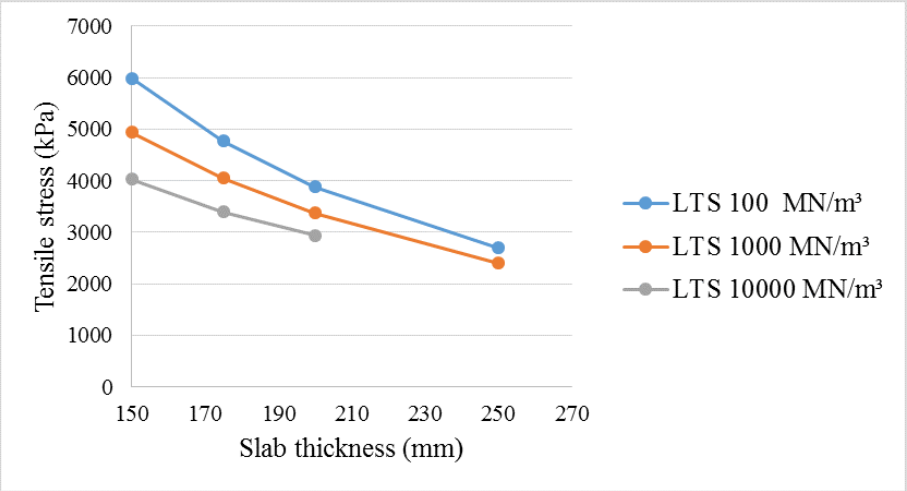

Figure 7.14: *Results for tensile stress at different slab thicknesses with different joint stiffnesses and slab length 4 m*

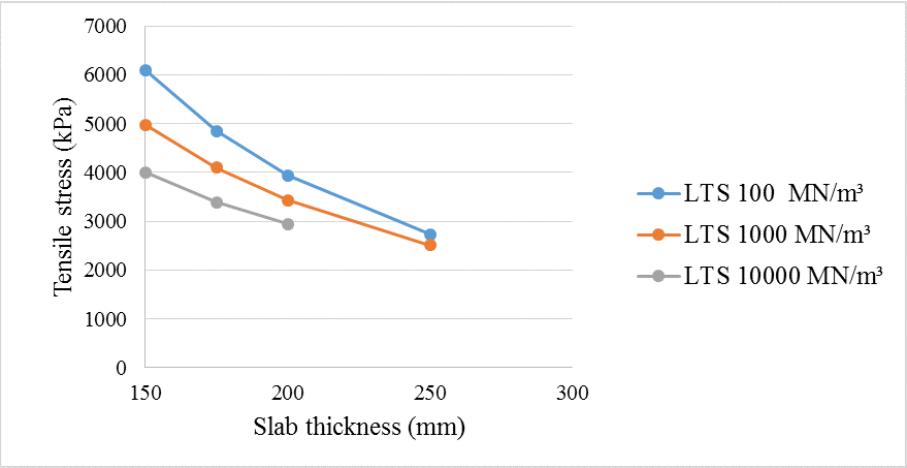

Figure 7.15: *Results for tensile stress at different slab thicknesses with different joint stiffnesses and slab length 3.6 m*

Furthermore, shear stresses along the transverse joint obtained from KENSLAB analysis are presented in Figures 7.16, 7.17, 7.18 and 7.19. It can be observed that increasing load transfer stiffness increased the shear stress. The percentage increase in shear stress, when the load transfer stiffness increased from 100 MN/m^3 - 10000 MN/m^3, reached to three times of minimum load transfer stiffness for a slab thickness of 250 mm and two times for a slab thickness of 150 mm at slab lengths 4.5 m and 3.6 m respectively.

However, when increasing slab thickness from 150 mm to 250 mm the shear stress reduced by about 13% at slab length 4.5 m and 9.5% at slab length 3.6 m as shown in Figures 7.20, 7.21 and 7.22. The effect of slab length on shear stress was negligible, with a variation of 1.9% for a slab thickness of 250 mm and 1.7% for a slab thickness of 150 mm. The full set of results for different slab thicknesses and lengths is given in Appendix B. It can be concluded that shear stresses increased with increasing load transfer stiffness to allow transferring the load in the joint but decreased with increasing slab thickness.

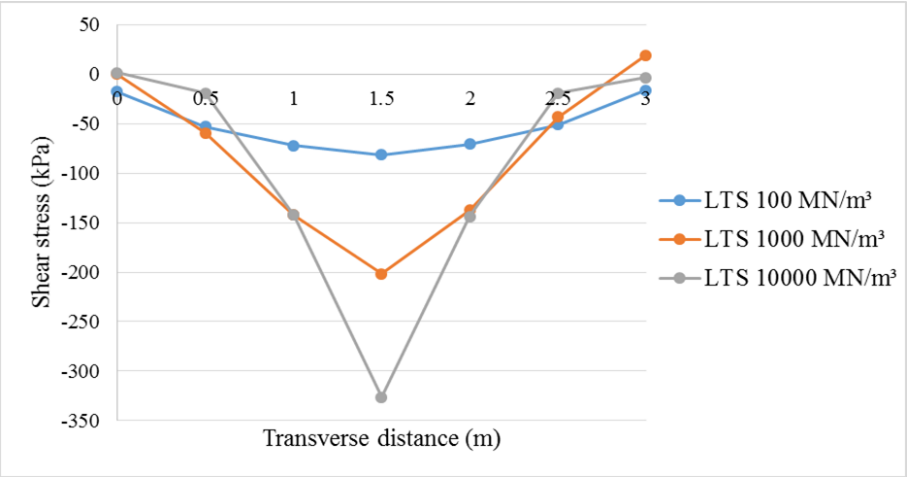

Figure 7.16: *Relationship between shear stress and transverse distance along the joint at slab thickness 250 mm and slab length 4.5 m*

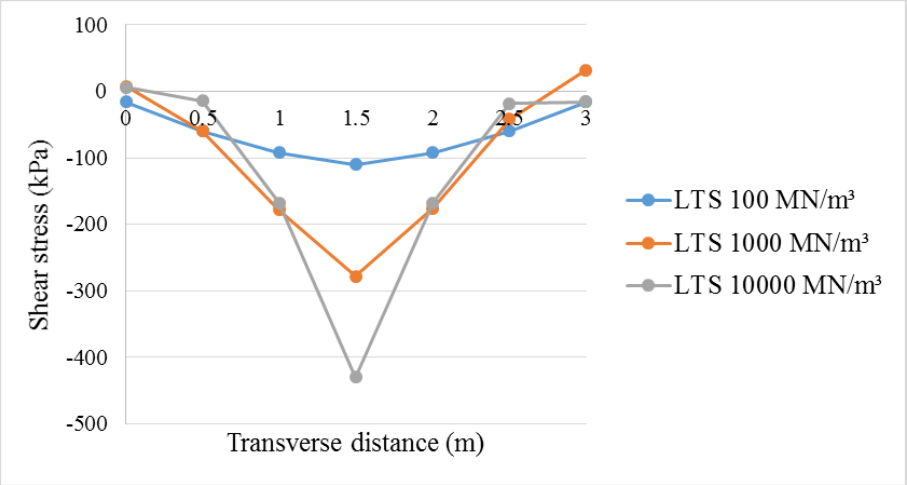

Figure 7.17: *Relationship between shear stress and transverse distance along the joint at slab thickness 200 mm and slab length 4.5 m*

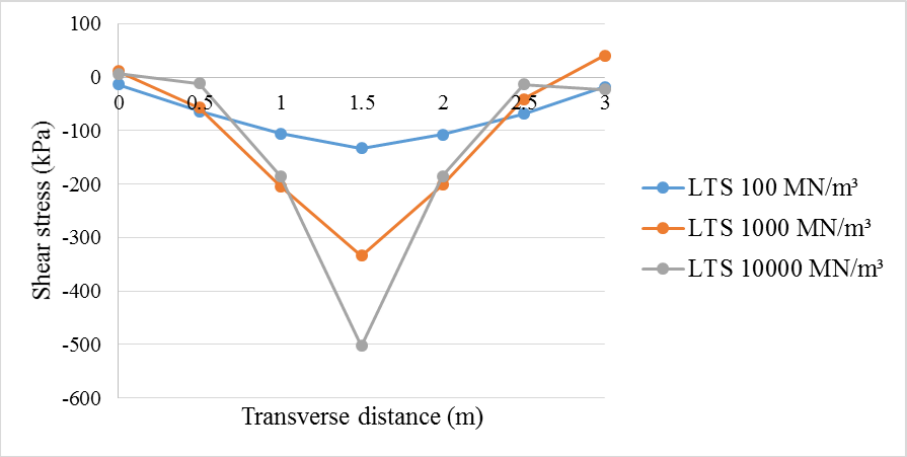

Figure 7.18: *Relationship between shear stress and transverse distance along the joint at slab thickness 175 mm and slab length 4.5 m*

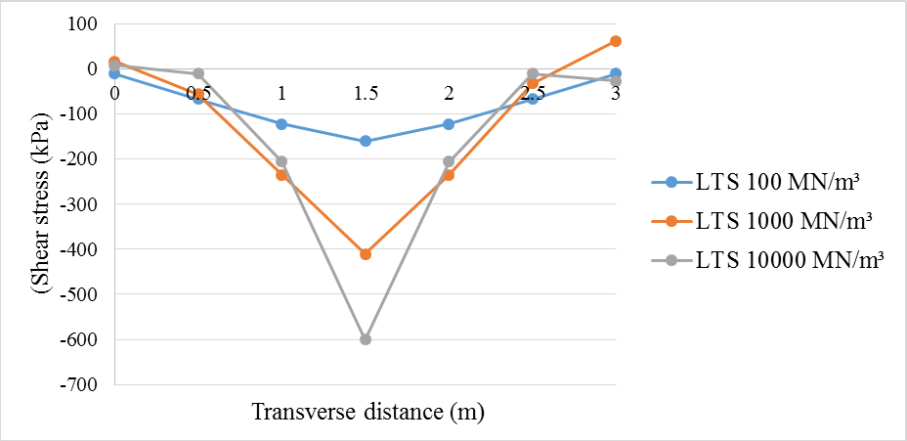

Figure 7.19: *Relationship between shear stress and transverse distance along the joint at slab thickness 150 mm and slab length 4.5 m*

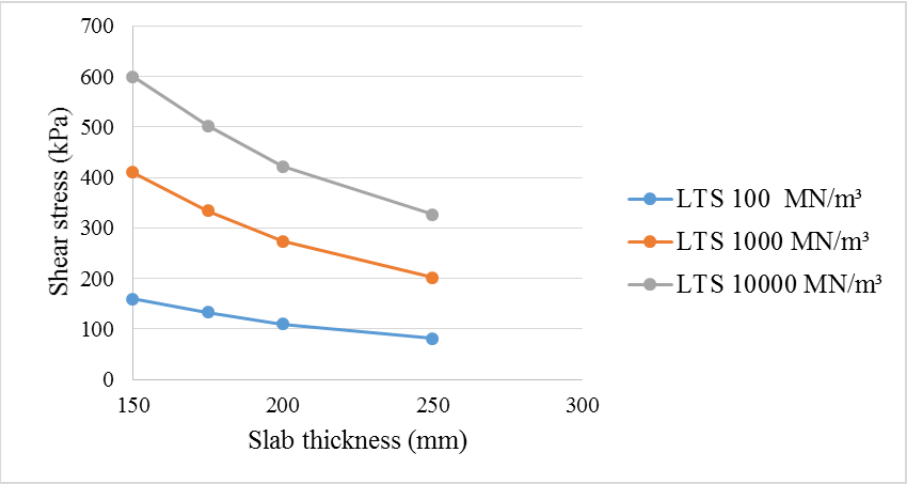

Figure 7.20: *Results for shear stress at different slab thicknesses with different joint stiffnesses and slab length 4.5 m*

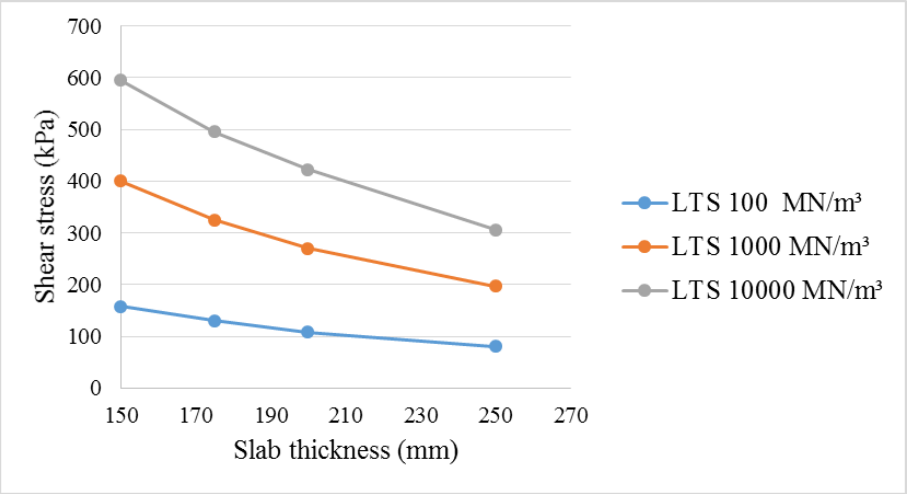

Figure 7.21: *Results for shear stress at different slab thicknesses with different joint stiffnesses and slab length 4 m*

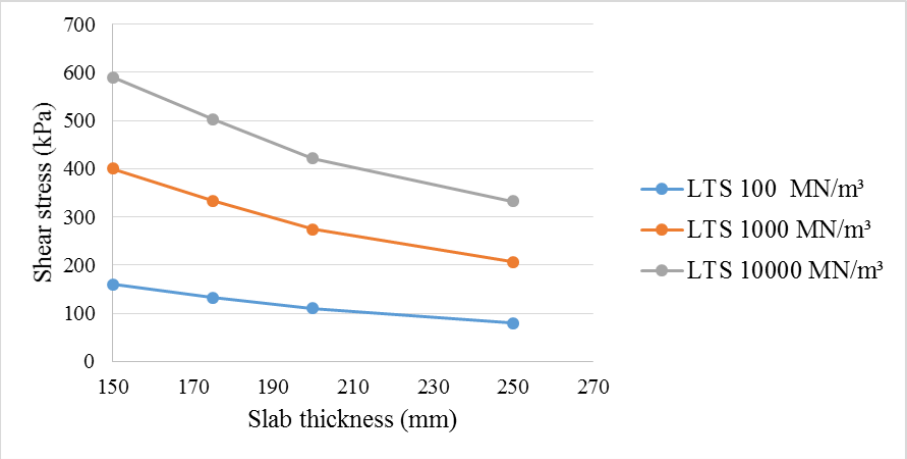

Figure 7.22: *Results for shear stress at different slab thicknesses with different joint stiffnesses and slab length 3.6 m*

7.6.2 Results of deflections for two-layer RCC pavement

As a result of applying traffic load, deflections occur on the two side of the joint/crack as shown in Figure 7.23.

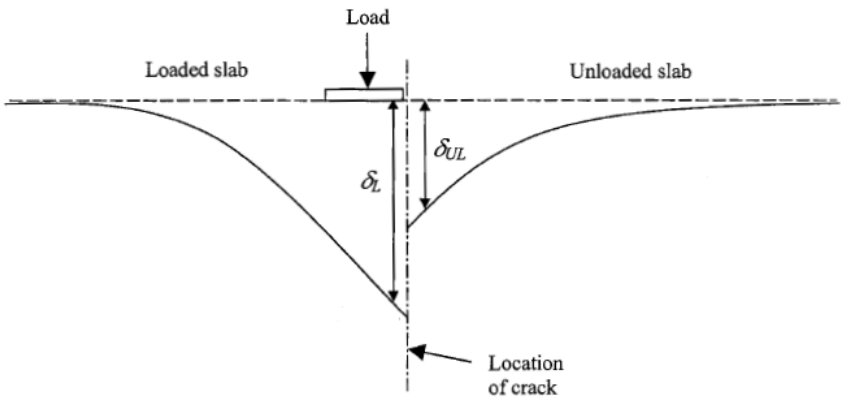

Figure 7.23: *The effect of load on two slabs with crack (Huang, 2004)*

It can be noted that the highest deflection is under the load adjacent to the crack; therefore, the load transfer stiffness will have a significant effect on the deflection. From KENSLAB analysis, the maximum deflection for different slab thicknesses and lengths was computed depending on different load transfer stiffnesses.

Figures 7.24, 7.25, 7.26 and 7.27 show the maximum deflection of a RCC pavement along the transverse joint for different slab thicknesses. It can be seen from these figures that the maximum deflection reduced with increasing load transfer stiffness and slab depth. The reduction is very significant when changing the load transfer stiffness from 100 MN/m^3 to 10000 MN/m^3, about 50% for a slab length of 3.6 m and 45.7% for a slab length of 4.5 m at slab thickness 200 mm as shown in Figures 7.28, 7.29 and 7.30. Also when increasing slab thickness, a significant reduction in deflections occur which can reach to 45% when increase the slab thickness from 150

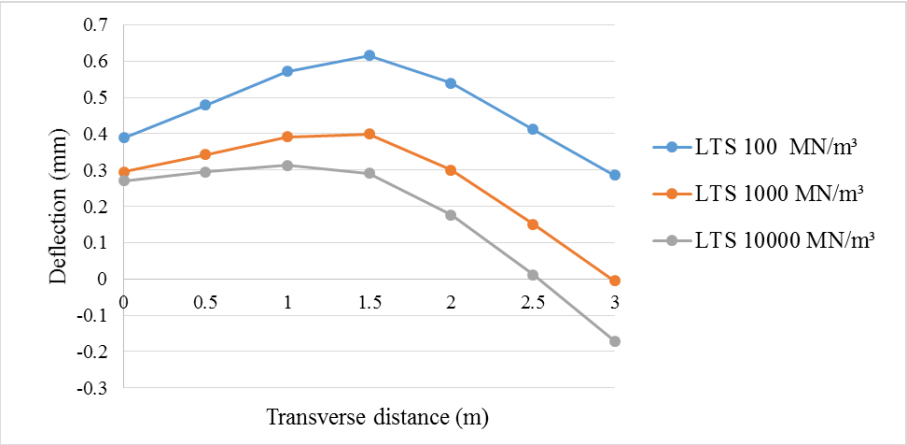

Figure 7.24: *Relationship between deflection and transverse distance along the joint at slab thickness 250 mm and slab length 4.5 m*

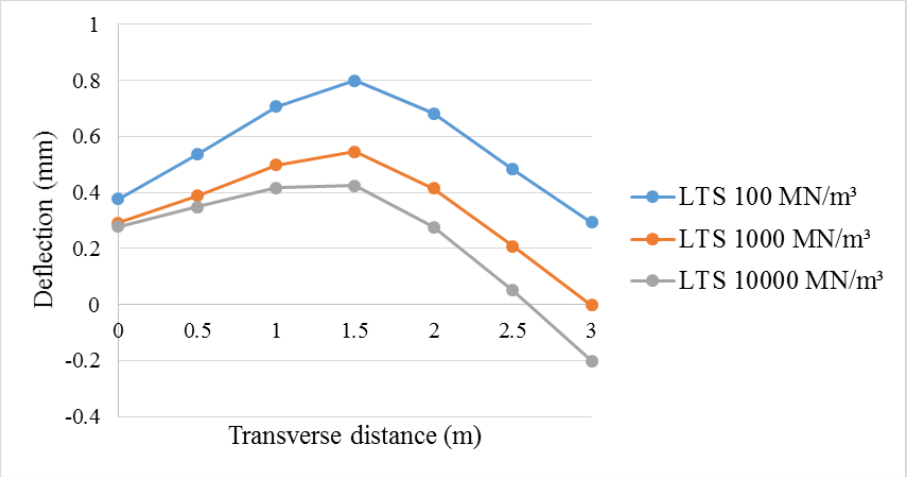

Figure 7.25: *Relationship between deflection and transverse distance along the joint at slab thickness 200 mm and slab length 4.5 m*

mm to 250 mm at 100 MN/m^3 and 4.5 m slab length. However, the slab length has a small effect on deflection of the two-layer RCC system. Therefore, it is important to have adequate load transfer stiffness with reasonable slab thickness in order to reduce the deflections.

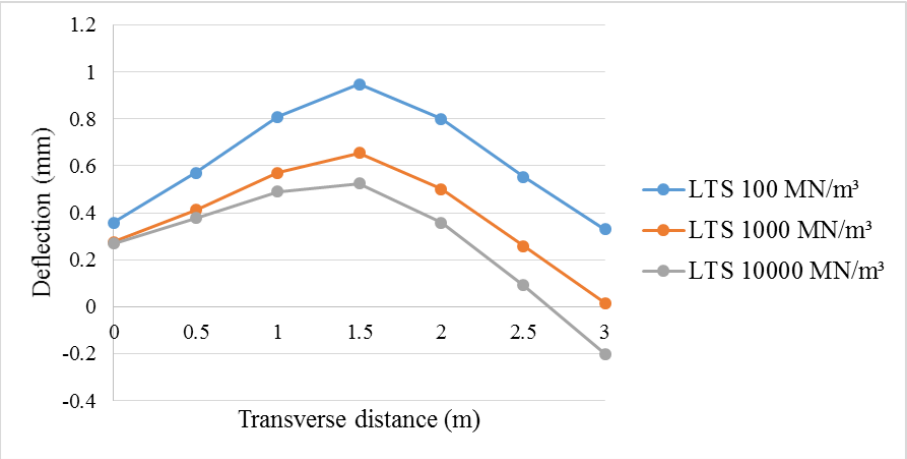

Figure 7.26: *Relationship between deflection and transverse distance along the joint at slab thickness 175 mm and slab length 4.5 m*

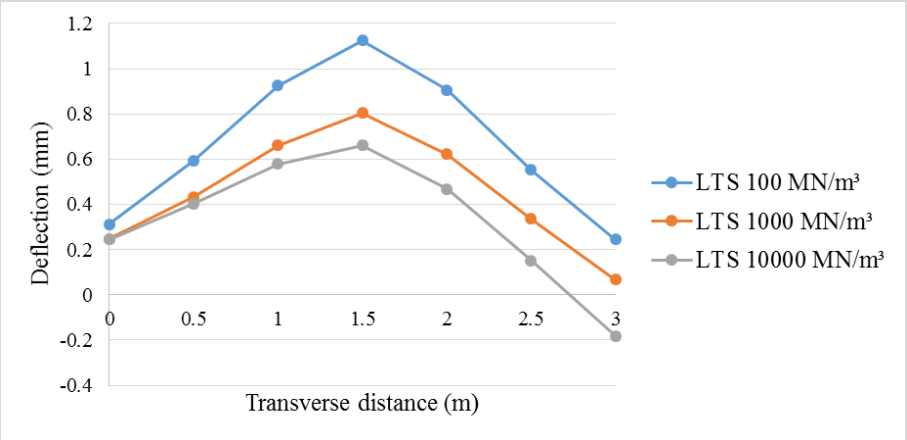

Figure 7.27: *Relationship between deflection and transverse distance along the joint at slab thickness 150 mm and slab length 4.5 m*

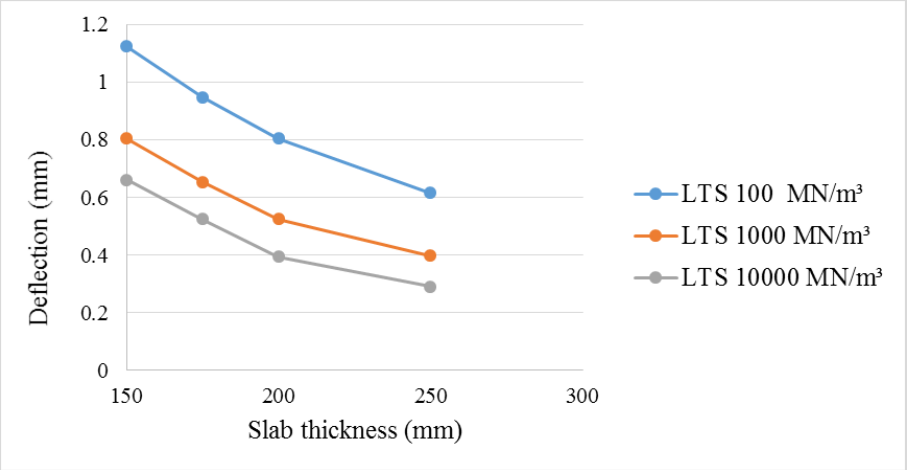

Figure 7.28: *Results for deflection with different slab thicknesses and load transfer stiffnesses at 4.5 m slab length*

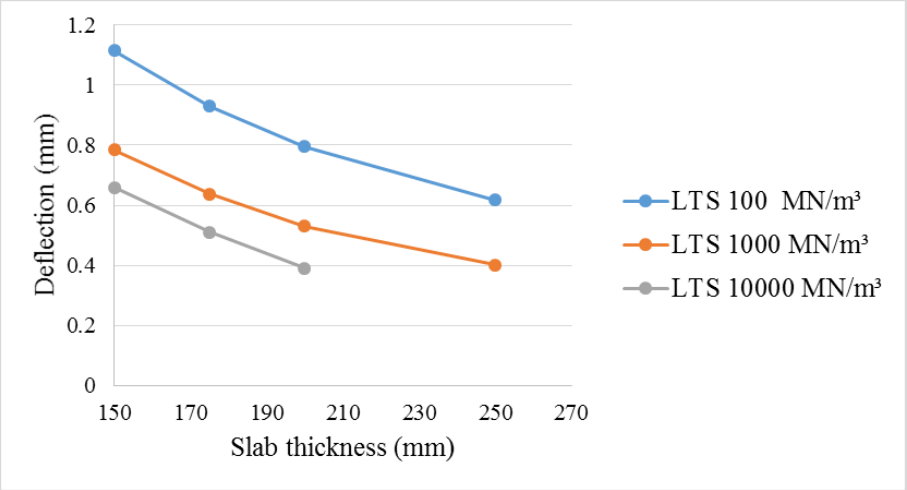

Figure 7.29: *Results for deflection with different slab thicknesses and load transfer stiffnesses at 4 m slab length*

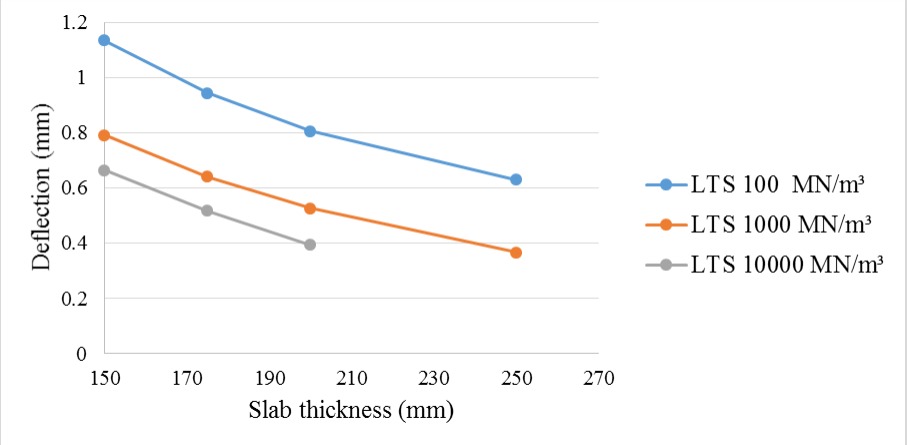

Figure 7.30: *Results for deflection with different slab thicknesses and load transfer stiffnesses at 3.6 m slab length*

7.7 Combined effect of differential temperature and traffic load on two-layer RCC pavement

In concrete pavements, the repeated application of traffic loads along with temperature variation may lead to initiation of cracks at highly stressed locations. The effect of differential temperature between top and bottom of a concrete pavement slab results in curling stresses. Variation in temperature affects the stresses in a concrete slab in two ways. The daily variation in temperature causes relatively quick changes in thermal gradients through the depth of the concrete slab, while seasonal variation results in different average temperatures in the concrete slab and therefore different joint/crack widths. The concrete slab will tend to curl upward or downward when it is subjected to an increasing or decreasing temperature variation through its depth (Maitra et al., 2013). Therefore, joints are used to reduce the curling stresses since these stresses are relieved when concrete cracks. Narrow cracks will not greatly affect the performance of the concrete pavement as long as good load transfer occurs across the cracks (Huang, 2004).

Huang (2004) assumed that the maximum temperature gradient would be between 0.055 and 0.077° C/mm of slab thickness during the day and about half the value in the night. In addition, in the AASHO Road Test, the maximum standard temperature differential for the months of June and July averaged about 10.2° C when the slab curled down and −4.9° C when it curled up, these values correspond to temperature gradients of 0.07° C/mm and 0.03° C/mm, respectively. Figure 7.31 shows the curling of a concrete slab on a liquid foundation.

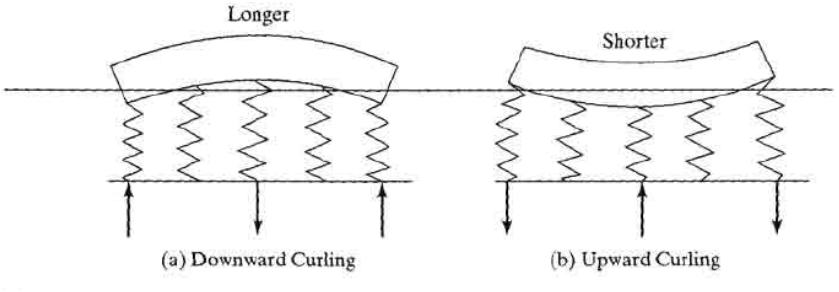

Figure 7.31: *Curling of slab due to temperature gradient (Huang, 2004)*

7.7.1 Results of combined effect on two-layer RCC pavement

The variation of temperature between day and night for different seasons will affect the performance of a RCC pavement. The effect of temperature changes in the slab on the load transfer of joints is seen in two ways. One is by changing the average temperature of the slab. Cooling temperatures cause a larger joint opening or crack width and consequently a reduced load transfer, and vice versa. The other way that temperature affects the load transfer due to aggregate interlock is by creating temperature differentials in the slab, between the top and the bottom (Pittman, 1994).

The results of the differential temperature effect, together with traffic load, on the tensile stress of two-layer RCC are presented in Figures 7.32 and 7.33 for different slab lengths. The results cover the variation of tensile stress during a year for different differential temperatures depending on load transfer stiffness where a negative gradient indicates that the slab curls down and a positive gradient indicates the slab curls up. An increase in load transfer stiffness results in a significant reduction in tensile stress with 200 mm slab thickness while slab length has only a minor effect.

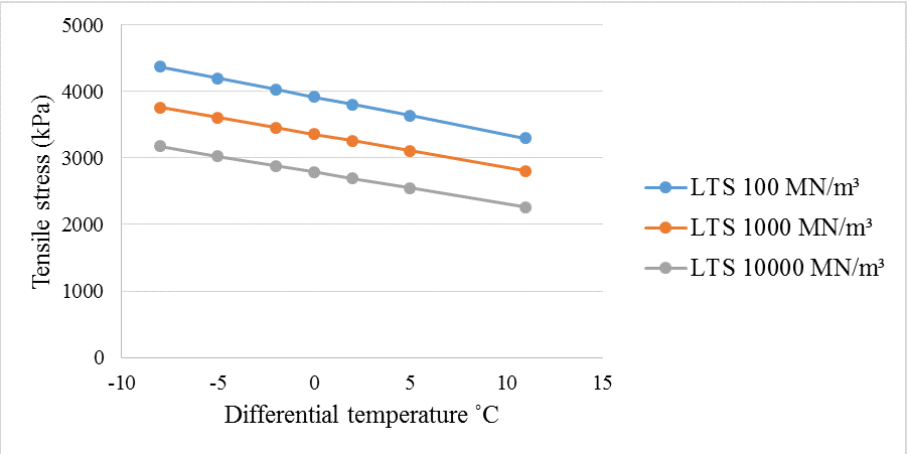

Figure 7.32: *Relationship between tensile stress and differential temperature depending on load transfer stiffness and slab length 4.5 m*

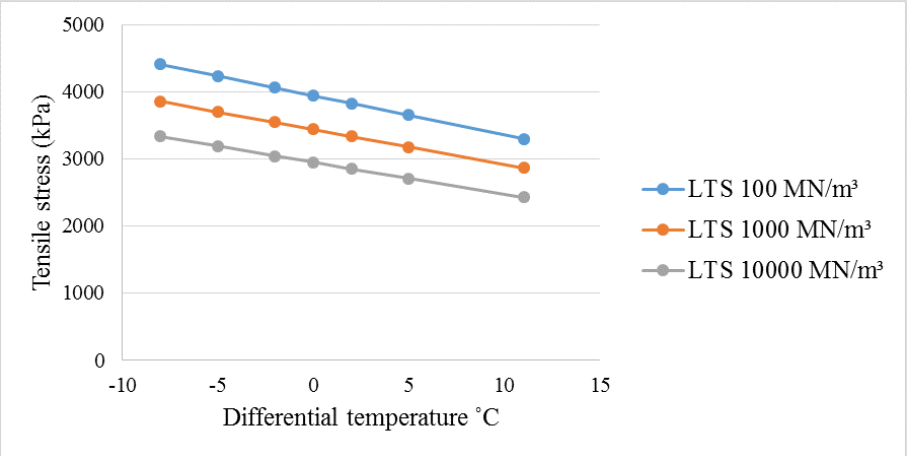

Figure 7.33: *Relationship between tensile stress and differential temperature depending on load transfer stiffness and slab length 3.6 m*

Furthermore, the effect of maximum and minimum differential temperatures on tensile stress for different slab thicknesses is summarised in Figures 7.34, 7.35, 7.36 and 7.37 depending on high and low load transfer stiffness. It can be observed that negative gradient of temperature causes higher tensile stress than a positive gradient. If the temperature of the upper surface of the slab is higher than the bottom surface then the top surface tends to expand and the bottom surface tends to contract resulting in compressive stress at the top and tensile stress at bottom and vice versa. Thus, the

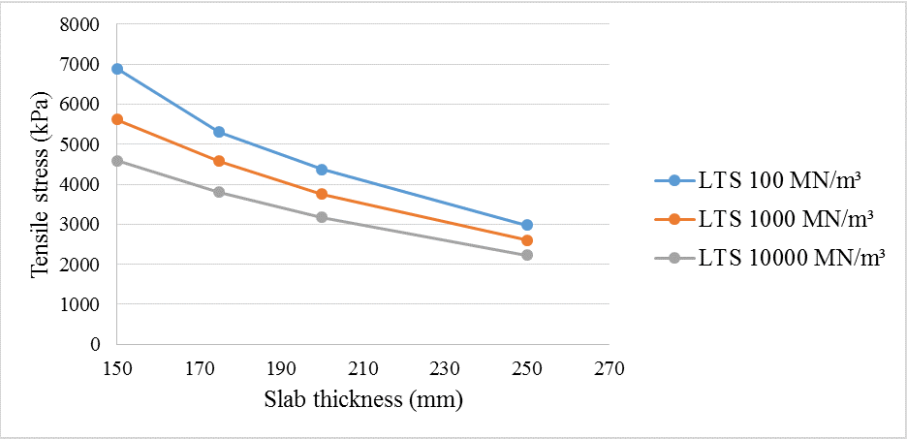

Figure 7.34: *Relationship between tensile stress and differential temperature depending on load transfer stiffness and slab length 4.5 m at −8° C*

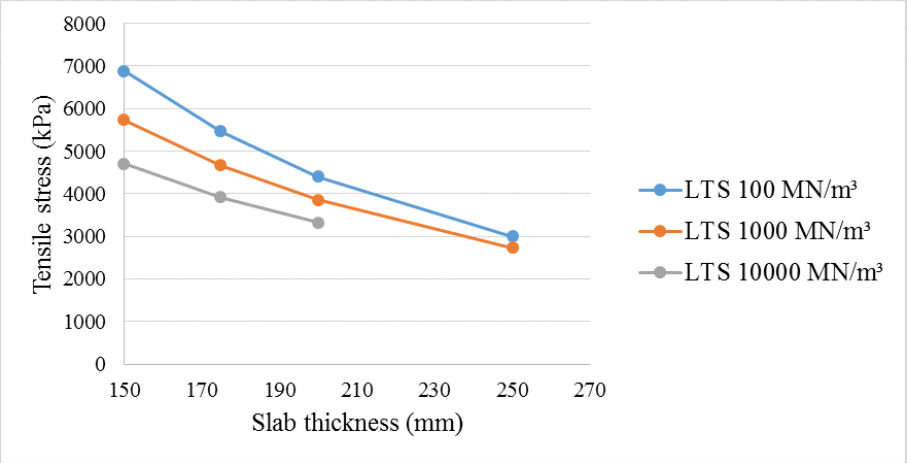

Figure 7.35: *Relationship between tensile stress and differential temperature depending on load transfer stiffness and slab length 3.6 m at −8° C*

stresses resulting from combined effect will increase significantly, where the percentage of increasing for slab thickness of 200 mm reached to 7.2% at 1000 MN/m^3.

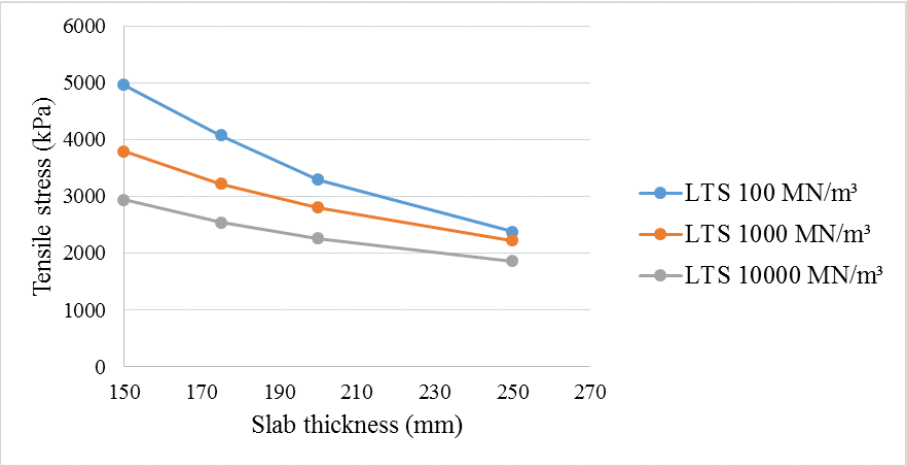

Figure 7.36: *Relationship between tensile stress and differential temperature depending on load transfer stiffness and slab length 4.5 m at +11° C*

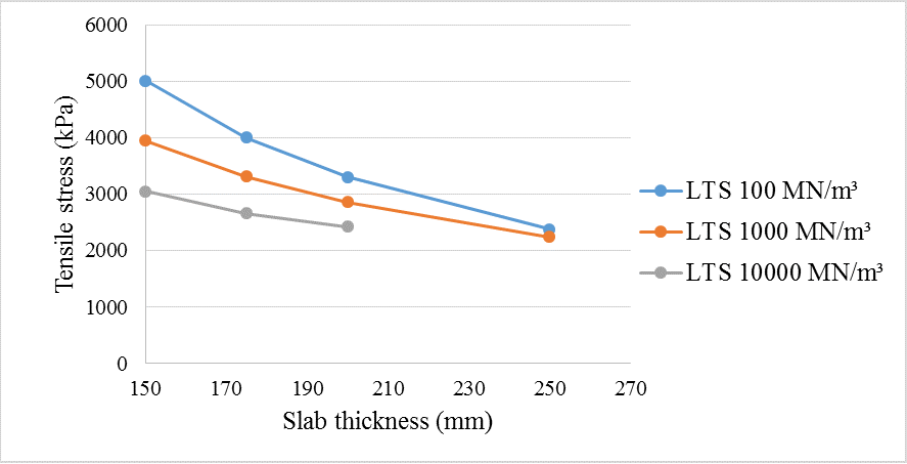

Figure 7.37: *Relationship between tensile stress and differential temperature depending on load transfer stiffness and slab length 3.6 m at +11° C*

7.7.2 Effect of temperature changes on joint spacing

The daily and seasonal temperature variations in a concrete slab have a significant effect on joint spacing. The average temperature of the concrete pavement therfore influences load transfer of joints according to the degree of aggregate interlock. The temperature differential between the top and bottom surfaces determines the degree of warping and the curling conditions at the joint which cause variability in stiffness along the joint (Armaghani et al., 1986). A prediction of joint opening and movement is necessary in order to assess the effects of the environment, concrete material properties and slab geometry on concrete pavement performance. In this research, the prediction of joint opening in two-layer RCC is approximated using Equation 7.1 from the AASHTO pavement design guide (AASHTO 1993) (Roesler and Wang, 2008):

$$\Delta L = CL(\alpha \Delta T + \varepsilon) \tag{7.1}$$

where ΔL = joint opening due to temperature and moisture changes in a concrete pavement (mm); L= slab length (mm); α = coefficient of thermal expansion/contraction of roller compacted concrete (RCC) (strain/°C); ΔT= temperature change (°C); ε = RCC coefficient of drying shrinkage (mm/mm); C = adjustment coefficient to account for the slab-base frictional restraint (0.65 for stabilized bases and 0.8 for granular bases). Figure 7.38 shows the relationship between joint spacing and joint opening calculated from Equation 7.1 with typical values of concrete pavement properties (thermal coefficient and coefficient of drying shrinkage) and a temperature change of 25 °C which is suggested the average joint opening in yearly time interval. Three different slab lengths have been used to pre-

dict joint opening, 3.6 m, 4 m, and 4.5 m. It can be observed that joint opening increases when joint spacing increases at a given temperature. Accurate prediction for joint opening is complex and there many parameters that affect it.

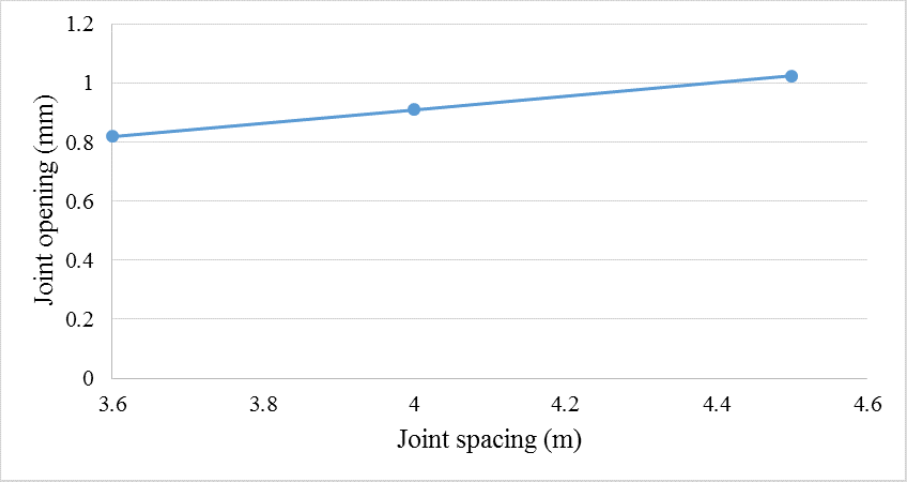

Figure 7.38: *Relationship between joint spacing and joint opening*

7.8 Pavement design sensitivity analysis

The evaluation of the performance of the two-layer RCC pavement was carried out in terms of fatigue life according to the tensile stresses obtained. The fatigue life calculations were made according to laboratory results; Table 6.1 presented the fatigue equations derived in this research. Previous sections showed that the maximum tensile stresses occurred at the bottom of the base layer of the RCC, which mean that these are the stresses appropriate for design purposes.

The fatigue equation used in calculating the fatigue life of two-layer RCC is shown below:

$$LogN_f = 18.45 - 18.09SR \tag{7.2}$$

where N_f is the number of cycles to failure and SR is the stress ratio.

Figures 7.39, 7.40 and 7.41 show the number of cycles to failure with different slab thicknesses for load transfer stiffness between 100 MN/m^3 and 10000 MN/m^3, and slab length 3.6 m, 4 m and 4.5 m. These figures demonstrate that the effect of increasing load transfer stiffness is to increase the number of cycles to failure which means better performance of the two-layer RCC.

However, with the combined effect of traffic load and differential temperature, there is a significant reduction in the number of cycles, particularly at lower load transfer stiffness and slab thickness as shown in figure 7.42. The differential temperature used in this analysis was $-8°$ C as it is showed maximum stresses in the base layer.

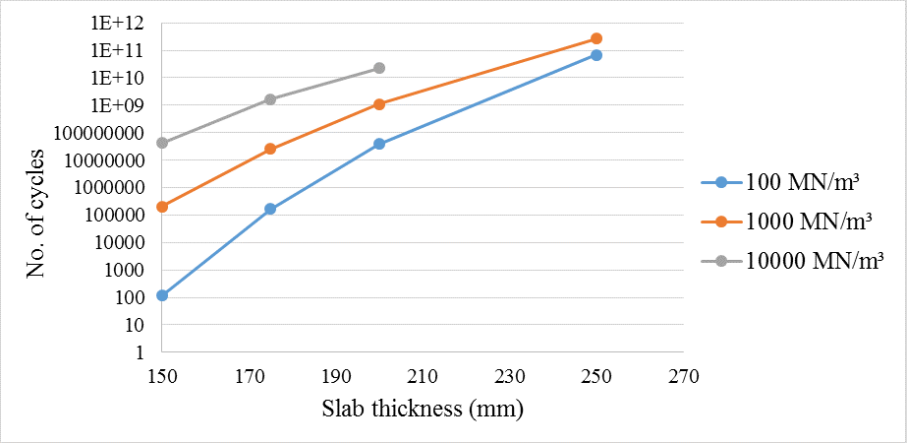

Figure 7.39: *Relationship between number of cycles to failure and slab thicknesses depending on load transfer stiffness at 4.5 m slab length*

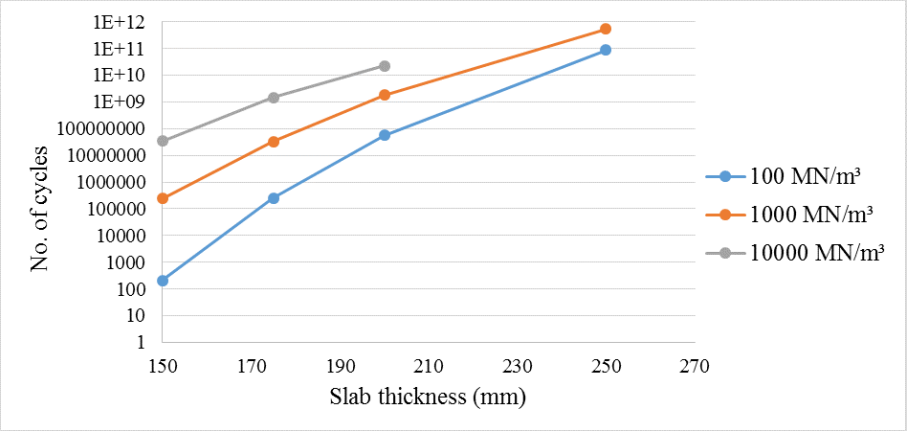

Figure 7.40: *Relationship between number of cycles to failure and slab thicknesses depending on load transfer stiffness at 4 m slab length*

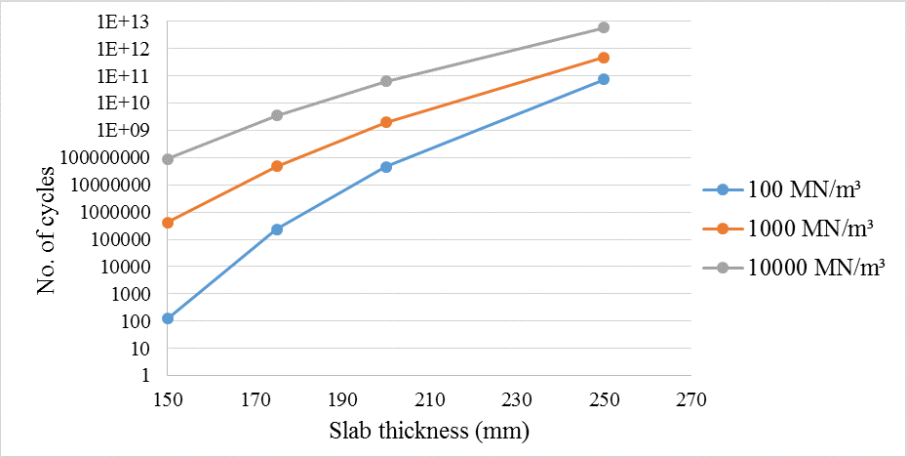

Figure 7.41: *Relationship between number of cycles to failure and slab thicknesses depending on load transfer stiffness at 3.6 m slab length*

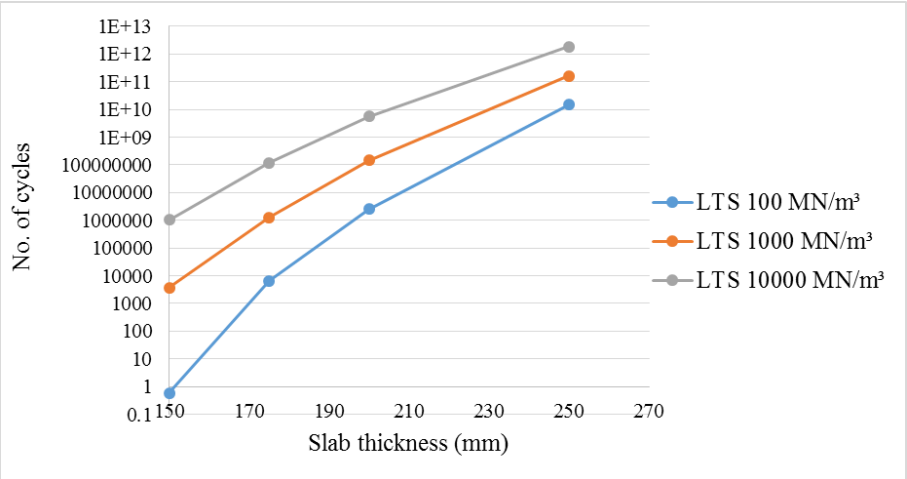

Figure 7.42: *Relationship between number of cycles to failure and load transfer stiffnesses for different slab thickness at −8° C and slab length 4.5 m*

7.8.1 Example design for two-layer RCC pavement

A design example for a major arterial road with an average annual daily traffic (AADT) of 1500, based on ACI 325.12R design charts, for a two-layer RCC pavement has been generated by KENSLAB by calculating the allowable load repetitions for different load transfer stiffnesses and slab widths for a design period of 30 years. Figure 7.43 shows a flowchart of the design methodology for the two-layer RCC pavement depending design parameters such as slab thickness, slab length, subgrade reaction, the stiffness of each layer, the estimated differential temperature and load transfer stiffness. From these inputs, tensile stresses were obtained, then the fatigue life was calculated to check the adequate design life of RCC with reasonable thickness. Finally, the joint deterioration was determined based on reduction in number of cycles to failure as a 90% of life damage. Table 7.1 summarises the values of input data for this example according to laboratory tests and ACI design procedures.

Table 7.1: *Input values of two-layer RCC design example*

Input data	Value
Flexural strength	6.5 MPa
Stiffness of the upper layer	31530 MPa
Stiffness of the lower layer	33470 MPa
Subgrade reaction	50 MPa/m
Differential temperature	-8° C
Thickness of the upper layer	50 mm
Thickness of the lower layer	150 mm
joint spacing	4.5 m, 3.6 m
Single axle load	80 kN

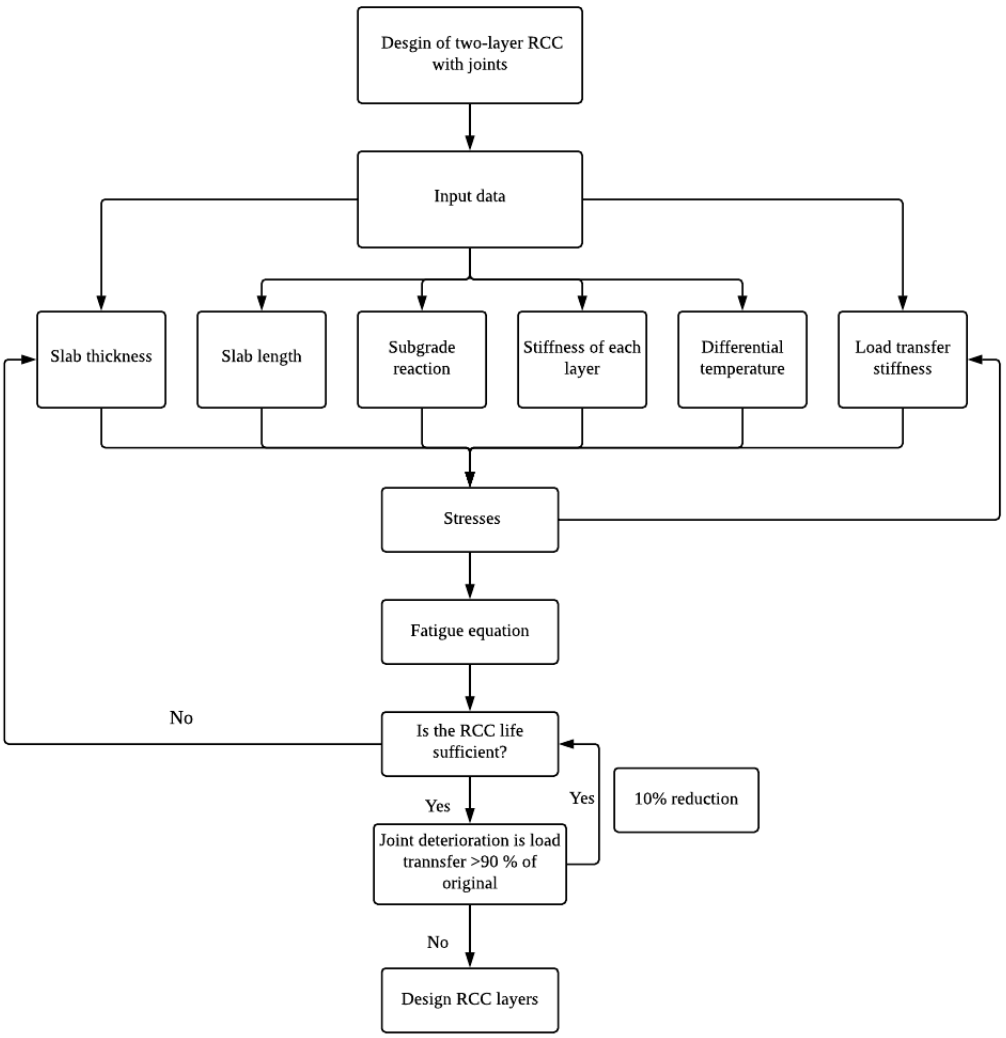

Figure 7.43: *Design flowchart for two-layer RCC pavement*

From this information, stresses are calculated for a range of load transfer stiffnesses from 100 MN/m^3 to 10000 MN/m^3. Then, from the computed fatigue equation in Chapter 6, the number of cycles are obtained. Figure 7.44 presents the number of cycles with different load transfer stiffness at slab widths of 3.6 m and 4.5 m.

Figure 7.43 demonstrates the relationship between load transfer stiffnesses and the number of cycles to failure of two-layer RCC. It can be concluded that in this case the obtained number of cycles is higher than the number

of repetition for 30 years design life (estimated as 16 x 10^6) at load transfer stiffness higher than 100 MN/m^3.

Therefore, in this case 200 mm slab thickness is adequate to achieve good performance of two-layer RCC with a large number of repetitions for long service life. For comparison, the thickness design of RCC based on PCA charts and available information, will be 280 mm and according to ACI-325.12R (2002) will be 230 mm. Thus, the calculated slab thickness is more economical with a large number of allowable load applications.

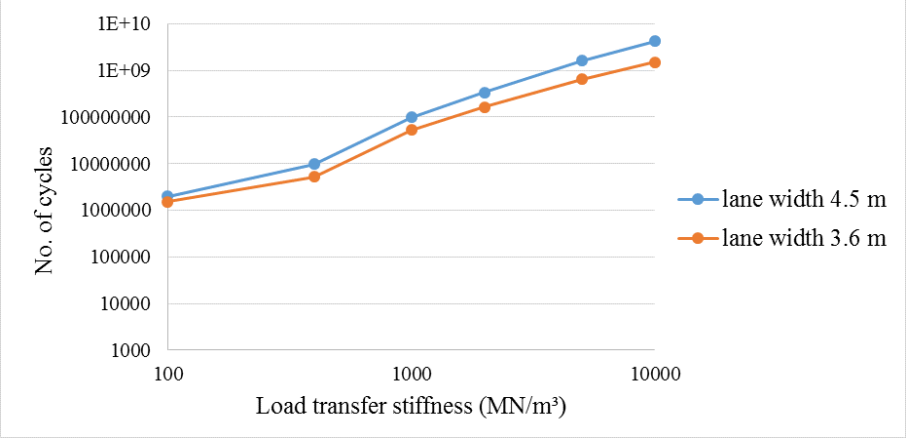

Figure 7.44: *Results for number of cycles to failure aganist load transfer stiffness at slab thickness 200 mm*

7.8.2 Joints deterioration in two-layer RCC

Adequate load transfer through aggregate interlock over a large number of heavy-truck load applications is critical to the satisfactory long-term performance of concrete pavements. Joint deterioration will be taking place throughout the lift of the road and this will have an effect on the service life of the pavements. Therefore, the degree of deterioration expected should be computed.

Colley and Humphrey (1967) found that 90% of the decrease in load transfer stiffness occurred during the first 500,000 load repetitions. Moreover, Raja and Snyder (1991) studied the effect of a number of variables on the rate of deterioration of load transfer capacity through aggregate interlock of transverse cracks and joints in concrete pavements and they found that these parameters have a significant effect on load transfer through aggregate interlock. These variables are:

- Width of crack opening,
- Type and size of coarse aggregate,
- Compressive strength of concrete,
- Applied load magnitude and repetitions,
- Foundation support

Panchmatia et al. (2014) stated that deterioration of joints in concrete pavements can be a function of three issues: structural design, construction practice and material properties. Joint spacing and saw cut depth are examples of structural design parameters that might contribute to joint deterioration. Once this deterioration progresses, it decreases ride quality, increases maintenance costs, and disrupts traffic during maintenance.

Joint deterioration has been calculated approximately in this research from Equation 6.10 with regard to the design example to predict the deterioration of the joints assuming a small crack width of 0.24 mm and initial load transfer stiffness of 1000 MN/m^3.

Figure 7.45 shows the predicted deterioration in this case based on a KENSLAB analysis of shear stress across joints. It can be concluded that the deterioration in this case is relatively moderate reaching to 60%.

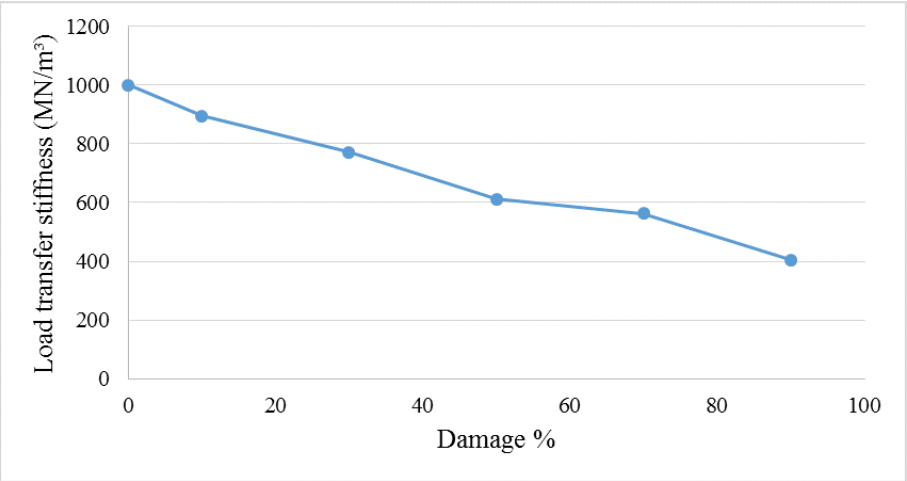

Figure 7.45: *Relationship between load transfer stiffness and the damage ratio at slab thickness 200 mm*

This is a simple example to predict the deterioration of joints in two-layer RCC for pavements. There are many factors have a significant effect on the deterioration such as the differential temperatures between day and night and for different seasons that influenced the crack opening and therefore the load transfer stiffness. Due to limited time of this research, it is recommended to make comprehensive investigation for the deterioration of joints in RCC and concrete pavements.

7.9 Summary

This chapter has summarized the concepts of the design and analysis of concrete pavement and the two-layer RCC system. It presents the most important criteria for designing the thickness according to the allowable load repetitions depending on previous theories and specifications. Theoretical analysis of two-layer RCC has been generated by KENSLAB, a finite element program, for pavement analysis and design in order to compute the maximum stresses and deflections.

Four slabs with four joints have been analysed in this study and the effect of load transfer stiffness on stresses and deflections has been observed. Also, different slab depths and lengths have been evaluated to investigate the best performance of two-layer RCC pavements. The results show the significant effect of load transfer stiffness on stresses and deflections, where increasing it leads to reduced tensile stresses in the base layer and reduced deflections as well.

In addition, the influence of increasing slab thickness is clear with regard to increasing the bending stiffness of the layer, while slab length has only a small effect, especially at higher load transfer stiffness. Moreover, the differential temperature effect together with traffic load shows higher stresses and deflections and therefore lower number of cycles to failure. The effect of temperature changes also was observed to predict the joint opening.

Finally, a design example shows the highest number of cycles with a 200 mm slab thickness that can be withstood successfully with acceptable load transfer stiffness and high strength of RCC. The joint deterioration has been estimated for slab thickness of 200 mm and the results show a rea-

sonable reduction depending on initial load transfer stiffness.

Chapter 8

Conclusions and Recommendations

8.1 Introduction

In this thesis, an investigation and evaluation of a two-layer roller compacted concrete (RCC) system for pavements has been performed. With this purpose, design of the two RCC mixtures with different aggregate sizes and types was studied in Chapter 3 in order to assess the mechanical properties of each RCC mixture.

The bond strength properties of the two-layer RCC with different top layer placement conditions were investigated in Chapter 4 with regard to shear bond strength and indirect tensile strength. In addition, the durability of the two-layer RCC system was evaluated in terms of freezing and thawing cycles.

A brief study of the surface characteristics of the top RCC layer was presented in Chapter 5. Skid resistance and texture depth measurements were carried out on RCC with granite aggregate and maximum size 10 mm.

Furthermore, the performance of the two-layer RCC system under cyclic load was evaluated with regard to fatigue damage and joint deterioration

using a four-point bending test and a cyclic shear test in Chapter 6.
Finally, design and analysis of two-layer RCC systems for pavements was carried out in Chapter 7. The KENSLAB program was used to evaluate the performance of the two-layer system with joints and maximum stresses and deflections calculated. A simple example was also performed to illustrate the potential effectiveness of a two-layer RCC design with a substantial design life.
This chapter summarizes the main issues that discussed in each of the previous chapters. The main conclusions and findings are presented in section 8.2. Some recommendations are given in section 8.3. for future work.

8.2 Conclusions

8.2.1 RCC mix design and production

The design and production of RCC mixtures were investigated in Chapter 3 to determine the best proportions of materials and to achieve suitable density, compacity and mechanical properties. Two mixtures were chosen for the two-layer RCC system with different aggregate sizes and types in order to evaluate general pavement applications.
Two methods of producing RCC samples were trialled in this research, namely a laboratory roller compactor and a vibrating hammer in order to evaluate the effectiveness of the laboratory roller compactor for RCC mixture.
The mechanical properties measured in this evaluations were compressive strength, flexural strength, indirect tensile strength and modulus of elasticity. Based on the laboratory experiments and analyses, the following

conclusions can be drawn:

- It can be concluded that RCC mixes provided sufficient mechanical performance when using granite and limestone aggregates in the two-layer RCC pavement comparable to conventional concrete (wet-formed concrete).
- Use of the laboratory roller compactor delivered well mixtures for both RCC layers, although compaction was slightly less than with the vibrating hammer. Thus, it can be concluded that using a laboratory roller compactor has an advantage in producing RCC specimens as it can simulates the real situation in the field.

8.2.2 The two-layer RCC system

The purpose of the two-layer RCC system was discussed in Chapter 4. The system was assessed with regard to bond strength between the two layers with different placement conditions in terms of shear bond strength and indirect tensile strength.

Three cases were chosen as the most reasonable options for placing the two layers of RCC in the field. These cases were Case 1, where the two layers were placed within one hour, Case 2, where the upper layer was placed three hours after the lower layer, and Case 3, where the upper layer was placed 24 hours after the lower layer. The durability of each case was then investigated with regard to freezing and thawing test. The conclusions of the study can be summarized as follows:

- Users should seek to place the upper layer of RCC within one hour of placing the first, in order to achieve good bond strength and mono-

lithic lifts. If this cannot be guaranteed the pavement life reduction of 57 % should be expected for three hours delay of placement.

- Case 1 showed the best bond strength, the bond between the two layers being as strong as continuous concrete (one layer concrete). However, for Case 2 and Case 3 the delay in placement affected the bond strength, Case 3 showing the lowest value.

- The results for durability indicated good performance for Case 1 and Case 2, while much poorer durability was achieved in Case 3. It can be concluded that a weak bond between the two layers will cause reduced durability due to increased voids and localised weak points in the mixture.

- In order to improve the bond strength for Case 2 and Case 3, two different methods were trialled, namely roughening of the lower surface before placing the upper layer and using an interlayer bonding agent, i.e. cement mortar between the two layers. The results showed limited effect for Case 3 when using cement mortar as interlayer bond. While roughening did not influence the bond strength.

8.2.3 Surface characteristics of RCC

The characteristics of the surface of the upper layer of RCC in this research was presented briefly in Chapter 5. The main limitations of using RCC in highways and normal roads are the surface texture and surface evenness. Therefore, this research suggested a two-layer RCC system with a surface-appropriate upper layer. The results for the upper layer RCC with granite aggregate and maximum size 10 mm indicated that the surface met

the minimum requirement for skid resistance and texture depth based on standard specifications.

Therefore, it is possible to make RCC pavement which can be directly traffic without necessarily giving rise to skid resistance issues, however, proper aggregate size and type should be chosen and proper mixture for good texture with low noise should be designed.

8.2.4 Performance under cyclic load

In Chapter 6, the effect of repeated load on the two RCC layers was evaluated with reference to fatigue damage and load transfer stiffness at joints. The fatigue life of each RCC mixture for the three placement cases was measured using the four-point bending test in order to determine a relationship between stress ratio and number of cycles to failure. The results demonstrated similar fatigue behaviour for RCC mixtures to that of conventional concrete pavement or other types of cement bound materials with acceptable fatigue strength for each mixture. However, Cases 2 and 3 showed reduced fatigue life compared to Case 1, where the reduction were 25% for Case 2 and 67% for Case 3.

Therefore, delayed placement of the second layer of a RCC system can result in 50-70% reduction in pavement life compared with a two-layer RCC pavement in which the second layer is added within one hour.

The load transfer stiffness of the two-layer RCC system was assessed based on cyclic shear test with different crack widths, applied shear stresses and placement conditions. It can be concluded from the results that the crack width has a major effect on the load transfer stiffness, more than the other parameters, as increasing the crack width reduced the friction connection

across the joint due to loss of aggregate interlock. Moreover, increasing the applied shear stress increased the load transfer stiffness and the delay in placement of the upper layer reduced the load transfer stiffness.
To predict the joint deterioration, an approximate equation was developed based on laboratory results, related to material strength, crack width, shear stress and number of load applications.

8.2.5 Design and analysis of two-layer RCC

Chapter 7 discussed the structural design and modelling of RCC pavement with a two-layer system. Four slabs with four joints were modelled in KENSLAB, a finite element program, in order to perform analysis and design. Different slab lengths and thicknesses were evaluated with a wide range of load transfer stiffness across the joints, under the effect of traffic load and differential temperatures. As a result of this study, the following conclusions are put forward:

- The maximum RCC stresses and deflections were found under the load in the base layer along the joint.
- Load transfer stiffness has a significant effect on stresses and deflections, where increasing load transfer stiffness reduced stresses and deflections.
- Increasing slab thickness reduces the stresses and deflections. However, slab length was observed to have only a minor influence on stresses and deflections.
- The design example for the two-layer RCC in pavement showed that

the fatigue life of this type of pavement depended on load transfer stiffness. It can be concluded that to get a long-lasting design without excessive thickness, it is necessary to select a mix strength and layer joint spacings according to procedures discussed in Chapter 7.

- Joints deterioration was computed depending on the equation from Chapter 6. It can be concluded that two-layer RCC can be designed to have an acceptable range of deterioration of load transfer stiffness at realistic crack or joint width.

8.3 Recommendations for further research

Due to the limited time and resources available for this study, some research areas need more investigation to expand the applications of two-layer RCC in pavements. These can be summarised as follows:

1- RCC in highway pavements has limitations related to evenness of the surface texture. Improvements may be possible using additives such as viscosity modifying admixtures for the concrete mixture to increase viscosity of concrete during compaction or by plant-based techniques (i.e. digital rolling control). Such research would require a large scale field trial.

2- Roughening the lower layer of RCC was used to improve the bond strength properties in the two-layer RCC system when a delay occurred. However, in static tests, namely shear bond strength and indirect tensile strength, roughening did not improve the bond properties. In contrast, in dynamic tests, namely cyclic shear test, the results showed a significant improvement in load transfer stiffness. Therefore, it is suggested that shear stresses with and without roughening should be investigated using an advanced finite element program.

3- There is a significant effect of moisture and differential temperature on load transfer stiffness and crack or joint width and therefore on two-layer systems of RCC with different placement conditions. It is recommended to make comprehensive analysis of the influence of these parameters on two-layer RCC with joints in pavements.

4- The delay in placing two layers has an impact on bond properties. In this research, two methods have been used to improve bond strength when the delay in placement more than three hours with mixed success. It is

suggested that different ways to develop good bond in multi-lift concrete pavements should still be sought.

5- Joint deterioration was assessed based on laboratory results and an approximate equation developed. It is suggested to make a site investigation for the deterioration of joints in two-layer RCC and compare it with the current study. This investigation could be carried out by a falling weight deflectometer (FWD) and finite element program.

6- As the two-layer RCC system showed good properties and performance, it is suggested to make field trials to compute stresses and deflections in different types of road in order to compare the site results with laboratory results obtained from this research.

7- To cover all aspects of two-layer RCC in pavements, a life cycle cost analysis is recommended. This should include the use of recycled materials to reduce cost and develop more environmentally friendly RCC pavements

8- The advantages of RCC in pavements makes it a good choice for many pavement applications. However, a reliability analysis with probabilistic model for long design life would be beneficial for the two-layer RCC system to predict the actual service life and reduce maintenance and rehabilitations.

References

Abdel-Maksoud, M. G., Hawkins, N., & Barenberg, E. (1997). Behavior of concrete joints under cyclic shear. In: *Aircraft/Pavement Technology In the Midst of Change*.

ACI-116 (2000). Cement and concrete terminology. Technical report, ACI Committee 116.

ACI-207.5R (1999). Roller-compacted mass concrete. Technical report, ACI Committee 207.

ACI-309 (2000). Compaction of roller compacted concrete. Technical report, ACI Committee 309.5R.

ACI-325.10R (2001). Report on roller-compacted concrete pavements. Technical report, ACI Committee 325.

ACI-325.12R (2002). Guide for design of jointed concrete pavements for streets and local roads. Technical report, ACI Committee 325.

Adaska, W. S. (2006). Roller-compacted concrete (rcc). In: *Significance of Tests and Properties of Concrete and Concrete-making Materials*. ASTM International.

Ahsan, R. (1982). Fatigue in concrete structures. In: *BSRM Seminar on fatigue properties of construction steel*.

Alshareef, H. N. (2011). Assessing asphalt and concrete surface texture in the field. Master's thesis, university of baghdad.

Ameen, P. & Szymanski, M. (2006). Fatigue in plain concrete. *Phenomenon and Methods of Analysis, Chalmers University, Goteborg, Sweden*.

Amer, N. H., Storey, C. S., & Delatte, N. J. (2008). Effect of density on mechanical properties and durability of roller compacted concrete. Technical report, Portland Cement Association.

Antrim, J. D. (1965). A study of the mechanism of fatigue in cement paste and plain concrete. Technical report, Purdue University.

Armaghani, J. M., Lybas, J. M., Tia, M., & Ruth, B. E. (1986). Concrete pavement joint stiffness evaluation. *Transportation Research Record*, 1099:22–36.

Arnold, S. J. (2004). *Load transfer across cracks and joints in concrete slabs on grade*. PhD thesis, Loughborough University.

ASTM-E1845 (2001). Standard practice for calculating pavement macrotexture mean profile depth. Technical report, ASTM International, West Conshohocken, PA.

ASTM-E303 (2013). Measuring surface frictional properties using the british pendulum tester. Technical report, ASTM International, West Conshohocken, PA.

Babu, D. S. (2009). *Mechanical and deformational properties, and shrinkage cracking behaviour of lightweight concretes*. PhD thesis.

Brown, S. F. (2013). An introduction to asphalt pavement design in the uk. In: *Proceedings of the Institution of Civil Engineers-Transport*, volume 166, pages 189–202. Thomas Telford Ltd.

Burwell, Brent Oklahoma, A., Byers, M., Delatte, N., Edwards, J., Fightmaster, M., Flynn, M., Forrestel, S., et al. (2014). *Roller-Compacted Concrete Pavements as Exposed Wearing Surface*. ACPA Guide Specification, Version 1.2.

Cable, J. K., Frentress, D. P., & Williams, J. A. (2004). Two-lift portland cement concrete pavements to meet public needs. Technical report, Center for Transportation Research and Education Iowa State University, final report DTF61-01-X-00042 (Project 8).

Cackler, E. T., Harrington, D. S., & Ferragut, T. (2006). Evaluation of us and european concrete pavement noise reduction methods. Technical report, Federal Highway Administration (FHWA), National Concrete Pavement Technology Center Iowa State University.

Chen, H. (2005). Evaluation of finite element software for pavement stress analysis. In: *Masters Abstracts International*, volume 47.

Choi, Y.-K. & Groom, J. L. (2001). Rcc mix design—soils approach. *Journal of materials in Civil Engineering*, 13(1):71–76.

Chun, Y., Naik, T., & Kraus, R. (2008). Roller-compacted concrete pavements. Technical report, University Of Wisconsin, Report No. CBU-2008-03.

Colley, B. & Humphrey, H. (1967). *Aggregate interlock at joints in concrete pavements*. Portland Cement Association Illinois.

Darestani, M. Y. (2007). *Response of concrete pavements under moving vehicular loads and environmental effects*. PhD thesis, Queensland University of Technology.

de Oliveira, J. R. M. (2006). *Grouted macadam: material characterisation for pavement design*. PhD thesis, University of Nottingham.

Deen, R. C., Havens, J. H., Rahal, A. S., Azevedo, W., et al. (1979). Cracking in concrete pavement.

Delatte, N. (2004). Simplified design of roller-compacted concrete composite pavement. *Transportation Research Record: Journal of the Transportation Research Board*, (1896):57–65.

Delatte, N. J. (2014). *Concrete pavement design, construction, and performance*. CRC Press.

Donegan, J. P. (2011). *Roller compacted concrete*, chapter 48, ICE Manual of Highway Design and Management. Institution of Civil Engineers.

Ergun, M., Iyinam, S., & Iyinam, A. F. (2005). Prediction of road surface friction coefficient using only macro-and microtexture measurements. *Journal of Transportation Engineering*, 131(4):311–319.

ERMCO-Guide (2013). Ermco guide to roller compacted concrete for pavements. *ERMCO, European Ready Mixed Concrete Organization*.

Farhan, A. H. (2016). *Characterization of rubberized cement-stabilized roadbase mixtures*. PhD thesis, University of Nottingham.

FHWA, F. H. A. (1990). Concrete pavement joints, technical advisory 5040.30. *FHWA, US Department of Transportation*.

Fuchs, F. (1991). Achieving and maintaining the evenness of concrete pavements. Technical report, Permanent International Association of Road Congresses.

Fuhrman, R. L. (2000). *Engineering and design roller compacted concrete by us army corps*, (manual no. 1110-2-2006 ed.). U.S. Army Corps of Engineers.

Gallaway, B. M., Epps, J. A., & Tomita, H. (1971). Effects of pavement surface characteristics and textures on skid resistance. Technical report, Texas Transportation Institute.

Garber, S., Rasmussen, R. O., & Harrington, D. (2011). Guide to cement-based integrated pavement solutions. Technical report, Institute for Transportation Iowa State University and Portland Cement Association.

Griffiths, G. & Thom, N. (2007). *Concrete pavement design guidance notes*. CRC Press.

Grove, J. & Taylor, P. (2010). Two-lift construction to address today's challenges. In: *11th 7 International Symposium on Concrete Roads, Seville, Spain*.

Guyer, J. P. (2013). Introduction to roller compacted concrete pavements. Technical report, Continuing Education and Development.

Halsted, G. (2009). Roller-compacted concrete pavements for highways and streets. In: *Annual conference and exhibition of the transportation association of Canada-transportation in a climate of change, Vancouver, British Columbia*.

Hammons, M. I. & Ioannides, A. M. (1997). Advanced pavement design: Finite element modeling for rigid pavement joints. report 1: Background investigation. Technical report, Army engineer waterways experiment station vicksburg ms Geotechnical lab.

Hammons, M. J. (1998). Advanced pavement design: Finite element modeling for rigid pavement joints, report ii: Model development. Technical report, Army engineer waterways experiment station vicksburg ms.

Harrington, D., Abdo, F., Adaska, W., Hazaree, C. V., Ceylan, H., & Bektas, F. (2010). Guide for roller-compacted concrete pavements.

HD36/06 (2006). *Surfacing Materials for New and Maintenance Construction*, (volume 7, section 5, part 1 ed.). Design manual for roads and bridges.

Hiller, J. E. (2001). Optimizing the efficiency of transverse joints and cracks in roller-compacted concrete (rcc) pavements. Technical report, Portland Cement Association, RD No. 2421.

Hosking, R. (1992). *Road aggregates and skidding.* HMSO publications centre.

Hu, J., Siddiqui, M. S., & David Whitney, P. (2014). Two-lift concrete paving–case studies and reviews from sustainability, cost effectiveness and construction perspectives. In: *TRB 93rd Annual Meeting Compendium of Papers.*

Huang, Y. H. (2004). *Pavement analysis and design.* Pearson prentice hall, Pearson education, Inc.

Ioannides, A. M. & Korovesis, G. T. (1990). Aggregate interlock: A pure-shear load transfer mechanism. *Transportation Research Record*, (1286).

Jafarifar, N. (2012). *Shrinkage behaviour of steel-fibre-reinforced-concrete pavements*. PhD thesis, University of Sheffield.

Keifer, O. (1986). Paving with roller compacted concrete. *Concrete Construction*, pages 287–297.

Khayat, K. H. & Libre, P. N. A. (2014). Roller compacted concrete: Field evaluation and mixture optimization. *Center for Transportation Infrastructure and Safety/NUTC program Missouri University of Science and Technology*, 363.

Knutson, M. (1990). Fast-track bonded overlays. *Concrete Construction*, 35(12).

Kokkalis, A. G. & Panagouli, O. K. (1998). Fractal evaluation of pavement skid resistance variations. ii: surface wear. *Chaos, solitons & fractals*, 9(11):1891–1899.

Kreuer, B. R. (2006). *Bond Shear Strength of a Rigid Pavement System with a Roller Compacted Concrete Base*. PhD thesis, Portland Cement Association.

Li, H., Zhang, M.-h., & Ou, J.-p. (2007). Flexural fatigue performance of concrete containing nano-particles for pavement. *International Journal of fatigue*, 29(7):1292–1301.

Maitra, S. R., Reddy, K., & Ramachandra, L. (2013). Estimation of critical stress in jointed concrete pavement. *Procedia-Social and Behavioral Sciences*, 104:208–217.

Marchand, J., Gagne, R., Ouellet, E., & Lepage, S. (1997). Mixture proportioning of roller compacted concrete-a review. *Special Publication*, 171:457–486.

Mardani-Aghabaglou, A., Andiç-Çakir, Ö., & Ramyar, K. (2013). Freeze & thaw resistance and transport properties of high-volume fly ash roller compacted concrete designed by maximum density method. *Cement and Concrete Composites*, 37:259–266.

Marques Filho, J., Paulon, V. A., Monteiro, P. J., de Andrade, W. P., & Dal Molin, D. (2008). Development of laboratory device to simulate roller-compacted concrete placement. *Materials Journal*, 105(2):125–130.

Mathew, T. V. & Rao, K. V. (2007). *Rigid pavement design*, chapter 29. NPTEL.

MCHW-1000 (2016). *Notes for Guidance on the Specification for Highway Works*, (volume 2 ed.). Design manual for roads and bridges.

MCHW-800 (2009). Manual of contract documents for highway works, volume 1 specification for highway works.

MCHW-900 (2012). *Interim advice note 154/12*. Highways England.

McLellan, J. (1982). Pavement thickness, surface evenness and construction practice. *NASA STI/Recon Technical Report N*, 82.

Mohammed, B. S. & Adamu, M. (2018). Mechanical performance of roller compacted concrete pavement containing crumb rubber and nano silica. *Construction and Building Materials*, 159:234–251.

Momayez, A., Ramezanianpour, A., Rajaie, H., & Ehsani, M. (2004). Bi-surface shear test for evaluating bond between existing and new concrete. *Materials Journal*, 101(2):99–106.

Naik, T., Singh, S., & Ye, C. (1993). Fatigue behavior of plain concrete made with or without fly ash. *A Progress Report Submitted to EPRI.*

Nanni, A. (1989). Abrasion resistance of roller compacted concrete. *ACI Materials Journal*, 86(6):559–565.

Neville, A. M. (2011). *Properties of concrete*, volume 5. Longman London.

Nicholls, J. (1997). *Laboratory tests on high-friction surfaces for highways.* Number 176. Thomas Telford.

Packard, R. G. (1984). Thickness design for concrete highway and street pavements.

Panchmatia, P., Olek, J., & Whiting, N. (2014). Joint deterioration in concrete pavements.

Parjoko, Y. (2012). Sensitivity analysis of concrete performance using finite element approach. In: *Civil Engineering Forum*, volume 21.

Parsons, A. W. et al. (1992). *Compaction of soils and granular materials: a review of research performed at the Transport Research Laboratory.* HMSO.

Pidwerbesky, B., Waters, J., Gransberg, D., & Stemprok, R. (2006). Road surface texture measurement using digital image processing and information theory. *Land Transport New Zealand Research Report*, 290:65–79.

Piggott, R. W. (1999). *Roller-compacted concrete pavements: A study of long term performance*. Portland Cement Association.

Pittman, D. W. (1994). *Development of a design procedure for roller-compacted concrete (RCC) pavements*. PhD thesis, U.S. Army Corps of Engineers and Waterways Experiment Station.

Pittman, D. W. & Ragan, S. A. (1998). Drying shrinkage of roller-compacted concrete for pavement applications. *Materials Journal*, 95(1):19–26.

Prusinski, J. R. (2013). Roller-compacted concrete: A value-added pavement solution.

Raja, Z. I. & Snyder, M. B. (1991). *Factors affecting deterioration of transverse cracks in jointed reinforced concrete pavements*. Number 1307.

Rao, S., Darter, M., Tompkins, D., Vancura, M., Khazanovich, L., Signore, J., Coleri, E., Wu, R., Harvey, J., & J, V. (2013). Composite pavement systems volume 2 pcc/pcc composite pavements. Technical report, Sharp 2 report sharp 2, Report S2-R21-RR-3.

RD/GN/032, H. D. (2007). *Guidance notes on road surface requirements for expressways and high speed roads*. Guidance Notes No. RD/GN/032, Hong Kong.

Roesler, J. & Wang, D. (2008). An analytical approach to computing joint opening in concrete pavements. *Pavement Cracking: Mechanisms, Modeling, Detection, Testing and Case Histories*, 79.

Sarsam, S. I., Al-Rawi, A. A., & Abdul-Rahim, A. S. (2012). Laboratory

investigation on roller compaction technique in concrete construction. *Journal of Engineering,Volume 18 April 2012*.

Saucier, K. (1994). Roller-compacted concrete (rcc). In: *Significance of Tests and Properties of Concrete and Concrete-Making Materials*. ASTM International.

Shin, K. J. & Carboneau, N. (2010). The indiana local technical assistance program roller compacted concrete pavement manual for local government agencies. Technical report, Indiana Local Technical Assistance Program.

Shoenberger, J. E. (1994). User's guide: Roller-compacted concrete pavement. Technical report, DTIC Document.

Sobhan, K. & Mashnad, M. (2000). Fatigue durability of stabilized recycled aggregate base course containing fly ash and waste-plastic strip reinforcement. *Final Rep. Submitted to the Recycled Materials Resource Centre, Univ. of New Hampshire*.

Solanki, P. & Zaman, M. (2013). Behavior of stabilized subgrade soils under indirect tension and flexure. *Journal of Materials in Civil Engineering*, 26(5):833–844.

Spielhofer, R. (2007). Describing longitudinal evenness. In: *Proc., Young Researchers Seminar, Transport Research Centre, Brno, Czech Republic*.

Tangtermsirikul, S., Kaewkhluab, T., & Jitvutikrai, P. (2004). A compressive strength model for roller-compacted concrete with fly ash. *Magazine of Concrete Research*, 56(1):35–44.

Thompson, I. (2001). *Use of steel fibres to reinforce cement bound roadbase.* PhD thesis, University of Nottingham.

Tompkins, D., Khazanovich, L., Darter, M., & Fleischer, W. (2009). Design and construction of sustainable pavements: Austrian and german two-layer concrete pavements. *Transportation Research Record: Journal of the Transportation Research Board*, (2098):75–85.

Vahidi, E. K. & Malekabadi, M. M. (2012). Joints in roller compacted concrete pavements. In: *International Conference on Transport, Environment and Civil Engineering (ICTECE'2012) August 25-26, 2012 Kuala Lumpur (Malaysia).*

White, T. D. (1986). *Mix Design, Thickness Design, and Construction of Roller-Compacted Concrete Pavement.* Number 1062.

Williams, R. (1988). Cement treated pavements. *Australian Road Research*, 18(1).

Xu, Y. (2014). *Sustainable Design of "Green" Concrete Overlays - Shear Failure at Cracks and Inadequate Resistance to Reflection Cracking.* PhD thesis, Engineering and Computing,Coventry University.

Zollinger, C. (2015). Recent advances and uses of roller compacted concrete pavements in the united states. *Paving Solutions CEMEX, Inc, Houston, TX USA.*

Appendices

Appendix A

Results of shear cyclic test

This appendix illustrates the relationship between applied load and shear slip for different crack widths, applied loads and placement conditions of two-layer RCC.

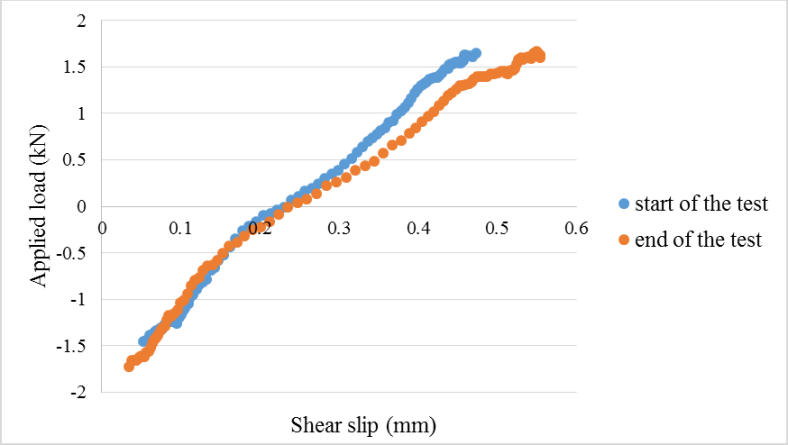

Figure A.1: *Relationship between applied load and shear slip for crack width 0.2 mm at 1.8 kN Case 1*

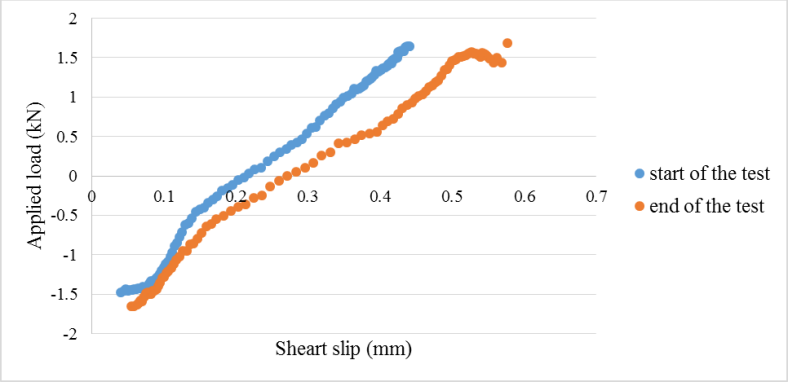

Figure A.2: *Relationship between applied load and shear slip for crack width 0.2 mm at 1.8 kN Case 2*

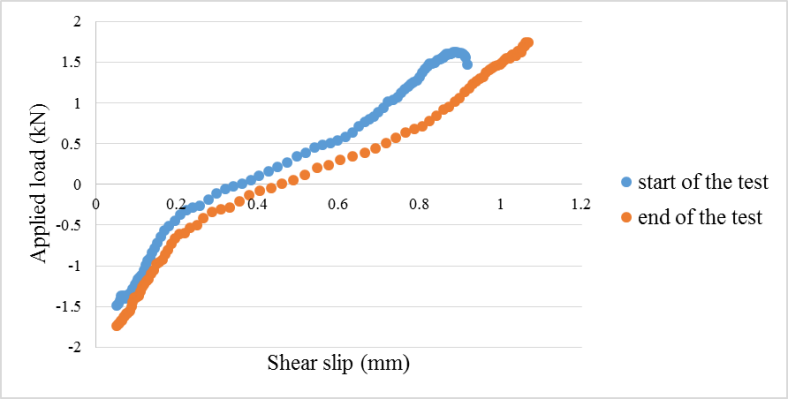

Figure A.3: *Relationship between applied load and shear slip for crack width 0.2 mm at 1.8 kN Case 3*

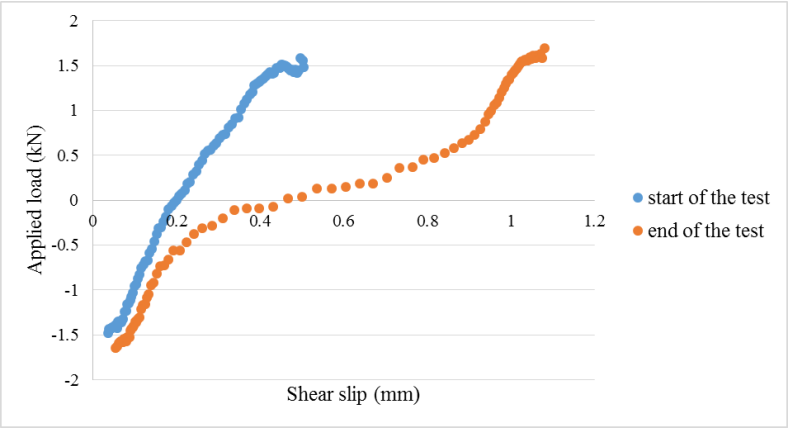

Figure A.4: *Relationship between applied load and shear slip for crack width 1 mm at 1.8 kN Case 1*

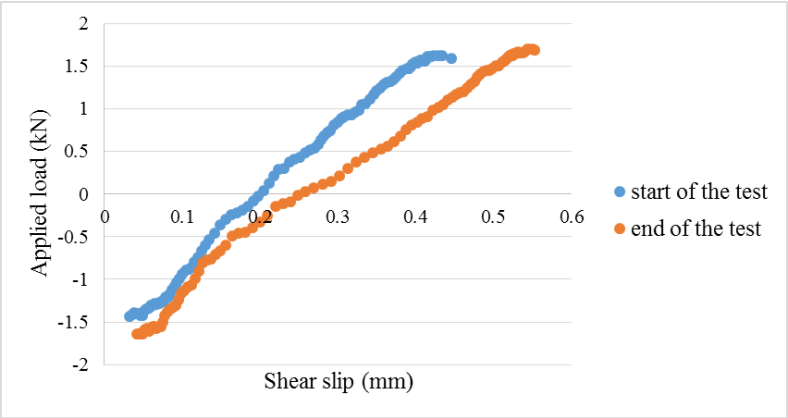

Figure A.5: *Relationship between applied load and shear slip for crack width 0.5 mm at 1.8 kN Case 2*

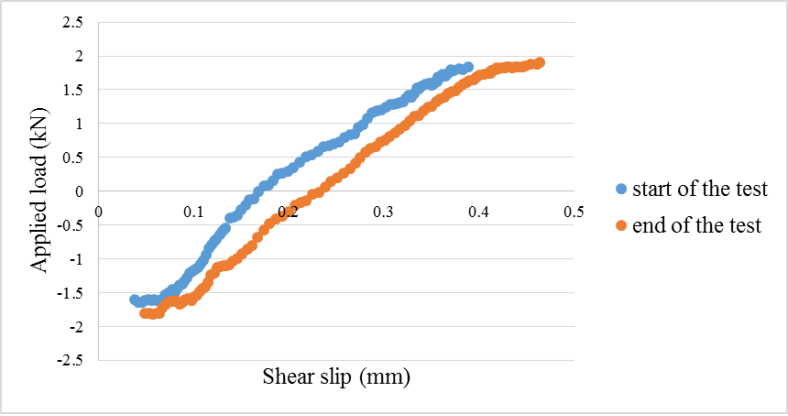

Figure A.6: *Relationship between applied load and shear slip for crack width 0.5 mm at 1.8 kN Case 3*

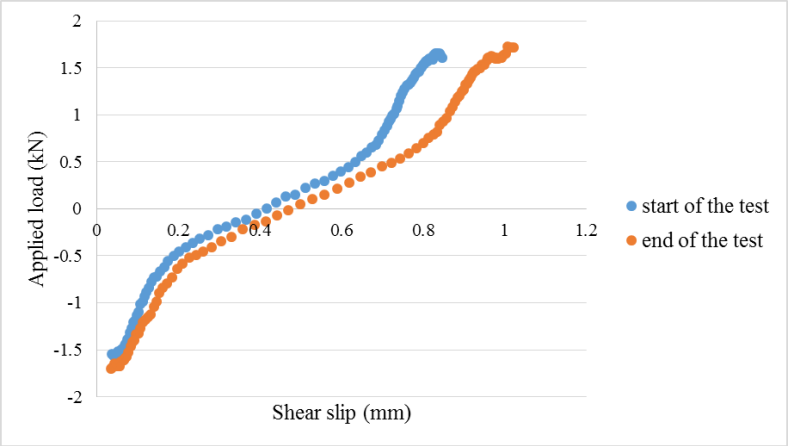

Figure A.7: *Relationship between applied load and shear slip for crack width 0.5 mm at 1.8 kN Case 1*

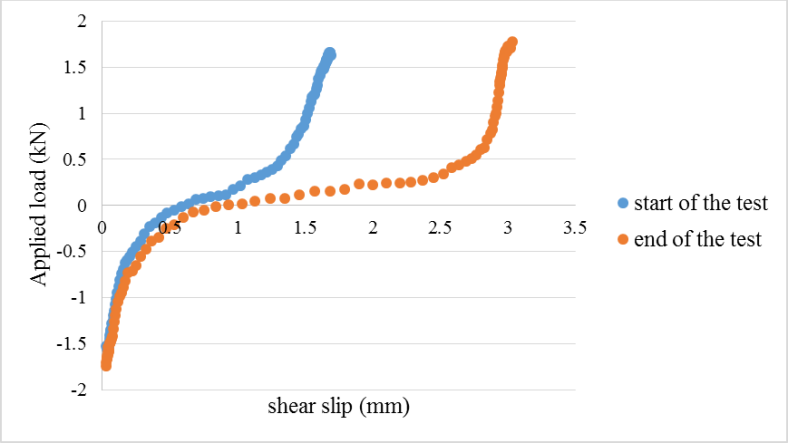

Figure A.8: *Relationship between applied load and shear slip for crack width 1 mm at 1.8 kN Case 3*

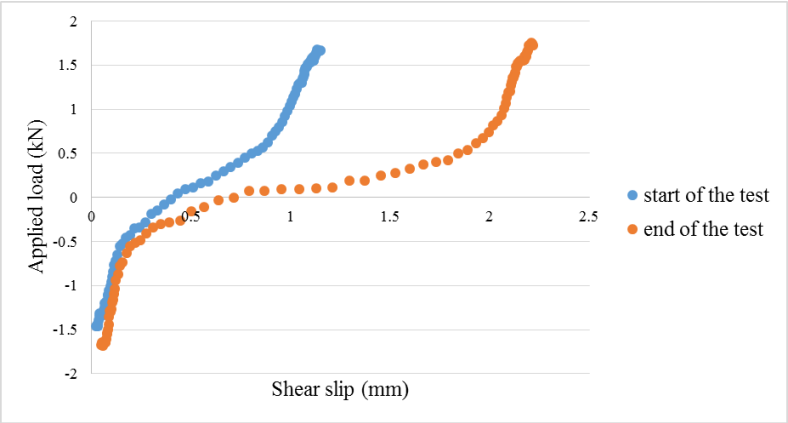

Figure A.9: *Relationship between applied load and shear slip for crack width 1 mm at 1.8 kN Case 2*

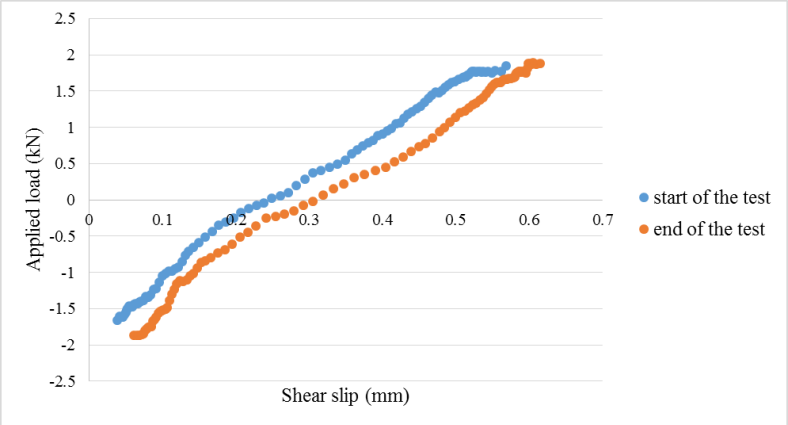

Figure A.10: *Relationship between applied load and shear slip for crack width 0.2 mm at 2 kN Case 1*

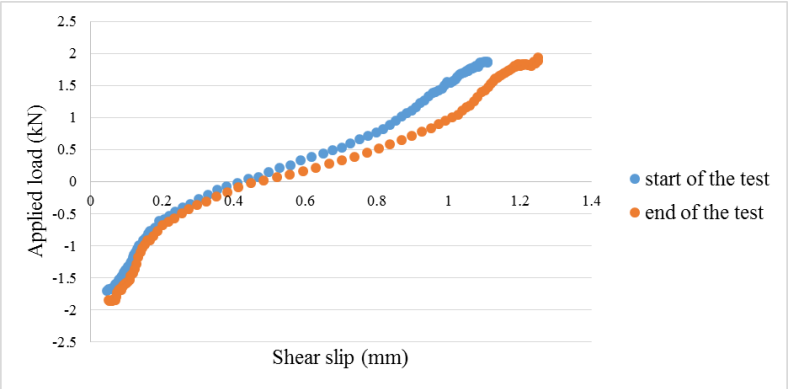

Figure A.11: *Relationship between applied load and shear slip for crack width 0.2 mm at 2 kN Case 3*

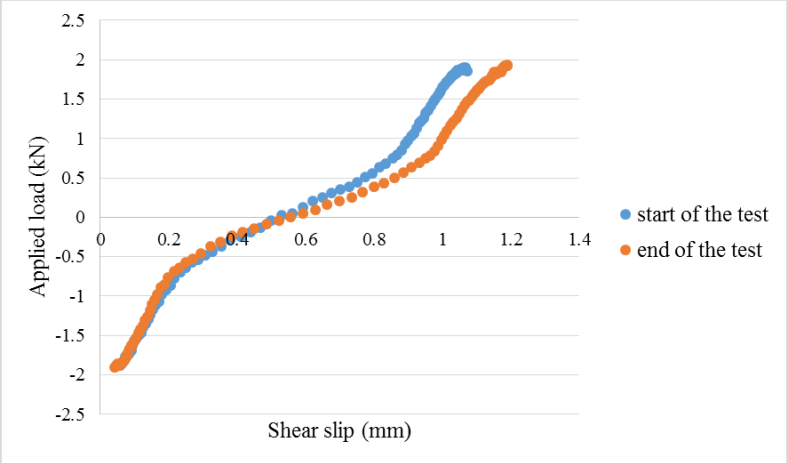

Figure A.12: *Relationship between applied load and shear slip for crack width 1 mm at 2 kN Case 1*

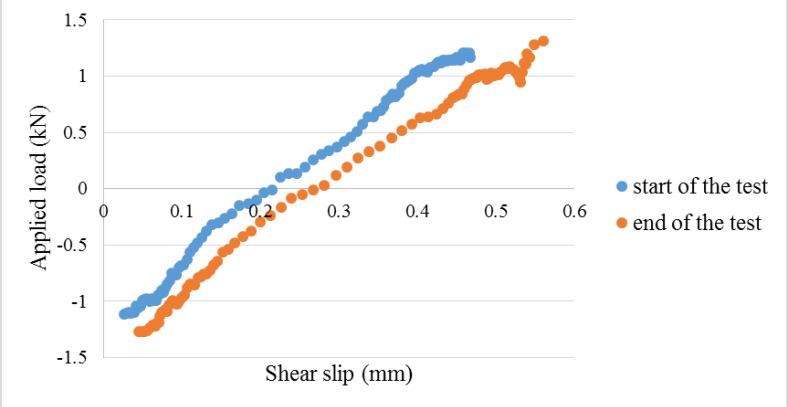

Figure A.13: *Relationship between applied load and shear slip for crack width 0.5 mm at 1.4 kN Case 2*

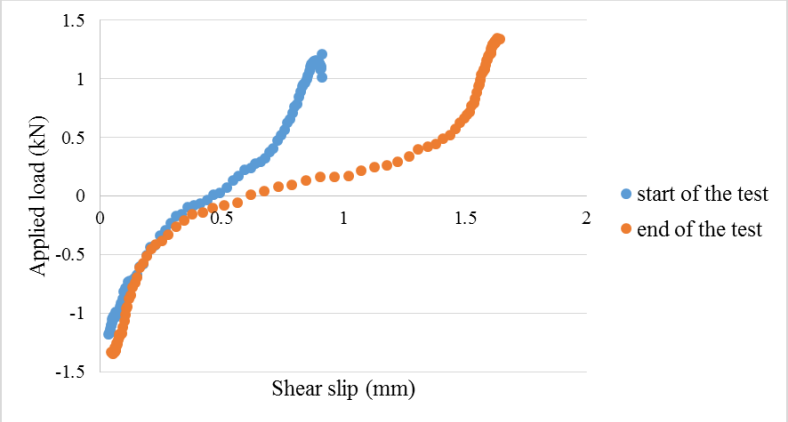

Figure A.14: *Relationship between applied load and shear slip for crack width 1 mm at 1.4 kN Case 2*

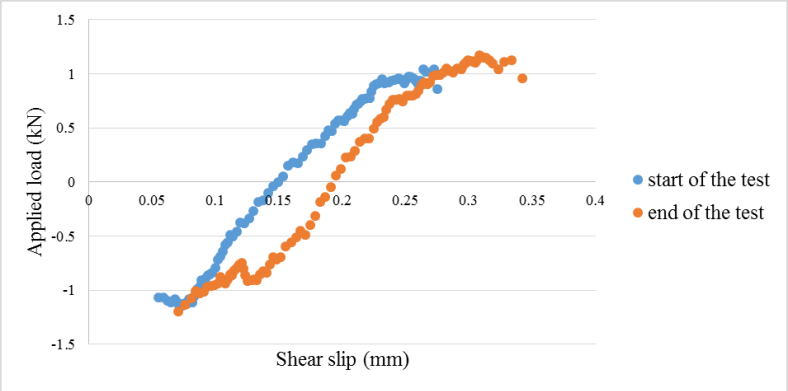

Figure A.15: *Relationship between applied load and shear slip for crack width 0.5 mm at 1.4 kN Case 3*

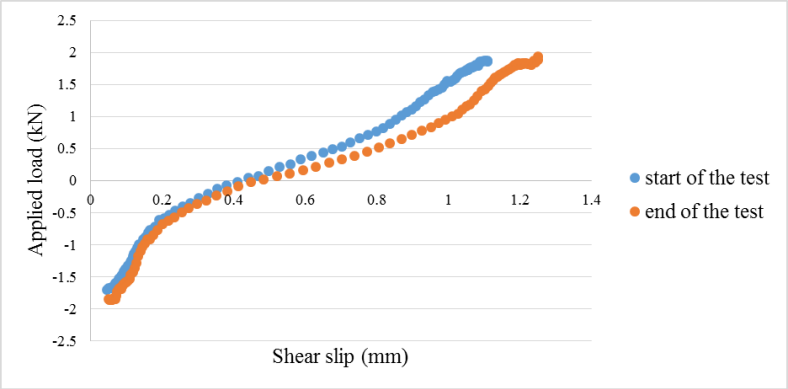

Figure A.16: *Relationship between applied load and shear slip for crack width 0.2 mm at 2 kN Case 3*

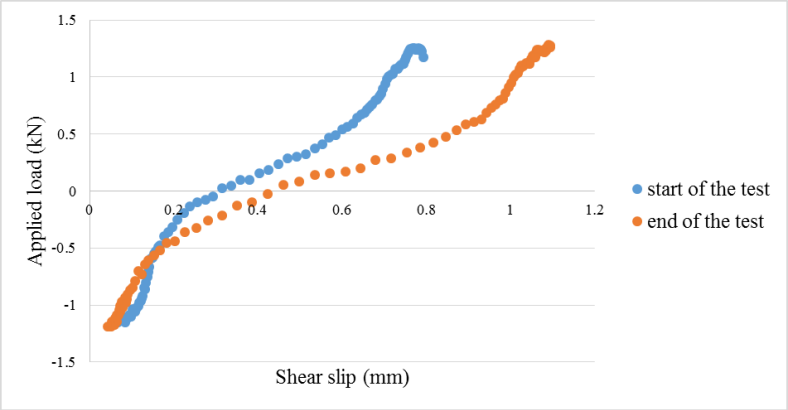

Figure A.17: *Relationship between applied load and shear slip for crack width 1 mm at 1.4 kN Case 3*

Appendix B

Results of KENSLAB

This appendix presents the results of stresses and deflections of two-layer RCC with different slab thicknesses and lengths and different load transfer stiffnesses.

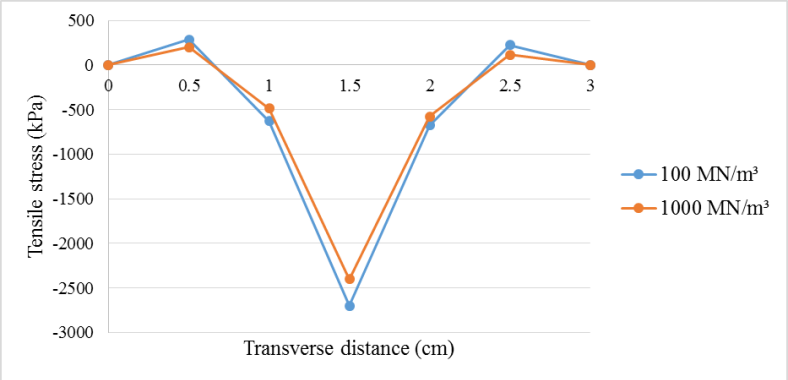

Figure B.1: *Relationship between tensile stress and transverse distance along the joint at slab thickness 250 mm and slab length 4 m*

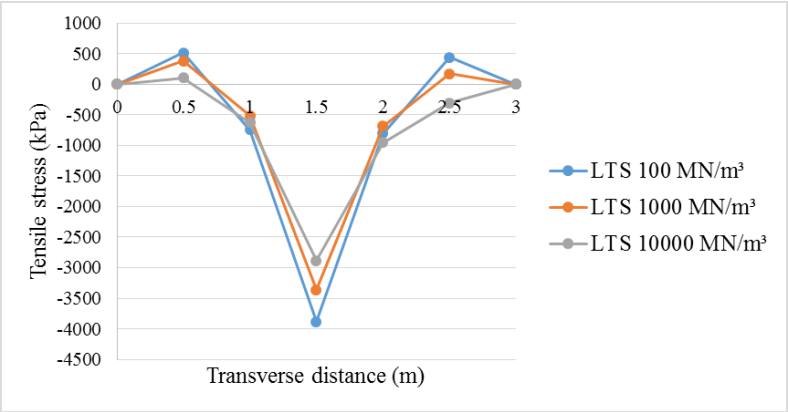

Figure B.2: *Relationship between tensile stress and transverse distance along the joint at slab thickness 200 mm and slab length 4 m*

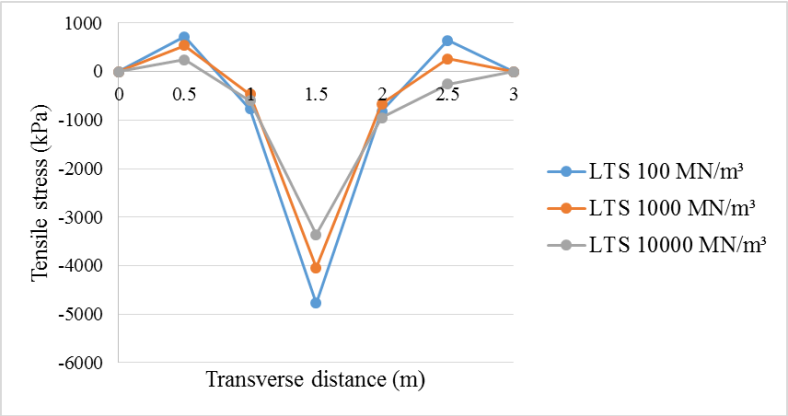

Figure B.3: *Relationship between tensile stress and transverse distance along the joint at slab thickness 175 mm and slab length 4 m*

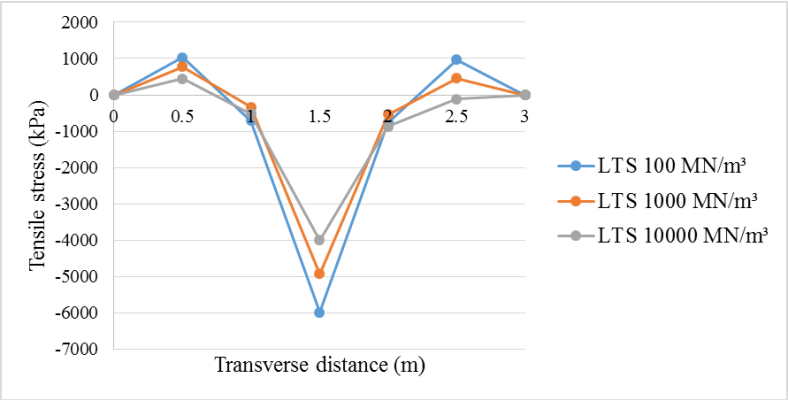

Figure B.4: *Relationship between tensile stress and transverse distance along the joint at slab thickness 150 mm and slab length 4 m*

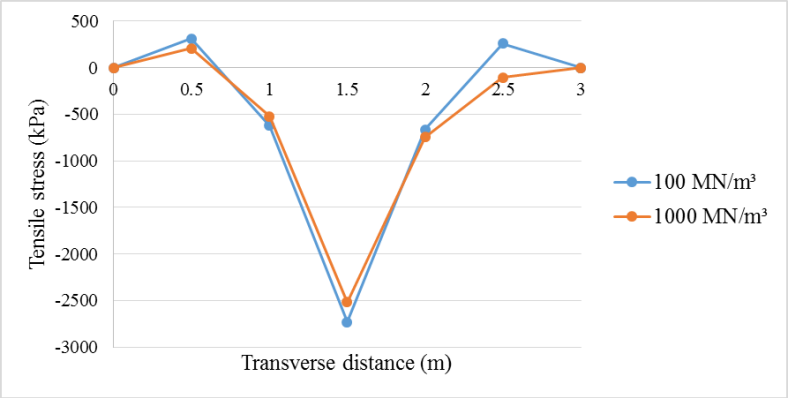

Figure B.5: *Relationship between tensile stress and transverse distance along the joint at slab thickness 250 mm and slab length 3.6 m*

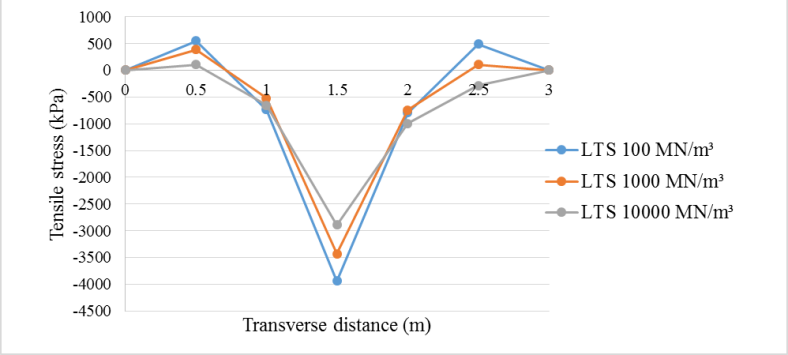

Figure B.6: *Relationship between tensile stress and transverse distance along the joint at slab thickness 200 mm and slab length 3.6 m*

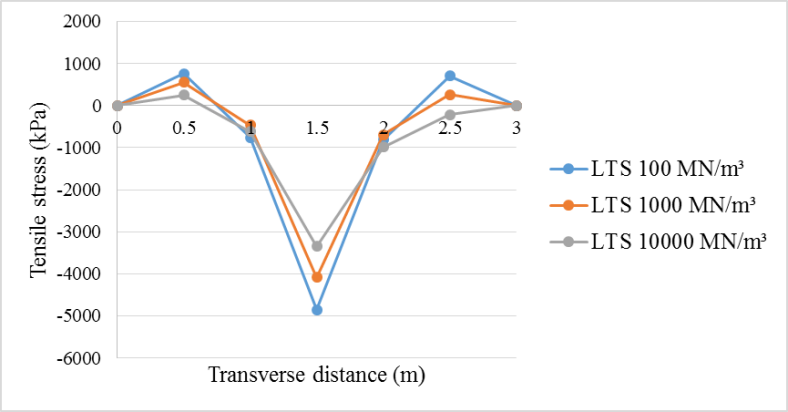

Figure B.7: *Relationship between tensile stress and transverse distance along the joint at slab thickness 175 mm and slab length 3.6 m*

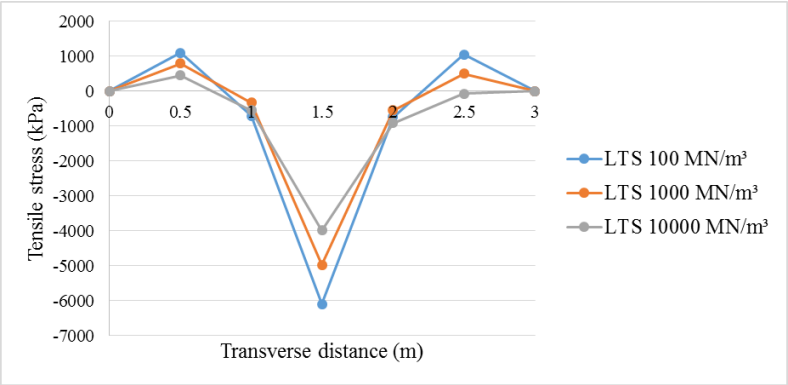

Figure B.8: *Relationship between tensile stress and transverse distance along the joint at slab thickness 150 mm and slab length 3.6 m*

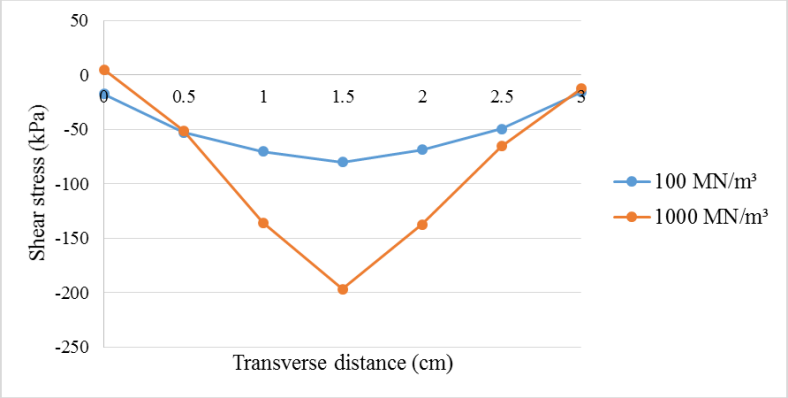

Figure B.9: *Relationship between shear stress and transverse distance along the joint at slab thickness 250 mm and slab length 4 m*

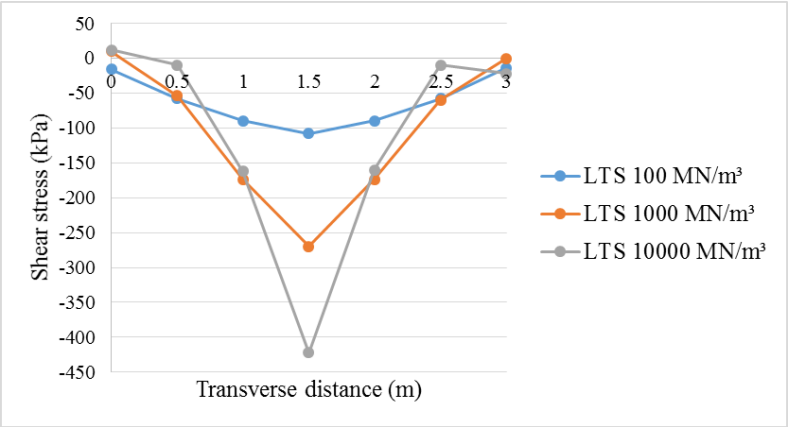

Figure B.10: *Relationship between shear stress and transverse distance along the joint at slab thickness 200 mm and slab length 4 m*

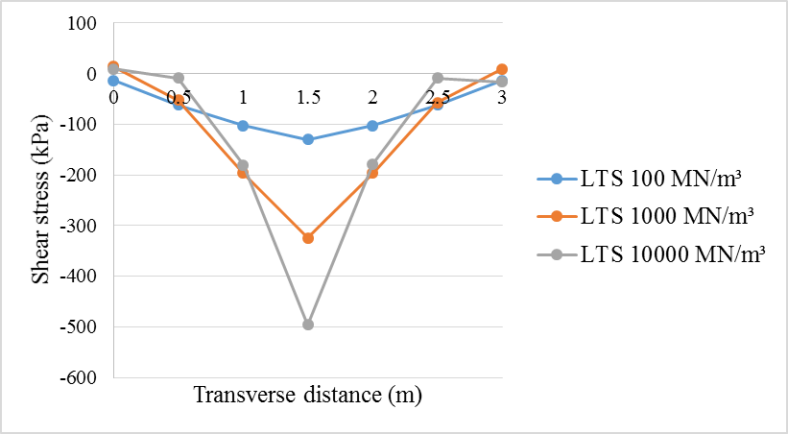

Figure B.11: *Relationship between shear stress and transverse distance along the joint at slab thickness 175 mm and slab length 4 m*

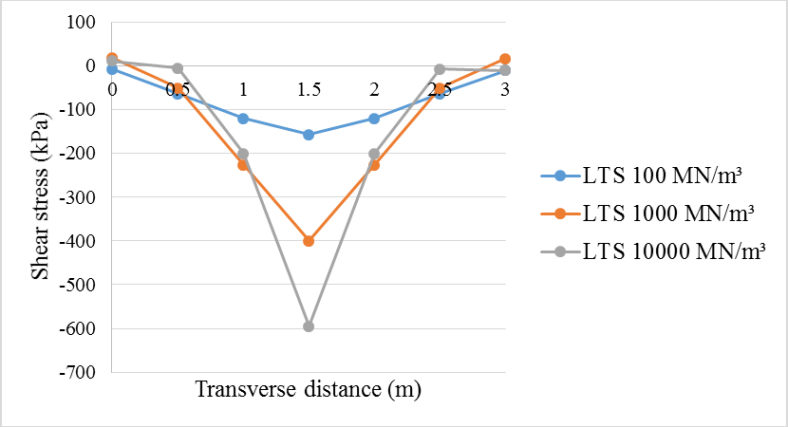

Figure B.12: *Relationship between shear stress and transverse distance along the joint at slab thickness 150 mm and slab length 4 m*

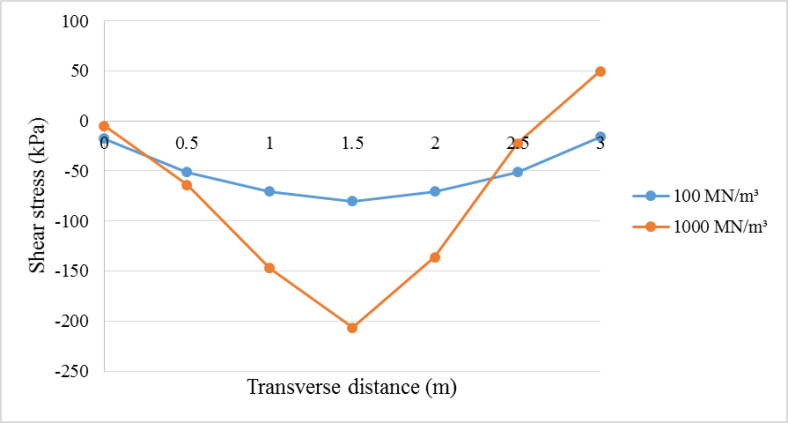

Figure B.13: *Relationship between shear stress and transverse distance along the joint at slab thickness 250 mm and slab length 3.6 m*

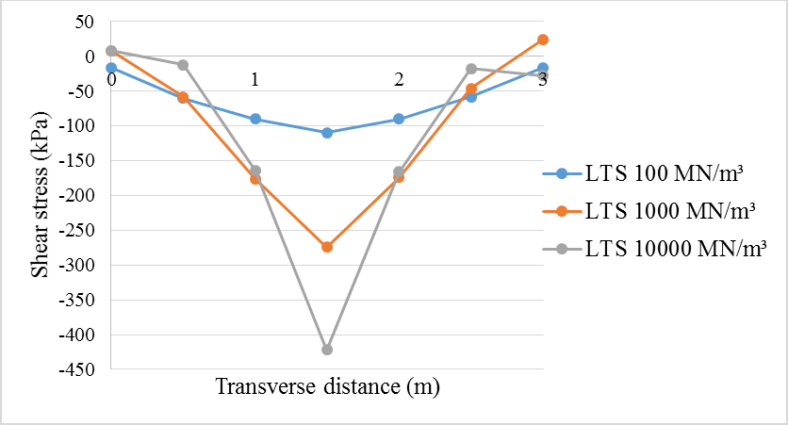

Figure B.14: *Relationship between shear stress and transverse distance along the joint at slab thickness 200 mm and slab length 3.6 m*

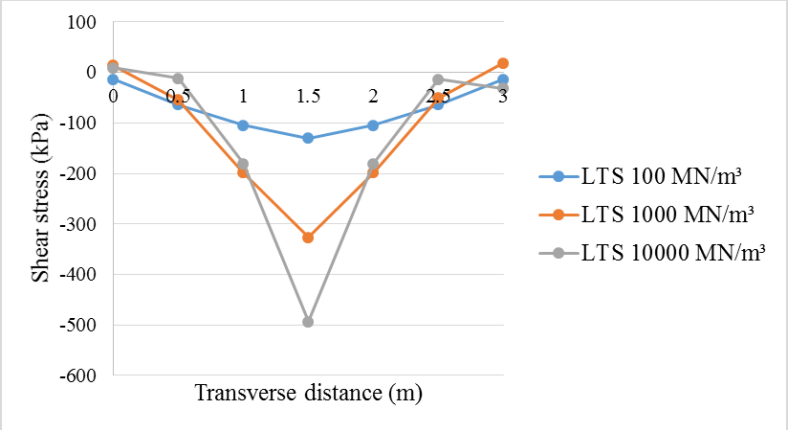

Figure B.15: *Relationship between shear stress and transverse distance along the joint at slab thickness 175 mm and slab length 3.6 m*

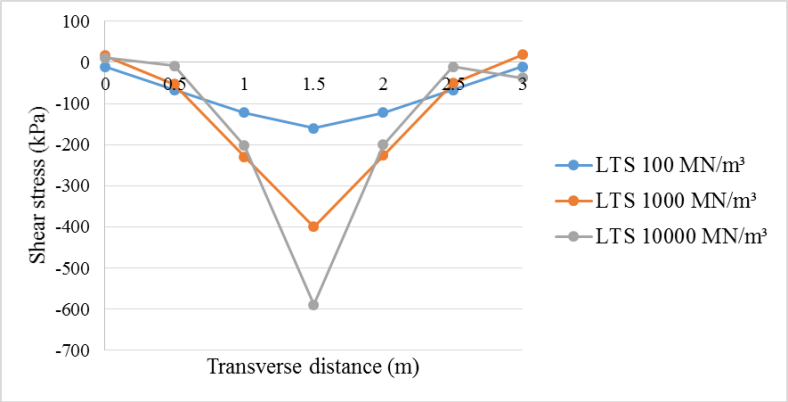

Figure B.16: *Relationship between shear stress and transverse distance along the joint at slab thickness 150 mm and slab length 3.6 m*

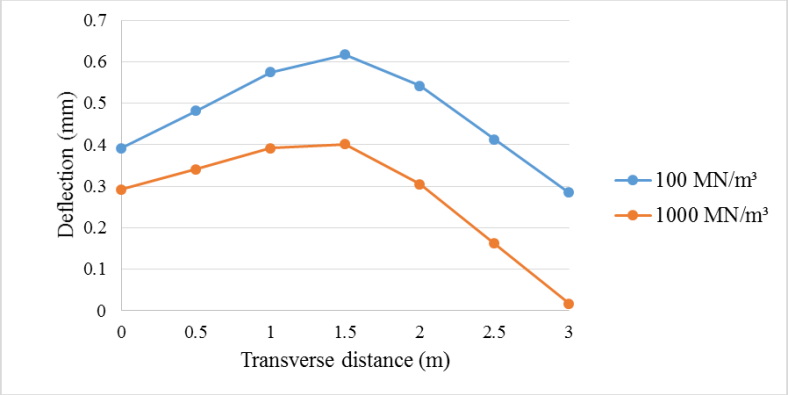

Figure B.17: *Relationship between deflection and transverse distance along the joint at slab thickness 250 mm and slab length 4 m*

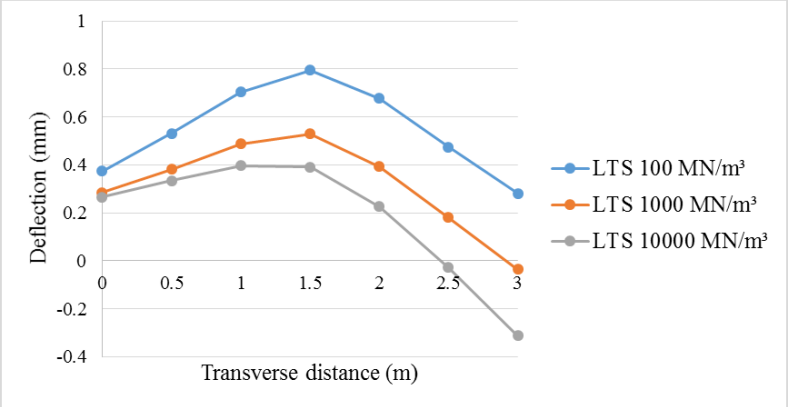

Figure B.18: *Relationship between deflection and transverse distance along the joint at slab thickness 200 mm and slab length 4 m*

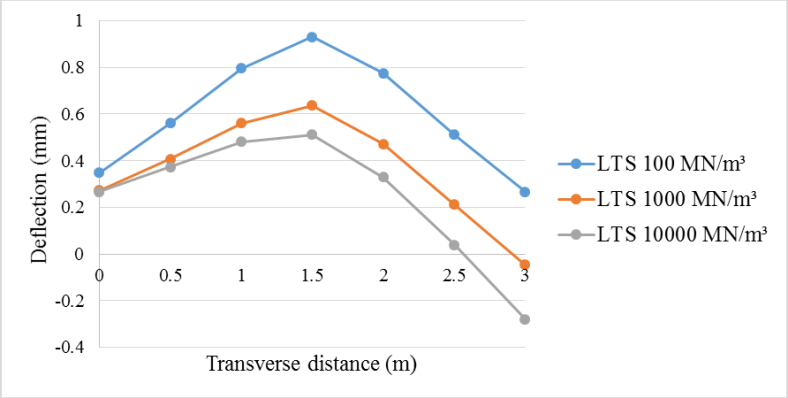

Figure B.19: *Relationship between deflection and transverse distance along the joint at slab thickness 175 mm and slab length 4 m*

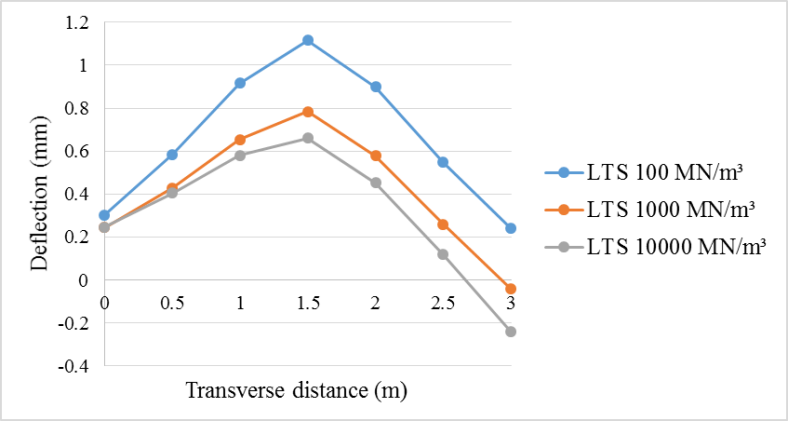

Figure B.20: *Relationship between deflection and transverse distance along the joint at slab thickness 150 mm and slab length 4 m*

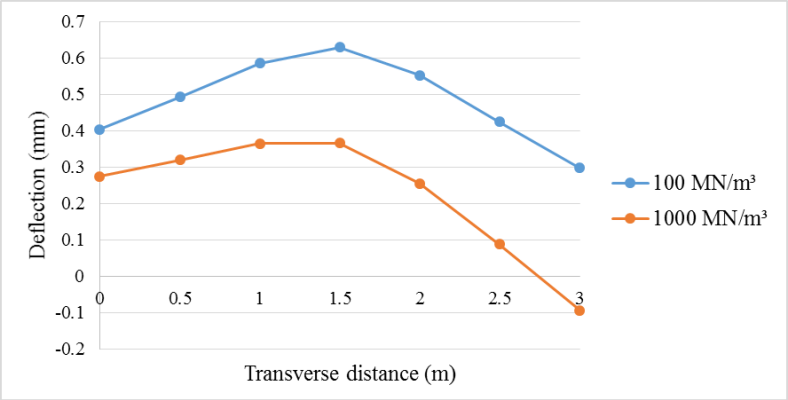

Figure B.21: *Relationship between deflection and transverse distance along the joint at slab thickness 250 mm and slab length 3.6 m*

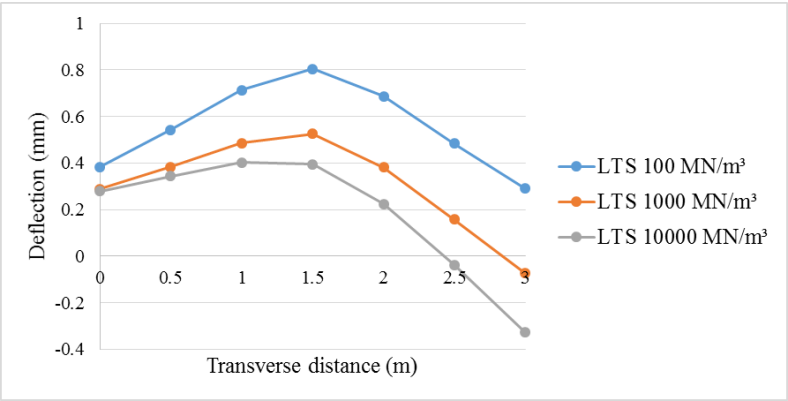

Figure B.22: *Relationship between deflection and transverse distance along the joint at slab thickness 200 mm and slab length 3.6 m*

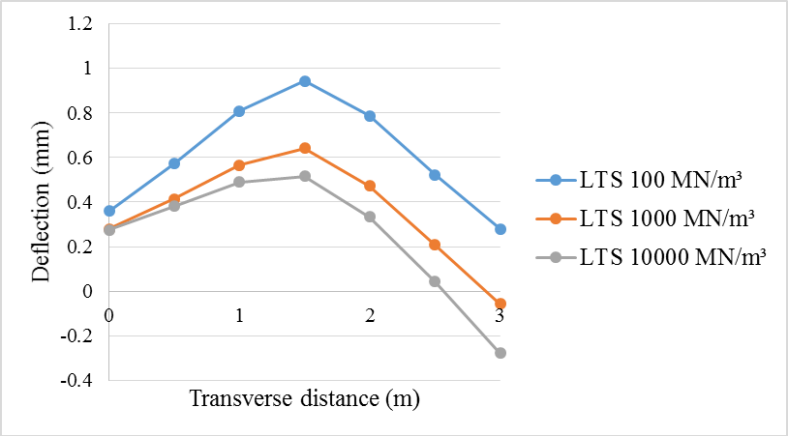

Figure B.23: *Relationship between deflection and transverse distance along the joint at slab thickness 175 mm and slab length 3.6 m*

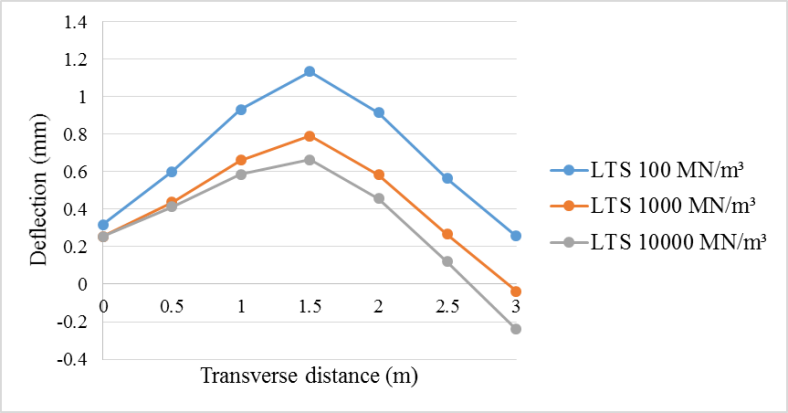

Figure B.24: *Relationship between deflection and transverse distance along the joint at slab thickness 150 mm and slab length 3.6 m*

Appendix C

KENSLAB design example

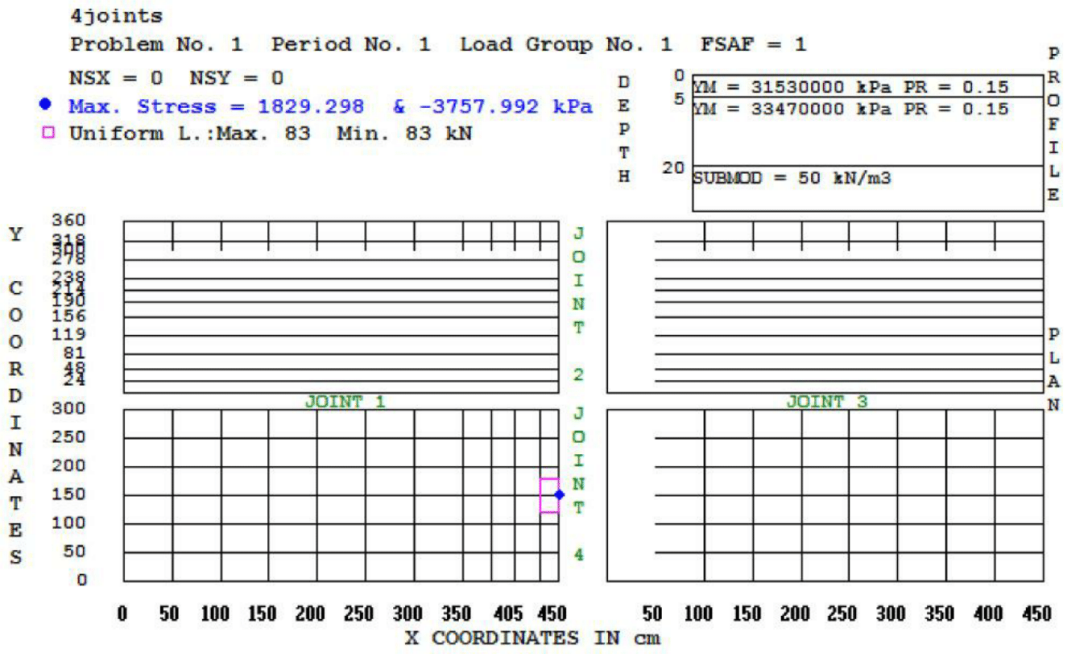

```
INPUT FILE NAME  -D:\kenpave\thermal effect-20-8-20.TXT

NUMBER OF PROBLEMS TO BE SOLVED =  1

TITLE -4joints

TYPE OF FOUNDATION (NFOUND)             =               0
TYPE OF DAMAGE ANALYSIS (NDAMA)         =               0
NUMBER OF PERIODS PER YEAR (NPY)        =               1
NUMBER OF LOAD GROUPS (NLG)             =               1
TOTAL NUMBER OF SLABS (NSLAB)           =               4
TOTAL NUMBER OF JOINTS (NJOINT)         =               4

ARRANGEMENT OF SLABS
SLAB   NO. NODES (NX)   NO. NODES (NY)    JOINT NO. AT FOUR SIDES (JONO)
 NO.   IN X DIRECTION   IN Y DIRECTION        LEFT  RIGHT  BOTTOM   TOP
  1          12              7                0     4      0      1
  2          12             12                0     2      1      0
  3           9              7                4     0      0      3
  4           9             12                2     0      3      0

NUMBER OF LAYERS (NLAYER)-------------------------------------=  2
NODAL NUMBER USED TO CHECK CONVERGENCE (NNCK)-----------------=  81
NUMBER OF NODES NOT IN CONTACT (NOTCON)-----------------------=  0
NUMBER OF GAPS (NGAP)-----------------------------------------=  0
NUMBER OF POINTS FOR PRINTOUT (NPRINT)------------------------=  0
CODE FOR INPUT OF GAPS OR PRECOMPRESSIONS (INPUT)- -----------=  0
BOND BETWEEN TWO LAYERS (NBOND)-------------------------------=  1
CONDITION OF WARPING (NTEMP)----------------------------------=  1
CODE INDICATING WHETHER SLAB WEIGHT IS CONSIDERED (NWT)-------=  0
MAX NO. OF CYCLES FOR CHECKING CONTACT (NCYCLE)---------------=  1
NUMBER OF ADDITIONAL THICKNESSES FOR SLAB LAYER 1 (NAT1)------=  0
NUMBER OF ADDITIONAL THICKNESSES FOR SLAB LAYER 2 (NAT2)------=  0
NUMBER OF POINTS ON X AXIS OF SYMMETRY (NSX)------------------=  0
NUMBER OF POINTS ON Y AXIS OF SYMMETRY (NSY)------------------=  0
MORE DETAILED PRINTOUT FOR EACH CONTACT CYCLE (MDPO)----------=  0
TOLERANCE FOR ITERATIONS (DEL)--------------------------------=  0.001
MAXIMUM ALLOWABLE VERTICAL DISPLACEMENT (FMAX)----------------=  2.54
DIFFERENCE IN TEMP. BETWEEN TOP AND BOTTOM OF SLAB (TEMP)-----= -8
COEFFICIENT OF THERMAL EXPANSION (CT)-------------------------=  0.000009

SYSTEM OF UNITS (NUNIT)---------------------------------------=  1
Length in cm, force in kN, stress in kPa, unit weight in kN/m^3
subgrade and dowel K value in MN/m^3, and temperature in C

FOR SLAB NO. 1 COORDINATES OF FINITE ELEMENT GRID ARE:
X =  0  50  100  150  200  250  300  350  380  405  430  450
Y =  0  50  100  150  200  250  300

FOR SLAB NO. 2 COORDINATES OF FINITE ELEMENT GRID ARE:
X =  0  50  100  150  200  250  300  350  380  405  430  450
Y =  300  24  48  81  119  156  190  214  238  278  318  360

FOR SLAB NO. 3 COORDINATES OF FINITE ELEMENT GRID ARE:
X =  50  100  150  200  250  300  350  400  450
Y =  0  50  100  150  200  250  300

FOR SLAB NO. 4 COORDINATES OF FINITE ELEMENT GRID ARE:
X =  50  100  150  200  250  300  350  400  450
Y =  300  24  48  81  119  156  190  214  238  278  318  360

LAYER        THICKNESS (T)        POISSON'S         YOUNG'S
 NO.                              RATIO (PR)      MODULUS (YM)
```

```
 1             5.00000             0.15000          3.153E+07
 2            15.00000             0.15000          3.347E+07

No. OF LOADED AREAS (NUDL) FOR EACH LOAD GROUP ARE:  1
NO. OF NODAL FORCES (NCNF) AND MOMENTS (NCMX AND NCMY) ARE: 0  0  0

FOR LOAD GROUP NO. 1 LOADS ARE APPLIED AS FOLLOWS:
SLAB NO.    X COORDINATES           Y COORDINATES       INTENSITY
   (LS)    (XL1)       (XL2)       (YL1)       (YL2)       (QQ)
    1   430.00000   450.00000   120.00000   180.00000   690.00000

FOUNDATION ADJUSTMENT FACTOR (FSAF) FOR EACH PERIOD ARE: 1

NUMBER OF ADDITIONAL SUBGRADE MODULI (NAS) TO BE READ IN-----=  0
SUBGRADE MODULUS (SUBMOD)-----------------------------------= 50

NODAL COORDINATES (XN AND YN) OF INDIVIDUAL SLAB ARE:
    1     0.000     0.000    2     0.000    50.000    3     0.000   100.000
    4     0.000   150.000    5     0.000   200.000    6     0.000   250.000
    7     0.000   300.000    8    50.000     0.000    9    50.000    50.000
   10    50.000   100.000   11    50.000   150.000   12    50.000   200.000
   13    50.000   250.000   14    50.000   300.000   15   100.000     0.000
   16   100.000    50.000   17   100.000   100.000   18   100.000   150.000
   19   100.000   200.000   20   100.000   250.000   21   100.000   300.000
   22   150.000     0.000   23   150.000    50.000   24   150.000   100.000
   25   150.000   150.000   26   150.000   200.000   27   150.000   250.000
   28   150.000   300.000   29   200.000     0.000   30   200.000    50.000
   31   200.000   100.000   32   200.000   150.000   33   200.000   200.000
   34   200.000   250.000   35   200.000   300.000   36   250.000     0.000
   37   250.000    50.000   38   250.000   100.000   39   250.000   150.000
   40   250.000   200.000   41   250.000   250.000   42   250.000   300.000
   43   300.000     0.000   44   300.000    50.000   45   300.000   100.000
   46   300.000   150.000   47   300.000   200.000   48   300.000   250.000
   49   300.000   300.000   50   350.000     0.000   51   350.000    50.000
   52   350.000   100.000   53   350.000   150.000   54   350.000   200.000
   55   350.000   250.000   56   350.000   300.000   57   380.000     0.000
   58   380.000    50.000   59   380.000   100.000   60   380.000   150.000
   61   380.000   200.000   62   380.000   250.000   63   380.000   300.000
   64   405.000     0.000   65   405.000    50.000   66   405.000   100.000
   67   405.000   150.000   68   405.000   200.000   69   405.000   250.000
   70   405.000   300.000   71   430.000     0.000   72   430.000    50.000
   73   430.000   100.000   74   430.000   150.000   75   430.000   200.000
   76   430.000   250.000   77   430.000   300.000   78   450.000     0.000
   79   450.000    50.000   80   450.000   100.000   81   450.000   150.000
   82   450.000   200.000   83   450.000   250.000   84   450.000   300.000
   85     0.000   300.000   86     0.000    24.000   87     0.000    48.000
   88     0.000    81.000   89     0.000   119.000   90     0.000   156.000
   91     0.000   190.000   92     0.000   214.000   93     0.000   238.000
   94     0.000   278.000   95     0.000   318.000   96     0.000   360.000
   97    50.000   300.000   98    50.000    24.000   99    50.000    48.000
  100    50.000    81.000  101    50.000   119.000  102    50.000   156.000
  103    50.000   190.000  104    50.000   214.000  105    50.000   238.000
  106    50.000   278.000  107    50.000   318.000  108    50.000   360.000
  109   100.000   300.000  110   100.000    24.000  111   100.000    48.000
  112   100.000    81.000  113   100.000   119.000  114   100.000   156.000
  115   100.000   190.000  116   100.000   214.000  117   100.000   238.000
  118   100.000   278.000  119   100.000   318.000  120   100.000   360.000
  121   150.000   300.000  122   150.000    24.000  123   150.000    48.000
  124   150.000    81.000  125   150.000   119.000  126   150.000   156.000
  127   150.000   190.000  128   150.000   214.000  129   150.000   238.000
  130   150.000   278.000  131   150.000   318.000  132   150.000   360.000
  133   200.000   300.000  134   200.000    24.000  135   200.000    48.000
  136   200.000    81.000  137   200.000   119.000  138   200.000   156.000
  139   200.000   190.000  140   200.000   214.000  141   200.000   238.000
```

142	200.000	278.000	143	200.000	318.000	144	200.000	360.000
145	250.000	300.000	146	250.000	24.000	147	250.000	48.000
148	250.000	81.000	149	250.000	119.000	150	250.000	156.000
151	250.000	190.000	152	250.000	214.000	153	250.000	238.000
154	250.000	278.000	155	250.000	318.000	156	250.000	360.000
157	300.000	300.000	158	300.000	24.000	159	300.000	48.000
160	300.000	81.000	161	300.000	119.000	162	300.000	156.000
163	300.000	190.000	164	300.000	214.000	165	300.000	238.000
166	300.000	278.000	167	300.000	318.000	168	300.000	360.000
169	350.000	300.000	170	350.000	24.000	171	350.000	48.000
172	350.000	81.000	173	350.000	119.000	174	350.000	156.000
175	350.000	190.000	176	350.000	214.000	177	350.000	238.000
178	350.000	278.000	179	350.000	318.000	180	350.000	360.000
181	380.000	300.000	182	380.000	24.000	183	380.000	48.000
184	380.000	81.000	185	380.000	119.000	186	380.000	156.000
187	380.000	190.000	188	380.000	214.000	189	380.000	238.000
190	380.000	278.000	191	380.000	318.000	192	380.000	360.000
193	405.000	300.000	194	405.000	24.000	195	405.000	48.000
196	405.000	81.000	197	405.000	119.000	198	405.000	156.000
199	405.000	190.000	200	405.000	214.000	201	405.000	238.000
202	405.000	278.000	203	405.000	318.000	204	405.000	360.000
205	430.000	300.000	206	430.000	24.000	207	430.000	48.000
208	430.000	81.000	209	430.000	119.000	210	430.000	156.000
211	430.000	190.000	212	430.000	214.000	213	430.000	238.000
214	430.000	278.000	215	430.000	318.000	216	430.000	360.000
217	450.000	300.000	218	450.000	24.000	219	450.000	48.000
220	450.000	81.000	221	450.000	119.000	222	450.000	156.000
223	450.000	190.000	224	450.000	214.000	225	450.000	238.000
226	450.000	278.000	227	450.000	318.000	228	450.000	360.000
229	50.000	0.000	230	50.000	50.000	231	50.000	100.000
232	50.000	150.000	233	50.000	200.000	234	50.000	250.000
235	50.000	300.000	236	100.000	0.000	237	100.000	50.000
238	100.000	100.000	239	100.000	150.000	240	100.000	200.000
241	100.000	250.000	242	100.000	300.000	243	150.000	0.000
244	150.000	50.000	245	150.000	100.000	246	150.000	150.000
247	150.000	200.000	248	150.000	250.000	249	150.000	300.000
250	200.000	0.000	251	200.000	50.000	252	200.000	100.000
253	200.000	150.000	254	200.000	200.000	255	200.000	250.000
256	200.000	300.000	257	250.000	0.000	258	250.000	50.000
259	250.000	100.000	260	250.000	150.000	261	250.000	200.000
262	250.000	250.000	263	250.000	300.000	264	300.000	0.000
265	300.000	50.000	266	300.000	100.000	267	300.000	150.000
268	300.000	200.000	269	300.000	250.000	270	300.000	300.000
271	350.000	0.000	272	350.000	50.000	273	350.000	100.000
274	350.000	150.000	275	350.000	200.000	276	350.000	250.000
277	350.000	300.000	278	400.000	0.000	279	400.000	50.000
280	400.000	100.000	281	400.000	150.000	282	400.000	200.000
283	400.000	250.000	284	400.000	300.000	285	450.000	0.000
286	450.000	50.000	287	450.000	100.000	288	450.000	150.000
289	450.000	200.000	290	450.000	250.000	291	450.000	300.000
292	50.000	300.000	293	50.000	24.000	294	50.000	48.000
295	50.000	81.000	296	50.000	119.000	297	50.000	156.000
298	50.000	190.000	299	50.000	214.000	300	50.000	238.000
301	50.000	278.000	302	50.000	318.000	303	50.000	360.000
304	100.000	300.000	305	100.000	24.000	306	100.000	48.000
307	100.000	81.000	308	100.000	119.000	309	100.000	156.000
310	100.000	190.000	311	100.000	214.000	312	100.000	238.000
313	100.000	278.000	314	100.000	318.000	315	100.000	360.000
316	150.000	300.000	317	150.000	24.000	318	150.000	48.000
319	150.000	81.000	320	150.000	119.000	321	150.000	156.000
322	150.000	190.000	323	150.000	214.000	324	150.000	238.000
325	150.000	278.000	326	150.000	318.000	327	150.000	360.000
328	200.000	300.000	329	200.000	24.000	330	200.000	48.000
331	200.000	81.000	332	200.000	119.000	333	200.000	156.000

```
  334   200.000   190.000  335   200.000   214.000  336   200.000   238.000
  337   200.000   278.000  338   200.000   318.000  339   200.000   360.000
  340   250.000   300.000  341   250.000    24.000  342   250.000    48.000
  343   250.000    81.000  344   250.000   119.000  345   250.000   156.000
  346   250.000   190.000  347   250.000   214.000  348   250.000   238.000
  349   250.000   278.000  350   250.000   318.000  351   250.000   360.000
  352   300.000   300.000  353   300.000    24.000  354   300.000    48.000
  355   300.000    81.000  356   300.000   119.000  357   300.000   156.000
  358   300.000   190.000  359   300.000   214.000  360   300.000   238.000
  361   300.000   278.000  362   300.000   318.000  363   300.000   360.000
  364   350.000   300.000  365   350.000    24.000  366   350.000    48.000
  367   350.000    81.000  368   350.000   119.000  369   350.000   156.000
  370   350.000   190.000  371   350.000   214.000  372   350.000   238.000
  373   350.000   278.000  374   350.000   318.000  375   350.000   360.000
  376   400.000   300.000  377   400.000    24.000  378   400.000    48.000
  379   400.000    81.000  380   400.000   119.000  381   400.000   156.000
  382   400.000   190.000  383   400.000   214.000  384   400.000   238.000
  385   400.000   278.000  386   400.000   318.000  387   400.000   360.000
  388   450.000   300.000  389   450.000    24.000  390   450.000    48.000
  391   450.000    81.000  392   450.000   119.000  393   450.000   156.000
  394   450.000   190.000  395   450.000   214.000  396   450.000   238.000
  397   450.000   278.000  398   450.000   318.000  399   450.000   360.000

AMOUNT OF INITIAL CURLING AND GAP (CURL) AT THE NODES IS
    1  -0.13163    2  -0.10913    3  -0.09563    4  -0.09113    5  -0.09563
    6  -0.10913    7  -0.13163    8  -0.09563    9  -0.07313   10  -0.05963
   11  -0.05513   12  -0.05963   13  -0.07313   14  -0.09563   15  -0.06863
   16  -0.04613   17  -0.03263   18  -0.02813   19  -0.03263   20  -0.04613
   21  -0.06863   22  -0.05063   23  -0.02813   24  -0.01463   25  -0.01013
   26  -0.01463   27  -0.02813   28  -0.05063   29  -0.04163   30  -0.01913
   31  -0.00563   32  -0.00113   33  -0.00563   34  -0.01913   35  -0.04163
   36  -0.04163   37  -0.01913   38  -0.00563   39  -0.00113   40  -0.00563
   41  -0.01913   42  -0.04163   43  -0.05063   44  -0.02813   45  -0.01463
   46  -0.01013   47  -0.01463   48  -0.02813   49  -0.05063   50  -0.06863
   51  -0.04613   52  -0.03263   53  -0.02813   54  -0.03263   55  -0.04613
   56  -0.06863   57  -0.08375   58  -0.06125   59  -0.04775   60  -0.04325
   61  -0.04775   62  -0.06125   63  -0.08375   64  -0.09882   65  -0.07632
   66  -0.06282   67  -0.05832   68  -0.06282   69  -0.07632   70  -0.09882
   71  -0.11615   72  -0.09365   73  -0.08015   74  -0.07565   75  -0.08015
   76  -0.09365   77  -0.11615   78  -0.13163   79  -0.10913   80  -0.09563
   81  -0.09113   82  -0.09563   83  -0.10913   84  -0.13163   85  -0.11705
   86  -0.13493   87  -0.12249   88  -0.10877   89  -0.09782   90  -0.09216
   91  -0.09131   92  -0.09321   93  -0.09718   94  -0.10841   95  -0.12540
   96  -0.14945   97  -0.08105   98  -0.09893   99  -0.08649  100  -0.07277
  101  -0.06182  102  -0.05616  103  -0.05531  104  -0.05721  105  -0.06118
  106  -0.07241  107  -0.08940  108  -0.11345  109  -0.05405  110  -0.07193
  111  -0.05949  112  -0.04577  113  -0.03482  114  -0.02916  115  -0.02831
  116  -0.03021  117  -0.03418  118  -0.04541  119  -0.06240  120  -0.08645
  121  -0.03605  122  -0.05393  123  -0.04149  124  -0.02777  125  -0.01682
  126  -0.01116  127  -0.01031  128  -0.01221  129  -0.01618  130  -0.02741
  131  -0.04440  132  -0.06845  133  -0.02705  134  -0.04493  135  -0.03249
  136  -0.01877  137  -0.00782  138  -0.00216  139  -0.00131  140  -0.00321
  141  -0.00718  142  -0.01841  143  -0.03540  144  -0.05945  145  -0.02705
  146  -0.04493  147  -0.03249  148  -0.01877  149  -0.00782  150  -0.00216
  151  -0.00131  152  -0.00321  153  -0.00718  154  -0.01841  155  -0.03540
  156  -0.05945  157  -0.03605  158  -0.05393  159  -0.04149  160  -0.02777
  161  -0.01682  162  -0.01116  163  -0.01031  164  -0.01221  165  -0.01618
  166  -0.02741  167  -0.04440  168  -0.06845  169  -0.05405  170  -0.07193
  171  -0.05949  172  -0.04577  173  -0.03482  174  -0.02916  175  -0.02831
  176  -0.03021  177  -0.03418  178  -0.04541  179  -0.06240  180  -0.08645
  181  -0.06917  182  -0.08705  183  -0.07461  184  -0.06089  185  -0.04994
  186  -0.04428  187  -0.04343  188  -0.04533  189  -0.04930  190  -0.06053
  191  -0.07752  192  -0.10157  193  -0.08424  194  -0.10212  195  -0.08968
  196  -0.07596  197  -0.06502  198  -0.05936  199  -0.05850  200  -0.06040
```

```
 201  -0.06438 202  -0.07561 203  -0.09260 204  -0.11664 205  -0.10157
 206  -0.11945 207  -0.10701 208  -0.09329 209  -0.08234 210  -0.07668
 211  -0.07583 212  -0.07773 213  -0.08170 214  -0.09293 215  -0.10992
 216  -0.13397 217  -0.11705 218  -0.13493 219  -0.12249 220  -0.10877
 221  -0.09782 222  -0.09216 223  -0.09131 224  -0.09321 225  -0.09718
 226  -0.10841 227  -0.12540 228  -0.14945 229  -0.09563 230  -0.07313
 231  -0.05963 232  -0.05513 233  -0.05963 234  -0.07313 235  -0.09563
 236  -0.06863 237  -0.04613 238  -0.03263 239  -0.02813 240  -0.03263
 241  -0.04613 242  -0.06863 243  -0.05063 244  -0.02813 245  -0.01463
 246  -0.01013 247  -0.01463 248  -0.02813 249  -0.05063 250  -0.04163
 251  -0.01913 252  -0.00563 253  -0.00113 254  -0.00563 255  -0.01913
 256  -0.04163 257  -0.04163 258  -0.01913 259  -0.00563 260  -0.00113
 261  -0.00563 262  -0.01913 263  -0.04163 264  -0.05063 265  -0.02813
 266  -0.01463 267  -0.01013 268  -0.01463 269  -0.02813 270  -0.05063
 271  -0.06863 272  -0.04613 273  -0.03263 274  -0.02813 275  -0.03263
 276  -0.04613 277  -0.06863 278  -0.09563 279  -0.07313 280  -0.05963
 281  -0.05513 282  -0.05963 283  -0.07313 284  -0.09563 285  -0.13163
 286  -0.10913 287  -0.09563 288  -0.09113 289  -0.09563 290  -0.10913
 291  -0.13163 292  -0.08105 293  -0.09893 294  -0.08649 295  -0.07277
 296  -0.06182 297  -0.05616 298  -0.05531 299  -0.05721 300  -0.06118
 301  -0.07241 302  -0.08940 303  -0.11345 304  -0.05405 305  -0.07193
 306  -0.05949 307  -0.04577 308  -0.03482 309  -0.02916 310  -0.02831
 311  -0.03021 312  -0.03418 313  -0.04541 314  -0.06240 315  -0.08645
 316  -0.03605 317  -0.05393 318  -0.04149 319  -0.02777 320  -0.01682
 321  -0.01116 322  -0.01031 323  -0.01221 324  -0.01618 325  -0.02741
 326  -0.04440 327  -0.06845 328  -0.02705 329  -0.04493 330  -0.03249
 331  -0.01877 332  -0.00782 333  -0.00216 334  -0.00131 335  -0.00321
 336  -0.00718 337  -0.01841 338  -0.03540 339  -0.05945 340  -0.02705
 341  -0.04493 342  -0.03249 343  -0.01877 344  -0.00782 345  -0.00216
 346  -0.00131 347  -0.00321 348  -0.00718 349  -0.01841 350  -0.03540
 351  -0.05945 352  -0.03605 353  -0.05393 354  -0.04149 355  -0.02777
 356  -0.01682 357  -0.01116 358  -0.01031 359  -0.01221 360  -0.01618
 361  -0.02741 362  -0.04440 363  -0.06845 364  -0.05405 365  -0.07193
 366  -0.05949 367  -0.04577 368  -0.03482 369  -0.02916 370  -0.02831
 371  -0.03021 372  -0.03418 373  -0.04541 374  -0.06240 375  -0.08645
 376  -0.08105 377  -0.09893 378  -0.08649 379  -0.07277 380  -0.06182
 381  -0.05616 382  -0.05531 383  -0.05721 384  -0.06118 385  -0.07241
 386  -0.08940 387  -0.11345 388  -0.11705 389  -0.13493 390  -0.12249
 391  -0.10877 392  -0.09782 393  -0.09216 394  -0.09131 395  -0.09321
 396  -0.09718 397  -0.10841 398  -0.12540 399  -0.14945

YOUNG MODULUS OF DOWEL BAR (YMSB)   = 0.000E+00
POISSON RATIO OF DOWEL BAR (PRSB)   =   0.00000

JOINT  SPRING CONSTANT  MODULUS OF  DOWEL   DOWEL   JOINT     GAP   NODE
 NO.   SHEAR     MOMENT   DOWEL SUP.  DIA.  SPACING  WIDTH    DOWEL  JOINT
     (SPCON1)  (SPCON2)   (SCKV)     (BD)    (BS)    (WJ)    (GDC)  (NNAJ)
  1 2.000E+01 0.000E+00 0.000E+00   0.000    0.000   0.000  0.00000    0
  2 2.000E+01 0.000E+00 0.000E+00   0.000    0.000   0.000  0.00000    0
  3 2.000E+01 0.000E+00 0.000E+00   0.000    0.000   0.000  0.00000    0
  4 2.000E+01 0.000E+00 0.000E+00   0.000    0.000   0.000  0.00000    0

HALF BAND WIDTH (NB) =  63

PERIOD 1 LOAD GROUP 1 AND CYCLE NO. 1

DEFLECTIONS OF SLABS (F) ARE: (DOWNWARD POSITIVE)
    1   0.04140    2   0.02545    3   0.01757    4   0.01663    5   0.02235
    6   0.03565    7   0.05777    8   0.02317    9   0.00703   10  -0.00113
   11  -0.00251   12   0.00258   13   0.01500   14   0.03609   15   0.01248
   16  -0.00381   17  -0.01213   18  -0.01389   19  -0.00951   20   0.00183
   21   0.02163   22   0.00716   23  -0.00909   24  -0.01742   25  -0.01948
   26  -0.01584   27  -0.00573   28   0.01248   29   0.00557   30  -0.01027
   31  -0.01840   32  -0.02064   33  -0.01772   34  -0.00890   35   0.00756
```

36	0.00748	37	-0.00747	38	-0.01507	39	-0.01736	40	-0.01520
41	-0.00777	42	0.00696	43	0.01425	44	0.00078	45	-0.00582
46	-0.00801	47	-0.00693	48	-0.00142	49	0.01109	50	0.02850
51	0.01709	52	0.01224	53	0.01043	54	0.00967	55	0.01195
56	0.02090	57	0.04187	58	0.03188	59	0.02860	60	0.02736
61	0.02483	62	0.02428	63	0.03046	64	0.05619	65	0.04734
66	0.04571	67	0.04535	68	0.04075	69	0.03732	70	0.04109
71	0.07351	72	0.06560	73	0.06576	74	0.06670	75	0.05948
76	0.05292	77	0.05445	78	0.08938	79	0.08207	80	0.08364
81	0.08568	82	0.07627	83	0.06714	84	0.06710	85	0.04841
86	0.05244	87	0.05721	88	0.05416	89	0.04681	90	0.03986
91	0.03481	92	0.03235	93	0.03105	94	0.03197	95	0.03768
96	0.04971	97	0.02369	98	0.01308	99	0.01546	100	0.01519
101	0.01331	102	0.01089	103	0.00892	104	0.00809	105	0.00804
106	0.01047	107	0.01711	108	0.02973	109	0.00843	110	-0.01285
111	-0.01360	112	-0.00994	113	-0.00718	114	-0.00658	115	-0.00670
116	-0.00657	117	-0.00587	118	-0.00253	119	0.00476	120	0.01796
121	-0.00183	122	-0.01701	123	-0.01704	124	-0.01466	125	-0.01334
126	-0.01341	127	-0.01367	128	-0.01347	129	-0.01264	130	-0.00902
131	-0.00144	132	0.01217	133	-0.00833	134	-0.00881	135	-0.00550
136	-0.00785	137	-0.01151	138	-0.01411	139	-0.01540	140	-0.01555
141	-0.01487	142	-0.01133	143	-0.00369	144	0.01008	145	-0.00830
146	-0.00884	147	-0.00554	148	-0.00767	149	-0.01110	150	-0.01357
151	-0.01481	152	-0.01493	153	-0.01426	154	-0.01073	155	-0.00313
156	0.01056	157	-0.00192	158	-0.01632	159	-0.01619	160	-0.01327
161	-0.01142	162	-0.01119	163	-0.01131	164	-0.01109	165	-0.01025
166	-0.00670	167	0.00077	168	0.01416	169	0.00800	170	-0.00981
171	-0.00988	172	-0.00538	173	-0.00198	174	-0.00106	175	-0.00106
176	-0.00092	177	-0.00024	178	0.00300	179	0.01010	180	0.02300
181	0.01615	182	0.00581	183	0.00799	184	0.01056	185	0.01158
186	0.01099	187	0.01007	188	0.00973	189	0.01002	190	0.01276
191	0.01949	192	0.03203	193	0.02536	194	0.02403	195	0.02855
196	0.02914	197	0.02733	198	0.02480	199	0.02267	200	0.02170
201	0.02149	202	0.02364	203	0.02998	204	0.04221	205	0.03756
206	0.04487	207	0.05124	208	0.05076	209	0.04648	210	0.04188
211	0.03831	212	0.03657	213	0.03575	214	0.03716	215	0.04303
216	0.05500	217	0.04944	218	0.06309	219	0.07056	220	0.06980
221	0.06390	222	0.05767	223	0.05289	224	0.05046	225	0.04909
226	0.04983	227	0.05529	228	0.06707	229	0.05680	230	0.04562
231	0.04129	232	0.03850	233	0.03349	234	0.02825	235	0.02731
236	0.03371	237	0.02068	238	0.01430	239	0.01118	240	0.00918
241	0.00923	242	0.01437	243	0.01924	244	0.00470	245	-0.00280
246	-0.00570	247	-0.00527	248	-0.00077	249	0.01026	250	0.01153
251	-0.00405	252	-0.01209	253	-0.01456	254	-0.01231	255	-0.00447
256	0.01116	257	0.00854	258	-0.00766	259	-0.01596	260	-0.01810
261	-0.01468	262	-0.00479	263	0.01352	264	0.00910	265	-0.00739
266	-0.01584	267	-0.01781	268	-0.01382	269	-0.00302	270	0.01630
271	0.01346	272	-0.00310	273	-0.01164	274	-0.01359	275	-0.00944
276	0.00159	277	0.02099	278	0.02316	279	0.00664	280	-0.00195
281	-0.00394	282	0.00019	283	0.01118	284	0.03038	285	0.04031
286	0.02388	287	0.01532	288	0.01329	289	0.01731	290	0.02814
291	0.04716	292	0.00066	293	0.02699	294	0.03130	295	0.03295
296	0.02961	297	0.02419	298	0.01939	299	0.01681	300	0.01526
301	0.01568	302	0.02084	303	0.03223	304	-0.00476	305	0.00997
306	0.01427	307	0.01459	308	0.01131	309	0.00690	310	0.00323
311	0.00138	312	0.00048	313	0.00179	314	0.00760	315	0.01954
316	-0.00397	317	-0.00234	318	0.00091	319	0.00122	320	-0.00079
321	-0.00365	322	-0.00607	323	-0.00719	324	-0.00750	325	-0.00543
326	0.00094	327	0.01347	328	-0.00045	329	-0.01168	330	-0.01050
331	-0.00859	332	-0.00825	333	-0.00939	334	-0.01068	335	-0.01121
336	-0.01104	337	-0.00839	338	-0.00156	339	0.01148	340	0.00214
341	-0.01289	342	-0.01237	343	-0.01051	344	-0.00994	345	-0.01075
346	-0.01172	347	-0.01201	348	-0.01164	349	-0.00867	350	-0.00155
351	0.01178	352	0.00352	353	-0.00618	354	-0.00449	355	-0.00481

356	-0.00647	357	-0.00839	358	-0.00976	359	-0.01015	360	-0.00978
361	-0.00673	362	0.00050	363	0.01392	364	0.00710	365	0.00091
366	0.00315	367	0.00197	368	-0.00074	369	-0.00324	370	-0.00484
371	-0.00529	372	-0.00492	373	-0.00183	374	0.00544	375	0.01882
376	0.01623	377	0.00647	378	0.00772	379	0.00814	380	0.00708
381	0.00550	382	0.00438	383	0.00416	384	0.00468	385	0.00793
386	0.01526	387	0.02856	388	0.03251	389	0.01779	390	0.01816
391	0.01996	392	0.02105	393	0.02098	394	0.02071	395	0.02085
396	0.02159	397	0.02500	398	0.03236	399	0.04557		

FOR JOINT NO. 1 SHEAR (FAJ1) AND MOMENT (FAJ2) AT THE NODES ARE:

7	2.6	0.0	14	2.2	0.0	21	1.4	0.0
28	0.3	0.0	35	-1.3	0.0	42	-0.7	0.0
49	1.6	0.0	56	1.3	0.0	63	0.1	0.0
70	-0.6	0.0	77	-1.0	0.0	84	-0.6	0.0

FOR JOINT NO. 2 SHEAR (FAJ1) AND MOMENT (FAJ2) AT THE NODES ARE:

217	-3.1	0.0	218	0.3	0.0	219	-1.9	0.0
220	-0.6	0.0	221	1.3	0.0	222	1.8	0.0
223	1.5	0.0	224	1.1	0.0	225	1.4	0.0
226	1.8	0.0	227	1.6	0.0	228	1.2	0.0

FOR JOINT NO. 3 SHEAR (FAJ1) AND MOMENT (FAJ2) AT THE NODES ARE:

235	-12.1	0.0	242	-4.6	0.0	249	0.3	0.0
256	3.0	0.0	263	3.2	0.0	270	1.8	0.0
277	0.7	0.0	284	0.4	0.0	291	0.3	0.0
226	0.0	0.0	227	0.0	0.0	228	0.0	0.0

FOR JOINT NO. 4 SHEAR (FAJ1) AND MOMENT (FAJ2) AT THE NODES ARE:

78	1.7	0.0	79	-0.5	0.0	80	-6.4	0.0
81	-11.2	0.0	82	-6.8	0.0	83	-2.9	0.0
84	-1.9	0.0						

NODAL NUMBER AND REACTIVE PRESSURE (SUBR) ARE: (COMPRESSION POSITIVE)

1	20.698	2	12.724	3	8.786	4	8.315	5	11.176
6	17.824	7	28.885	8	11.587	9	3.513	10	-0.566
11	-1.254	12	1.288	13	7.499	14	18.047	15	6.239
16	-1.907	17	-6.066	18	-6.943	19	-4.756	20	0.914
21	10.813	22	3.579	23	-4.543	24	-8.710	25	-9.738
26	-7.918	27	-2.866	28	6.238	29	2.786	30	-5.134
31	-9.198	32	-10.320	33	-8.859	34	-4.452	35	3.781
36	3.740	37	-3.733	38	-7.533	39	-8.682	40	-7.602
41	-3.885	42	3.481	43	7.127	44	0.392	45	-2.909
46	-4.007	47	-3.463	48	-0.708	49	5.545	50	14.251
51	8.547	52	6.118	53	5.213	54	4.833	55	5.975
56	10.449	57	20.934	58	15.939	59	14.299	60	13.679
61	12.413	62	12.138	63	15.230	64	28.096	65	23.670
66	22.855	67	22.674	68	20.376	69	18.662	70	20.544
71	36.755	72	32.802	73	32.879	74	33.350	75	29.742
76	26.459	77	27.225	78	44.691	79	41.035	80	41.821
81	42.842	82	38.135	83	33.569	84	33.550	85	24.207
86	26.219	87	28.607	88	27.081	89	23.407	90	19.928
91	17.405	92	16.177	93	15.523	94	15.986	95	18.838
96	24.853	97	11.846	98	6.541	99	7.728	100	7.594
101	6.657	102	5.446	103	4.458	104	4.043	105	4.019
106	5.233	107	8.556	108	14.867	109	4.214	110	-6.424
111	-6.798	112	-4.971	113	-3.592	114	-3.290	115	-3.352
116	-3.287	117	-2.936	118	-1.264	119	2.378	120	8.982
121	-0.915	122	-8.504	123	-8.520	124	-7.328	125	-6.672
126	-6.706	127	-6.833	128	-6.736	129	-6.318	130	-4.512
131	-0.722	132	6.086	133	-4.167	134	-4.404	135	-2.752
136	-3.923	137	-5.754	138	-7.054	139	-7.702	140	-7.774
141	-7.437	142	-5.666	143	-1.847	144	5.041	145	-4.149
146	-4.419	147	-2.768	148	-3.833	149	-5.551	150	-6.784

151	-7.403	152	-7.466	153	-7.128	154	-5.365	155	-1.567
156	5.282	157	-0.960	158	-8.162	159	-8.094	160	-6.633
161	-5.711	162	-5.593	163	-5.656	164	-5.543	165	-5.126
166	-3.349	167	0.383	168	7.082	169	3.998	170	-4.903
171	-4.938	172	-2.692	173	-0.992	174	-0.528	175	-0.531
176	-0.460	177	-0.120	178	1.498	179	5.050	180	11.499
181	8.076	182	2.907	183	3.993	184	5.280	185	5.790
186	5.497	187	5.035	188	4.865	189	5.010	190	6.380
191	9.747	192	16.016	193	12.679	194	12.014	195	14.276
196	14.569	197	13.666	198	12.400	199	11.333	200	10.848
201	10.747	202	11.818	203	14.989	204	21.107	205	18.782
206	22.434	207	25.621	208	25.379	209	23.242	210	20.939
211	19.156	212	18.284	213	17.877	214	18.580	215	21.517
216	27.499	217	24.720	218	31.547	219	35.282	220	34.898
221	31.951	222	28.836	223	26.443	224	25.228	225	24.547
226	24.917	227	27.643	228	33.533	229	28.399	230	22.809
231	20.644	232	19.248	233	16.747	234	14.124	235	13.655
236	16.856	237	10.338	238	7.150	239	5.591	240	4.592
241	4.613	242	7.185	243	9.619	244	2.348	245	-1.401
246	-2.848	247	-2.636	248	-0.387	249	5.131	250	5.766
251	-2.023	252	-6.043	253	-7.281	254	-6.157	255	-2.234
256	5.582	257	4.268	258	-3.829	259	-7.980	260	-9.049
261	-7.341	262	-2.397	263	6.762	264	4.549	265	-3.695
266	-7.919	267	-8.903	268	-6.911	269	-1.512	270	8.149
271	6.728	272	-1.552	273	-5.821	274	-6.794	275	-4.718
276	0.796	277	10.496	278	11.579	279	3.321	280	-0.974
281	-1.969	282	0.096	283	5.588	284	15.191	285	20.154
286	11.939	287	7.658	288	6.645	289	8.655	290	14.068
291	23.578	292	0.332	293	13.496	294	15.652	295	16.474
296	14.805	297	12.093	298	9.697	299	8.406	300	7.629
301	7.838	302	10.419	303	16.115	304	-2.381	305	4.985
306	7.134	307	7.295	308	5.653	309	3.450	310	1.614
311	0.691	312	0.241	313	0.896	314	3.799	315	9.770
316	-1.986	317	-1.170	318	0.454	319	0.609	320	-0.394
321	-1.823	322	-3.034	323	-3.595	324	-3.749	325	-2.717
326	0.470	327	6.737	328	-0.223	329	-5.841	330	-5.249
331	-4.294	332	-4.126	333	-4.694	334	-5.341	335	-5.604
336	-5.522	337	-4.196	338	-0.778	339	5.740	340	1.071
341	-6.447	342	-6.183	343	-5.255	344	-4.972	345	-5.376
346	-5.858	347	-6.006	348	-5.818	349	-4.335	350	-0.777
351	5.892	352	1.758	353	-3.092	354	-2.246	355	-2.405
356	-3.235	357	-4.193	358	-4.878	359	-5.073	360	-4.889
361	-3.367	362	0.248	363	6.962	364	3.550	365	0.455
366	1.576	367	0.983	368	-0.369	369	-1.619	370	-2.422
371	-2.645	372	-2.461	373	-0.914	374	2.722	375	9.412
376	8.115	377	3.236	378	3.858	379	4.069	380	3.540
381	2.752	382	2.191	383	2.078	384	2.339	385	3.966
386	7.632	387	14.279	388	16.256	389	8.893	390	9.079
391	9.980	392	10.523	393	10.492	394	10.355	395	10.423
396	10.794	397	12.502	398	16.178	399	22.786		

SUM OF FORCES (FOSUM) = 82.8 SUM OF REACTIONS (SUBSUM) = 82.9

NODE	LAYER	STRESS X	STRESS Y	STRESS XY	MAX.SHEAR	MAJOR	MINOR
1	1	0.000	0.000	0.000	0.000	0.000	0.000
1	2	0.000	0.000	0.000	0.000	0.000	0.000
2	1	0.000	53.571	0.000	26.786	53.571	0.000
2	2	0.000	-110.054	0.000	55.027	0.000	-110.054
3	1	0.000	144.897	0.000	72.448	144.897	0.000
3	2	0.000	-297.667	0.000	148.833	0.000	-297.667
4	1	0.000	165.694	0.000	82.847	165.694	0.000
4	2	0.000	-340.391	0.000	170.196	0.000	-340.391
5	1	0.000	97.531	0.000	48.765	97.531	0.000
5	2	0.000	-200.361	0.000	100.180	0.000	-200.361

6	1	0.000	-7.261	0.000	3.631	0.000	-7.261
6	2	0.000	14.917	0.000	7.459	14.917	0.000
7	1	0.000	0.000	0.000	0.000	0.000	0.000
7	2	0.000	0.000	0.000	0.000	0.000	0.000
8	1	81.679	0.000	0.000	40.839	81.679	0.000
8	2	-167.795	0.000	0.000	83.898	0.000	-167.795
9	1	93.846	76.780	-9.195	12.544	97.857	72.769
9	2	-192.790	-157.732	18.889	25.769	-149.492	-201.030
10	1	100.752	169.232	-16.774	38.128	173.120	96.864
10	2	-206.978	-347.659	34.459	78.328	-198.991	-355.647
11	1	100.856	193.347	-29.959	55.102	202.203	92.000
11	2	-207.193	-397.200	61.546	113.197	-188.999	-415.393
12	1	95.523	128.814	-46.624	49.507	161.675	62.662
12	2	-196.237	-264.628	95.782	101.703	-128.730	-332.136
13	1	93.160	20.969	-62.042	71.778	128.843	-14.714
13	2	-191.382	-43.078	127.456	147.457	30.227	-264.687
14	1	112.222	0.000	-61.815	83.484	139.595	-27.373
14	2	-230.541	0.000	126.989	171.503	56.233	-286.774
15	1	241.128	0.000	0.000	120.564	241.128	0.000
15	2	-495.357	0.000	0.000	247.678	0.000	-495.357
16	1	243.841	102.363	-2.193	70.773	243.875	102.329
16	2	-500.931	-210.288	4.505	145.391	-210.218	-501.001
17	1	250.790	206.740	-11.026	24.630	253.395	204.135
17	2	-515.206	-424.714	22.651	50.599	-419.361	-520.559
18	1	250.659	237.787	-29.249	29.949	274.172	214.275
18	2	-514.938	-488.494	60.087	61.524	-440.192	-563.241
19	1	243.185	176.573	-53.442	62.971	272.850	146.908
19	2	-499.583	-362.739	109.788	129.364	-301.797	-560.525
20	1	236.287	61.689	-76.768	116.252	265.240	32.736
20	2	-485.414	-126.729	157.708	238.821	-67.250	-544.892
21	1	248.139	0.000	-80.612	147.958	272.027	-23.888
21	2	-509.761	0.000	165.603	303.955	49.074	-558.835
22	1	355.772	0.000	0.000	177.886	355.772	0.000
22	2	-730.876	0.000	0.000	365.438	0.000	-730.876
23	1	350.563	123.756	10.320	113.872	351.032	123.287
23	2	-720.174	-254.236	-21.201	233.932	-253.273	-721.137
24	1	354.190	241.382	-3.151	56.492	354.278	241.294
24	2	-727.625	-495.880	6.473	116.053	-495.700	-727.806
25	1	352.757	281.661	-26.495	44.336	361.545	272.873
25	2	-724.682	-578.625	54.429	91.081	-560.573	-742.734
26	1	342.158	225.739	-56.403	81.053	365.002	202.895
26	2	-702.908	-463.743	115.870	166.511	-416.814	-749.836
27	1	326.160	103.506	-86.217	140.808	355.641	74.025
27	2	-670.041	-212.637	177.118	289.267	-152.072	-730.606
28	1	323.718	0.000	-97.842	189.133	350.992	-27.274
28	2	-665.026	0.000	200.999	388.543	56.030	-721.056
29	1	373.684	0.000	0.000	186.842	373.684	0.000
29	2	-767.671	0.000	0.000	383.836	0.000	-767.671
30	1	361.755	138.593	29.458	115.404	365.578	134.770
30	2	-743.165	-284.716	-60.516	237.078	-276.862	-751.019
31	1	361.298	268.462	8.167	47.131	362.011	267.749
31	2	-742.228	-551.512	-16.778	96.823	-550.047	-743.692
32	1	359.980	317.787	-22.923	31.153	370.037	307.731
32	2	-739.520	-652.842	47.091	63.999	-632.183	-760.180
33	1	352.434	265.159	-57.612	72.273	381.070	236.523
33	2	-724.019	-544.725	118.355	148.474	-485.899	-782.846
34	1	334.437	139.219	-87.413	131.029	367.857	105.799
34	2	-687.046	-286.002	179.576	269.178	-217.347	-755.702
35	1	299.621	0.000	-101.172	180.773	330.584	-30.963
35	2	-615.522	0.000	207.841	371.369	63.608	-679.130
36	1	281.838	0.000	0.000	140.919	281.838	0.000
36	2	-578.989	0.000	0.000	289.495	0.000	-578.989
37	1	264.181	146.724	55.631	80.894	286.346	124.558
37	2	-542.715	-301.421	-114.286	166.184	-255.885	-588.252

38	1	257.485	291.209	24.380	29.643	303.990	244.704
38	2	-528.960	-598.240	-50.085	60.897	-502.703	-624.497
39	1	258.072	350.720	-23.389	51.894	356.289	252.502
39	2	-530.166	-720.496	48.048	106.607	-518.724	-731.938
40	1	266.696	294.013	-70.646	71.955	352.309	208.400
40	2	-547.884	-604.000	145.132	147.819	-428.123	-723.761
41	1	276.417	153.543	-98.714	116.271	331.251	98.708
41	2	-567.852	-315.428	202.792	238.860	-202.780	-680.501
42	1	277.279	0.000	-109.583	176.718	315.358	-38.079
42	2	-569.625	0.000	225.120	363.039	78.226	-647.851
43	1	102.614	0.000	0.000	51.307	102.614	0.000
43	2	-210.803	0.000	0.000	105.401	0.000	-210.803
44	1	83.146	145.336	89.972	95.194	209.435	19.047
44	2	-170.810	-298.568	-184.834	195.561	-39.128	-430.250
45	1	63.366	321.507	52.123	139.198	331.634	53.239
45	2	-130.175	-660.483	-107.078	285.959	-109.371	-681.288
46	1	61.302	404.449	-32.615	174.646	407.521	58.230
46	2	-125.936	-830.873	67.002	358.781	-119.624	-837.185
47	1	97.518	326.822	-116.858	163.710	375.880	48.460
47	2	-200.335	-671.402	240.066	336.315	-99.554	-772.184
48	1	156.263	148.334	-151.989	152.041	304.339	0.257
48	2	-321.016	-304.728	312.237	312.343	-0.529	-625.215
49	1	240.056	0.000	-163.933	203.177	323.205	-83.149
49	2	-493.154	0.000	336.774	417.393	170.816	-663.971
50	1	-98.317	0.000	0.000	49.159	0.000	-98.317
50	2	201.977	0.000	0.000	100.989	201.977	0.000
51	1	-105.189	120.790	131.198	173.146	180.947	-165.345
51	2	216.093	-248.143	-269.524	355.700	339.674	-371.725
52	1	-145.057	378.586	103.120	281.397	398.162	-164.632
52	2	297.995	-777.743	-211.843	578.084	338.209	-817.958
53	1	-167.495	538.506	-49.873	356.506	542.011	-171.001
53	2	344.091	-1106.271	102.457	732.383	351.293	-1113.473
54	1	-96.654	387.868	-205.395	317.612	463.219	-172.005
54	2	198.559	-796.810	421.950	652.481	353.355	-951.607
55	1	-5.336	129.763	-238.240	247.631	309.844	-185.418
55	2	10.962	-266.576	489.424	508.717	380.910	-636.524
56	1	70.442	0.000	-240.897	243.458	278.679	-208.237
56	2	-144.712	0.000	494.882	500.144	427.788	-572.500
57	1	-179.065	0.000	0.000	89.533	0.000	-179.065
57	2	367.860	0.000	0.000	183.930	367.860	0.000
58	1	-154.788	82.515	154.172	194.544	158.407	-230.680
58	2	317.986	-169.513	-316.722	399.658	473.894	-325.422
59	1	-188.737	429.527	160.464	348.298	468.693	-227.903
59	2	387.730	-882.392	-329.647	715.521	468.190	-962.852
60	1	-240.885	721.192	-61.453	484.948	725.102	-244.795
60	2	494.859	-1481.571	126.244	996.246	502.890	-1489.602
61	1	-143.006	441.738	-286.876	409.609	558.974	-260.243
61	2	293.783	-907.477	589.340	841.474	534.627	-1148.321
62	1	-65.253	96.972	-287.652	298.869	314.729	-283.010
62	2	134.052	-199.213	590.933	613.977	581.396	-646.558
63	1	-56.906	0.000	-266.705	268.218	239.765	-296.671
63	2	116.905	0.000	547.901	551.010	609.463	-492.558
64	1	-206.464	0.000	0.000	103.232	0.000	-206.464
64	2	424.147	0.000	0.000	212.074	424.147	0.000
65	1	-145.285	28.782	159.299	181.524	123.272	-239.776
65	2	298.465	-59.127	-327.253	372.911	492.580	-253.242
66	1	-119.295	459.443	214.001	359.904	529.978	-189.830
66	2	245.072	-943.849	-439.630	739.363	389.974	-1088.752
67	1	-192.353	1003.073	-69.873	601.783	1007.143	-196.424
67	2	395.159	-2060.648	143.543	1236.265	403.520	-2069.010
68	1	-82.321	473.727	-357.910	453.207	648.911	-257.504
68	2	169.114	-973.194	735.267	931.040	529.000	-1333.080
69	1	-76.664	42.902	-304.943	310.748	293.867	-327.629
69	2	157.494	-88.136	626.456	638.381	673.061	-603.702

70	1	-140.539	0.000	-248.708	258.444	188.175	-328.713
70	2	288.713	0.000	510.929	530.931	675.288	-386.574
71	1	-157.209	0.000	0.000	78.605	0.000	-157.209
71	2	322.960	0.000	0.000	161.480	322.960	0.000
72	1	-93.475	-40.753	145.509	147.878	80.764	-214.992
72	2	192.029	83.721	-298.925	303.790	441.665	-165.916
73	1	10.773	441.318	211.882	302.054	528.099	-76.008
73	2	-22.132	-906.616	-435.278	620.520	156.146	-1084.893
74	1	223.125	1473.204	-75.681	629.605	1477.769	218.560
74	2	-458.373	-3026.454	155.475	1293.419	-448.995	-3035.833
75	1	29.920	459.270	-367.561	425.660	670.255	-181.064
75	2	-61.466	-943.495	755.093	874.447	371.967	-1376.928
76	1	-51.884	-40.682	-294.436	294.489	248.206	-340.772
76	2	106.587	83.574	604.871	604.980	700.061	-509.899
77	1	-145.497	0.000	-215.793	227.726	154.977	-300.474
77	2	298.900	0.000	443.312	467.825	617.275	-318.375
78	1	0.000	0.000	0.000	0.000	0.000	0.000
78	2	0.000	0.000	0.000	0.000	0.000	0.000
79	1	0.000	-129.701	141.277	155.451	90.600	-220.301
79	2	0.000	266.450	-290.231	319.348	452.573	-186.123
80	1	0.000	401.115	209.492	290.018	490.575	-89.460
80	2	0.000	-824.024	-430.367	595.794	183.781	-1007.806
81	1	0.000	1826.051	-77.070	916.273	1829.298	-3.247
81	2	0.000	-3751.322	158.327	1882.331	6.670	-3757.992
82	1	0.000	427.898	-368.724	426.300	640.249	-212.351
82	2	0.000	-879.046	757.484	875.764	436.241	-1315.287
83	1	0.000	-159.909	-290.128	300.944	220.989	-380.899
83	2	0.000	328.507	596.021	618.240	782.494	-453.986
84	1	0.000	0.000	-200.269	200.269	200.269	-200.269
84	2	0.000	0.000	411.420	411.420	411.420	-411.420

MAXIMUM STRESS (SMAX) IN LAYER 1 IS 1829.298 (NODE 81)

MAXIMUM NEGATIVE STRESS IN X DIRECTION = -240.9 (NODE 60)
MAXIMUM POSITIVE STRESS IN X DIRECTION = 373.7 (NODE 29)
MAXIMUM NEGATIVE STRESS IN Y DIRECTION = -159.9 (NODE 83)
MAXIMUM POSITIVE STRESS IN Y DIRECTION = 1826.1 (NODE 81)

MAXIMUM STRESS (SMAX) IN LAYER 2 IS -3757.992 (NODE 81)

MAXIMUM NEGATIVE STRESS IN X DIRECTION = -767.7 (NODE 29)
MAXIMUM POSITIVE STRESS IN X DIRECTION = 494.9 (NODE 60)
MAXIMUM NEGATIVE STRESS IN Y DIRECTION = -3751.3 (NODE 81)
MAXIMUM POSITIVE STRESS IN Y DIRECTION = 328.5 (NODE 83)